KAZAN SCIENCE WEEK 2023

ABSTRACTS


300 лет
Российская Академия Наук

KAZAN SCIENCE WEEK

ABSTRACTS OF THE
INTERNATIONAL CONFERENCES
"MODERN DEVELOPMENT OF MAGNETIC RESONANCE"
AND
"SPIN PHYSICS, SPIN CHEMISTRY, AND SPIN TECHNOLOGY"

Editor:
KEV M. SALIKHOV

KAZAN, SEPTEMBER 25–30, 2023

Published by Zavoisky Physical-Technical Institute, FRC Kazan Scientific Center of RAS, Kazan
www.kfti.knc.ru

Conferences are supported by:

Ministry of Science and Higher Education of the Russian Federation

Ministry of Education and Science of the Republic of Tatarstan

Federal Research Center "Kazan Scientific Center of the Russian Academy of Sciences"

Zavoisky Physical-Technical Institute FRC KazanSC RAS

Kazan Federal University

Academy of Sciences of the Republic of Tatarstan

Government of the Republic of Tatarstan

ЭЛемент

"НАУКА"
Центр Технического Сопровождения

CRYOTRADE engineering

CHAIRMEN

Kalachev A.A.
Khantimerov S.M.
Salikhov K.M.

PROGRAM COMMITTEE

Tagirov L.R., chairman (Russia)
Voronkova V.K., chairman (Russia)
Atsarkin V.A. (Russia)
Bagryanskaya E.G. (Russia)
Baranov P.G. (Russia)
Demishev S.V. (Russia)
Eremina R.M. (Russia)
Fedin M.V. (Russia)
Gafurov M.R. (Russia)
Goldfarb D. (Israel)
Kalachev A.A. (Russia)
Ohta H. (Japan)
Salikhov K.M. (Russia)
Smirnov A.I. (Russia)
Tarasov V.F. (Russia)

SCIENTIFIC SECRETARIAT

Gavrilova T.P.
Kandrashkin Yu.E.
Kamashev A.A.
Latypov I.Z.
Latypov V.A.
Mosina L.V.

LOCAL ORGANIZING COMMITTEE

Khantimerov S.M., chairman
Tagirov L.R., scientific secretary
Voronkova V.K., scientific secretary
Gavrilova T.P., secretary
Akhmetgalieva A.M.
Akhmin S.M.
Falin M.L.
Garipov R.R.
Gubaidulina A.Z.
Guseva R.R.
Ilmatova D.V.
Kandrashkin Yu.E.
Kamashev A.A.
Khabibullina V.I.
Konovalov D.A.
Latypov V.A.
Likerov R.F.
Lvov S.G.
Mosina L.V.
Morozova A.S.
Novikov H.A.
Oladoshkin Yu.V.
Pushkova V.V.
Salikhov K.M.
Yagfarova A.R.
Yanduganova O.B.

CONTENTS

ZAVOISKY AWARD LECTURE

PLENARY LECTURES

MODERN DEVELOPMENT OF MAGNETIC RESONANCE

SPIN PHYSICS, SPIN CHEMISTRY, AND SPIN TECHNOLOGY

ZAVOISKY AWARD LECTURE

The application of advanced EPR methods to study molecular macrosystems containing electron spins

E.G. Bagryanskaya

N.N. Vorozhtsov Novosibirsk Institute of Organic Chemistry of the Siberian Branch of the Russian Academy of Sciences, Novosibirsk, Russia,
e-mail: egbagryanskaya@nioch.nsc.ru

Pulsed dipole EPR spectroscopy is widely used to study the structure and functions of biological molecules – proteins and nucleic acids [1]. The method is based on the use of special pulse sequences PELDOR, DEER, SIFTER, which allow measuring nanometre distances between spin tags selectively inserted into biomolecules. Recently we presented an X-band pulse EPR spectrometer with high throughput and excellent sensitivity in the 8.5–11.5 GHz range [2] and illustrated the capabilities and performance of the spectrometer by measurements on free radicals and biradicals in solids and liquids. The advantages of direct detection of highly stable deuterated nitroxides and the simplicity of the measurements of electron spin relaxation times will be demonstrated. Nitroxyl and triarylmethyl radicals as well as gadolinium and copper complexes are used as spin tags.

The report gives an overview of the works on the application of spin labels based on triarylmethyl [3–6] and stereo-substituted nitroxyl radicals [7] to study the complex of human ribosomes and RNA modelling translation [8, 9], membrane complexes of colabumin B12 transport [10, 11], and to study the processes of penetration of unstructured RL2 proteins into lung cancer cells [12].

Another approach concerns the combination of fluorine labeling and pulsed electron-nuclear double resonance (ENDOR) and was proposed by M. Benatti et al. [13] to be used for the measurements of short nanometer distances. We showed the capability of Mims19F ENDOR experiments on reporting intermolecular distances in trityl- and19F-labeled DNA duplexes [14].

This work was supported by Russian Science Foundation № 21–14–00219.1.

1. Schiemann D. et al.: J. Am. Chem. Soc. **143**, 17875 (2021)
2. Isaev N.P. et al.: JMRO 14-15, 100092 (2023)
3. Krumkacheva O., Bagryanskaya E.: Trityl radicals as spin labels, in book: Electron Paramagnetic Resonance. RSC, Oxford, pp. 35–60, 2016.
4. Krumkacheva O., Bagryanskaya E.: J. Magn. Res. **280**, 117 (2017)
5. Tormyshev V.M., Bagryanskaya E.: Russian Chemical Review **12**, 2278 (2021)
6. Timofeev, I.O. et al.: Phys. Chem. Chem. Phys. **24**(7), 4475–4484 (2022)
7. Dobrynin, S.A. et al.: Molecules **26**(19), 5761 (2021)
8. Bulygin, K.N. et al.: Comput. Struct. Biotechn. J. **19**, 47026 (2021)
9. Malygin A.A. et al.: NAR **47**, 11850 (2019). NARr **46**, 897 (2018)
10. Joseph B. et al.: Chem.- A Europ. Journ. 27, 2299 (2021)
11. Ketter S. et al.: J. of Magn. Reson. Open. 10-11, 100041 (2022)
12. Ovcherenko S.S. et al.: Molecules 26, 5442 (2021)
13. Meyer et al.: Angew. Chemie – Int. Ed. 59, 373–379 (2020)
14. Asanbaeva N.B. et al: PCCP (2023), DOI: 10.1039/D3CP02969G

PLENARY LECTURES

P1

THz ESR applications to the study of Dzyaloshinskii-Moriya interaction in quantum spin systems

H. Ohta[1,2], S. Okubo[1,2], E. Ohmichi[2], T. Sakurai[3], H. Takahashi[1,2], S. Hara[3]

[1]Molecular Photoscience Research Center, Kobe University, Kobe, Hyogo, Japan
[2]Graduate School of Science, Kobe University, Kobe, Hyogo, Japan
[3]Research Facility Center for Science and Technology, Kobe University, Kobe, Hyogo, Japan

Our multi-extreme THz ESR covers the frequency region between 0.03 and 7 THz [1], the temperature region between 1.8 and 300 K [1], the magnetic field region up to 55 T [1], and the pressure region is extended from 1.5 GPa [2] to 2.5 GPa using the hybrid-type pressure cell [3]. It also includes our mechanically detected ESR [4] measurements using a commercially available membrane-type surface stress sensor, which is the extension from our micro-cantilever ESR [5]. Our multi-extreme THz ESR and other related topics on THz ESR are summarized in the special issue "Terahertz Spectroscopy" of Appl. Mag. Reson. [6].

HO recently published a review article "Experimental Studies of Dzyaloshinskii-Moriya Interaction in Quantum Spin Systems: High-frequency High-field Electron Spin Resonance (ESR) Measurements" [7] in the JPSJ Special Topics "Dzyaloshinskii-Moriya Interaction: Physics of Inversion Symmetry Breaking". In this presentation, some topics from the review, such as THz ESR studies of Shastry-Sutherland model substance $SrCu_2(BO_3)_2$ [8], triangular antiferromagnets Cs_2CuC_{l4} [9] and $CsCuC_{l3}$ [10] under high pressure will be presented.

1. Ohta H. et al.: J. Low Temp. Phys. **170**, 511 (2013)
2. Sakurai T. et al.: Rev. Sci. Inst. **78**, 065107 (2007)
3. Fujimoto K. et al.: Appl. Mag. Reson. **44**, 893 (2013); Ohta H. et al.: J. Phys. Chem. B **119**, 13755 (2015); Sakurai T. et al.: J. Mag. Res. **259**, 108 (2015); Sakurai T. et al.: J. Phys. Soc. Jpn. **87**, 033701 (2018)
4. Takahashi H. et al.: Rev. Sci. Intrum. **89**, 036108 (2018)
5. Ohta H. et al.: AIP Conf. Proceedings **850**, 1643 (2006); Ohmichi E. et al.: Rev. Sci. Instrum. **79**, 103903 (2008); Takahashi H., Ohmichi E., Ohta H.: Appl. Phys. Lett. **107**, 182405 (2015)
6. Ohta H., Sakai T. (eds.): Appl. Mag. Reson. **52**(4), 263–564 (2021), Special Issue "Terahertz Spectroscopy".
7. Ohta H.: J. Phys. Soc. Jpn. **92**, 081003 (2023)
8. Sakurai T., Hirao Y., Hijii K., Okubo S., Ohta H., Uwatoko Y., Kudo K., Koike Y.: J. Phys. Soc. Jpn. **87**, 033701 (2018)
9. Zvyagin S.A., Graf D., Sakurai T., Kimura S., Nojiri H., Wosnitza J., Ohta H., Ono T., Tanaka H.: Nat. Commun. **10**, 1064 (2019)
10. Yamamoto D., Sakurai T., Okuto R., Okubo S., Ohta H., Tanaka H., Uwatoko Y.: Nat. Commun. **12**, 4263 (2021)

P2

Antiferromagnetic spintronics and magnonics

S.A. Nikitov[1,2], D.V. Kalyabin[1,2], A.R. Safin[1,3]

[1]Kotel'nikov Institute of Radioengineering and Electronics, RAS, Moscow, Russia
[2]Moscow Institute of Physics and Tecnology, National Research University, Dolgoprudny, Russia
[3]Moscow Power UIniversity, National Research University, Moscow, Russia

State-of-the-art studies of antiferromagnetic (AFM) dielectric magnon spintronics and magnonics are reviewed and discussed. Theoretical and experimental approaches to exploring physical processes in and calculations of the parameters of magnonic micro- and nanostructures are described. We discuss the basic concepts of antiferromagnetic magnon spintronics, the underlying physical phenomena, and the prospects for applying antiferromagnetic magnon spintronics for data processing, transmission, and reception. Special attention is paid to the feasibility of boosting the operating frequencies of magnonic devices from the gigahertz to terahertz frequency range. We also discuss specific implementations of the component base of magnonics and ways to further develop it.

Furthermore, we discuss effects of giant and tunnel magnetoresistance, spin Hall effect (inverse spin Hall effect) and spin transfer torque in AFM, spintronic nanoocillators, and, finally, neuromorphic applications. Partly results of this work were published in a number of original papers and in a review paper [1].

The research of this work was done under financial support of Russian Science Foundation (grant 19-19-00607).

1. Nikitov S.A., Safin A.R., Kalyabin D.V. et al.: Physics – Uspekhi **63**, 945–974 (2020)

P3

Gd(III)-^{19}F distance measurements in solution and in cells by electron-nuclear double resonance

D. Goldfarb

Department of Chemical and Biological Physics Weizmann Institute of Science, Rehovot, Israel

Double electron-electron resonance (DEER) technique can track proteins' conformations in the cell by providing distance distributions between two attached spin labels. This technique, however, cannot access distances below 1.5 nm. Very recently, nitroxide-^{19}F [1], trityl-^{19}F [2] and Gd(III)-^{19}F [3] electron-nuclear double resonance (ENDOR) have been shown to efficiently determine the distances below 1.5 nm. Here we present Gd(III)-^{19}F Mims ENDOR distance measurements in the range of 0.9 nm to 1.5 nm on several model complexes and ^{19}F labeled GB1 and ubiquitin (Ub) proteins, spin-labeled with rigid Gd(III) tags. We further extended these studies to Gb1 and ubiquitin delivered into Hela cells, thus adding ^{19}F ENDOR to the tool-box allowing exporlating protein in their native environment, the cell [4]. The solution and in-cell derived Gd(III)-^{19}F distances were essentially identical and lie in the 1–1.5 nm range revealing that both, GB1 and Ub, retained their overall structure in the cell. Methods incresing the sensetivity of ^{19}F Mims ENDOR and incresing the accessible distance range will be presented.

1. Meyer A., Dechert S., Dey S., Höbartner C., Bennati M.: Angew. Chem. Int. Ed. **59**, 373–379 (2020)
2. Asanbaeva N.B., Sukhanov A.A., Diveikina A.A., Rogozhnikova O.Y., Trukhin D.V., Tormyshev V.M., Chubarov A.S., Maryasov A.G., Genaev A.M., Shernyukov A.V., Salnikov G.E., Lomzov A.A., Pyshnyi D.V., Bagryanskaya E.G.: Phys. Chem. Chem. Phys. **24**, 5982–6001 (2022)
3. Martyna J., Qi M., Harmer J.R., Huber T., Godt A., Savitsky A., Otting G., Cox N.: Phys. Chem. Chem. Phys. **24**, 25214–25226 (2022)
4. Seal M., Zhu W., Dalaloyan A., Feintuch A., Bogdanov A., Frydman V., Su X.C., Gronenborn A.M., Goldfarb D.: Angew. Chem. Int. Ed. **62** (20), e202218780 (2023)

P4

Magnetic resonance spectroscopy of excited states in semiconductors and based nanostructures

P.G. Baranov

Ioffe Institute, Saint Petersburg, Russia

To describe manipulations on rapidly changing objects, the phrase is often used: “Shoe a galloping horse”. Magnetic resonance measurements in short-lived objects, in particular excited states, from this field. Obtaining information about spin states in an excited state is critical to the implementation of ultrafast, all-optical methods of spin control. Electron and nuclear spins coherently coupled to photons in solids provide promising resources for information processing and quantum sensing. For a short-lived excited state, a sufficiently strong microwave field must be applied to induce a significant transition probability during that lifetime. The report will consider several characteristic examples of the use of magnetic resonance spectroscopy methods for studying short-lived excited states in semiconductors and based nanostructures.

(1) Excitons.

(i) Self-trapped excitons in wide-band-gap materials. Pulse methods, electron spin echo, electron-nuclear double resonance on the example of self-trapped excitons in silver halides.

(ii) Excitons in semiconductor quantum wells and superlattices. Type-I and type-II superlattices. Localization of excitons at opposite interfaces.

(2) Excited states of spin-1 and spin-3/2 centers in diamond and silicon carbide.

(3) All-optical methods of magnetic resonance: level anticrossing (LAC) and cross-relaxation (CR) in luminescence. The use of LAC and CR in all-optical sensorics with submicron spatial resolution.

This work was supported by the Russian Science Foundation № 23-12-00152, https://rscf.ru/project/23-12-00152/

P5

MR & the intricacies of radical initiation by radical-SAM enzymes

B.M. Hoffman

Departments of Chemistry and Molecular Biosciences, Northwestern University, Evanston, USA

Radical reactions are central to enzymatic catalysis, and in large part are carried out by the largest enzyme superfamily in Nature, the radical S-adenosyl-L-methionine (SAM) enzymes (RS enzymes), with over 700,00 members spanning all kingdoms of life and exhibiting remarkable functional diversity. These reactions are initiated through H-atom abstraction from substrate by the 5′-deoxyadenosyl (5′-dAdo•) radical, which is created by reductive cleavage of the S-C5′ bond of SAM upon electron transfer from a [4Fe-4S]$^{1+}$ cluster, which chelates the amino-acid moiety of SAM. This talk first reviews the efforts of our group, in collaboration with that of Prof. Joan Broderick, which showed that the catalytic process involves the obligatory formation of a bio-organometallic intermediate, denoted, Ω. It them proceeds to describe: the EPR/ENDOR characterization of this intermediate and of a biomimetic synthetic complex; an extension of the BS-DFT computational technique developed in collaboration with Prof. Martin Mosquera to treat such organometallic complexes; then describes the elusive 5′-dAdo• and gives a surprising ENDOR/EPR demonstration of the intimate chaperoning of this reactive intermediate by the radical-SAM active site.

P6

Ultrafast spin dynamics and magnetic phase transitions

V.I. Belotelov

Faculty of Physics, Lomonosov Moscow State University, Moscow, Russia;
Russian Quantum Center, Skolkovo, Moscow, Russia;
Vernadsky Crimean Federal University, Simferopol, Russia

Ferrimagnets containing several partially compensated magnetic sublattices are considered the most promising materials for all-optical data storage and for ultrafast communications based on spin waves. There are two magnetic phases of the ferrimagnets: collinear and non-collinear ones. Up to now spin dynamics in ferrimagnets has been studied mostly in the collinear state without paying much attention to the kind of the magnetic phase. Here we investigate laser induced ultrafast spin dynamics in a rare-earth iron garnet film in the noncollinear phase as well.

We identify an importance of the magnetic phase of a ferrimagnet for its ultrafast spin behavior. A rare-earth iron garnet near magnetization compensation temperature was considered. We demonstrated several crucial peculiarities of spin dynamics in a non-collinear state that contrast sharply with the usually observed spin dynamics of the exchange and ferromagnetic modes in a collinear state far from the compensation point. In particular, when temperature approaches the compensation point the frequencies of quasi-antiferromagnetic (q-AFM) and quasi-ferromagnetic (q-FM) modes (Fig. 1) behave oppositely: the former decreases, while the latter one grows. The situation changes after crossing the compensation point for higher temperatures. We also discovered that the transition from the non-collinear phase to the collinear one is accompanied with softening of the q-FM mode which leads to a huge increase of the excitation efficiency and amplitude. The amplitude of the soft mode becomes more than 4 times larger than for the collinear state and up to 10 times higher than for the non-collinear phase. As the deflection angle of the soft mode was found to reach ~7°, it can be interesting for all-optical switching and nonlinear magnonics.

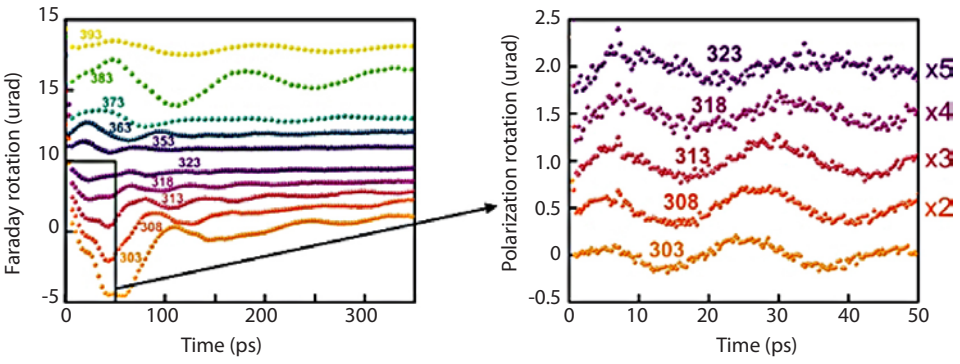

Fig. 1. Ultrafast magnetization dynamics represented by the probe Faraday transients for different temperatures from 303 K (below compensation) to 393 K (above compensation).

P6

The other crucial property of the non-collinear phase is bistability of the Neel vector. It is described by the double well potential energy. If the number of spins in a sample is small enough (~100) then probability of tunneling between two states becomes noticable and the film will behaves in a quantum regime. In this case macroscopic quantum tunneling takes place and one could consider a nanodisk of rare earth iron garnet with compnesation point as a kind of magneitc qubit. The latter might be promissing for future quantum technologies.

Support by the Russian Science Foundation, project N 23-62-10024 is acknowledged.

This work was financially supported by the Ministry of Science and Higher Education of the Russian Federation, Megagrant project N 075-15-2022-1108.

P7

Spin-fluctuation transitions revealed by electron paramagnetic resonance and small-angle neutron scattering

S.V. Demishev

Prokhorov General Physics Institute of RAS, Moscow, Russia

A spin-fluctuation transition (SFT) is a change in the characteristics of spin fluctuations in a magnet under the influence of control parameters (for example, temperature or material composition) that is not directly related to the formation of phases with long-range magnetic order [1, 2]. Therefore, SFT in most cases go beyond the standard theory of phase transitions, which is characterized by the consideration of fluctuations as some phenomenon accompanying the magnetic transition. The present work considers the SFT problem state of the art from the theoretical and experimental point of view, including as the examples helical magnets MnSi and $Mn_{1-x}Fe_xSi$, magnetic semiconductors $Hg_{1-x}Mn_xTe$, doped compensated semiconductors Ge:As(Ga), and strongly correlated metal with hidden order CeB_6.

The detection of SFTs has become possible due to the development of experimental methods, primarily electron paramagnetic resonance (EPR) and small-angle neutron scattering. The analysis of the EPR line width W is of special importance as long as just this parameter contains direct information about spin fluctuation magnitude. The improvement of experimental technique made it possible not to be limited by the classically recognized, "smooth" dependences of the correlation length and width of the EPR line. As a result, a "window of opportunity" has opened up for experimentalists to observe a sharp change in the parameters of spin fluctuations.

A systematic study of spin-fluctuation transitions is in the very beginning. Nevertheless, the available experimental data and theoretical results allow us to propose an outline of classification of spin fluctuation transitions:

SFT disorder–disorder. Transitions of this type reflect a change in the nature of magnetic fluctuations in the paramagnetic phase of $Hg_{1-x}Mn_xTe$ magnetic semiconductors and MnSi-based helical magnets. Such SFTs can be diagnosed by changes in EPR line width as well as in magnetization and magnetic susceptibility, in reasonable agreement with evolution of neutron scattering pattern. From a theoretical point of view, to describe the SFT for MnSi and $Mn_{1-x}FexSi$, it is necessary to take into account the coexistence of classical and quantum fluctuations.

The study of the disordered Ising model has shown the occurrence of SFT, which consists in a sharp change in the amplitude of spin fluctuations and the distribution function of the exchange energy with a change in the concentration of magnetic centers randomly located in space. It is interesting that this type of SFT arises for both ferromagnetic and antiferromagnetic exchange. Doped compensated semiconductors like Ge:As(Ga)may turn out to be promising objects for testing the predictions of the theory.

SFT disorder-hidden (quadrupole) order. This is a magnetic transition to the spin nematic phase, in which the anisotropy of spin fluctuations changes. In the paramagnetic phase, the average spin at the site is zero, and the spin fluctuations (mean square of the spin) are the same in all directions. Upon transition to a phase with a quadrupole

P7

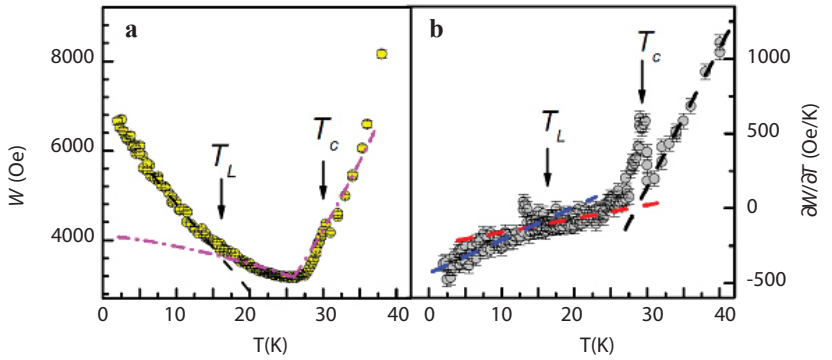

Fig. 1. Temperature dependences of the EPR line width W (**a**) and the derivative $\partial W/\partial T$ (**b**). Arrows indicate characteristic temperatures T_c and T_L (see text). On panel **a**: points – experiment; dash-dotted line – model calculation; dashed line is the guide to the eye. On panel **b**: dots are the derivative calculated from experimental data, dashed lines are the guides to the eye. From Ref. 3.

order, the average spin will still be equal to zero, and the average spin square will be different along different directions. The spin nematic effect was discovered in the antiferroquadrupole phase of CeB_6 by studying the angular dependences of the EPR and magnetoresistance.

The orientational SFT consists in changing the preferred direction of anisotropic spin fluctuations and was experimentally observed in the antiferroquadrupole phase of CeB_6 with varying temperature.

SFT order-order. An EPR study made it possible to detect a spin-fluctuation transition at $T_L \sim 15$ K in the magnetically ordered (spin-polarized) phase of MnSi [3], which is due to quantum fluctuations (Fig. 1). It is noteworthy that this SPT occurs at a temperature much lower than the temperature of the transition to the magnetically ordered phase ($T_c \sim 30$ K) and is outside the limits of the classical fluctuation region.

The studied objects, where SFTs are detected, look at first glance as essentially different. We suggest that the fundamental reason for the appearance of SFT may be understood in the framework of spin-polaron model. Generally, spin polaron may be considered as a quasi-bound state of an itinerant electron and localized magnetic moment. In this model, spin fluctuations naturally appear as a result of transition between continuum and bound states, and, therefore SFTs reflect changes in the spin-polaron states. This opportunity has not been studied yet in sufficient detail, and further research in this direction may turn out to be one of the points of growth in modern physics of magnetic phenomena.

1. Demishev S.V.: Applied Magnetic Resonance **51**, 473–522 (2020)
2. Demishev S.V.: Physics-Uspekhi, in press. DOI: 10.3367/UFNr.2023.05.039363
3. Demishev S.V. et al.: JETP Lett. **115**, 673–678 (2022)

P8

Long-range p–d exchange interaction in a ferromagnet-semiconductor hybrid structure

Yu.G. Kusrayev

Ioffe Institute, Russian Academy of Sciences, St. Petersburg, Russia

The proximity effect is widely used in modern condensed matter physics to search for new hybrid structures with new interface properties. The hybrid structure obtained by the contact of two materials not only combines the properties of the ancestors, but also acquires qualitatively new properties generated by the interactions of these systems.

There are various types of such structures composed of different materials and demonstrating proximity effect. For example, in semiconductor/ferromagnetic layer; interacting ferromagnetic layer and a semiconductor quantum well (QW) are separated by barrier. They allow one to control the spin dynamics of carriers in semiconductors, on the one hand, and the magnetization of a ferromagnet on the other. Voltage control of ferromagnetism on the nanometer scale is highly appealing for the development of novel electronic devices with low power consumption, high operation speed and compatibility with semiconductor technology.

For coupling the magnetic properties, an exchange interaction has to be implemented which typically depends on wave function overlap and is therefore short-ranged, so that it may negatively affect the state of the hybrid interface.. Here we study a hybrid structure consisting of a ferromagnetic Co layer and a semiconducting CdTe quantum well, separated by a thin (Cd, Mg)Te barrier [1, 2]. In contrast to the expected p–d exchange that decreases exponentially with the wave function overlap of quantum well holes and magnetic atoms, we find a long-ranged, robust coupling that does not vary with barrier width up to more than 30 nm. We suggest that the resulting spin polarization of acceptor-bound holes is induced by an effective p–d exchange that is mediated by elliptically polarized phonons.

Further, we demonstrate the electrical control of the exchange coupling in a hybrid consisting of a ferromagnetic Co layer and a semiconductor CdTe quantum well [3]. The electric field controls the phononic ac Stark effect – the indirect exchange mechanism that is mediated by elliptically polarized phonons emitted from the ferromagnet. The effective magnetic field of the exchange interaction reaches up to 2.5 Tesla and can be turned on and off by application of 1V bias across the heterostructure. The physical mechanism underlying the electrical control of the exchange coupling is related to a change in the tuning of the magnitude of the heavy and light hole level splitting from the energy of the magnon-phonon resonance.

The presence of the long-range exchange interaction along with the possibility of its electrical control offers prospects in the development of low-voltage spintronic devices compatible with existing semiconductor electronics.

This work was partially supported by the RFBR project No. 19-52-12066.

1. Korenev V.L. et al.: Nat. Phys. **12**, 85 (2016)
2. Kalitukha I.V. et al.: Nano Letters **21**, 6, 2370 (2021)
3. Korenev V.L. et al.: Nat. Commun. **10**, 2899 (2019)

MODERN DEVELOPMENT OF MAGNETIC RESONANCE

I1

The latest developments of EPR/ODMR instrument complex and its application to material research

R.A. Babunts

Ioffe Institute, Saint Petersburg, Russia

Combination of a line of high-frequency EPR spectrometers and an autonomous closed-cycle magneto-optical system with the capability to detect magnetic resonance through microwave and optical channels in pulse and cw modes, creates a powerful synergistic effect for the study of condensed materials. An inclusion in the instrumental EPR/ODMR instrumental complex of a low-frequency scanning ODMR spectrometer created by us on the basis of confocal and atomic force microscopes greatly expands the possibilities of conducting magnetic resonance studies. The high-frequency EPR/ODMR spectrometer has a number of unique features that distinguish it from industrial instruments. These features include an optical access through four windows, a cryogen-free system, a wide operating range of magnetic fields from –7 to +7 T, a crossing of zero magnetic field, temperature range of 1.7–300 K, unified bridge schemes for W- and D-bands. A highly stable solid-state oscillator with low phase noise, a sensitive superheterodyne IQ receiver, compact bridges non-sensitive to magnetic fields are used.

The non-destructive method for express diagnostics of local stresses/strains and local concentrations of substitutive nitrogen donors in diamond under environmental conditions is proposed. An optical quantum thermometer and a magnetometer with submicron resolution based on the anticrossing effect in silicon carbide are developed. Coherent manipulations of spin ensembles of triplet neutral divacancies in 6H-SiC crystals with more than tenfold increase in the content of the ^{13}C isotope in high magnetic fields are demonstrated. Hyperfine electron-nuclear interactions in spin centers in these crystals are optically detected without microwave.

Two-dimensional materials having a layered crystal structure with tight bonds in the plane, where the layers are coupled with each other by weak van der Waals forces, have been studied using high-frequency EPR spectroscopy. Anisotropic electron paramagnetic resonance spectra in a WS_2 single crystal under optical excitation have been detected. These spectra assumingly belong to localized carriers near the valence band and reflect features of the 5d shell of the crystal.

Detailed information on the location of magnetic Mn^{2+} ions implemented in semiconductor CdSe/(Cd,Mn)S nanoplatelets, spin dynamics, and interaction of surface Mn^{2+} ions with ^1H nuclei belonging to acid ligands that passivate the nanoplatelets surface has been obtained. High frequency EPR has made it possible to observe non-Kramers ions, such as Tb^{3+} in YAG, and Fe^{2+} in β-Ga_2O_3.

This work was supported by the Russian Science Foundation № 23-12-00152, https://rscf.ru/project/23-12-00152/

Electron spin relaxation times of lanthanide complexes with lanmodulin and the 3,4,3-LI(1,2-HOPO) chelator

G.R. Eaton[1], S.S. Eaton[1], W.B. Larrinaga[2], J.A. Cotruvo Jr.[2]

[1]Department of Chemistry and Biochemistry, University of Denver, Denver, CO, USA
[2]Department of Chemistry, The Pennsylvania State University, University Park, PA, USA

The EPR properties of 7 lanthanide(III) ions bound to the natural lanthanide-binding protein, lanmodulin (LanM), and the synthetic small-molecule chelator, 3,4,3-LI(1,2-HOPO) ("HOPO") were studied. Echo-detected pulsed EPR spectra reveal intense signals from ions for which the normal continuous-wave first-derivative spectra are negligibly different from zero. Spectra of Kramers lanthanide ions Ce^{3+}, Nd^{3+}, Sm^{3+}, Er^{3+}, and Yb^{3+}, and non-Kramers Tb^{3+} and Tm^{3+}, bound to LanM are more similar to the ions in dilute aqueous:ethanol solution than to those coordinated with HOPO. Spin echo dephasing rates ($1/T_m$) are faster for lanthanides than for most transition metals. The trend in $1/T_m$ at 4–6 K is $Sm^{3+} < Ce^{3+} < Nd^{3+} < Tm^{3+} < Yb^{3+} < Tb^{3+} < Er^{3+}$ with some pairwise swaps depending on ligation, which is approximately the order of increasing values of quantum number J. For Sm^{3+}, Er^{3+}, Tm^{3+} and Yb^{3+}, $1/T_1$ decreases in the order 1:1 water:ethanol > LanM > HOPO, which is the same as the order for $1/T_m$. For Nd^{3+} and Tb^{3+}, $1/T_1$ decreases in the order LanM > water:ethanol ~ HOPO, and for Ce^{3+} the order is 1:1 water:ethanol ~ HOPO > LanM. The EPR spectra and relaxation times are sensitive to the coordination environment and are emerging tools for characterization of both small-molecule and biomolecule interactions with lanthanides.

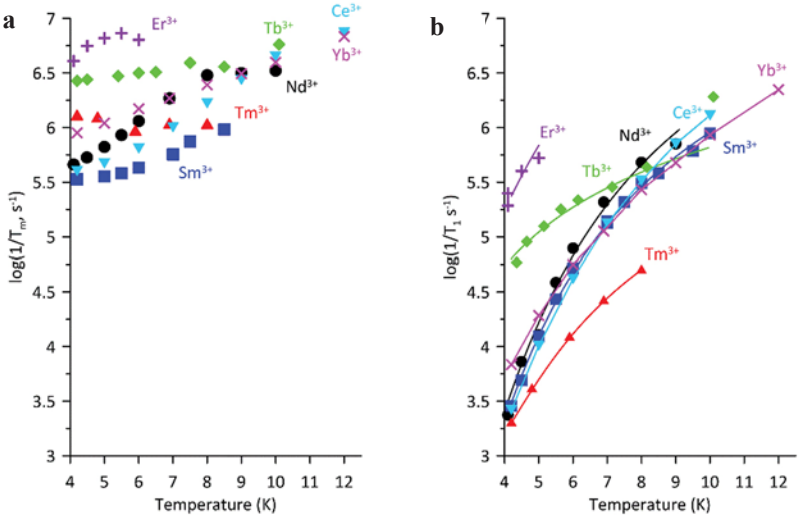

Fig. 1. a Temperature dependence of $1/T_m$ for complexes of LanM complexes with (▼) Ce^{3+}, (•) Nd^{3+}, (■) Sm^{3+}, (◆) Tb^{3+}, (+) Er^{3+}, (▲) Tm^{3+}, (×) Yb^{3+}. **b** Temperature dependence of $1/T_1$ for (▼) Ce^{3+}, (•) Nd^{3+}, (■) Sm^{3+}, (◆) Tb^{3+}, (+) Er^{3+}, (▲) Tm^{3+}, (×) Yb^{3+}. The solid lines are fits to the experimental data for $1/T_1$.

I3

Microstructure of mixtures of ionic liquids $[bmim]^+A^-$ with water

V.I. Chizhik, V.V. Matveev, M. Ubovich

Saint-Petersburg State University, Saint Petersburg, Russia,
e-mail: v.chizhik@spbu.ru

Room temperature ionic liquids (ILs) are ionic compounds consisting of asymmetric organic cations or anions and counterions of almost any type. In contrast to typical salts these substances remain in liquid phase at the room temperature or at temperatures close to it. Unique physical and chemical properties of ionic liquids (neat and in solutions) such as high thermal stability, low vapor pressure, high boiling point, and the ability to dissolve a wide range of chemical species, determine numerous applications in "green" chemistry and material science. More recently, systems based on IL are considered as promising for use in electrochemical devices of a new generation. For the development of applications in the latter aspect, it is important to know the features of the microstructure and molecular dynamics of mixtures of IL with different solvents. This work presents the results of a study of the microstructure of mixtures of ionic liquids $[bmim]^+A^-$ with water. The presence of water may have a negative effect on the properties of electrochemical devices, in particular, it may narrow the electrochemical window.

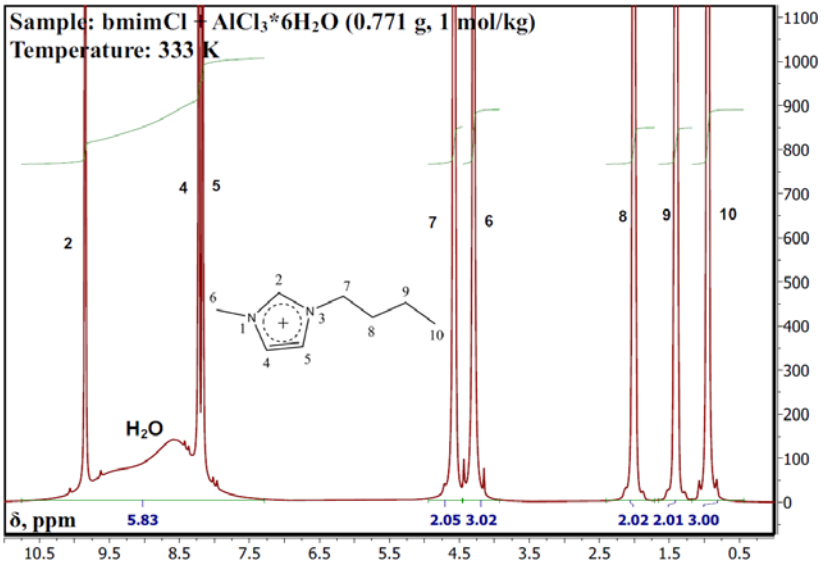

Fig. 1. The example of the ^{1}H spectrum for the system [bmim]Cl–$AlCl_3$–H_2O at 333 K. The line numbering is in accordance with the numbers of molecular groups in the cation scheme (insertion). The integral line intensities are indicated under the spectrum.

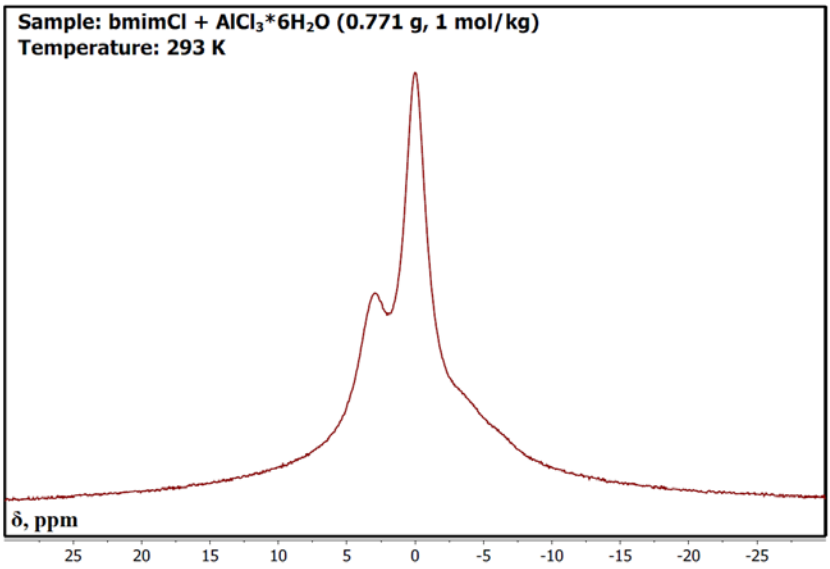

Fig. 2. The example of the ^{27}Al spectrum for the system [bmim]Cl–$AlCl_3$–H_2O at 293 K.

Previously, we developed a model of "IL $[bmim]^+A^-$–water" mixtures [1] (in a contrast to the "water pocket" model of Japanese colleagues), as well as established the fact of the impossibility of dehydration of IL systems containing Al^{3+} ions [2].

Liquid electrolytes based on solutions of aluminum salts in ILs are considered as promising systems for metal-ion batteries of the next generations. The sample was prepared using crystalline hydrate $AlCl_3 \cdot 6H_2O$ and ionic liquid [bmim]Cl. Both neat IL and the solution were undergone the standard drying procedure under low pressure (≈10^{-6} mbar) and 80 °C but as expected [2] it could not remove the water completely. Therefore, after preparing the sample by gravimetric method the water concentration was verified using integral intensities of the ^1H spectral lines of $[bmim]^+$ and water. As a result, we have determined the following molar ratios for the $AlCl_3$–[bmim]Cl–H_2O mixture: 1 Al^{3+}:5.7 $[bmim]^+$:7.5 H_2O. NMR measurements were carried out using Bruker Avance III 500 MHz Spectrometer at 500 MHz for ^1H nucleus and 130 MHz for ^{27}Al one. The examples of spectra are provided in Fig. 1 and 2. We used the temperature range between 293 and 363 K.

For the first time, the splitting of the spectral lines *in such systems* due to the occurrence of complex associates has been recorded. Based on the obtained spectra of ^1H and ^{27}Al nuclei, it was concluded that, in the studied electrolyte system, water molecules are located in the vicinity of aluminum cations at least in two nonequivalent structures. Our data show the existence of exchange between these substructures, and the exchange rate can be estimated from the obtained proton spectra. It has also been established that with temperature variation the relative concentration of these substructures changes (on the background of the exchange process). Some features of

the spectra of quadrupole nuclei ^{27}Al, in particular, of the spectral line width, allow us to conclude that the symmetry of the environment of aluminum cations has changed with temperature. It is worth noting that the ^{27}Al lines in the sample investigated are at least three times broader than the lines in $Al(NO_3)_3$ solutions in EAN or water (see [2]), and this fact might be an indication of the partial penetration of the Cl^- ion into the first solvation shell of the Al^{3+} cation.

All NMR measurements were carried out in the Center for Magnetic Resonance of Research Park of Saint Petersburg State University.

This work was supported by the Russian Science Foundation (project № 23-23-00049).

1. Bystrov S.S., Matveev V.V., Egorov A.V., Chernyshev Yu.S., Konovalov V.A., Balevičius V., Chizhik V.I.: J. Phys. Chem. B **123(43)**, 9187–9197 (2019)
2. Matveev V.V., Ievleva A.V., Vovk M.A., Cabeza O., Salgado-Carballo J., Parajó J.J., Rodríguez J.R., de la Fuente R., Lähderanta E., Varela L.M.: J. Molec. Liquids **278**, 239–246 (2019)

I4

Embedding and employing electron spins in porous functional materials

M.V. Fedin, A.S. Poryvaev, D.M. Polyukhov, O.D. Bakulina, M.Yu. Ivanov

International Tomography Center SB RAS, Novosibirsk, Russia

Nano- and mesoporous materials attract great interest in modern chemistry and materials science and are used, in particular, in catalytic applications, sorption, separation of mixtures, gas storage, etc. The embedding of electron spins into porous materials can lead to the onset of new functional properties and, at the same time, provide opportunities for studying these materials by magnetic resonance techniques. In particular, the encapsulation of nitroxide spin probes into metal-organic frameworks (MOFs) allows application of electron paramagnetic resonance (EPR) to study the sorption and separation of hydrocarbon mixtures [1, 2], as well as to study the amorphization of MOFs under external pressure and to develop ways to minimize these effects [3]. The introduction of triazinyl radicals into mesoporous organosilica materials opens up new possibilities for quantum computing [4]. In addition, these materials are effective NO_x sorbents from the air and can be used in a number of environmental applications [5]. Finally, targeted optimization of the MOF structure with the introduction of paramagnetic metals opens up the possibility of creating efficient catalysts of ortho-para conversion of hydrogen for its liquefaction and storage, which is important for future hydrogen energy [6].

Another type of intriguing media refers to ionic liquid glasses, which possess inherent heterogeneities [7]. These media can themselves be considered as partially nanoporous, and they can also be coupled with MOFs to create functional composites [8]. In recent studies we demonstrate new capabilities of paramagnetic probes in studies of nanostructuring in such unusual media [9–10].

Financial support of the Russian Science Foundation (19-13-00071-П) is greatly acknowledged.

1. Polyukhov D.M., Poryvaev A.S., Gromilov S.A., Fedin M.V.: Nano Lett. **19**, 6506–6510 (2019)
2. Polyukhov D.M., Poryvaev A.S., Sukhikh A.S., Gromilov S.A., Fedin M.V.: ACS Appl. Mater. Interf. **13**, 40830–40836 (2021)
3. Poryvaev A.S., Polyukhov D.M., Fedin M.V..: ACS Appl. Mater. Interf. **12**, 16655–16661 (2020)
4. Poryvaev A.S., Gjuzi E., Polyukhov D.M., Hoffmann F., Fröba M., Fedin M.V.: Angew. Chem. Int. Ed. **60**, 8683–8688 (2021)
5. Poryvaev A.S., Gjuzi E., Yazikova A.A., Polyukhov D.M., Albrekht Y.N., Efremov A.A., Kudriavykh N.A., Yanshole V.V., Hoffmann F., Fröba M., Fedin M.V.: ACS Appl. Mater. Interf. **15**, 5191–5197 (2023)
6. Polyukhov D.M., Kudriavykh N.A., Gromilov S.A., Kiryutin A.S., Poryvaev A.S., Fedin M.V.: ACS Energy Lett. **7**, 4336–4341 (2022)
7. Ivanov M.Yu., Surovtsev N.V., Fedin M.V.: Russ. Chem. Rev. **91**, RCR5031 (2022)
8. Ivanov M.Yu., Poryvaev A.S., Polyukhov D.M., Prikhod'ko S.A., Adonin N.Yu., Fedin M.V.: Nanoscale **12**, 23480–23487 (2020)
9. Ivanov M.Yu., Bakulina O.D., Polienko Y.F., Kirilyuk I.A., Prikhod'ko S.A., Adonin N.Yu., Fedin M.V.: J. Mol. Liquids **381**, 121830 (2023)
10. Bakulina O.D., Ivanov M.Yu., Prikhod'ko S.A., Adonin N.Yu., Fedin M.V.: Nanomaterials (2023)

I5

Double electron-electron resonance for c-centers in diamond: optimization, coherent control and concentration measurements

O.R. Rubinas[1,2,3], V.V. Soshenko[2,3], I.S. Cojocaru[1,2,3], S.V. Bolshedvorskii[2,3], P.G. Vilyuzhanina[4], E.A. Primak[5], A.M. Kozodaev[4], S.M. Drofa[5], V.G. Vins[6], V.N. Sorokin[2,3], A.N. Smolyaninov[3], A.V. Akimov[1,2,3]

[1]Russian Quantum Center, Moscow, Russia
[2]P.N. Lebedev Institute RAS, Moscow, Russia
[3]LLC Sensor Spin Technologies, Moscow, Russia
[4]National Research Nuclear University "MEPhI", Russia
[5]Moscow Institute of Physics and Technology, Dolgoprudny, Moscow Region, Russia
[6]LLC Velman, Novosibirsk, Russia

NV-centers in diamond recommend themselves as good sensors of environmental fields as well as detectors of diamond impurities. The sensitivity of a sensor depends on coherence properties of NV centers, their concentration and so on. Thus, optimization of sensitivity of a sensor is hard experimental task. Both wat of sensor operation and diamond plates use for sensing are subject of such an optimization. In the latter case a lot of attention lately were dedicated to post grown procedures of diamond.

One of the key factors affecting sensitivity of NV center-based sensors are C-centers, often also called p_1-centers. These centers are on one side source of electrons for NV centers on another one of the main sources of decoherence. The relative concentration of C-centers and NV center more specifically negatively charged NV centers is often the focus of diamond plates optimization. The C-center themselves may be detected using in-diamond NV center magnetometer via so called double electron-electron resonance, thus providing insight into local distribution of impurities.

The double electron-electron resonance can also be used to measure the C-center concentration. Here, we measured the concentration of C-centers in several diamond plates and compared results with often used infrared spectroscopy method. We also investigated an influence of the free precession time of the NV-center on the observed contrast of double electron-electron resonance spectrum. The dependence of the resonance amplitudes and widths on the concentration of C-centers as well as the length of the combined C-center driving and NV-center π-pulse is discussed. The optimal contrast-free precession time was determined for each C-center concentration, showing a strong correlation with both the concentration of C-centers and the NV-center T_2 time.

Besides, series of experiments on optimization of NV-centers to C-centers concentration ratio, or yield of NV centers, in electron beam irradiation post processing with consequent annealing was performed along with study of associated coherence properties change. The optimization was performed for cases of medium and high concentration of nitrogen in a diamond, for which optimal procedures were established. As high as 37(4)% conversion efficiency of C-centers into negatively charged NV centers was demonstrated.

Recombination of X-ray-generated radical ion pairs assembles optically inaccessible exciplexes from perfluoro-para-oligophenylenes with N,N-dimethylaniline showing red-shifted magnetosensitive emission

D.V. Stass[1,2], E.M. Glebov[1,3], R.G. Fedunov[1], L.V. Kuibida[1], P.V. Nikul'shin[4], A.M. Maksimov[5]

[1]V.V. Voevodsky Institute of Chemical Kinetics and Combustion, Novosibirsk, Russia
[2]International Tomography Center, Novosibirsk, Russia
[3]Novosibirsk State University, Novosibirsk, Russia
[4]A.V. Topchiev Institute of Petrochemical Synthesis, Moscow, Russia
[5]N.N. Vorozhtsov Novosibirsk Institute of Organic Chemistry, Novosibirsk, Russia

A series of perfluorinated para-oligophenylenes C_6F_5-$(C_6F_4)_n$-C_6F_5 (n = 1–3) produce exciplexes with N,N-dimethylaniline (DMA) in degassed X-irradiated n-dodecane solutions. While their short fluorescence lifetimes (ca. 1.2 ns) and UV-Vis absorption spectra overlapping with the spectrum of DMA with molar absorption coefficients of $2.7–4.6 \cdot 10^4$ $M^{-1} \cdot cm^{-1}$ preclude standard photochemical exciplex formation pathway, under X-rays the efficient assembly of such exciplexes proceeds via recombination of radical ion pairs, which delivers the two partners close to each other and ensures sufficient energy deposition. The recombination nature of the exciplexes results in magnetic field sensitivity of the exciplex emission band inherited from magnetic field sensitivity of recombination of spin-correlated radical ion pairs. Exciplex formation in such systems is supported by DFT calculations. These first exciplexes from a series of fully fluorinated compounds show the largest known red shift of the exciplex emission from the local emission band, suggesting the potential of perfluorocompounds for optimizing optical emitters, while the similarity of X-ray generated reaction cascade to electroluminescence scenario in OLEDs may lead to development of a new class of all-organic magnetosensitive functional devices.

1. Nikul'shin P.V., Fedunov R.G., Kuibida L.V., Maksimov A.M., Glebov E.M. Stass D.V.: Int. J. Mol. Sci. **24**, 7568 (2023)

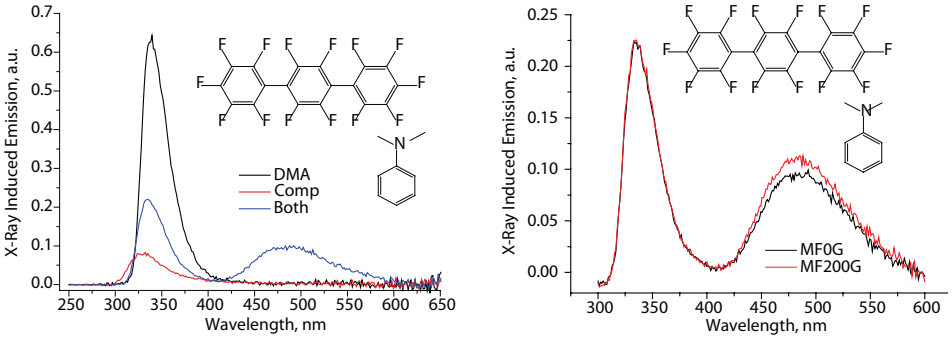

Fig. 1. A new exciplex emission band appearing in the spectra of radiation-induced luminescence for a mixture of perfluoro-PTP and DMA in n-dodecane (left) and its sensitivity to magnetic field (right)

Study of the photophysical mechanisms of thermally activated delayed fluorescence (TADF) emitters with time-resolved optical and magnetic resonance spectroscopic methods

J. Zhao

State Key Laboratory of Fine Chemicals, Frontier Science Center for Smart Materials, School of Chemical Engineering, Dalian University of Technology, Dalian, P. R. China, e-mail: zhaojzh@dlut.edu.cn

Thermally activated delayed fluorescence (TADF) emitters based on molecular structures of electron donor-acceptor in in particular of interest, because of the features of precious metal atom-free and the efficient harvesting of the singlet and triplet excitons in OLED. Moreover, the photophysical processes involved in these compounds upon photoexcitation is also interesting. However, it is still a challenge to unveil the photophysical processes of these compounds, because a few states exists and they share similar energy, such as the localized states (singlet and triplet LE state, ^{1}LE and ^{3}LE) and the charge separated states (^{1}CS and ^{3}CS). Previously, the transient species of these compounds formed upon photoexcitation were usually studied with transient luminescence spectral methods. However, in this case only the emissive states are detected, the dark states (non-emissive states), for instants the ^{3}CS and the ^{3}LE states, cannot be directly detected.

Recently, we [1, 2] and other groups [3, 4] used femtosecond and nanosecond transient absorption (fs-TA and ns-TA) spectroscopic methods to study the photophysical processes of the TADF emitters, especially to detect the darks states and the interconversion between these states. Time-resolved electron paramagnetic resonance (TREPR) spectral method was used to study the electron spin selectivity of the intersystem crossing (ISC) of the compounds. New in-depth understanding was achieved, and experimental evidence for the spin-vibronic coupling enhanced reverse ISC (rISC) was observed.

1. Zhao X., Sukhanov A.A., Jiang X., Zhao J., Voronkova V.K.: J. Phys. Chem. Lett. **13**, 2533−2539 (2022)
2. Zhang X., Liu X., Taddei M., Bussotti L., Kurganskii I., Li M., Jiang X., Zhao J., Di Donato M., Wan Y., Fedin M.V.: Chem. Eur. J., **28**, e202200510 (2022)
3. Drummond B.H., Aizawa N., Zhang Y., Myers W.K., Xiong Y., Cooper M.W., Barlow S., Q. Gu, Weiss L.R., Gillett A.J., Credgington D., Pu Y.-J., Marder S.R., Evans E.W.: Nature Commun. **12**, 4532 (2021)
4. Hosokai T., Matsuzaki H., Nakanotani H., Tokumaru K., Tsutsui T., Furube A., Nasu K., Nomura H., Yahiro M., Adachi C.: Sci. Adv. **3**, e1603282 (2017)

On electron spin decoherence caused by the nuclear spin bath

G. Jeschke

ETH Zurich, Department of Chemistry and Applied Biosciences, Zurich, Switzerland

At sufficiently low concentration and sufficiently low temperature, phase memory loss (decoherence) of electron spins is usually dominated by interaction with the nuclear spin bath. In most applications of pulsed EPR, protons almost exclusively contribute to this decay. We have recently obtained a data set on nitroxide model compounds that separates contribution from methyl groups on the nitroxide from those of protons of a water-glycerol matrix (spin bath) and quantifies the effect of dynamical decoupling on both contributions [1].

The contribution by the spin bath to Hahn spin echo decay can be quantitatively predicted from a molecular-dynamics model of the water-glycerol matrix based on an analytical expression for nuclear-pair electron spin echo envelope modulation and a pair-product approximation (Fig. 1) [2]. The same approach provides a spin-noise spectrum that also quantitatively predicts the decay at very low computational cost. However, predictions become worse for Carr-Purcell dynamical decoupling sequences, in particular, if the number of p refocusing pulses is even. Under microwave irradiation, electron spin magnetization decays more slowly and it does so with different decay times in the spin-lock direction ($T_{1\rho}$) and perpendicular to this direction ($T_{2\rho}$) [3]. We rationalize this behavior by hyperfine decoupling.

1. Soetbeer J., Millen M., Zouboulis K., Hülsmann M., Godt A., Polyhach Y., Jeschke G.: Phys. Chem. Chem. Phys. **23**, 5332–5369 (2021)
2. Jeschke G.: J. Magn. Reson. Open **14-15**, 100094 (2023)
3. Wili N., Hintz H., Vanas A., Godt A., Jeschke G.: Magn. Reson. (Gött.) **1**, 75–87 (2020)

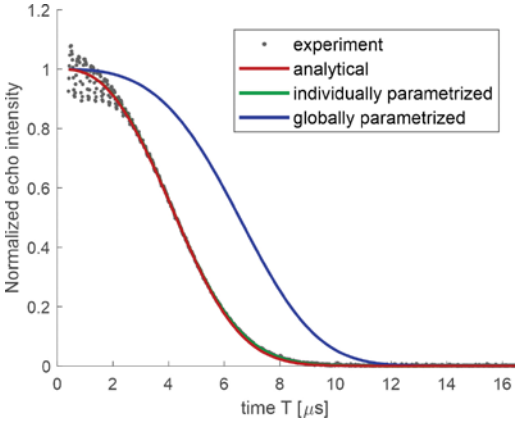

Fig. 1. Analytical theory predicts Hahn echo decay of a nitroxide in water-glycerol glass almost perfectly from a molecular-dynamics simulated nuclear spin bath model. The same applies to a noise spectrum parametrized for only Hahn echo decay. A noise spectrum globally parametrized to a series of Carr-Purcell dynamical decoupling experiments fails to predict the experimental decay.

Structure, dynamics and transformations in coordination sphere of iridium (IV) complexes

A.I. Kokorin[1,2,3], N.A. Chumakova[1,4], T.A. Tereshina[5], O.V. Rudnitskaya[5], V.N. Khrustalev[5]

[1]N.N.Semenov FRC for Chemical Physics RAS, Moscow, Russia
[2]Plekhanov Russian University of Economics, Moscow, Russia
[3]Infochemistry Scientific Center of ITMO University, St. Petersburg Russia
[4]Chemistry Department, M.V. Lomonosov MSU, Moscow, Russia
[5]Peoples' Friendship University of Russia (RUDN), Moscow, Russia
[6]Zelinsky Institute of Organic Chemistry RAS, Moscow, Russia

Transition metal complexes bearing dimethyl sulfoxide ($O=S(CH_3)_2$, DMSO) as a ligand, including platinum metals, are well known. A number of Ir(I) and Ir(III)-derived chloride−DMSO complexes were elucidated and described structurally [1–3] but the first Ir(IV) chloride−DMSO complexes were recently reported in [4, 5]. As an example, the X-ray structure of $[H(dmso)][trans\text{-}IrCl_4(dmso)_2]$ complex is shown in Fig. 1.

Iridium complexes were characterized using chemical analysis, UV-Vis, FTIR, NMR, and CW X-band EPR spectroscopy, and X-ray diffraction techniques applied both to single-crystal and polycrystalline powder. The reaction of $H_2IrCl_6 \cdot 6H_2O$ with DMSO results in a slow reduction of Ir(IV) to Ir(III) at elevated temperatures avoiding the formation of Ir(IV)-$O=S(CH_3)_2$ complexes, which were isolated and solved their crystal structure. The DMSO ligand is coordinated to the Ir site via the oxygen atom. Typical changes in EPR spectra are shown in Fig. 2. It was also revealed that $\{IrCl_5[(CH_3)_2CO]\}^-$ species are formed in acetone solutions of $H_2IrCl_6 \cdot 6H_2O$ upon storage. This reaction dominated by $\{IrCl_5[(CH_3)_2CO]\}^-$ affords a novel Ir(IV) chloride-DMSO salt.

The reduction kinetics (Fig. 2) is linearized in co-ordinates of the first order reaction and is accompanied by the incorporation of DMSO molecules into the coordination

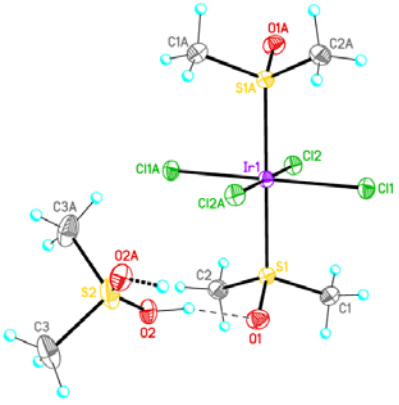

Fig. 1. X-ray structure of [H(dmso)] [trans-$IrCl_4(dmso)_2$].

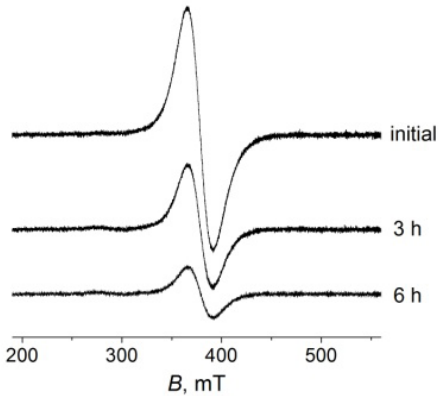

Fig. 2. EPR spectra at 90 K of $H_2IrCl_6 \cdot 6H_2O$ complex in DMSO after 0, 3 and 6 h at 150 °C.

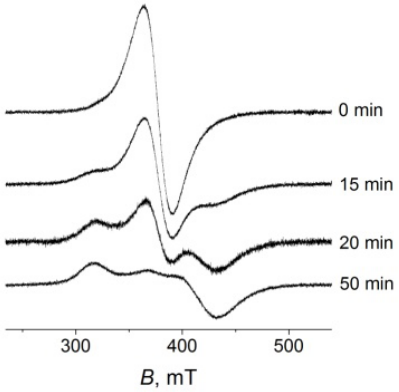

Fig. 3. EPR spectra at 90 K of $H_2IrCl_6 \cdot 6H_2O$ complex in acetone after aging at 40 °C.

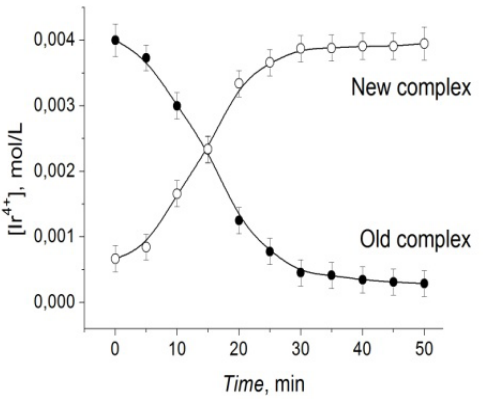

Fig. 4. Experimental kinetics of H_2IrCl_6 decay (●) and $[IrCl_5(Me_2CO)]^-$ (○) generation at 40 °C.

sphere of iridium. In the case of acetone solutions, heating at mild temperatures (40 °C) of $H_2[IrCl_6]$ complex results in introduction of $O{=}C(CH_3)_2$ molecules as a ligand to the co-ordination sphere preserving the Ir(IV) valence.

Figure 3 demonstrates spectral changes occurring at 40 °C. The initial signal has $g_0 = 1.780 \pm 0.003$ and the peak-to-peak linewidth $\Delta B = 26 \pm 0.5$ mT. The new spectra characterize novel species with the axial symmetry and EPR parameters $g_{\|} = 2.115 \pm 0.005$ and $g_{\perp} = 1.62 \pm 0.01$, i.e. we observe a $[IrCl_6]^{2-} \rightarrow [IrCl_5(Me_2CO)]^-$ conversion. We would note that the integral intensity, i.e. the number of Ir(IV) paramagnetic centers, does not change during the total time of the experiment. Experimental kinetics of H_2IrCl_6 decay and $[IrCl_5(Me_2CO)]^-$ generation at 40 °C are shown in Fig. 4. A fact that the measured value of the axial signal starts not from a zero point, most likely, reflects a situation that during several minutes between the sample preparation, its freezing and recording EPR spectrum, some chemical changes occurs. The reduction process ($Ir^{IV} \rightarrow Ir^{III}$) starts noticeably later at ambient conditions or at higher temperatures.

This work was funded within the framework of the Program of Fundamental Research of the Russian Federation (Reg. № 122040500068-0).

1. Dorta R., Rozenberg H., Shimon L.J.W., Milstein D.: J. Am. Chem. Soc. **124**, 188−189 (2002)
2. Lagos Y., Palou-Mir J., Bauza A., Fiol J.J., Garcia-Raso Á.G., Terron À. et al.: Polyhedron **102**, 735−740 (2015)
3. Ridgway B.M., Foi A., Corrêa R.S., Bikiel D.E., Ellena J., Doctorovich F., Di Salvo F.: Acta Crystallogr. Sect. B: Struct. Sci. **73**, 1032−1042 (2017)
4. Rudnitskaya O.V., Tereshina T.A., Dobrokhotova E.V. et al.: Eur. J. Inorg. Chem. no. 33, e202200463 (2022)
5. Rudnitskaya O.V., Tereshina T.A., Dobrokhotova E.V. et al.: ACS Omega **8**, 20569−20578 (2023)

I10

Hydration, ionic and water molecular mobility in solid electrolytes studied by NMR

V. Volkov[1,2], A. Chernyak[1,2], N. Slesarenko[1], I. Avilova[1]

[1]Federal Research Center of Problems of Chemical Physics and Medicinal Chemistry RAS, Chernogolovka, Russia
[2]Osipyan Institute of Solid State Physics RAS, Chernogolovka, Russia,
e-mail: vitwolf@mail.ru

Solid electrolytes like ion-exchange membranes [1–8], polymer electrolytes for lithium batteries [9, 10], cesium acid sulfates and phosphates [5, 11] attract keen attention of scientists in view of the development of modern environmentally clean and energy efficient technologies. The design of novel materials requires fundamental scientific knowledge of the mechanisms of ion and molecular transport at the different spatial scales and ion solvation (hydration) particularities.

Highly attractive method that allow the mentioned information to be acquired is NMR. The following possibilities of magnetic resonance techniques are:

NMR spectroscopy. The most popular method is ^{1}H NMR, which was used to study hydration processes in ion exchange membranes. Information on hydration of ionic channels in membranes is fundamental importance for understanding the mechanism of migration of cations and water molecules. NMR of studies of ^{7}Li, ^{23}Na, ^{31}P, ^{133}Cs and ^{19}F cations and anions in membranes and in gel and solid electrolytes for lithium cells reported [1–10]. The analysis of concentration dependences of chemical shifts and the shapes of NMR lines for these nuclei provided information on the mechanisms of interaction of alkali metal ions with ionogenic groups and on the cation mobility.

NMR relaxation provides unique information on the local mobility of ions and molecules [6–8]. Unfortunately, the quantitative treatment of experimental data was difficult due to the wide distribution of the correlation times of the ionic and molecular motion and the presence of paramagnetic impurities in these systems.

The pulsed field gradient NMR method (PFG NMR) makes it possible to directly measure the ionic and molecular partial self-diffusion coefficients.

In our presentation, the application of these NMR techniques for cation-exchange membranes and model systems is mainly discussed. Nafion membranes are the more used and investigated among of ion exchangers. Membranes MSC based on polyethylene and grafted sulfonated polystyrene show a high selectivity for alkaline metal cation separation. Polystyrene acid and its lithium, sodium, cesium salts films also have been investigated as model systems. Correlation times of local mobilities of Li^{+}, Na^{+}, Cs^{+} cations and water molecules was estimated by ^{1}H, ^{7}Li, ^{23}Na, ^{133}Cs spin relaxation technique. The calculated cation and water molecule self-diffusion coefficients were compared with experimental values measured by PFG NMR. It was shown, that macroscopic mass transfer is controlled by molecule and ion motion near sulfonate groups. Lithium and sodium cations which hydrated energy is higher than water hydrogen bond energy are moving together with water molecules. Cesium cation in possession of low hydrated energy is jumping between neighboring sulfonate groups directly. Cation Li^{+}, Na^{+}, Cs^{+} hydration numbers (h) in membranes were calculated from ^{1}H chemical shift

water molecule temperature dependences. The *h* values are 5.0±1.0, 6.0±1.0, 1.0±0.2 and 4.1±1.0, 5.0±1.0, 3.1±1.0 for Li^+, Na^+ Cs^+ ionic forms of Nafion and MSC membranes correspondingly. At high water content in MSC membrane cation self-diffusion coefficients increased in the row $Li^+ < Na^+ < Cs^+$. Cation self-diffusion coefficients sequence was $Li^+ \geq Na^+ > Cs^+$ in Nafion membranes. Calculated from Nernst-Einstein equation and experimental conductivity values are close to each other in Nafion membranes. In MSC membranes calculated conductivities are one order of magnitude more comparing the experimental ones which is explained by heterogeneity of membrane pore and channel system. Water molecules as well as lithium cations self-diffusion and local mobility in poly(4-styrenesulfonic acid), and its lithium, sodium and cesium salts were investigated by pulsed field gradient NMR and NMR relaxation techniques.

Comparison of self-diffusion coefficients measured by PFG NMR with self-diffusion coefficients calculated from correlation times has shown that macroscopic water molecules and lithium cations transfer is also control local particle jumping between neighboring sulfonated groups. Therefore ionogenic transport channels forming in polystyrenesulfonic films are regular structure. It was concluded that polystyrenesulfonic polymer films are appropriate model of homogeneous sulfonic cation-exchangers.

Therefore the detailed NMR investigations gave opportunity to understand the microscopic mechanism of membrane selectivity to the alkaline metal cations.

NMR techniques such as high-resolution NMR, solid-state NMR, magic angle spinning (MAS) NMR, NMR relaxation, and PFG NMR applications for polymer electrolytes for lithium batteries are discussed [9, 10].

NMR measurements were performed using equipment of the Multi-User Analytical Center of the Federal Research Center of Problems of Chemical Physics and Medicinal Chemistry RAS and Scientific Center in Chernogolovka of the Institute of Solid State Physics named Yu. A. Osipyan RAS Assignment of the Federal Research Center of Problems of Chemical Physics and Medicinal Chemistry RAS (state registration No AAAA-A19-119071190044-3).

1. Volkov V.I., Chernyak A.V., Golubenko D.V., Shevlyakova N.V., Tverskoy V.A., Yaroslavtsev A.B.: Membr. Membr. Technol. **2**, 54–62 (2020)
2. Volkov V.I., Chernyak A.V., Golubenko D.V., Tverskoy V.A., Lochin G.A., Odjigaeva E.S., Yaroslavtsev A.B.: Membranes **10**, 272 (2020)
3. Volkov V.I., Chernyak A.V., Avilova I.A., Slesarenko N.A., Melnikova D.L., Skirda V.D.: Membranes **11**, 385 (2021)
4. Volkov V.I., Chernyak A.V., Gnezdilov O.I., Skirda V.D.: Solid State Ionics **364**, 115627 (2021)
5. Volkov V.I., Chernyak A.V., Slesarenko N.A., Avilova I.A.: Int. J. Mol. Sci. **23**, 5011 (2022)
6. Slesarenko N.A., Chernyak A.V., Avilova I.A., Zabrodin V.A., Volkov V.I.: Mendeleev Commun. **32**, 534–536 (2022)
7. Volkov V.I., Slesarenko N.A., Chernyak A.V., Zabrodin V.A., Golubenko D.V., Tverskoy V.A., Yaroslavtsev A.B.: Membr. Membr. Technol. **4**, 189–194 (2022)
8. Slesarenko N.A., Chernyak A.V., Avilova I.A., Tarasov V.P., Volkov V.I.: Mendeleev Commun. **33**, 215–217 (2023)
9. Chernyak A.V., Slesarenko N.A., Slesarenko A.A., Baymuratova G.R., Tulibaeva G.Z., Yudina A.V., Volkov V.I., Shestakov A.F., Yarmolenko O.V.: Membranes **12**, 11112022 (2022)
10. Volkov V.I., Yarmolenko O.V., Chernyak A.V., Slesarenko N.A., Avilova I.A., Baymuratova G.R., Yudina A.V.: Membranes **12**, 416 (2022)
11. Chernyak A.V., Volkov V.I.: Appl. Magn. Reson. **45**, 287–299 (2014)

I11

Low-frequency EPR imaging of reactive oxygen species in excised mouse lungs

S.S. Eaton[1], G.R. Eaton[1], L.B. Woodcock[1], T.A. Hovey[1], G.A. Rinard[1], A. Canny[1], H.B. Elajaili[2], N.M. Dee[2], E.S. Nozik[2], J.P.Y. Kao[3]

[1]Department of Chemistry and Biochemistry, University of Denver, Denver, CO USA
[2]Cardiovascular Pulmonary Research Laboratories and Pediatric Critical Care Medicine, University of Colorado Anschutz Medical Campus, Aurora CO USA
[3]Center for Biomedical Engineering and Technology and Department of Physiology, University of Maryland School of Medicine, Baltimore, MD USA

A rapid scan EPR spectrometer operating at a microwave frequency of about 1 GHz achieves a spin sensitivity of ~$2 \cdot 10^{14}$ spins for an aqueous nitroxide sample in a 9 mm diameter resonator. The magnet and rapid scan driver and coils are similar to those reported by Buchanan et al. [1], but the signal detection path was simplified to minimize loss and increase detection sensitivity. One application measured nitroxide radicals in excised injured mouse lungs. Free radicals generated in a lipopolysaccharide (LPS)-induced mouse model of acute respiratory distress syndrome (ARDS) reacted with two cyclic hydroxylamines (1-hydroxy-3-carboxy-2,2,5,5-tetramethyl pyrrolidine hydrochloride and 4-acetoxymethoxycarbonyl-1-hydroxy-2,2,5,5-tetramethylpyrrolidine-3-carboxylic acid), which were converted into nitroxide radicals CP$^{\bullet}$ and DCP$^{\bullet}$, respectively. The small number of radicals trapped results in low signal-to-noise in the spectra and images. However, since the spectral properties of the nitroxides are known, we can use the prior knowledge of the line shape and hyperfine splitting to fit the noisy data, yielding well-defined images. Two-dimensional spectral-spatial images are shown for lung samples containing $(4.5 \pm 0.5) \cdot 10^{14}$ and $(9.9 \pm 1) \cdot 10^{14}$ spins. This work was supported by NIH RO1CA1262159 (GRE) and R33 HL157907 (ESN and SSE).

1. Buchanan L.A., Rinard G.A., Quine R.W., Eaton S.S., Eaton G.R.: Conc. Magn. Reson. B, Magn. Reson. Engin. **48B**, e21384 (2018)

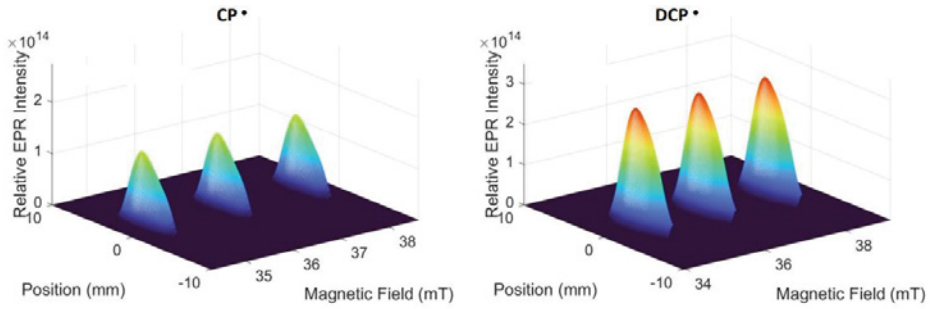

Fig. 1. Spectral-spatial images of the signals from CP$^{\bullet}$ or DCP$^{\bullet}$ in the lungs of LPS-treated mice that contained $(4.5 \pm 0.5) \cdot 10^{14}$ and $(9.9 \pm 1) \cdot 10^{14}$ nitroxide spins, respectively.

I12

Damping of the magnetization precession in graded epitaxial films of Pd-Fe alloy studied by ferromagnetic resonance

I.V. Yanilkin[1,2], I.A. Golovchanskiy[3,4], A.I. Gumarov[1,2], B.F. Gabbasov[1,2], R.V. Yusupov[1], M.N. Aliyev[5], L.R. Tagirov[2]

[1]Institute of Physics, Kazan Federal University, Kazan, Russia
[2]Zavoisky Physical-Technical Institute, FRC Kazan Scientific Center of RAS, Kazan, Russia
[3]Moscow Institute of Physics and Technology, National Research University, Dolgoprudny, Russia
[4]University of Science and Technology MISIS, Moscow, Russia
[5]Baku State University, Baku, Azerbaijan

The Pd-Fe alloy is a promising tunable material for magnonics [1–3]. The damping of the magnetization precession is the most important parameter for magnonics; it has not been studied yet in the Pd-Fe alloy. In this work, we investigate experimentally the Gilbert damping α in epitaxial Pd-Fe alloy films at different iron contents x either with homogeneous or graded across the thickness $Pd_{1-x}Fe_x$ compositions. For this, homogeneous $Pd_{1-x}Fe_x$ films with x in the range of 0.01–0.08 and graded Pd-Fe films with different profiles of the iron content were prepared. The attenuation study was carried out using a broadband-FMR flip-chip approach and cavity-FMR. As can be seen from Fig. 1, an increase in the iron concentration in homogeneous samples leads to a decrease in damping (Fig. 1a). For example, for x = 0.02, α = 0.0290, while α = 0.0193 for x = 0.08 composition. Similar frequency dependences of the linewidth were established for the spin wave resonance modes in graded films (Fig. 1b), however, the correlation of large/small linewidth (and high/low damping parameter α) with the

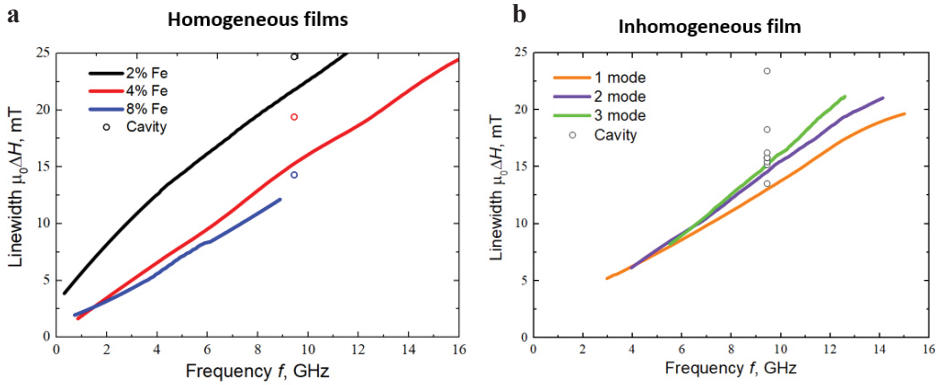

Fig. 1. Frequency dependence of the resonance linewidth for the broadband-FMR (lines) and cavity-FMR (symbols) for homogeneous (**a**) and graded (**b**) Pd-Fe films with constant gradient in the interval 2–10% of iron. The film thickness is 200 nm.

regions of different iron concentration is not unambiguous. Modelling the *ac* field absorption across the film thickness [3] makes it possible to assign low-damping modes to regions with a higher iron concentration.

This work was supported by the Russian Science Foundation (Project № 22-22-00629, https://rscf.ru/en/project/22-22-00629/).

1. Esmaeili A. et al.: Science China Materials **64**, 1246 (2021)
2. Golovchanskiy I.A. et al.: Phys. Rev. Materials **6**, 064406 (2022)
3. Yanilkin I.V. et al.: Nanomaterials **12**, 4361 (2022)

I13

^{175}Lu and ^{11}B NMR in LuB_{12}

O.M. Vyaselev[1], A.A. Gippius[2], N.E. Sluchanko[3], N.Y. Shitsevalova[4], V.B. Filipov[4]

[1]Institute of Solid State Physics, Russian Academy of Sciences, Chernogolovka, Russia
[2]Moscow State University, Moscow, Russia
[3]General Physics Institute, Russian Academy of Sciences, Moscow, Russia
[4]Institute for Problems of Materials Science, National Academy of Sciences of Ukraine, Kyiv, Ukraine

Lutetium dodecaboride was studied by means of ^{175}Lu and ^{11}B NMR in order to study a lattice instability related with dynamic Jahn-Teller effect, as a possible reason for low superconducting critical temperature $T_C \approx 0.4$ K as compared to ZrB_{12} where $T_C \approx 6$ K [1].

In an idealized cubic lattice of LuB_{12}, space group *Fm*-3*m*, Lu atom occupies a centrosymmetric position. Due to huge quadrupole moment of spin-7/2 ^{175}Lu, its NMR spectrum is extremely sensitive to crystal structure defects: any disturbance of the cubic symmetry (displacement of Lu from the cube center, vacancies in the surroundings etc.) cause the I-order perturbation theory quadrupole shift of the "satellite" transitions ($\pm 7/2 \leftrightarrow \pm 5/2$, $\pm 5/2 \leftrightarrow \pm 3/2$, $\pm 3/2 \leftrightarrow \pm 1/2$). In the case of random lattice defects this results in broadening of the NMR line, serving as a measure of the lattice defectiveness.

^{175}Lu NMR spectrum in LuB_{12} is represented by a superposition of two Lorentzian-shaped peaks, centered at the same frequency but nearly two orders of magnitude different in breadth, $\Delta_{1/2}$ (Fig. 1). The broad peak originates from the "satellite" transitions while the narrow one corresponds to $+1/2 \leftrightarrow -1/2$ "central" transition not receptive to quadrupole interactions in I-order. The temperature dependence of the broad line width $\Delta_{1/2}$ is hysteretic (Fig. 2).

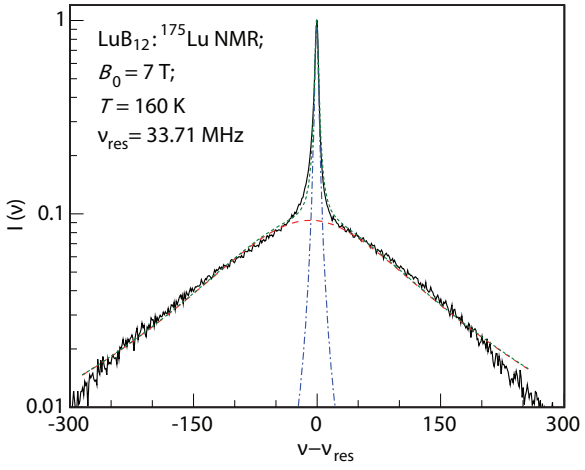

Fig. 1. ^{175}Lu NMR spectrum in LuB_{12}.

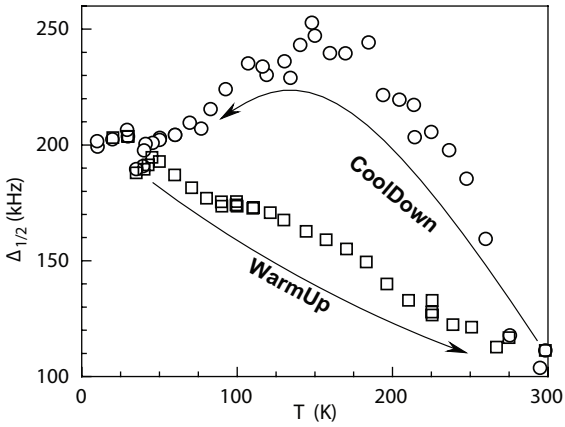

Fig. 2. Temperature dependence of the width of the broad contribution to ^{175}Lu NMR peak.

The increase of $\Delta_{1/2}$ with cooling down to 150 K related to the growth of the lattice defectiveness, signifies the escalation of the lattice instability. Further cooling results in a decrease in $\Delta_{1/2}$ that can be associated with formation of a certain low-temperature configuration, maybe ordering, of lattice defects. This low-temperature configuration is obviously more stable: it disintegrates monotonously upon warm-up, determining the temperature hysteresis in $\Delta_{1/2}(T)$.

^{175}Lu spin-lattice relaxation, $1/T_1$, at $T < 25$ K is linear in temperature signifying the magnetic relaxation via itinerant electron spins. At $25 < T < 140$ K a gap-like T-behaviour $1/T_1 \propto \exp(-\delta/T)$ with $\delta = 204$ K prevails, and at higher temperature $1/T_1 \propto T^4$. The two latter contributions to ^{175}Lu spin-lattice relaxation are presumably of quadrupolar origin.

^{11}B spin-lattice relaxation measured in $B_0 = 7$ and 2.4 T indicates the enhancement, in the temperature range 100–200 K, of low-frequency spin dynamics at $\nu = 33.7$ MHz ($B_0 = 2.4$ T) that corresponds to ^{175}Lu NMR frequency at 7 T.

1. Azarevich A. et al.: Phys. Rev. B. **103**, 104515 (2021)

I14

The mechanism of the formation of biologically active paramagnetic mononuclear dinitrosyl iron complexes in living organisms

A.F. Vanin

N.N. Semenov Federal Research Center of Chemical Physics Russian Academy of Sciences, Moscow, Russia, e-mail: vanin.dnic@gmail.com

The capacity of NO molecules to operate in the disproportionation reaction when binding in pair with Fe^{2+} ion determines in high extent the mechanism of the formation of mononuclear EPR-active dinitrosyl iron complexes (M-DNIC) in living organisms. The reaction results in the appearance of nitrosonium cation (NO^+) and nitroxyl anion (NO^-) in iron ligand sphere. The release of the NO^- from the sphere after its transformation into HNO molecule is terminateed by another NO molecule including into iron ligand sphere resulting in the formation of M-DNIC characterized with resonance structure $[(L^-)_2Fe^{2+}(NO)(NO^+)]^+$, where L^- is an anionic ligand. The complex is stabilized when anionic thiol-containing compounds (RS^-) include into the M-DNIC ligands and DNIC with thiol-containing ligands begins to function in living organisms as "working form" of the universal regulator of various biological processes – nitric oxide. Including of the latter into the complexes leads to NO stabilization thereby providing its transfer between cells and tissues in the forms of NO molecules and NO^+ cations. Both agents releasing from the M-DNIC exert on living organisms positive, regulatory or negative, toxic effects respectively.

Selective release NO^+ from M-DNIC with thiol-containing ligands (as well as from binuclear form of DNIC) can be induced with the dithiocarbamate derivatives ($R_2NCS_2^-$) action on the complexes. The derivatives are capable of taking up iron-mononitrosyl group from iron-dinitrosyl fragments of the DNICs that results in the formation of stable mononitrosyl iron complexes with dithiocarbamate derivatives. As a result of that the DNICs exert only cytotoxic action on the biological objects induced by NO^+ cations. It was discovered the ability of these cations appeared in the system DNIC+dithiocarbamate derivative to block efficiently "COVID" infection (induced by SARS-CoV-2 virus) in Syrian hamsters.

Probing of dietary fiber conformation by EPR spectroscopy

V.N. Syryamina[1,2], X. Wu[2], S. Boulos[2], L. Nyström[2], M. Yulikov[3]

[1]Voevodsky Institute of Chemical Kinetics and Combustion, Novosibirsk, Russia
[2]Institute of Food, Nutrition and Health, Zurich, Switzerland
[3]Institute for Molecular Physical Science, Zurich, Switzerland

Dietary fibers (DFs) from plant foods are a significant part of the human diet required for a healthy diet. The DFs are weakly digestible natural polysaccharide chains and can therefore work as 'molecular carriers' that bind and remove various small molecules from the human body. Since the structure and nutritional properties of different DFs are not alike, establishing the structure-function relationship would be a fundamental basis for understanding the nutritional properties of dietary fibers. For neutral soluble DFs, the interaction between the fiber chain and food constituents can be transient and so weak that it presents a challenge not only to describe the binding efficiency or binding sites in the polymer chain, but also to prove the presence of this interaction. Therefore, it is valuable to introduce spectroscopic techniques that are sensitive to weak interactions and that provide a detailed picture of the conformations and interactions of such DF chains at the molecular level.

Here we summarize our recent studies of polysaccharide chain conformations and conformational changes using electron paramagnetic resonance (EPR) spectroscopy. We will focus on the results of the multiple stochastic labeling of the polysaccharide chain [1], the features of pulse dipolar EPR spectroscopy (PDS) for spin-labeled fibers [2, 3], as well as various approaches to DFs modeling – coarse-grained one and the atomistic-resolution modeling [3]. We anticipate that the proposed EPR and modeling toolkit is not limited to polysaccharide chains and can be extended to describe the structure or structural changes of various weakly ordered or disordered materials.

1. Wu X., Boulos S., Yulikov M., Nyström L.: Carb. Polymers **293**, 119724 (2022)
2. Wu X., Boulos S., Syryamina V., Nyström L., Yulikov M.: Carb. Polymers **309**, 120698 (2023)
3. Syryamina V.N., Wu X., Boulos S., Nyström L., Yulikov M.: Carb. Polymers **319**, 121167 (2023)

ESR observation of magnons, their bound states and spinons in a frustrated triangular magnet Cs_2CoBr_4

A.I. Smirnov[1], T.A. Soldatov[1], A.V. Syromyatnikov[2]

[1]P. L. Kapitza Institute for Physical Problems RAS, Russia
[2]Petersburg Nuclear Physics Institute named by B.P. Konstantinov of National Research Center "Kurchatov Institute", St. Petersburg, Russia

We report a multimode ESR of ordered phases of Cs_2CoBr_4 in a magnetic field and its theoretical interpretation. The spin structure of this material consists of weakly interacting triangular-lattice planes of Co^{2+} magnetic ions (S = 3/2) [1]. The exchange interaction along the lateral sides of triangles is frustrated in presence of the strongest exchange along the base of triangles. For this reason the exchange network may be considered as weakly coupled spin chains. The strong single-ion anisotropy gives a possibility to consider the system on the base of a pseudospin-1/2 model at low temperatures [1]. The pseudospin representation implies a strong anisotropy of the exchange interaction of about 25% (see, e.g., [2]). Thus, Cs_2CoBr_4 gives an example of a magnet, simultaneously demonstrating features of a frustrated triangular system and of a quasi-one-dimensiomal S = 1/2 antiferromagnet with a strongly anisotropic exchange. Our ESR data taken at the temperature of 0.5 K (which is below the Néel temperature of 1.3 K) in the range 25–250 GHz reveal up to seven branches of magnetic resonance at a given magnetic field. These branches arise due to interplay of frustration, low dimensionality and strong anisotropy. For the low-field collinear phase, the spin-resonance modes are spin-1 and spin-0 quasiparticles which are obtained theoretically using the bond-operator technique [3]. These excitations are conventional magnons and bound states of these magnons, respectively. Besides, the magnon modes demonstrate satellites which arise due to four magnetic ions in a crystal cell. In contrast, excitations lying above 200 GHz [4] are not captured by theory [3] due to pronounced one-dimensional correlations inside spin chains which govern the spin dynamics at high energies. They were successfully interpreted as bound states of domain walls in adjacent chains known as "Zeeman ladder" in anisotropic spin chains [4]. Thus, the ordered state of Cs_2CoBr_4 demonstrates dynamic excitations of both two-dimensional and one-dimensional quantum magnet.

In the intermediate temperature range between the Néel temperature and a temperature destroying the exchange correlations (about 6 K) we observe a two component ESR signals corresponding to a spinon-like resonances of spin S = 1/2 anisotropic spin chains [2].

We acknowledge the support by the Russian Science Foundation: Grant No. 22-12-00259 for experiment and Grant No. 22-22-00028 for theory.

1. Povarov K.Yu., Facheris L., Velja. S., Blosser D., Yan Z., Gvasaliya S., Zheludev A.: Phys. Rev. Res. **2**, 043384 (2020)
2. Bruognolo B., Weichselbaum A., Jan von Delft, Garst M.: Phys. Rev. B **94**, 085136 (2016)
3. Syromyatnikov A.V.: Phys. Rev. B **98**, 184421 (2018)
4. Fachers L., Nabi S. D., Glezer Moshe A., Nagel U., Room T., Povarov K. Yu., Stewart J. R., Yan Z., Zheludev A.: Phys. Rev. Lett. **130,** 256702 (2023)

Peculiarities of spin centers in titania-based nanoheterostructures

E.A. Konstantinova[1,2], T.P. Savchuk[1,3], A.V. Semeno[2], S.V. Demishev[2]

[1]Physics Department, M.V. Lomonosov Moscow State University, Moscow, Russia
[2]Prokhorov General Physics Institute of RAS, Moscow, Russia
[3]National Research University of Electronic Technology – MIET, Zelenograd, Moscow, Russia

The main area of application titania is photocatalysis [1–3]. Note that the functional characteristics (photoactivity, rate of chemical decomposition of organic impurities, including toxic) of titania are determined by its physicochemical properties. In recent years the efforts of many scientific groups are directed to the development of energy-efficient TiO_2 based photocatalysts for the decomposition of toxic impurities, viruses in air and water and the conversion of CO_2 into more energy-intensive hydrocarbons [1–3]. For this purpose, it is important to know the type and properties of defects in the structure of the titania, since they are involved in redox reactions that determine the efficiency of photocatalysis. The aim of our study is to investigate the features of the behavior of defects in titania nanotubes (NT) based composites.

The formation of nanotube arrays of anodic titanium oxide doped with carbon (TiO_2-C NT) occurred by two-stage electrochemical oxidation of Ti-foil BT1-0 [3]. For formation of the TiO_2-C-Cu composites the solution for the precipitation of copper nanoparticles was prepared as follows: 0.4 M copper sulfate was added to a 3 M aqueous solution of lactic acid and stirred. The pH was then adjusted to 3–4 with 5 M NaOH aqueous solution. After that, copper nanoparticles were deposited on the surface of TiO_2-C NT at a temperature of 20 °C and a potential of –1.5 V relative to Ag/AgCl (3M). After the deposition process, the TiO_2-C-Cu samples were washed in deionized water and dried in an air stream.

The EPR spectra at 300 K were recorded with a Bruker spectrometer ELEXSYS-E500 (X-band). EPR measurements at low temperatures were carried out at Prokhorov General Physcics Institute RAS using a spectrometer based on Agilent PNA network analyzer [4]. In this experiment the sample was put on the bottom plate a cylindrical cavity operating at a frequency f = 60 GHz in TE011 resonance mode.

The EPR spectrum of the TiO_2-C NT samples at 300 K consists of a single line with g = 2.0027 ± 0.0005, which can be attributed to carbon dangling bonds [5]. The EPR spectrum of the TiO_2-C-Cu NT samples is a superposition of several EPR signals. Firstly, in the magnetic field range 2600–3100 G, a strong EPR signal is recorded from copper ions Cu^{2+} embedded in the structure of titania during synthesis (g = 2.3212±0.0005, line width ΔH = 330 G) [6]. In the interval 3000–3300 G, there is an EPR signal with parameters g = 2.1635±0.0005, line width ΔH = 320 G from copper ions Cu^{2+} in the CuO phase [6]. The latter indicates partial oxidation of the deposited metallic copper. Note that such a large width of EPR line from copper ions can be due to unresolved hyperfine splitting (copper nucleus spin is equal 3/2), and also to dipole–dipole and/or exchange interactions. Also in the EPR spectrum (H = 3406 G) there is a narrow line from dangling carbon bonds observed in the initial samples (without copper). We calculated the concentration of carbon dangling bonds, which amounted to $1.3 \cdot 10^{15}$

g^{-1} for both the TiO_2-C NT and TiO_2-C-Cu NT samples. This indicates that there is no interaction between Cu^{2+} ions embedded in titania nanotubes and intrinsic defects such as carbon dangling bonds. We performed also EPR measurements at a frequency f = 60 GHz in the ΔT range from 50 to 1.8 K. We determined the g-factors of the narrow EPR lines: g_I = 1.996 (H = 2.13 T) and g_{II} = 1.972 (H = 2.16 T). According to literature data defects with such parameters are the Ti^{3+}/V_o (oxygen vacancy) centers [7]. A broad EPR line with $g \approx 2.1$ (H = 2.06 T) can be attributed to the Cu^{2+} centers [6]. It was established that the intensity of EPR lines from Ti^{3+}/V_o centers varies nonmonotonically with decreasing temperature. Thus, in the temperature range ΔT from 50 K to 4 K, the Curie law is fulfilled (EPR signal intensity I_{EPR} increases with decreasing temperature). At the same time, in the range of ΔT from 4 to 1.8 K, instead of the expected further increase of the intensity of the EPR signal, due to the Curie law, there is a decrease of the I_{EPR} value. We have determined the activation energies from the temperature dependences. They amounted to E_I = 1.08 and E_{II} = 0.9 eV. We believe that the majority of energy levels of defects are ionized up to the temperatures of about 5 K: Ti^{3+}–V_o–Ti^{4+}). With a further decrease in temperature, the contribution of non-ionized defects increases: Ti^{3+}–V_o– Ti^{3+}. Probably, in this case, a situation occurs when it is energetically favorable to form the next center with a total spin equal to zero: Ti^{4+}–↑↓–Ti^{4+}. This hypothesis allows us to explain the anomalous temperature dependence $I_{EPR}(T)$ in the interval ΔT = 4–1.8 K.

The obtained data is very important for the development of TiO_2-C-Cu energy effective photocatalysts. The experiments were performed using the facilities of the Collective Use Center at the Moscow State University. The study was supported by a grant from Russian Science Foundation № 21-19-00494.

1. Chiesa M., Livraghi S., Paganini M.C., Salvadori E., Giamello E.: Chem. Sci. **11**(26), 6623–6631 (2020)
2. Low J., Yu J., Jaroniec M., Wageh S., Al-Ghamdi A.A.: Adv. Mater. **29**, 1601694 (2017)
3. Gavrilin I., Dronov A., Volkov R., Savchuk T., Dronova D., Borgardt N., Pavlikov A., Gavrilov S., Gromov D.: Appl. Surf. Sci. **516**, 146120 (2020)
4. Samarin A.N., Semeno A.V., Gilmanov M.I., Glushkov V.V., Lobanova I.I., Samarin N.A., Sluchanko N.E., Sannikov I.I., Chubova N.M., Dyadkin V.A., Grigoriev S.V., Demishev S.V.: Phys Procedia **71**, 337–342 (2015)
5. Savchuk T., Gavrilin I., Konstantinova E., Dronov A., Volkov R., Borgardt N., Maniecki T., Gavrilov S., Zaitsev V.: Nanotechnology **33**, 55706 (2022)
6. Martín-Gómez J., Hidalgo-Carrillo J., Montes V., Estévez-Toledano R.C., Escamilla J.C., Marinas A., Urbano F.J.: J. Environ. Chem. Eng. **9**(4), 105336 (2021)
7. Kokorin A.I.: Electron spin resonance of nanostructured oxide semiconductors, in: Chemical physics of nanostructured semiconductors edited by Kokorin A.I.,. Bahnemann D.W. Boston: VSP–Brill Academic Publishers (2003), 236 p.

I18

Magnetic resonance in the high-field phases of low-temperature paramagnets

V.N. Glazkov

P. Kapitza Institute for Physical Problems RAS, 119334 Moscow, Russia

Conventional behavior of the exchange-coupled spins on a regular lattice at low temperatures is to order magnetically at a temperature $k_B T_c \sim J$, here J is a characteristic strength of the exchange interaction. Last decades revealed existence of the class of exchange-coupled systems, which do not follow this 'traditional' route. Despite of the presence of a strong exchange coupling these systems remain in a disordered paramagnetic state down to low temperatures $k_B T \ll J$. Microscopically this unusual behavior of low-temperature paramagnets is due to specific geometry of the exchange bonds' network frequently involving low-dimensional patterns or frustration of different interactions.

A subclass of particular interest are the low-temperature paramagnets with gapped excitation spectrum. These systems have a singlet ground state separated from the magnetic excitations by an energy gap Δ. At low temperatures these systems has two independent energy scales and two characteristic magnetic fields: $H_{c1} \sim \Delta/(g\mu_B)$ and $H_{c2} \sim J/(g\mu_B)$. The former field corresponds to the closing of the energy gap, while the later corresponds to the saturation of spin system. Formation of the ordered or disordered high-field phases of low-temperature paramagnets at $H_{c1} < H < H_{c2}$ was actively studied by different techniques (see, e.g., [1]).

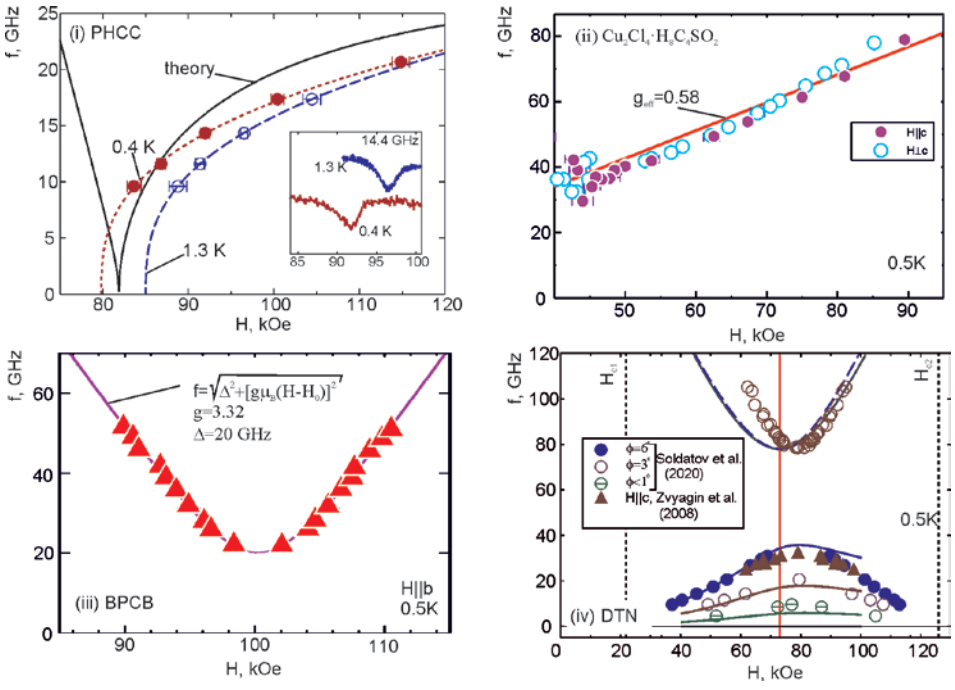

Fig. 1. Examples of frequency-field diagrams for electron spin resonance in the high-field phases of various low-temperature paramagnets (see text for details).

Magnetic resonance technique has proved to be a powerful and sensitive tool to study unusual high-field phases of low-temperature paramagnets [2]. It allows to probe low-energy spin dynamics, to follow closing and re-opening of the energy gaps, to observe collective modes of spin precession characteristic of different phases. Experimental facilities of P.Kapitza Institute allows to measure electron spin resonance spectra at frequencies 1–300 GHz, in the fields up to 12 T and at the temperatures down to 0.1 K providing access to the low-temperature phases of various low-temperature paramagnets.

We will discuss four different examples of spin-dynamics in the high-field phases of various low-temperature paramagnets:

(i) "Conventional" field-induced antiferromagnetic ordering in a quasy-2D magnet PHCC ($(C_4H_{12}N_2)Cu_2Cl_6$). Here we observe characteristic low-frequency antiferromagnetic resonance mode, which is a non-Goldstone mode due to the presence of anisotropic spin-spin interactions [2]. The frequency of this mode is quantitatively described within the hydrodynamic model [3].

(ii) Non-commensurate helical ordering in a quasy-1D "spin-tube"-type magnet $Cu_2Cl_4{\cdot}H_8C_4SO_2$. Here we observe antiferromagnetic resonance mode with non-Larmor slope ($g_{eff} = 0.58$) [2]. Such a mode is inherent feature of helicoidal spin ordering, its observation allows to discern commensurate and incommensurate antiferromagnetic structures in a electron spin resonance experiment [4].

(iii) Solitonic excitations in the Tomonaga-Luttinger liquid phase of a 1D strong-rung ladder BPCB [5]. Low-energy dynamics close to the point where the system is half-magnetized can be mapped on a pseudo-spin model of a gapless easy plane chain in zero field. We observed orientation-dependent spin gap at $H \approx (H_{c1} + H_{c2})/2$ and anomalous effective g-factor values ($g_{eff} \approx 3.5$). Analysis demonstrates that the observed low-energy excitation modes are solitonic excitations caused by Dzyaloshinskii-Moriya interaction presence.

(iv) Non-Goldstone antiferromagnetic resonance modes in a strongly anisotropic spin-chain magnet DTN ($NiCl_2{\cdot}4SC(NH_2)_2$) in slightly canted magnetic field [6]. Tetragonal symmetry of DTN makes it one of the most perfect candidates to observe "true" Goldstone mode in the field-induced antiferromagnetically ordered phase [1]. Experiment [7] revealed that non-Goldstone low-frequency mode appears in the ordered phase if the field is tilted by 1–6° away from the symmetry axis. Pseudospin mapping model [6] combining results of strong coupling limit approach and traditional mean field description of antiferromagnetic resonance quantitatively describes this effect.

Author thanks Prof. A.I. Smirnov, Dr. Yu. Krasnikova, Dr. T. Soldatov (Kapitza Institute), and Dr. K. Povarov and Prof. A. Zheludev (ETH Zurich) for their involvement on different stages of this research project. Samples for the study were kindly provided by Prof. A. Zheludev (ETH Zurich). The work was supported by Russia Science Foundation Grants 17-12-01505 (ESR experiments) and 22-12-00259 (final data analysis).

1. Zapf V., Jaime M., Batista C.D.: Rev. Mod. Phys. **86**, 563 (2014)
2. Glazkov V.N.: JETP **131**, 46 (2020)
3. Farutin A.M., Marchenko V.I.: JETP, **104**, 751 (2007)
4. Svistov L.E., Prozorova L.A., Farutin A.M. et al.: JETP **108**, 1000 (2009)
5. Krasnikova Yu.V., Furuya S.C., Glazkov V.N. et al.: Phys. Rev. Lett. **125**, 027204 (2020)
6. Glazkov V.N.: JETP Letters, **112**, 647 (2020)
7. Soldatov T.A., Smirnov A.I., Povarov K.Yu. et.al.: Phys. Rev. B **101**, 104410 (2020)

New EPR data on the nature of optically active centers in plastically deformed natural diamonds

V.A. Nadolinny[1], Yu.N. Palyanov[2], A.Yu. Komarovskikh[1], M.I. Rakhmanova[1]

[1]Nikolaev Institute of Inorganic Chemistry SB RAS, Novosibirsk, Russia
[2]Sobolev Institute of Geology and Mineralogy SB RAS, Novosibirsk, Russia

In this study, the natural diamonds of different types IaB, IaAB, and low-nitrogen diamond crystals from Yakutian province with plastic deformation characteristic features have been investigated. It is shown that for low-nitrogen and type IaB diamonds, plastic deformation does not lead to brown coloration of crystals raising the question about the nature of optically active centers. The electron paramagnetic resonance (EPR) spectra of the brown samples revealed the W7 centers, which are pairs of nitrogen atoms separated by two carbon atoms and formed from the A-centers as a result of plastic deformation, and the 490.7 single line related to dangling bonds in the dislocation cores. For these plastically deformed diamonds the narrowing of the 490.7 EPR line and the dynamical broadening of the W7 lines were observed with a temperature increase from 77 to 300 K. The hypothesis was proposed regarding a charge transfer from W7 defects to dangling bonds in the dislocation cores. The observed change in the EPR spectra can be explained by the mobility of electrons localized on dangling carbon bonds, leading to the polarization of W7 orbitals and modulation of the hyperfine structure from nitrogen atoms. In this case, the resulting charge transfer complexes can be responsible for the 550 nm band in the optical absorption spectra and, consequently, for a brown coloration of plastically deformed IaAB diamond samples. To investigate the complexes where dangling bonds in the channels of dislocation cores act as electron acceptors for nitrogen centers, experiments were conducted to passivate carbon dangling bonds by annealing in a hydrogen-containing medium. This should reduce the probability of charge-transfer complex formation and weaken the corresponding 550 nm band in the optical absorption spectra. Annealing in a TiH1.19 medium at 1500 °C and a pressure of 7.8 GPa for 21 hours resulted in discoloration of the diamond crystal. Simultaneously, a broadened band appeared in the IR spectra in the region of 2960 cm^{-1}, which corresponds to the vibrations of the C-H bonds. A similar manifestation of C-H bonds vibrations in this region was observed during the hydrogenation of the surface of CVD diamonds. As the brown color weakens, the intensity of the W7 EPR spectrum decreases, the EPR spectrum of substitutional nitrogen appears, and the EPR line from dangling bonds in the dislocation cores broadens. These effects suggest that passivating dangling bonds in the dislocation cores leads to a decrease in the intensity of the 550 nm band in the optical absorption spectra. Along with the W7 and 490.7 nm centers, the EPR spectra of some brown plastically deformed natural diamonds also displayed the presence of N1 centers with the structure of two nitrogen atoms separated by one carbon atom. The N1 center has an electron spin of $S = 1/2$, indicating the ionized state of this defect. The conducted studies on annealing at high pressures and temperatures of plastically deformed crystals showed that the N1 center could be annealed at 1400 °C. Furthermore, we observed that the disappearance of the N1 EPR

spectrum at a temperature of 1300 °C was due to the annealing of the center being an acceptor for the N1 defect. A technique has been developed for the ionization of the neutral N1 centers. By applying this technique to natural crystals of the IaAB type, we found that during the aggregation of single nitrogen atoms into A centers, a significant amount of neutral N1 centers accumulated in the crystals. This phenomenon can be explained by the fact that at the last stage of aggregation of two impurity nitrogen atoms, the energy barrier increases due to the strong Coulomb repulsion of unpaired electrons of nitrogen atoms. It means that in the absence of electron acceptors, the N1 center is the limiting step in the aggregation of nitrogen into A centers in both natural and synthetic diamonds.

1. Nadolinny V.A. et al.: Diamond and Related Materials **136**, 110073 (2023)

Extending spin coherence in open-shell donor-acceptor macromolecules

M.K. Bowman[1], J.D. Azoulay[2], N. Eedugurala[2]

[1]Department of Chemistry & Biochemistry, The University of Alabama, Tuscaloosa, Alabama, USA
[2]School of Chemistry and Biochemistry and School of Materials Science and Engineering, Georgia Institute of Technology, Atlanta, Georgia, USA

Long spin coherence lifetimes are important for many uses of electron spins in magnetic resonance spectroscopy, spintronics, and spin informatics. Spin decoherence is a major limiting factor in nanoscale distance measurement by pulse dipolar spectroscopy (PDS); in resolution in pulse hyperfine spectroscopy (PHS) and CW EPR; and in qubit applications in quantum informatics.

One major cause of spin decoherence is the time-dependent interaction with other spins. The time dependence can be driven by physical motion of a spin or by coherent evolution or relaxation of the other spin. Significant coherence lifetime increases are achieved simply by elimination motion, especially motion of rotating or tunneling methyl groups, and by decreasing interactions between spins.

Decreasing the interactions between spins by increasing distance between spins has been a productive strategy in some systems. Dilution of spins, including isotopic depletion of nuclear spins, can also significantly extend coherence lifetimes. But expanding the spatial extent of the electron spin can also be effective by increasing its distance from other spins when the electron spin is delocalized over many nanometers. We have explored such a strategy in a series of linear open-shell molecules with repeating donor-acceptor groups [1].

In relatively short molecules, we find rapid spin decoherence, from tens of nanoseconds to a couple of microseconds. But when molecules become so long that the singlet-triplet splitting is negligible, spin decoherence slows dramatically even at room temperature. In these systems, $T_1 = T_2$ at room temperature, simplifying manipulations on the Bloch sphere. Their very slow decoherence gives FT-EPR spectra with highly resolved *g*-factor anisotropy. Their 2D Rabi oscillations show nutation around tilted fields in the rotating frame.

Strong delocalization of the open shell electron spins means that even though the molecules contain many protons, nitrogen spins, and even several natural abundance ^{13}C spins, each nuclear spin interacts with only a minute fraction of the electron spin, causing little decoherence. Attempts to measure inter-electron interactions from the effects of instantaneous spectral diffusion show that interactions among electron spins are less than a several kHz in strength.

1. Mayer K.S., Adams D.J., Eedugurala N., Lockart M.M., Mahalingavelar P., Huang L., Galuska L.A., King E.R., Gu X., Bowman M.K., Azoulay J.D.: Cell Rep. Phys. Sci. **2**, 17 (2021)

I21

Optically detected magnetic resonance studies of the ChlF synthase enzyme

A. van der Est[1], A. Agostini[2], G. Shen[3], D. Bryant[3], J. Golbeck[3], D. Carbonera[2]

[1]Dept. of Chemistry, Brock University, St. Catharines ON, Canada
[2]Dept. of Chemical Sciences, University of Padua, Padua, Italy
[3]Dept. of Biochemistry and Molecular Biology, Penn State University, University Park, PA, USA

Photosynthetic organisms live in a wide variety of environments with very different and variable light conditions. In particular, plants and cyanobacteria living in shaded environments often receive very little visible light. It was recently discovered that some oxygenic organisms have a complex set of genes that allow them to adapt to the lack of visible light by absorbing far red light. These genes and the regulatory process associated with them are known as far red light photoacclimation (FaRLiP) [1]. One of the regulatory responses is to synthesize chlorophyll *f*, which absorbs further to red than chlorophyll *a* in a region of the spectrum that is not used under normal light conditions. Once it has been synthesized, the chlorophyll *f i*s then incorporated into the antenna systems of Photosystems I and II (PSI and PSII) allowing them to harvest the available light. The pathway by which the chlorophyll *f* synthesis takes place is not well known. However, it has been demonstrated that chlorophyll *f* synthesis depends on the expression of an unusual gene that shows very high sequence homology to one of the two core proteins of PS II [2]. This gene is a so-called "super-rogue" paralog of the *psbA* gene, and the associated protein has been named ChlF synthase. Very little is known about the structure and function of the ChlF enzyme but it has been shown that when it is illuminated at low temperature spin-polarized chlorophyll triplet states are observed. This allows the enzyme to be studied using optically detected magnetic resonance (ODMR) data. Fluorescence detected ODMR measurements reveal the presence of several different types of chlorophyll triplet states with different zero-field splitting parameters and optical properties. The triplet-minus-singlet spectrum obtained from absorption detected ODMR is remarkably similar to the spectrum of the triplet state of the primary donor $^3P_{680}$ of PSII, suggesting that ChlF may have an electron transfer pathway similar to that of PSII. The ODMR data also reveal the presence of chlorophyll *f* triplet states and carotenoid triplets. These clearly suggest that the enzyme is light activated and has a photoprotection mechanism as well. The site of chlorophyll *f* synthesis remains unknown but the similarity of the data to that of PSII points to the so-called Chl-Z site as a possibility.

1. Gan F., Zhang S., Rockwell N.C., Martin S.S., Lagarias J.C., Bryant D.A.: Science **345**, 1312–1317 (2014)
2. Ho M.Y., Shen G., Canniffe D.P., Zhao C., Bryant D.A.: Science **353(6302)**, aaf9178 (2016)

Decoherence of radical pairs due to spin selective recombination. Comparison of the results of three models

V.A. Bagryansky, A.O. Chetverikov, V.I. Borovkov, Yu.N. Molin

Voevodsky Institute of Chemical Kinetics and Combustion, Novosibirsk, Russia

Analytical solutions of the density matrix evolution of radical pairs caused by their spin-selective recombination and singlet-triplet transitions were obtained in the conventional model [1] and the Jones model [2]. The analytical solution in the Salikhov model obtained in [3] was also considered. Transitions were considered caused by interactions of electron spins with an external magnetic field and magnetic nuclei in a high magnetic field approximation. Time-independent exchange interaction of spins with each other was also taken into account. The solutions are complex functions of three parameters: the recombination rate constant, k, from the singlet state, the exchange integral, J, and the difference, Ω, in the precession frequencies of electron spins around the effective magnetic field, which is the sum of the external field and set by a certain configuration of spins of magnetic nuclei. The complete solution in this approximation requires averaging over these configurations.

The obtained solutions made it possible to propose a criterion for comparing the results of various models and to identify ranges of parameters in which the differences in predictions of these models are the most remarkable. A comparison of time dependencies of the singlet state occupancy ratios to the total number of radical pairs that have avoided recombination is proposed. In the conventional model for $J = 0$ and $k < 2\Omega$ time dependence of this ratio is undamped oscillations with a period that increases with an increase in the ratio of k/Ω. At the same time, in the Jones model, oscillations decay with a characteristic time of the order of magnitude of the inverse reaction constant. In the Salikhov model, this ratio does not decay and its form does not depend on the value of the recombination constant. Hypothetical experiments are discussed.

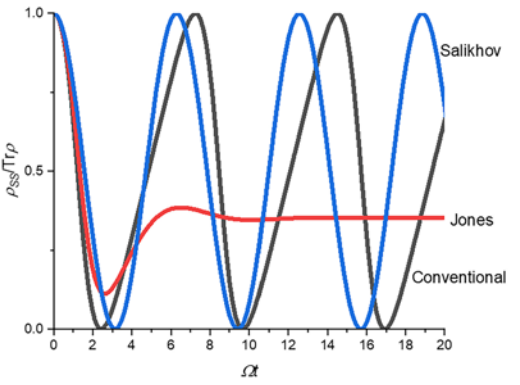

Fig. 1. Time dependences of ratios $\rho_{SS}(t)/\mathrm{Tr}\{\rho(t)\}$ for all three models at $J = 0$ and $k/\Omega = 1$.

The work was partially supported by the Russian Science Foundation (project 21-13-00278).

1. Haberkorn R.: Mol. Physics **32(5)**, 1491–1493 (1976)
2. Jones J.A., Hore P.J.: Chem. Phys. Lett. **488**, 90–93 (2010)
3. Salikhov K.M: Am. J. Phys. Chemistry **11(3)**, 67–74 (2022)

123

Analytical solution for the inverting pulses with constant adiabaticity

K.L. Ivanov[1], A.V. Snadin[1,2], A.S. Kiryutin[1,2], N.N. Lukzen[1,2]

[1]International Tomography Center, Siberian Branch of the Russian Academy of Sciences, Novosibirsk, Russia
[2]Novosibirsk State University, Novosibirsk, Russia

The exact solution was found for inverting pulses with constant adiabaticity for spin 1/2. The analytical relationship between the time-varying frequency of the microwave resonant field (or RF field in the case of NMR) and its amplitude time dependence such that the adiabaticity parameter remains constant for the single isochromat throughout the pulse is found. Comparison with EPR (hyperbolic tangent)-(hyperbolic secant) pulse method was carried out. On the basis of the analytical solution the pulses with different dependences of the microwave field amplitude conserving the constant adiabaticity have been constructed. The pulses exhibit rather sharp inversion selectivity that can be used in the field of EPR, NMR and MRI.

Authors acknowledge funding from Ministry of Science and Higher Education of the Russian Federation grant 075-15-2020-779.

I24

An updated view on the intermolecular contributions in the pulse dipolar EPR experiments

M. Yulikov

Department of Chemistry and Applied Bioscience, ETH Zurich, Switzerland

The routine application of any dipolar-interactions-related EPR pulse sequence besides that it needs understanding of the underlying electron spin pair dynamics also demands a description of the related contributions stemming from the interactions with the surrounding electron and nuclear spins. These additional "intermolecular" contributions form so-called background signal. In the most commonly used in pulse dipolar EPR double electron-electron resonance (DEER) experiment the properties of the intermolecular background are well investigated and analytically described. A handle of alternative pulse dipolar spectroscopy (PDS) techniques has been proposed and they attracted substantial attention in the past ten years as possible alternatives to DEER at some special conditions. In particular, single frequency PDS techniques were investigated in relation to the detection of dipolar interactions for species with either very narrow or very broad EPR spectrum. The case of narrow EPR spectrum is targeted by the double-quantum coherence (DQC) technique and single frequency technique for refocusing dipolar interactions (SIFTER). The case of broad EPR spectrum can be targeted by the relaxation-induced dipolar modulation enhancement (RIDME) technique. Rather quickly it revealed that understanding the intermolecular contributions may be the key to turn these single frequency PDS experiments into routinely applicable spectroscopic techniques.

In this presentation an overview of the recently made progress in understanding intermolecular electron-electron and electron-nuclear contributions in SIFTER and RIDME will be presented. The complications due to the interplay between electron-electron and electron-nuclear contributions, as well as the advantages related to the analysis of samples with heterogeneous local environments of electron spins will be discussed. In particular, we will mention the relevance of these techniques for studying soft materials, polymers and unfolded biopolymers solutions, as well as in designing methodology for dynamic nuclear polarization (DNP).

O1

Multifrequency EPR spectroscopy of Fe^{4+} color centers in amethyst

V.F. Tarasov[1], R.B. Zaripov[1], V.D. Scherbakov[2]

[1]Zavoisky Physical-Technical Institute, FRC Kazan Scientific Center of RAS, Kazan, Russia
[2]Kazan (Volga Region) Federal University, Kazan, Russia

Amethyst is a well-known violet colored kind of quartz (SiO_2). In most studies devoted to the nature of the color of amethyst, this color is attributed to the presence in crystals of impurity Fe^{4+} ions. Electric crystal field of SiO_2 splits the ground electron state of these ions with 4 unpaired electrons into two quasi-doublets $|\pm2\rangle$, $|\pm1\rangle$ and singlet $|0\rangle$. The large energy gap between these singlet levels makes it difficult to observe resonance transitions between them using widely used X-band EPR spectrometers with an operating frequency of about 10 GHz.

To determine the fine structure of the ground electron levels of the Fe^{4+} ion in amethyst, we measured the EPR spectra in the wide frequency range of 34–535 GHz. The measurements were carried out at cryogenic temperatures in a wide frequency range on the frequency-tunable submillimeter spectrometer operating in the frequency range of 64–535 GHz [1] and in the Q-band on an ELEXSYS E580 spectrometer. Measurements in the submillimeter range revealed resonance transitions at frequencies between 350 and 490 GHz (transitions 1–4 in Fig. 1). Temperature dependence of intensity of resonance transitions between levels of the quasidoublet $|\pm2\rangle$ (transition 5 in Fig. 1) shows that this quasidoublet is the ground spin state. This allowed us to determine scheme of five electron spin levels of Cr^{4+} in SiO_2 [2]. The magnetic field dependencies of these levels are presented in Fig. 1.

1. Tarasov V.F., Shakurov G.S.:Appl. Magn. Reson. **2**, 571–576 (1991)
2. Tarasov V.F., Zaripov R.B., Scherbakov V.D.: Appl. Magn. Reson. **54**, 679–686 (2023)

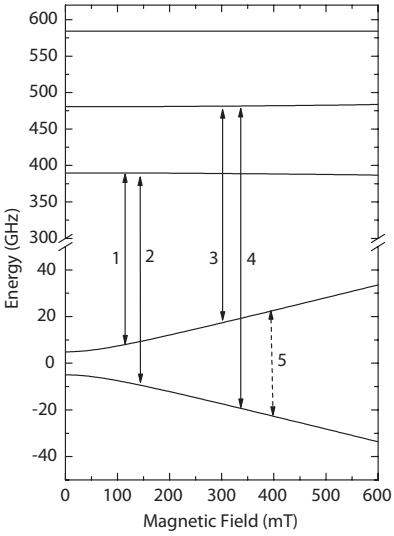

Fig. 1. Magnetic field dependencies of the energy of the electron spin levels of the Fe^{4+} impurity ion in amethyst. The solid and dashed lines show the resonance transitions observed in the submillimeter and Q bands, respectively.

O2

Features of solving the Bloch equation in a weak magnetic field for describing the character of changes in the magnetization of liquid media using the modulation method

A.A. Gol'dberg[1], V.V. Davydov[1], R.V. Davydov[1,2]

[1]Peter the Great St. Petersburg Polytechnic University, St. Petersburg, Russia
[2]Department of Bioinformatics and Mathematical Biology, Alferov University, St. Petersburg, Russia

Nuclear magnetic resonance (NMR) found many different applications in conducting research and monitoring the state of condensed media [1, 2]. One of the applications of NMR, which is now in high demand, is express monitoring of the state of liquid media at the sampling site [3]. To realize it, the times of longitudinal T_1 and transverse T_2 relaxation of the liquid medium are determined by the recorded NMR signal. In express control, depending on the tasks to be solved, taking into account the conditions of mobility of the device [4], either a pulse or a modulation technique is used to register the NMR signal. If it is necessary to move the NMR relaxometer operationally, preference is given to the modulation technique. The use of pulse methods (Hanna and Carr–Purcell spin echo) for measuring T_1 and T_2 requires a gap between the poles of the magnet of at least 80 mm to accommodate the coil system, which increases the weight of the device and the pulse voltage of several hundred volts (battery charge limits). In this case, the NMR signal is represented in the form of damped non-periodic oscillations ("wiggles"). Fig. 1 shows the recorded NMR signal from water with lithium hydroxide at T = 293.1 K.

The time T_2 is determined by the decline of the envelope constructed from the peaks (green curve) (Fig. 1) taking into account the inhomogeneity of the magnetic field in the area of the registration coil [1, 2, 4]. Difficulties arise with the measurement of time T_1. Experimental research has shown that the use of frequency measurements of the Julotto method [5] to determine T_1 in the design of a small-sized NMR relaxometer is extremely difficult. This is due to the fact that changing the modulation frequency in a weak field changes the frequency of NMR signal registration by fractions of hertz.

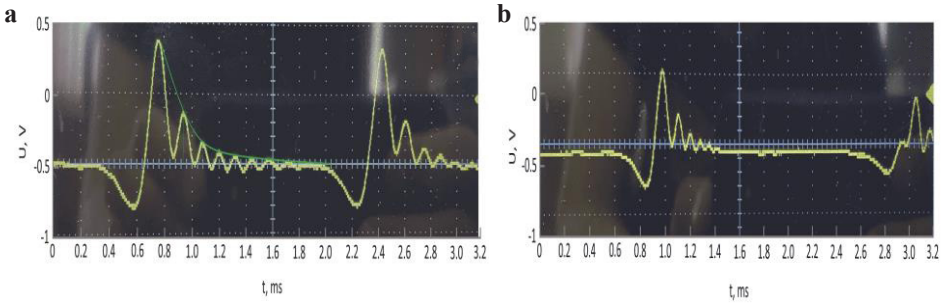

Fig. 1. Recorded NMR signal for lithium nuclei. Graphs (**a**) and (**b**) correspond to fm modulation frequencies in Hz: 702.0 and 360.

In the field, it is difficult to adjust to resonance with an accuracy of fractions of hertz. Therefore, we considered the Bloch equation, which took into account the use of a modulation technique for recording the NMR signal. For the NMR signal recorded at the resonant frequency of the field H0, for the case $T_1 = T_2$, this equation was solved with respect to the components of the magnetization vector M_z, M_x and M_y. At the resonant frequency, only the component of the magnetization vector M_z contributes to the amplitude of the recorded signal. Its change from the modulation frequency of the fm field H_0 by the following formula:

$$M = M_0[1 - (1 - \exp(-1/(f_m T_1))) / (1 + \exp(-1/(f_m T_1)))], \quad (1)$$

where $M_0 = \chi_0 B_0$ – he magnetization value of the condensed medium in the absence of magnetic field modulation, where χ_0 is the static nuclear magnetic susceptibility.

It follows from (1) that in order to measure T_1, it is necessary to measure the amplitude of the NMR signal at two different modulation frequencies (i.e. for two different τ) and graphically find the value of T_1. Experimental investigations have shown the following. In order to determine using (1) the T_1 time and it coincided with the measurement results on the Minispec mq-20M industrial NMR relaxometer, it is necessary that the f_m values between the two measurements of the NMR signal amplitude differ by an order of magnitude or more. In addition, it is necessary to ensure a maximum modulation depth and a signal/noise ratio of at least 1.3 (in this case, an NMR signal accumulation scheme can be used). In the case when the values of f_{m1}/f_{m2} are < 10, the use of formula (1) does not give a reliable result. In this case, the NMR signal is recorded in the f_m range from 0.5 to 1000 Hz. This feature of using formula (1) to determine the value of T_1 introduces limitations in the operation of small-sized NMR relaxometers and requires additional research. These investigations should establish under what approximations (boundary conditions) it is necessary to solve the Bloch equation with new coefficients that take into account the use of the modulation technique when registering the NMR signal. What is the maximum value of the inhomogeneity of the magnetic field during the registration of the NMR signal is permissible. How much should the amplitudes of the two recorded NMR signals differ from each other in order to be able to use (1) without limits on the f_m frequency.

1. Leshe A.: Nuclear induction. Veb Deustscher Verlag Der Wissenschaften, Berlin (1963), 464 p.
2. Jacobsohn B., Wangsness R.: Physical Review.**73**, 942–947 (1948)
3. Neronov Yu.I.: Measurement Techniques **63**, 667–673 (2021)
4. Davydov V.V., Dudkin V.I., Vysoczky M.G., Myazin N.S.: Applied Magnetic Resonance **51**, 653–666 (2020)
5. Giulotto L., Lanzi G., Tosca L.: Journal of Chem. Physics **24**, 632 – 644 (1956)

O3

Formation of a nutation signal in the flowing liquid at the noise level in the entire flow measurement range

I.D. Kochetkov[1], V.V. Davydov[1], R.V. Davydov[1,2]

[1]Peter the Great St. Petersburg Polytechnic University, St. Petersburg, Russia
[2]Department of Bioinformatics and Mathematical Biology, Alferov University, St. Petersburg, Russia

The development of scientific and technological progress, the use of new liquid media in the technical cycles of industrial production and electrical energy (nuclear power plants) [1, 2], as well as increased requirements for the control of hydrocarbons in the pipeline system [3] required the development of new devices or the modernization of those in operation. Devices based on the phenomenon of nuclear magnetic resonance (NMR) are one of the promising directions in solving new problems of monitoring the parameters of current media [2–4]. It is because they eliminate the contact of the measuring elements with the flowing medium, and the measurements carried out using NMR do not change the medium's physical structure and chemical composition.

At present, many different models of NMR flowmeters – relaxometers – have been developed in the world, in which pulse methods (Hann spin echo and Carr–Purcell sequence) [3] or a nutation line with a modulation technique for recording the NMR signal [4] are used to measure the liquid flow rate and relaxation times T_1 and T_2. Using the nutation line and the modulation technique makes it possible to measure the liquid flow q, and the range is 6–10 times greater than when using the pulse technique with an error of 0.5–1.0%. All these models of devices have one drawback, which is associated with an increase in the measurement error q with rapid changes in fluid flow. The method proposed earlier by us using the effect of parametric resonance of the magnetic field in the area where the nutation coil is located [2] has several difficulties when it is implemented at rapidly changing flow rates. Especially in the case of placing the nutation coil in an area with strong electromagnetic interference, which is possible when controlling the flow parameters of various media in nuclear power plants. The formation of satellites in the nutation line is disturbed, which interferes with the formation of the q measurement mode at the noise level [2]. The automatic

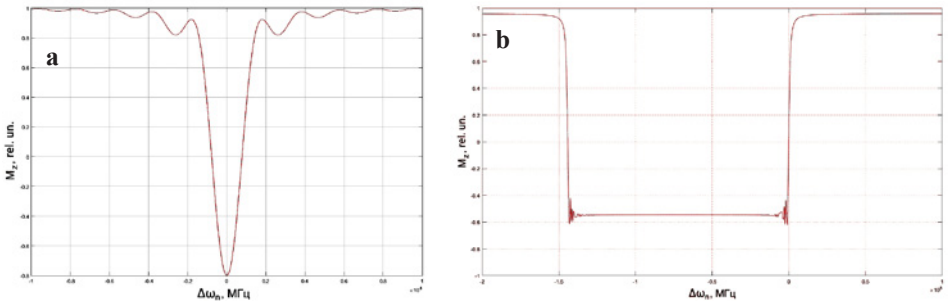

Fig. 1. The dependence of the change in the magnetization M_z on $\Delta\omega_n$. Graphs (**a**) and (**b**) corresponds the following values: $H_1 = 4.21$ A/m, $\Delta H_0 = 11.12$ A/m and $H_1 = 5.66$ A/m, $\Delta H_0 = 2698.21$ A/m.

system for adjusting the parameters of the modulation field does not have time to respond to a rapid change in the value of q. Measurements of q either stop or occur with large errors. Therefore, it is necessary to find a new solution to this problem. We propose implementing one of the possible options for solving this complex problem using a strong inhomogeneous magnetic field in the area where the nutation coil is located. Let us consider the system of Bloch equations for describing the formation of a nutation line in a flowing fluid. Let us introduce new coefficients into the Bloch equations, which allow us to consider the change in the inhomogeneity of the magnetic field ΔH_0 in the zone of the nutation coil. The shape of the nutation line is calculated from the change in the component of the magnetization vector M_z (the amplitude of the registered NMR signal is proportional to M_z, since the relation $T_1 > t_c \geq T_2$ is satisfied, where t_c is the time of liquid movement from the nutation coil to the registration coil).

$$\begin{aligned} &dM_x/dt + M_x/T_2 + [\Delta\omega_n + (\Delta H_0/t_n)\gamma t + \gamma H_m \sin(\omega_m t)]M_y = 0\ , \\ &dM_y/dt + M_y/T_2 - [\Delta\omega_n + (\Delta H_0/t_n)\gamma t + \gamma H_m \sin(\omega_m t)]M_x + \gamma H_1 M_z = 0, \\ &dM_z/dt + M_z/T_1 - \gamma H_1 M_y - M_0/T_1 = 0\ , \end{aligned} \quad (1)$$

where $t_n = V_n/q$ is the time spent by the liquid segment under the action of magnetic fields in the nutation coil, H_m and ω_m are the amplitude and frequency of the modulating field, $M_p = \chi_0 H_p \gg M_0 = \chi_0 \cdot H_0$.

Figure 1 shows, as an example, the nutation lines obtained based on solution (1) for various values of the inhomogeneity of the magnetic field ΔH_0, the flow rate of the flowing liquid q, and the field H_1.

The obtained results of the calculation of the nutation line show its broadening and decrease in the value of M_z to the zero level. Controlling the values of H_1 and ΔH_0 makes it possible to ensure the NMR signal registration at the noise level, which was previously achieved only with satellite lines (parametric resonance) [2]. It should also be noted that the method of controlling the shape of the nutation line proposed by us makes it possible with higher stability to ensure the fulfillment of the following relation $T_1 > t_c \geq T_2$ (where t_c is the time of liquid movement from the nutation coil to the registration coil), which ensures that the amplitude of the registered NMR signal is proportional to the value of M_z.

Comparison of the previously obtained results of the nutation line broadening in [2] with the calculations using (1) shows that in this NMR mode, the flowmeter-relaxometer will work more stably with a rapid change in the value of q. The margin for a rapid change in q for stable operation of the device is at least an order of magnitude greater than when using satellite lines. It should also be noted that in (1), a linear dependence of the change in the magnetic field inhomogeneity along the length of the nutation coil is presented. This dependence can be quadratic or cubic; modern designs of electromagnetic systems make it possible to do this. Therefore, it is necessary to continue these studies to determine the optimal variant for controlling the magnetic field inhomogeneity along the length of the nutation coil.

1. Sadovnikova M.A., Murzakhanov F.F., Mamin G.V., Gafurov M.R.: Energies **15**, 6204–6218 (2022)
2. Davydov V.V., Dudkin V.I., Vysoczkiy M.G., Myazin N.S., Rud' V.Y.: Applied Magnetic Resonance **49**, 665–678 (2018)
3. Kashaev R.S., Kien N.C., Tung T.V., Kozelkov O.V.: Journal of Applied Spectroscopy. **86**, 890–895 (2019)
4. Davydov V.V., Dudkin V.I., Karseev A.Y.: Russian Physics Journal **58**, 146–152 (2015)

O4

Quantum hashing via single-photon states with orbital angular momentum

D.O. Akat'ev[1], D.A. Turaykhanov[1], N.M. Shafeev[2], A.V. Vasiliev[1,2], F.M. Ablayev[2], A.A. Kalachev[1]

[1]Zavoisky Physical-Technical Institute, FRC Kazan Scientific Center of RAS, Kazan, Russia
[2]Kazan Federal University, Kazan, Russia

Quantum hashing is a promising generalization of the cryptographic hashing concept on the quantum domain. In this case, the hash function encodes a classical input state into a quantum state so that to optimize the trade-off between one-way property and collision resistance. The first means that restoring an input string from its hash (decoding) should be a computationally hard problem, while the second means that the situation when two different inputs have the same hash (which is called a collision) is hard to observe. In the present work, we consider a new version of quantum hashing technique wherein a quantum hash is constructed as a sequence of single-photon qubits [1] or qudits [2]. A proof-of-principle implementation of the quantum hashing protocol using orbital-angular momentum encoding of single photons demonstrates good agreement with theoretical predictions. In particular, it shows that the number of qudits decreases with increase of their dimension for an optimal ratio between collision probability and decoding probability of the hash [2]. In addition, we develop a scheme of the quantum hash verification that can be implemented with a single quantum hash state, which is crucial for cryptographic applications.

1. Turaykhanov D.A., Akat'ev D.O., Vasiliev A.V., Ablayev F.M., Kalachev A.A.: Physical Review A, **104**, 052606 (2021)
2. Akat'ev D.O., Vasiliev A.V., Shafeev N.M., Ablayev F.M., Kalachev A.A.: Laser Physics Letters **19**, 125205 (2022)

O5

Polarized luminescence of a single upconversion particle YVO_4:Yb, Er

V.G. Nikiforov, D.K. Zharkov, A.V. Leontyev, A.G. Shmelev, L.A. Nurtdinova, A.P. Chuklanov, N.I. Nurgazizov

Zavoisky Physical-Technical Institute, FRC Kazan Scientific Center of RAS, Kazan, Russia

As known, oxide nanoparticles exhibit low sensitivity to surface quenchers in water solutions. This feature makes them very attractive for various biological applications, such as bioimaging, phototherapy, opto- and thermo-genetics, drag delivery and so on.

This work focuses on the luminescence response registration of a single YVO_4:Yb, Er particle. We synthesized YVO_4:Yb, Er nanoparticles (in the size range from 0.05 μm up to 2 μm) by using hydrothermal method. Nanoparticles emitted bright green upconversion luminescence under 980 nm laser irradiation. Spectroscopic studies showed that Er^{3+} emission centers are excited by means of the Yb^{3+} to Er^{3+} energy transfer.

A clean 60×60 μm^2 square of a glass surface was prepared with atomic-force microscope. Then a single 1-μm particle has been placed in the middle. This sample allowed us to reveal significant difference between the collective luminescent response of a powder of synthesized nanoparticles and the selected single particle. We observed a pronounced polarization of the single particle upconversion luminescence and saturation effect in the laser power dependence of the luminescence intensity. These findings clear evidence high individuality of single particles. The presented example suggests that using an upconversion particle as a single sensor of the medium local parameters requires additional testing and calibration of its upconversion luminescence parameters.

The research was supported by RSF (project no. 23-42-10012).

Synthesis and photophysics of the rare-earth doped upconversion nano-luminophores designed for local temperature measurement

L.A. Nurtdinova, D.K. Zharkov, A.V. Leontyev, A.G. Shmelev, E.O. Mityushkin, V.G. Nikiforov

Zavoisky Physical-Technical Institute, FRC Kazan Scientific Center of RAS, Kazan, Russia

Spectroscopy of anisotropic emitters is attracting attention due to potential applications in microfluidics, individual particles tracking, high resolution bioimaging, etc. [1–3]. We report the results of the study of fluorescent properties of individual NaYF4:Yb, Er nanocrystals synthesized through hydrothermal process [4]. These rod-shaped particles exhibit highly anisotropic fluorescent emission in the range of 650–670 nm when excited by a 980 nm laser radiation. Upconversion particles of similar composition are widely used as local probes, most notably, including in living tissues [1, 5].

The substrate with the dispersed rods was processed using atomic force microscope in the contact mode. The resulted specimen was a 60×80 μm^2 clean area on a glass surface void of fluorescent objects, with the exception of a set of numbered rods with different orientations, suitable for obtaining fluorescent responses of individual selected particles using confocal optical spectroscopy.

The upconverted fluorescent emission of a single rod has a strong polarization anisotriopy. In contrast, the fluorescence of even a very small ensemble of disordered rods is virtually depolarized. Within studied set, the polarization properties of single particles were very close to each other with prominent dependence on nanocrystal orientation.

The research was supported by RSF (project No. 23-42-10012).

1. Rodríguez-Sevilla P. et al.: Nano letters **16**, 8005 (2016)
2. Shao B. et al.: Angewandte Chemie **132**, 18370 (2020)
3. Zharkov D.K. et. al.: Изв. РАН. Сер. физ. **86**, 12, 1727 (2022)
4. Ren G., Zeng S., Jianhua Hao J.: J. Phys. Chem. C. **115**, 20141 (2011)
5. Shmelev A.G. et. al.: Bull. RAS: Phys. **84**, 1696 (2020)

O7

EPR and in silico modeling insights into photodynamic treatment: spotlight on G-quadruplex DNA and human serum albumin complexes

N.E. Sannikova[1,2], M.I. Kolokolov[1,2], T.A. Khlynova[1,2], A.S. Chubarov[3], K.A. Zhdanova[4], M.V. Fedin[1], O.A. Krumkacheva[1]

[1]International Tomography Center SB RAS, Novosibirsk, Russia
[2]Novosibirsk State University, Novosibirsk, Russia
[3]Institute of Chemical Biology and Fundamental Medicine SB RAS, Novosibirsk, Russia
[4]MIREA – Russian Technological University, Moscow, Russia

The interaction of biomacromolecules with small ligands forms a pivotal facet of modern biomedical research. Central to this exploration are DNA, specifically G-quadruplex structures (G4s), and human serum albumin (HSA), the latter being indispensable for the transport and dispersion of myriad compounds in the bloodstream. In a groundbreaking application of laser-induced dipolar Electron Paramagnetic Resonance (EPR) spectroscopy, the interactions between G-quadruplex structures (G4s), specifically the human telomeric G-quadruplex (HTel-22), and photosensitizers were examined [1]. This study specifically delved into the binding and light-induced structural changes of HTel-22 when complexed with TMPyP4, a cationic porphyrin, highlighting the method's utility in understanding G4s′ dynamics in the context of photodynamic therapy (PDT). Remarkably, this approach unearthed G-quadruplex transformations, including unfolding and dimerization, upon light irradiation. Such revelations underscore the potential of EPR spectroscopy in elucidating G4 and photosensitizer interactions.

PDT's efficacy is closely tethered to photosensitizer (PS) interactions with transport proteins like HSA. Using EPR spectroscopy, we successfully elucidated the precise binding sites of the commonly employed photosensitizer, Chlorin E6 (Ce6), within the HSA framework [2]. Through a novel combination of orthogonal labels with photoexcited molecules, we identified two precise binding sites of Ce6 within the HSA. Furthermore, leveraging pulse dipolar EPR spectroscopy in conjunction with molecular docking, we shed light on the differential interactions of various photosensitizer groups with HSA. Our findings indicate that while the nature of the conjugated moieties and the presence of Zn(II) ions influence the localization of anionic and neutral photosensitizers within the HSA, they don't exhibit a similar impact on the binding sites of cationic porphyrins.

In conclusion, the fusion of EPR and in silico modeling has proven to be a valuable tool in exploring the intricate interactions between biomacromolecules and photosensitizers. While our findings primarily focus on the characterization of these complexes, they underscore the importance of robust methodologies in advancing our understanding of their behavior and interactions. Such insights pave the way for future research tailored to optimizing and evaluating the therapeutic potential of these molecular systems.

This research received support from the Ministry of Science and Higher Education of the Russian Federation (075-15-2021-580).

1. Phys. Chem. Chem. Phys. 2023. https://doi.org/10.1039/D3CP01775C
2. Sannikova N.E. et al.: Multicenter EPR Based Approach for the Localization of Photosensitizers in Biomolecules 2023, submitted.

O8

High-tech devices based on electron paramagnetic resonance: X- and W-band EPR spectrometers and NV-magnetometer from ZHONGTAI

A.M. Cherkasov, A.I. Chazov

ELEMENT company

Company ELEMENT presents a line of desktop and floor standing EPR spectrometers ZT series from ZHONGTAI (China). The company's work is based on high-precision quantum measurement technologies, the source of which since 2000 is the leading laboratory of microscale magnetic resonance of the Chinese Academy of Sciences at the University of Science and Technology of China. This laboratory focuses on the research of spin quantum control and its applications in novel quantum technologies, with various experimental routes including nuclear magnetic resonance (NMR), electron spin resonance (ESR), optically-detected magnetic resonance (ODMR), magnetic resonance force microscopy (MRFM), and electrically-detected magnetic resonance (EDMR) [1, 2].

The range of X-band EPR spectrometers includes the ZT6500 benchtop EPR spectrometer, the ZT15C research grade floor standing EPR spectrometer, and the ZT15P research grade pulsed EPR spectrometer. The ZT60W high-frequency W-band EPR spectrometer is also available in the line.

The model of the desktop spectrometer ZT6500 has worthy characteristics for its class of instruments: sensitivity $5 \cdot 10^9$ spin/G, signal:noise ratio at the level of 600:1, modulation frequency 10/50/100 kHz and small overall dimensions and weight. This spectrometer was used to study $W_{18}O_{49}$ as an oxygen-deficient drug delivery system [3] and $ZnSn(OH)_6$ with hydroxyl vacancies at ultralow temperature (6 K) [4].

ZT15C research class floor standing EPR spectrometer with the following characteristics: sensitivity $3 \cdot 10^9$ spin/G, magnetic field range –0.1 ~ 1.8 T, as well as the possibility of using cooling systems based on liquid helium and nitrogen. This spec-

Fig. 1. ZHONGTAI EPR spectrometers.

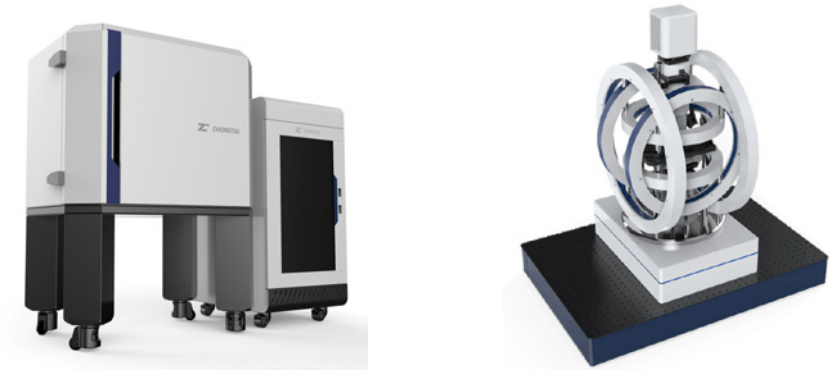

Fig. 2. ZHONGTAI NV magnetometer and NV-Microscope.

trometer was used to determine the stability of the radical cation [6]CPP⊂[12]CPP [5] and to study the structure of the H_2ADC ligand [6].

The research-grade pulsed EPR spectrometer ZT15P, in addition to the CW mode with characteristics similar to ZT15C, has decent performance for the pulsed mode: the microwave source pulse time resolution is 50 ps, the maximum output power of the solid-state power amplifier is 450 W, the microwave pulse phase stability is less than 3° in 1 ms, the maximum duration of the microwave pulse is 3 ms and up to 20,000 pulses per channel. An example of the use of such a device can be the study of the effect of an oxygen vacancy on the valence and chemical state of Co in the compound Co_3O_4 [7] .

In less than 5 years of production, ZHONGTAI has delivered about 30 competitive EPR spectrometers of high level of reliability and quality to the China market. Given the accumulated knowledge and experience, the company highly appreciates the growth opportunities in international markets, including the market of the Russian Federation.

Another two unique devices produced by the company ZHONGTAI. It is also associated with electron paramagnetic resonance, in this case, in the visible range. These are a Quantum Sensor Scanning NV-magnetometer and Quantum NV-Microscope – instruments for accurate measurement of the magnetic field which is based on NV centers – it is the nitrogen vacancy center in Diamond. The device has an ultra-high resolution in the magnetic field – it is about 10 nm and has a high magnetic field sensitivity of about 2 μT√HZ / 5 μT√HZ, respectively. These features of the NV magnetometer and NV-Microscope allow quantitative and non-invasive measurement of the magnetic field with excellent accuracy.

1. Yudi Ma, Ruijuan Liu, Lingjing Ji, Liyang Qiu, Saijun Wu, Dianqiang Su, Yanting Zhao, Ni Yao, Wei Fang: “Composite picosecond control of atomic state through a nanofiber interface”, arXiv preprint arXiv: 2203.06716 (2022), https://doi.org/10.48550/arXiv.2203.06716
2. Yue Li, Zhi-Cheng He, Xinxing Yuan, Mengxiang Zhang, Chang Liu, Yi-Xuan Wu, Mingdong Zhu, Xi Qin, Zheng-Yuan Xue, Yiheng Lin, Jiangfeng Du: “Experimental Demonstration of Swift Analytical Universal Control over Nearby Transitions”, arXiv preprint arXiv: 2201.06246 (2022), https://doi.org/10.48550/arXiv.2201.06246
3. Zhihuan Zhao, Shasha Yang, Pengfei Yang, Jianying Lin, Jimin Fan, Bing Zhang: “Study of oxygen-deficient $W_{18}O_{49}$-based drug delivery system readily absorbed through cellular internalization pathways in

tumor-targeted chemo-/photothermal therapy", Biomaterials Advances, Volume 136, 2022, 212772, ISSN 2772-9508, https://doi.org/10.1016/j.bioadv.2022.212772.

4. Yuhan Li, Bangfu Chen, Ping Ouyang, Youyu Duan, Wee-Jun Ong, Fan Dong: "Engineering $ZnSn(OH)_6$ with ternary active sites-directed hydroxyl vacancies for robust deep C_6H_6 photo-oxidation: Experiment and DFT calculations", Chemical Engineering Journal, Volume 451, Part 2, 2023, 138695, ISSN 1385-8947, https://doi.org/10.1016/j.cej.2022.138695.
5. Chong Zhao, Fupin Liu, Lai Feng, cMingzhe Nie, Yuxi Lu, Jie Zhang, Chunru Wang, Taishan Wang: "Construction of a double-walled carbon nanoring", Nanoscale, 2021, 13, 4880-4886, http://dx.doi.org/10.1039/D0NR08931A .
6. Hu, JX., Li, Q., Zhu, HL. et al.: "Achieving large thermal hysteresis in an anthracene-based manganese(II) complex via photo-induced electron transfer". Nat Commun 13, 2646 (2022). https://doi.org/10.1038/s41467-022-30425-1
7. Dongfang Chen, Lyuming Pan, Pucheng Pei, Shangwei Huang, Peng Ren, Xin Song: "Carbon-coated oxygen vacancies-rich Co_3O_4 nanoarrays grow on nickel foam as efficient bifunctional electrocatalysts for rechargeable zinc-air batteries", Energy, Volume 224, 2021, 120142, ISSN 0360-5442, https://doi.org/10.1016/j.energy.2021.120142.

Experimental confirmation of the "negative interference" of the exchange and dipole-dipole interaction in the transfer of spin coherence and the formation of collective modes of motion of spin magnetization in dilute solutions of nitroxyl radicals

K.M. Salikhov, M.M. Bakirov, I.T. Khairutdinov, R.B. Zaripov

Zavoisky Physical-Technical Institute, FRC Kazan Scientific Centre of RAS, Kazan, Russia

Annotation. The Heisenberg exchange interaction in random bimolecular collisions of paramagnetic particles in dilute solutions causes paramagnetic relaxation of the magnetization of the spins of unpaired electrons. In the simplest case of a solution of particles with two possible resonant spin frequencies, the contribution of spin exchange to the kinetic equations for the magnetization of these two spin subassemblies can be described as

$$(\partial M(\omega_1)/\partial t) = -K_{ex}CM(\omega_1) + K_{ex}CM(\omega_2) \quad (1)$$

for a sub-ensemble of spins with a frequency of ω_1 and a similar equation for the magnetization of the second sub-ensemble. Here K_{ex} is the rate constant of bimolecular spin exchange, C is the concentration of spins in each sub-assembly. In Eq. (1) the second term in the right part is of particular interest. It reflects the effect of the recoil of quantum coherence to the spin from the sub-ensemble 1 from the collision partner from the sub-ensemble 2. It is this return of quantum coherence that is responsible for the amazing manifestations of spin exchange in the form of EPR spectra as, e.g., the mixed (absorption+dispersion) form of resonance lines and the collapse of spectra into one homogeneously broadened Lorentzian line in the centre of gravity [1, 2].

For a long time, it was mistakenly believed that the dipole-dipole interaction in inviscid solutions does not give a contribution associated with the effect of recoil of the coherence to a given spin from other spins. In fact, as it was shown by K.M. Salikhov [3], the dipole-dipole interaction leads to an equation of type (1), there is an effect of the recoil of coherence from the partner spind. But the contribution of the coherence recoil effect to the kinetic equation of type (1) in the case of d-d interaction has a minus sign, and not a plus sign as in the case of spin exchange. Thus, two different interactions give contributions of different signs to the transfer of coherence from partner spins.

In inviscid solutions, the contributions of spin exchange and dipole-dipole interaction vary with temperature in the opposite way. This circumstance opens up the possibility to vary the total contribution of both interactions to the transfer of spin coherence $V = K_{ex}C - K_{d\text{-}d}C$ by changing the temperature. When the temperature changes, V can become equal to zero and change the sign.

In this work, for solutions of ^{15}N nitroxyl radical, it is shown that when the temperature changes, V changes sign. We determined the sign of V by the sign of the contribution of dispersion to the mixed form of the resonance lines of the EPR spectrum.

The recoil effect of quantum coherence forms collective modes of spin magnetization motion. For solutions of ^{14}N radicals, it was shown that the manifestation of the so-called collapse of EPR spectrum is not due to the equal resonance frequencies of all modes, in fact these modes have very different integral intensities. These experimental observations confirm a new paradigm of spin exchange [1, 2].

The analysis of experimental data showed that the dipole-dipole interaction of the spin of an unpaired electron with magnetic nuclei also contributes to the transfer of spin coherence. This contribution does not depend on concentration of paramagnetic particles.

1. Salikhov K.M.: Physics-Uspekhi **189**, 1017–1043 (2019)
2. Salikhov K.M.: Fundamentals of Spin Exchange. Story of a Paradigm Shift. Springer (2019)
3. Salikhov K.M., Semenov A.G., Tsvetkov Yu.D.: Electron Spin Echo and its Application. Novosibirsk: Nauka. Russia (1976)

O10

Enhancing the sensitivity of dynamic nuclear polarization using laser excitation and shaped pulses techniques

M.I. Kolokolov[1,2], O.A. Krumkacheva[1], A.R. Melnikov[1], A.S. Kiryutin[1], I.V. Zhukov[1], A.V. Yurkovskaya[1], M.V. Fedin[1]

[1]International Tomography Center, SB RAS, Novosibirsk, Russia
[2]Novosibirsk State University, Russia

Dynamic Nuclear Polarization (DNP) is a prevalent method for enhancing the sensitivity of Nuclear Magnetic Resonance (NMR) experiments by generating non-equilibrium spin populations. A primary limitation of this technique has been the requirement for extremely low temperatures (below 4 K) and high magnetic fields. A recent advancement in DNP involves utilizing photoexcited triplet spin labels, which display inverse population between states, and this approach has achieved almost complete spin polarization due to the selectivity of the excited singlet-triplet intercombination transition. Moreover, the incorporation of shaped pulse techniques in Electron Paramagnetic Resonance (EPR) has emerged as a novel strategy to augment EPR sensitivity through broader excitation bandwidth.

In this research, we present, for the first time, the application of shaped pulses in experiments with photoexcited labels. This new method has enabled achieving a significant DNP effect while relaxing experimental conditions, such as raising the minimum temperature requirement to 100 K. Specifically, WURST-shaped EPR pulses were optimized and integrated into the pi-DNP pulse sequence, and we investigated their influence on the transfer of light-induced electron polarization to nuclei.

The experiments were conducted using a Bruker E580 X-band EPR spectrometer, and the samples were excited with 100 Hz laser pulses at a wavelength of 532 nm. Nuclear polarization was detected through 400 MHz ^{1}H NMR measurements, using an ENDOR unit. Two different systems were employed: the OXO63 radical in D_{20}/d-glycerol/H_2O solution, which did not require photoexcitation, and pentacene in a p-terphenyl matrix, which was subject to laser excitation. We optimized the magnetic field, pulse length, and EPR pulse excitation bandwidth to attain maximum nuclear polarization. The results show that the pi-DNP sequence with rectangular pulses led to the least increase in NMR signal. Conversely, the NOVEL sequence with rectangular pulses boosted DNP efficiency between 2.3 and 3.6 times above the baseline, while the pi-DNP sequence with optimized WURST-shaped pulses increased efficiency by factors of 8.9 and 7 for the OXO63 and pentacene systems, respectively. These findings highlight the significant potential of combining photoexcited triplet states with shaped pulses to enhance NMR sensitivity.

This research received support from the Ministry of Science and Higher Education of the Russian Federation (075-15-2021-580).

O11

Investigation of orientation dependences of phase spin relaxation using broadband microwave pulses of the same duration

D.A. Kuznetsov[1,2], A.R. Melnikov[1,2], E.G. Bagryanskaya[1]

[1]N.N. Vorozhtsov Novosibirsk Institute of Organic Chemistry, SB RAS, Novosibirsk, Russia
[2]Novosibirsk State University, Novosibirsk, Russia

Pulsed Electron Paramagnetic Resonance (EPR) spectroscopy is a powerful experimental method for studying the structure, dynamic, and functional properties of various paramagnetic compounds. Typical pulsed EPR experiments use microwave rectangular pulses of nanosecond duration. The width of the EPR spectrum of the paramagnetic species in most cases exceeds the experimentally achievable bandwidth of the excitation pulses. For example, the EPR spectra of nitroxyl radicals, widely used as spin labels, have a width of more than 200 MHz in the X band in the solid state. In this regard, in experiments with rectangular pulses, it is not possible to excite the entire EPR spectrum of the sample.

One of the potential ways to solve this problem is to use adiabatic pulses with a linear frequency sweep. The first paper describing the use of adiabatic pulses in EPR was published in 2013 [1]. It was demonstrated that adiabatic broadband pulses can excite spins in the frequency range of several hundreds of megahertz, which can increase the sensitivity of measurements in a number of experiments.

Unlike rectangular pulses, the linear frequency sweep in adiabatic pulses results in a quadratic dependence of the signal phase on frequency. This makes the usually used integration of the spin echo signal in the time domain impossible. A special Bohlen-Bodenhausen scheme is typically used to solve the described phase problem [2]. However, the disadvantage of this scheme is that the signals of different components of the EPR spectrum evolve for different times. As a result, the shape of the obtained spectrum is distorted due to the different phase of nuclear modulation (ESEEM effect) and transverse relaxation..

Herein, we propose to use an alternative scheme of experiments using sequences of adiabatic pulses of the same duration. For this purpose, an experiment was carried out to measure the T_2 relaxation time simultaneously at all parts of the EPR spectrum of Finland triarylmethyl radical. All the experimental data were obtained using amplitude-corrected broadband pulses to account for the frequency response of the microwave cavity.

1. Doll A. et al.: Journal of Magnetic Resonance **230,** 27–39 (2013)
2. Doll A., Jeschke G.: Journal of Magnetic Resonance **246**, 18–26 (2014)

O12

Water molecules and lithium cations mobility in sulfonated polystyrene acid and alkaline metal salts films studied by NMR

N.A. Slesarenko[1], S.A. Bilyk[1,2], V.A. Tverskoy[3], A.V. Chernyak[1,4], I.A. Avilova[1], V.I. Volkov[1,4]

[1]Federal Research Center of Problems of Chemical Physics and Medicinal Chemistry RAS, Chernogolovka, Russia
[2]Lomonosov Moscow State University, Moscow, Russia
[3]Lomonosov Institute of Fine Chemical Technologies, MIREA–Russian Technological University
[4]Scientific Center in Chernogolovka of the Institute of Solid State Physics named by Yu. A. Osipyan RAS, Chernogolovka, Russia, e-mail: wownik007@mail.ru

In modern electrochemical technologies and ion separation processes ion exchange sulfonic cation membranes are widely used. For the interpretation of data in membranes, comparison with the results of studying low-molecular aqueous solutions of metal chlorides turned out to be very fruitful [1]. Obviously, for a deeper understanding of the mechanisms of ion transport in membranes and the formation of transport channels, it is necessary to study aqueous solutions of electrolytes, which are non-crosslinked polymer analogs of membranes. Such investigations have been carried out on polystyrene sulfonic acids and their alkaline metal salts. To obtain unique information about the structural and dynamic characteristics of complex molecular systems NMR is successfully used [2].

Films of poly(4-styrenesulfonic acid) and its Li^+, Na^+, Cs^+ salts were investigated which, from our opinion, are the model of ionogenic part of sulfonated cation exchange membranes. Self-diffusion coefficients and local mobility of water molecules and lithium cations were measured by pulsed field gradient NMR and NMR spin relaxation techniques, respectively. NMR measurements were carried out in temperature range from −20 °C to +50 °C.

Self-diffusion coefficients were measured for ^1H and ^7Li nuclei by pulsed field gradient technique. Unfortunately, spin-spin relaxation time T_2 of ^{23}Na and ^{133}Cs was too short in order applied PFG NMR technique. Temperature dependences of water

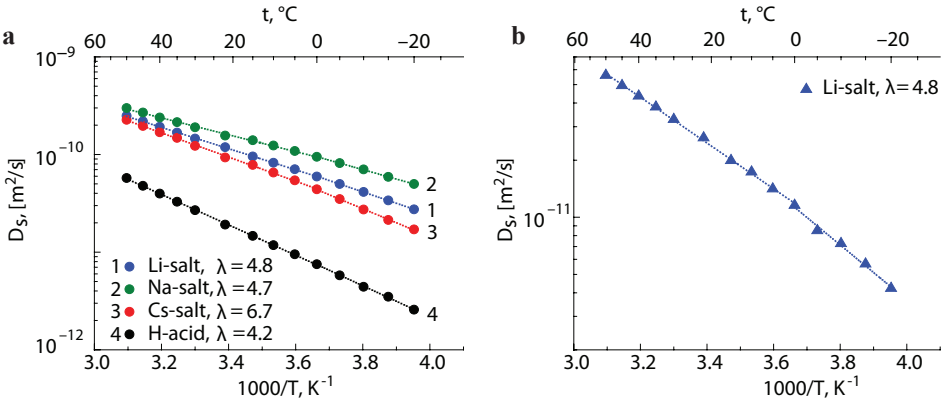

Fig. 1. Temperature dependences of water self-diffusion coefficients (**a**) polystyrene lithium (1), sodium (2), cesium (3) salts and polystyrene acid (4). Humidity λ (amount of water molecules per cation) is shown in insertion. Temperature dependence of Li^+ cation self-diffusion coefficient (**b**).

O12

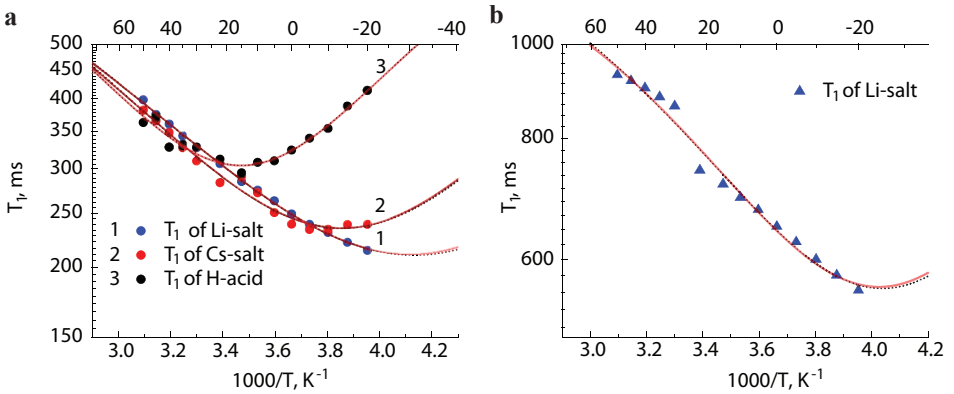

Fig. 2. Temperature dependence of ^{1}H nuclei spin-lattice relaxation times T_1 (**a**) in polystyrene lithium (1), cesium (2) salts and polystyrene acid (3). Temperature dependence of ^{7}Li nuclei spin-lattice relaxation times T_1 (**b**) in polystyrene lithium. Dotted and solid lines are Lorentz and Gauss functions approximations accordingly.

self-diffusion coefficients are shown in Fig. 1. The temperature dependences of the self-diffusion coefficient are approximated by the Arrhenius equation.

To study the local mobility of water molecules and Li^+ cations, spin relaxation was measured on nuclei ^{1}H and ^{7}Li, respectively. Temperature dependences of spin-lattice T_1 times are shown in Fig. 2.

Calculated self-diffusion coefficients were compared with experimental values measured by PFG NMR at temperatures equal to temperature of minimum T_1. In our previous paper a distance of local jumping length of water molecules and Li^+, Cs^+ cations for Nafion membrane was calculated [2, 3]. We have used these distances in order to estimate diffusion coefficients from Einstein relation. As it was shown water proton jumping at low humidity is 0.15 nm which is about hydrogen bond length [2, 4]. As result we have a good agreement between water macroscopic self-diffusion coefficients measured by PFG NMR and self-diffusion coefficients calculated from correlation times obtained by spin-relaxation which characterize average of water molecule jumping time.

Comparison of self-diffusion coefficients measured by PFG NMR with self-diffusion coefficients calculated from correlation times has shown that macroscopic water molecules and lithium cations transfer is control local particle jumping between neighboring sulfonated groups. Therefore, ionogenic transport channels forming in polystyrenesulfonic films are regular structure. It was concluded that polystyrenesulfonic polymer films are appropriate model of homogeneous sulfonic cation-exchangers.

NMR measurements were performed using equipment of the Multi-User Analytical Center of the Institute of Problems of Chemical Physics RAS and Science Center in Chernogolovka RAS with the support of State Assignment of the Institute of Problems of Chemical Physics RAS (state registration No 0089-2019-0010/AAAA-A19-119071190044-3).

1. Volkov V.I., Chernyak A.V., Golubenko D.V., Tverskoy V.A., Lochin G.A., Odjigaeva E.S., Yaroslavtsev A.B.: Membranes **10**, 272 (2020)
2. Volkov V.I., Slesarenko N.A., Chernyak A.V., Avilova I.A., Tarasov V.P.: Membranes **13**, 518 (2023)
3. Slesarenko N.A., Chernyak A.V., Avilova I.A., Tarasov V.P., Volkov V.I.: Mendeleev Commun. **33**, 215–217 (2023)
4. Slesarenko N.A., Chernyak A.V., Avilova I.A., Zabrodin V.A., Volkov V.I.: Mendeleev Commun. **32**, 534–536 (2022)

O13

Development of receiving sensors for new nuclei for specialized MRI system with a field of 0.4 T

A. Bayazitov, A. Fakhrutdinov, Ya. Fattakhov, V. Odivanov, V. Shagalov

Zavoisky Physical-Technical Institute, FRC Kazan Scientific Center of RAS, Kazan, Russia,
e-mail: alfisgdi5s5d@yandex.ru

The work was carried out as part of expanding the diagnostic capabilities of a specialized MRI system with a magnetic field of 0.4 T.

The work is devoted to the development of sensors with operating frequencies of 4.63 and 4.7 MHz. The diameters of the working part of the sensors are 20 mm and 125 mm.

In the course of the work, the coils of the circuits were optimized according to the criterion of a uniform distribution of the RF field of the coil at frequencies of 4.63 and 4.7 MHz. Coil № 1 has a working area diameter of 20 mm and is designed to study solutions in a test tube. Coil № 2 has a working area diameter of 125 mm and is designed to study larger objects.

Optimization was carried out according to the following parameters: inductance and length of the coil and uniformity of the RF field in the coil. The length and diameter of the coil affect the number of turns and the uniformity of the field in the working area. The number of turns and how they are turned on affects the magnitude of the signal (the amount of inductance) as well as the uniformity of the RF field. The value of the inductance is limited by the ability to tune the circuit to the operating frequency of the MRI.

The coils were optimized by mathematical modeling. The work was carried out taking into account the previously obtained results [1–3]. According to the results of the calculations, prototypes of sensors were made and images were obtained.

1. Bayazitov A.A., Fattakhov Ya.V., Fakhrutdinov A.R., Shagalov V.A.: J. Instruments and Experimental Techniques **63**, no. 6, 875–879 (2020)
2. Bayazitov A.A., Fattakhov Ya.V., Khundiryakov V.E.: J. Nauchnoe Priborostroenie **29**, no. 1, 92–98 (2019)
3. Bayazitov A.A., Fattakhov Ya.V., Zalyalyutdinova L.N., Fazliakhmetova D.A., Krylatykh N.A., Imanaeva A.Ya., Petrova A.A.: J. Nauchnoe Priborostroenie **29**, no. 1, 87–91 (2019)

O14

Application of a specialized MRI system for accelerated selection and control in biology and agriculture

Ya.V. Fattakhov[1], V.L. Odivanov[1], T.G. Khadeev[1], A.V. Kornienko[2], R.M. Nizamov[3], V.O. Ezhkov[4]

[1]Zavoisky Physical-Technical Institute, FRC Kazan Scientific Center of RAS, Kazan, Russia
[2]Mazlumov All-Russian Scientific Research Institute of Sugar Beet and Sugar, Voronezh
[3]Tatar Scientific Research Institute of Agriculture, FRC Kazan Scientific Center of RAS
[4]Tatar Scientific Research Institute of Agrochemistry and Soil Science, FRC Kazan Scientific Center of RAS

The use of a specialized magnetic resonance imaging system with induction of magnetic field 0.4 T to solve the problems of biology and agriculture will significantly deepen scientific research in these areas, opens up new unique opportunities for experiments. The first results of studies of the internal structure of agricultural crops were obtained: sugar beet, potatoes, carrots, corn, onions, various fruits, wheat and rye sprouts, as well as laboratory animals and poultry embryos. First of all, the advantage of this technique is in the non-invasive effect on living objects, in the ability to dynamically monitor the internal structure of plants with non-destructive methods, diagnose diseases at the latent stage of development, and determine developmental defects.

The analysis of tomographic images, for example, of sugar beet root crops, allows us to determine the number and thickness of parenchyma and xylem rings, and predict the productivity of the selected samples as the initial selection material for accelerated selection process. The use of non-destructive tomography methods is also a promising direction for the diagnosis of plant diseases at the latent stage of development.

To control the dynamics of plant growth, storage and processing in field and vegetation experiments and at sugar factories, it is possible to create a mobile version of a compact tomograph based on a car.

The effectiveness of the technique for early diagnosis of embryo development in poultry farming is shown.

Original computer programs have been created that allow to obtain the characteristics of biological objects in digital form with high spatial and temporal resolution.

O15

Hyperpolarization of ^{3}He in magnetized plasma and effect of temperature on the polarization process

A.S. Makarchenko, V.V. Kuzmin, K.R. Safiullin, M.S. Tagirov

Institute of Physics, Kazan Federal University, Kazan, Russia

Helium-3 is widely used in NMR, as a probe for porous media. It can be used for non-invasive study of different samples, including biological ones, since helium-3 is chemically inert. However, its application at room temperature is complicated by the low NMR signal due to the low gas density. This problem can be solved by using hyperpolarized helium-3 (hyperpolarized helium-3 is a gas with a nuclear polarization a few orders of magnitude higher than Boltzmann, at the Zeeman sublevels of nuclear spins).

Hyperpolarized helium-3 is used in scientific and medical applications. It is used for high-precision magnetometry, the study of porous media, neutron polarization and MRI of human lungs. However, the use of hyperpolarized helium-3 is limited by the complexity of its production. The most common methods of hyperpolarization of helium-3 are now SEOP and MEOP. These are optical polarization methods that are expensive and requires complex equipment.

Recently, a new method of hyperpolarization of helium-3 [1] has been proposed, which may become a good alternative to optical methods in future. This is the PAMP (polarization of atoms in a magnetized plasma) method. According to acronym, this method implies that helium-3 plasma is placed in magnetic field under certain conditions. In this report the progress in the study of the PAMP polarization method will be presented.

Experiments were conducted to study the polarization rate of helium-3 by the PAMP method at 10-mbar gas filling pressure. It turned out that the polarization rate by this method is relatively high, the time constant of the polarization process reaches ~1 s. The dependence of the polarization rate on the RF discharge power was investigated. Also the dependence of the steady-state polarization on temperature was found. The dependence of the polarization value on temperature was investigated in the range ~ 30 to 190 °C at different power of RF discharge pumping. A significant increase in the value of polarization was detected with an increase in temperature and there was no tendency to slow down this growth in the studied range, which indicates the need for research in a wider temperature range [2].

During the experiments, the optical fluorescent light spectrum of plasma was recorded in addition to the value of polarization and temperature. It was found that in addition to helium-3 lines, oxygen lines are present in the plasma radiation spectrum, the intensity of which strongly correlates with the temperature of the polarization cell. Based on this, it was assumed that the intensity of the oxygen lines reflects the temperature inside the polarization cell and it is a more relevant parameter than the temperature of the outer wall of the polarization cell.

1. Maul A., Blümler P., Nacher P. J., Otten E., Tastevin G., Heil W.: Physical Review A **98**(6), 063405 (2018)
2. Makarchenko A., Kuzmin V., Safiullin K., Tagirov M.: Physical Review A **106**(2), 023101 (2022)

O16

Investigation of ferromagnetic coupling for manganese pairs in a bulk layered gallium sulfide crystal by high-field high-frequency EPR method

R.A. Babunts[1], A.V. Batueva[1,2], A.S. Gurin[1], K.V. Likhachev[1,2], E.V. Edinach[1], P.G. Baranov[1]

[1]Ioffe Institute, 194021, St. Petersburg, Russia
[2]Northern (Arctic) Federal University, Arkhangelsk, Russia

Layered semiconductors, in particular, GaS, consisting of quasi-two-dimensional S-Ga-Ga-S monolayers, are of interest due to the wide possibilities of their application in optoelectronics and spintronics. The highly anisotropic structure leads to interesting properties, such as the relatively simple preparation of monolayers that differ significantly in optical characteristics from bulk crystals. By choosing the layer thickness

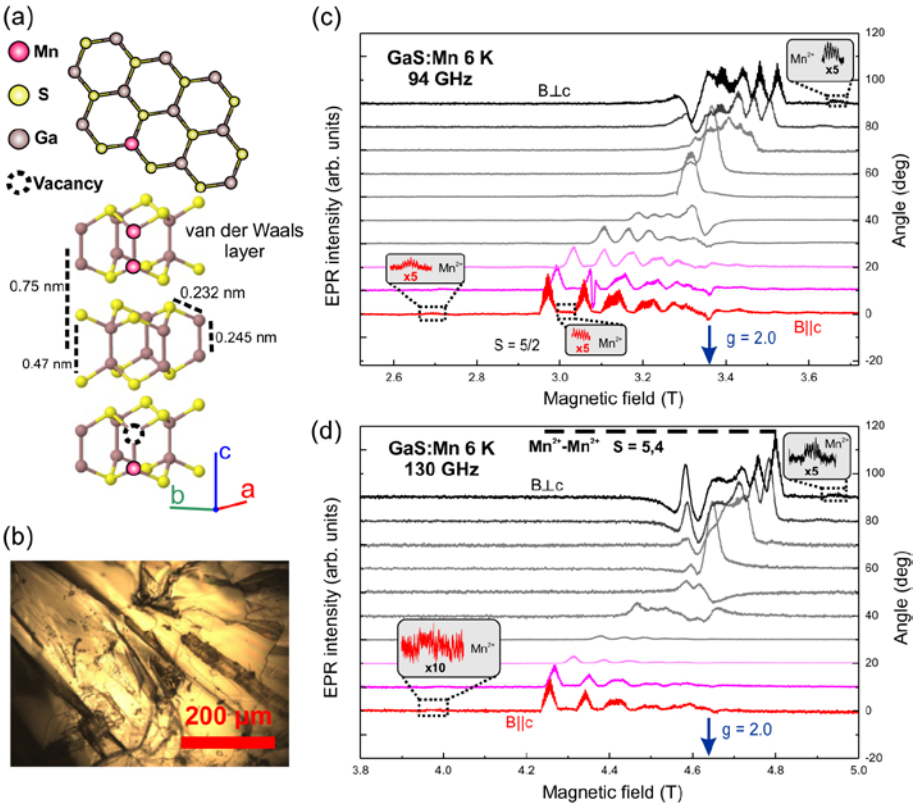

Fig. 1. a Sketch of the crystal structure of 2H-GaS, manganese Mn^{2+}-Mn^{2+} pairs and single Mn^{2+} ion. **b** Microscope picture of GaS:Mn sample. Orientation dependence of EPR signals related to Mn centers in a GaS:Mn sample, recorded at 94 GHz (**c**) and 130 GHz (**d**) at a temperature of 6 K.

O16

or by combining layers of different materials, it is possible to obtain structures with desired energy characteristics [1, 2]. Doping layered semiconductors with transition metals allows to obtain semi-insulating and magnetic materials, as well as to create spin centers, which can be used as information carriers in quantum computing due to the strong spin-orbit interaction [3]. High-frequency EPR provides opportunity of obtaining unique information about charge state, electronic structure and energy characteristics of spin centers in bulk single crystals.

In this work, the properties of paramagnetic centers in bulk layered GaS:Mn samples are investigated at the frequencies of 94 and 130 GHz at 6 K by the electron paramagnetic resonance (EPR) method. The experimental setup of high-field high-frequency EPR/ODMR spectrometer [4] developed at the Ioffe Institute.

The EPR spectra of ferromagnetically coupled Mn^{2+} (Mn_2^{4+}) pairs substituting covalently bonded Ga_2^{4+} pairs and located in the center of the GaS:Mn layer were obtained (Fig. 1). Sets of lines from multiplets with spin $S = 4$ and $S = 5$ are observed, which makes it possible to estimate the energy of isotropic exchange interaction J as ~ -0.5 cm^{-1}. The fine structure parameters for the lower multiplets with $S = 4$ and $S = 5$ were determined equal to $D = -0.040$ cm^{-1} and $D \approx -0.035$ cm^{-1}, respectively. For all registered transitions for Mn^{2+} pairs, as well as for single Mn^{2+} ions, a well-resolved hyperfine structure is observed. The hyperfine splitting for pairs is approximately half the hyperfine interaction constant for individual Mn^{2+} ions.

This work was supported by a grant from the Russian Science Foundation (project No. 23-12-00152).

1. Li X., Tao L., Chen Z., Fang H., Li X., Wang X., Xu J.-B., Zhu H.: Appl. Phys. Rev. **4(2)**, 021306 (2017)
2. Gutiérrez Y., Giangregorio M.M., Dicorato S., Palumbo F., Losurdo M.: Frontiers in Chemistry **9**, 781467 (2021)
3. Atatüre M., Englund D., Vamivakas N. et al.: Nat. Rev. Mater **3**, 38–51 (2018)
4. Babunts R.A., Badalyan A.G., Gurin A.S. et al.: Appl. Magn. Reson. **51**, 1125–1143 (2020)

O17

Application of EPR spectroscopy to study changes in the content of nitric monoxide and copper in the rats frontal lobes after modeling a combined injury of brain and spinal cord

Kh.L. Gainutdinov[1,2], V.A. Kulchitchky[3], V.V. Andrianov[1,2], L.V. Bazan[1,2], T.K. Bogodvid[2,4], G.G. Yafarova[2], E.V. Fedorova[3], T.A. Filipovich[3], A.V. Nagibovv[3]

[1]Zavoisky Physical-Technical Institute, FRC Kazan Scientific Center of RAS, Kazan, Russia
[2]Institute of Fundamental Medicine and Biology of Kazan Federal University, Kazan, Russia
[3]Institute of Physiology of Nat. Acad. of Sci. of Belarus, Minsk, Belarus
[4]Volga Region State University of Physical Culture, Sport and Tourism, Kazan, Russia,
e-mail: kh_gainutdinov@mail.ru

Nitric oxide (NO) is known as one of the most important signaling molecules regulating the physiological functions of the organism and the metabolism of cells [1]. Studies of the role of NO in the transmission of signals in the nervous system began shortly after its discovery [2]. It was found that the production of endogenous NO is observed in almost all tested groups of animals, as well as in plants, diatoms, slime molds and bacteria [3]. By activating soluble heme-containing guanylate cyclase and ADP-ribosyltransferase, NO participates in the regulation of intracellular concentration of Ca^{2+} ions, is involved in pH regulation against the background of cerebral ischemia [4]. The two main mechanisms stabilizing the unpaired electron $^{\bullet}NO$ are its reaction with other free radicals and interactions with d-orbitals of transition metals [5]. Since NO is a chemically highly reactive free radical capable of acting both as an oxidizer and as a reducing agent [1], there is an assumption about its diverse effects in biological tissues. Therefore, NO is an example of the classic two-faced Janus.

There are many methods of measuring NO production in biological systems. Precise measurement of both the steady concentration of NO and the speed of NO generation in biological systems is a difficult task due to the low activity of NO synthases and its short half-life. In last years electronic paramagnetic resonance (EPR) proved to be one of the most efficient methods for the detection and quantification of nitric oxide in biological tissues [2, 5]. Therefore, we conducted a study of the dynamics of NO production in injured and non-injured areas (frontal lobes) of the brain when modeling combined brain and spinal cord injury in rats.

We used EPR spectroscopy to study the dynamics of NO in the brain and heart of rats after modeling a number of pathological processes. The intensity of NO production by EPR spectroscopy was measured using the spin trap technique [1, 6], which is based on the reaction of a radical (in this case NO) with the spin trap. The complex of Fe^{2+} with diethyldithiocarbamate (DETC) was used to capture NO and to form a stable ternary complex $(DETC)_2$-Fe^{2+}-NO in the animal tissues. Those complexes are characterized by an easily recognizable EPR spectrum with *g*-factor $g = 2.035–2.040$ and a triplet hyperfine structure [6, 7]. The spectra of the complex $(DETC)_2$-Fe^{2+}-NO were measured on Brucker X spectrometers (9.50 GHz) EMX/plus with a temperature module ER 4112HV with a magnetic field modulation of 100 kHz and a modulation

amplitude of 2 G ,with a microwave power of 30 mW, a time constant of 200 ms and a temperature of 77 K in a finger Dewar of the Bruker company.

By the methods of EPR spectroscopy our team has evaluated effect of brain stroke on the intensity of NO production in the tissues of the brain of rats in vivo. A simulation of brain injury and then spinal cord injury was performed. Seven days after the operation, tissues were extracted from the injured and non-injured areas of the brain and measurements were made. The measurements of NO were carried out by EPR spectroscopy. The results of the analysis demonstrate a significant decrease in NO production 7 days after the simulation of trauma in the injured brain region by an average of 6 times (P = 0.029, Mann-Whitney) and also a significant decrease in NO production in the non-injured (contralateral) brain region by an average of 3 times. There is a difference in NO production in the injured and contralateral regions of the brain (P = 0.050, t-test).

The work was supported by the Russian Scientific Fund No. 23-45-10004 and Belarusian Republican Foundation for Basic Research (grant M23RNF-067).

1. Vanin A.F.: Nitric Oxide **54**, 15–29 (2016)
2. Boehning D., Snyder S.H.: Annu. Rev. Neurosci. **26**, 105–131 (2003)
3. Moroz L.L.: Am. Zool. **41**, 304–320 (2015)
4. Steinert J.R. et al.: Neuroscientist **16**, 435–452 (2010)
5. Santos R.M. et al.: Intern. J. Cell Biol., Article ID 391914 (2012)
6. Vanin A.F., Huisman A. et al.: Methods in Enzymology **359**, 27–42 (2003)
7. Mikoyan V.D., Kubrina L.N. et al.: Biochim. Biophys. Acta **1336**, no 2, 225–234 (1997)

O18

Role of dissipation in spin-flop transition in spiral magnets

S.K. Gotovko[1,2], V.I. Marchenko[1]

[1]P.L. Kapitza Institute for Physical Problems RAS, Moscow, Russia
[2]HSE University, Moscow, Russia

Dissipation processes play a crucial role in spin dynamics of magnetic structures and reorientation processes that occur in magnets. Here, we present theoretical study of the role of dissipation processes in spiral magnets at the proximity of critical point where spin-flop reorientation occurs.

Usually, a harbinger of spin-flop transition in antiferromagnets is the softening of the gap in spin-wave spectra (Fig. 1a). However, from the side of low fields, this rule is broken in spiral magnets [1–2]: the expected decrease in frequency is not observed (Fig. 1b). It has been shown that the peculiarity of the low-frequency spectra in spiral magnets at spin-flop transition can be explained when dissipation processes are taken into account. In this case, dissipation parameter changes its sign at the critical point, and instability of spin plane oscillations causes the spin-flop reorientation.

When approaching the critical point from the side of high fields, the usual vanishing of the frequency is observed. In this case, while instability of the magnetic structure at the critical point can also be explained when dissipation processes are taken into account, the occurrence of an unusual phenomenon – so-called marginal state – is predicted: the oscillation frequency vanishes before the critical point and stays equal to zero till the spin-flop reorientation. ESR frequency ω and dissipation parameter λ dependence on external magnetic field in the vicinity of the critical point H_{sf} is presented in Fig. 1c.

The work was supported by Russian Science Foundation (№ 22-12-00259).

1. Büttgen N., Krug von Nidda H.-A., Svistov L.E., Prozorova L.A., Prokofiev A., AßmusW .: Phys. Rev. B **76**, 014440 (2007)
2. Svistov L.E., Prozorova L.A., Farutin A.M., Gippius A.A., Okhotnikov K.S., Bush A.A., Kamentsev K.E., Tishchenko E.A.: JETP **108**, 1000–1009 (2009)

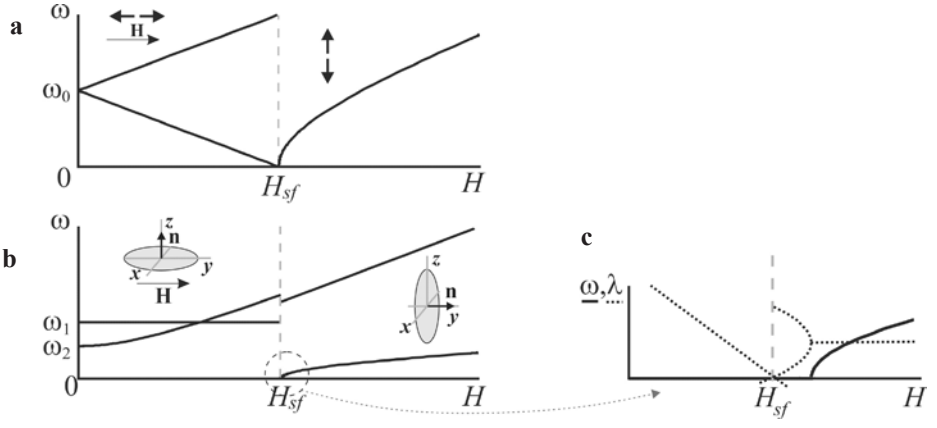

Fig. 1. a ESR spectra of collinear antiferromagnet. **b** ESR spectra of planar spiral magnet. **c** ESR spectra (solid lines) and dissipation parameter (dashed lines) in planar spiral magnet in the vicinity of critical point.

O19

Transformation of orbital moment and spin-orbit interaction induced by covalent bonding of 3d electrons with ligands

M.V. Eremin

Institute of Physics, Kazan (Volga Region) Federal University, Russia

The effects of covalent metal-ligand bonds in the compounds of 3d ions in nondegenerate orbital states are well described previously in [1]. In this work, the modification of spin-orbit coupling operators and the orbital magnetic moment of orbitally degenerate states caused by covalent bonds is discussed by the examples of $Fe^{2+}(^5E)$ and $Fe^{2+}(^5T_2)$ ions in tetrahedral and octahedral oxygen ion environments, respectively. It is known that the spin-orbit coupling parameter of the free ion $\varsigma = 404$ cm^{-1} decreases by the quantity $\Delta\varsigma$ due to covalent bonds. In addition, it is shown that an anisotropic term V_{SO} appears due to the covalent bonding of 3d electrons with ligands. It is convenient to write it down in terms of double irreducible tensor operators used in the theory of optical spectra [2]:

$$V_{SO} = \sqrt{3/7}\left(2\cdot W_{00}^{(11)} + W_{1,-1}^{(11)} + W_{-1,1}^{(11)}\right)\nu 1 + \left[-\sqrt{3/7}W_{00}^{(13)} + \sqrt{2/7}\left(W_{1,-1}^{(13)} + W_{-1,1}^{(13)}\right)\right]\nu 2$$
$$+\left[\sqrt{4/7}W_{00}^{(13)} + \sqrt{3/14}\left(W_{1,-1}^{(13)} + W_{-1,1}^{(13)}\right)\right]\nu 3 + \left[W_{03}^{(13)} + W_{0,-3}^{(13)} + \left(W_{12}^{(13)} + W_{-1,-2}^{(13)}\right)\sqrt{3}\right]\nu 4\,.$$

The parameters ν1, ν2, ν3, ν4 calculated in [3] multiplied by the corresponding reduced matrix elements

$$\left\langle d^6\,{}^5D \middle\| W^{(11)} \middle\| d^6\,{}^5D \right\rangle = \frac{3}{2}\sqrt{5},$$
$$\left\langle d^6\ D \middle\| W^{(13)} \middle\| d^6\,{}^5D \right\rangle = -\frac{1}{2}\sqrt{105}$$

are given in Table below

w, cm^{-1}	tetra	octa
$\Delta\varsigma$	–27.6	–18.9
$w1$	25.2	21.8
$w2$	108.7	97.8
$w3$	27.9	–114.5
$w4$	–36.9	–85.9

The expression for the orbital magnetic moment is deduced, which also contains additional operator forms with selection rules $\Delta M_L = 3$.

This work was supported by RNF Grant no. 19-12-00244.

1. Abragam A., Bleaney B.: Electron Paramagnetic Resonance of Transition Ions, Clarendon Press 1970.
2. Judd B.: Second Quantization in Atomic Spectroscopy, The Johns Hopkins Press, Baltimore 1967.
3. Eremin M.V., Vasin K.V., Nurmukhametov A.R.: JETP, accepted (2023)

O20

Principles and history of magnon Bose condensation discovery

Yu.M. Bunkov

Russian Quantum Center, Skolkovo, Moscow, Russia

Bose condensate is a macroscopic quantum state of matter. The explosive growth of interest to these systems is associated with the hypothetical possibility of using them for new types of quantum computations involving a macroscopic ensemble of particles. In particular, the interest to Bose condensates of magnetic excitations – magnons is connected with the variety of different states of the mBEC. In the frequently used films of yttrium iron garnet (YIG), the properties of magnons depend on the orientation of the magnetic field. When the film is magnetized in a plane, the minimum magnon energy corresponds to spin waves with a relatively large wave vector k. In this case, their state of the Bose condensate can be considered by analogy with the condensation of photons in matter. On the contrary, at an out of plane magnetized film, the minimum energy of magnons corresponds to zero k, which makes their Bose condensate similar to the atomic one. The properties of these two types of magnon BEC will be considered in the lecture.

Of particular interest to these systems is due to the fact that quantum phenomena can be observed even at room temperature, when their properties go beyond the scope of classical physics of Landau-Lifshitz-Gilbert (LLG) theory. It was first discovered in superfluid antiferromagnetic ^{3}He-B [1–3]. Upon pulsed excitation of magnetic resonance, the usual decay of the free induction signal to zero was observed. However, after a delay, the signal spontaneously recovered. The radiation of coherent state of magnons was observed, which existed 3 orders of magnitude longer than the initial induction signal. It decayed due to a decrease in the number of magnons with a simultaneous change in their chemical potential. Naturally, such behavior of the induction signal cannot be described by the semiclassical LLG theory.

The Hamiltonian of magnons in antiferromagnetic ^{3}He-B is similar to that in an out of plane magnetized yttrium iron garnet (YIG) film. Therefore, the properties of magnon Bose condensation should be similar. However, the Hilbert constant in YIG is three orders of magnitude larger than in ^{3}He-B. Consequently, it is very difficult to obtain the formation of a magnon BEC by the pulsed method. As shown in [4], at a density of excited magnons in a YIG film, corresponding to angles of deviation of the precessing magnetization of more than 3 degrees, a magnon BEC should form. We have developed an optical setup for measuring the amplitude and phase of magnetization precession using the Faraday rotation effect [5]. We carried out a specially designed experiment to test Bose magnon condensation. We used an elliptical YIG film and locally excited magnons with a strip line. We have found that at low magnon density they propagate beyond the excitation region in the form of spin waves, in full accordance with the LLG equations. We found that at a magnon density corresponding to a magnetization deviation of more than 3 degrees, the propagation pattern changes dramatically. Instead of spin waves, coherent precession appears, which demonstrates magnon condensation to Bose. However, the computer solution of the LLG equations for the experimental

O20

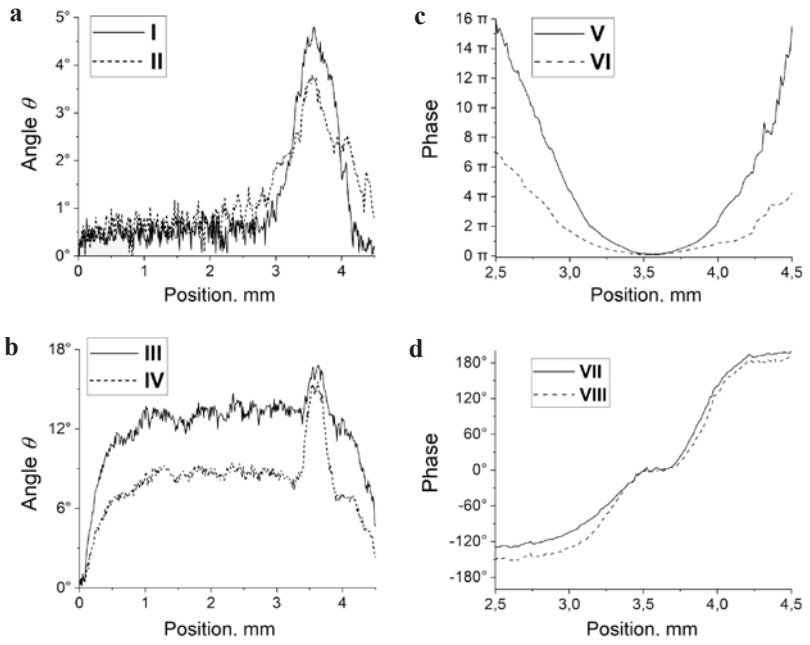

Fig. 1. (**a**)–(**b**) The spatial distribution of the magnon density in units of the magnetization deflection angle in the magnetic fields 2607 Oe and 2615 Oe at a pump energy of 0.05 mW (**a**) and 6 mW (**b**). (**c**)–(**d**) The spatial distribution of the magnon phase at fields 2615 Oe and 2607 Oe at a pump energy of 0.05 mW (**c**) and 6 mW (**d**).

conditions shows the formation of spin waves. Thus, we have shown that this result lies beyond the limits of the semiclassical LLG theory and corresponds to the quantum phenomenon of magnon Bose condensation into a coherent state.

Figure 1 (a, b) shows the spatial distribution of the magnon density at low (a) and high (b) excitation by a strip line located between 3.4 and 3.6 mm. On Fig. 1 (c, d) shows the spatial distribution of the precession phase, which corresponds to the pattern of a spin wave at low excitation (c) and a region with a coherent magnetization precession at a high magnon density (d). The magnon precession phase changes by about 180 degrees near the edge of the strip line. The phase gradient corresponds to the magnon superfluid flow and the boundary conditions on the strip line. The Bose condensation of magnons, considered in this experiment, is formed by magnons with $k = 0$. It has direct analogies with the atomic Bose condensate.

This work was supported by the Russian Science Foundation (project no. 22-12-00322)

1. Borovik-Romanov A.S. et al.: JETP Letters **40**, 1033 (1984)
2. Bunkov Yu.M.: J. Low Temp. Phys. **138**, 753 (2005)
3. Bunkov Yu.M., G.E. Volovik, Phys. Rev. Lett. **98**, 265302 (2007)
4. Bunkov Yu.M., V. L. Safonov, J. Magn. Magn. Mat. **452**, 30 (2018)
5. Petrov P.E. et al.: Optics Express **31**, 8335 (2023)

O21

Orientational ordering of graphene oxide membranes according to the data of spin probe technique and scanning electron microscopy

M.V. Matveev[1], N.A. Chumakova[1,2], N.A. Marnautov[3]

[1]M.V. Lomonosov Moscow State University, Chemistry Department, Moscow, Russia
[2]N.N. Semenov Federal Research Center for Chemical Physics of RAS, Moscow, Russia
[3]Emanuel Institute of Biochemical Physics of RAS, Moscow, Russia

Membranes formed by oxidized graphene planes (GOMs) are promising materials for water desalination and other barrier application due to their selective permeability for polar liquids and hydrated ions. It was found that more ordered GOMs pass water an order of magnitude faster than less ordered ones [1]. Until recently, ordering of GOM assessed qualitatively (visually) based on cross-section scanning electron microscopy (SEM) image. The resolution of the method allows estimating only the alignment of lamellas, while each lamella includes 15–30 oxidized graphene layers.

This report will present two novel methods that allow determining the orientational order of GOMs quantitatively. First technique is based on the analysis of EPR spectra of stable nitroxide radicals (spin probes) sorbed on inner surface of GOM. Orientational order parameters of the probes in the membrane that can be determined by joint simulation of a series of EPR spectra recorded at different orientation of the membrane relative to magnetic field lines (Fig. 1a), reflect both ordering and shape of the GO layers. Second technique is based on quantitative analysis of the cross-section SEM images of GOM (Fig. 1b) using the machine learning technology. This approach allows determining the order parameters of lamellas forming the membrane. The combined use of the described methods allows a detailed characterization of the internal structure of GOMs.

The work was supported by Foundation for Basic Research no. 23-23-0001,

1. Akbari A. et al.: Nat. Commun. **7**, no. 10891 (2016)

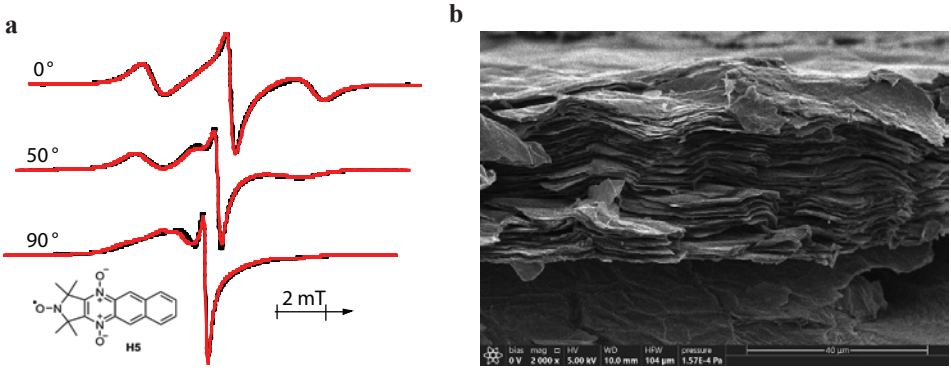

Fig. 1. a Angular dependence of EPR spectra of stable nitroxide radical in GOM; black lines – experimental spectra, red lines – result of simulation; **b** SEM microphotograph of the GOM.

O22

Study of spin centers in $TiO_2/BaTiO_3$ nanoheterostructures

E.V. Kytina[1,2], T.P. Savchuk[1,3], I.S. Kekiashkiev[1], A.V. Marikutsa[4], E.A. Konstantinova[1]

[1]Physics Department, M.V. Lomonosov Moscow State University, Moscow, Russia
[2]N.N. Semenov Federal Research Center for Chemical Physics, RAS, Moscow, Russia
[3]National Research University of Electronic Technology – MIET, Zelenograd, Moscow, Russia
[4]Chemistry Department, M.V. Lomonosov Moscow State University, Moscow, Russia

Titania (TiO_2) nanotubes is a promising material for use as photocatalyst or sensor [1]. In recent years, nanoheterostructures based on this material have been formed to improve absorption in the visible region of the spectrum and provide charge accumulation [2]. The purpose of this work was to obtain $TiO_2/BaTiO_3$ nanoheterostructures for sensor application. We have performed a study of defects (spin centers) in the structure of the samples in dark and under illumination.

The formation of TiO_2 nanotube arrays doped with carbon occurred by two-stage electrochemical oxidation of a previously prepared Ti-foil BT1-0 [2]. Nanoheterostructures $TiO_2/BaTiO_3$ were synthesized using a hydrothermal process with barium hydroxide.

The EPR spectra at 300 K were recorded with a Bruker spectrometer ELEXSYS-E500 (X-band). A xenon lamp with a total power of 500 W was used as a light source. A light flux of 100 mW/cm^2 was created through an AM1.5 filter.

The EPR spectrum of initial carbon doped TiO_2 nanotubes consists of a single line with g = 2.0027, which can be attributed to carbon dangling bonds [3]. The EPR spectrum of the $TiO_2/BaTiO_3$ samples is a superposition of several EPR lines. First of all, it is carbon dangling bond. Barium (g = 1.974) and oxygen (g = 1.958) vacancies are also detected [4].When the samples are illuminated, the intensity of EPR signals from all spin centers increases. After turning off the illumination, after about 24 hours, the intensity of the EPR signals returns to its original state. We attribute this effect to defect recharging because of its reversibility. The long relaxation time of EPR intensity is probably due to charge separation: a hole remains in titania, while an electron is injected into barium titanate. The results obtained open up new possibilities for the development of gas sensors with improved selectivity based on nanocrystalline $TiO_2/BaTiO_3$ The study was supported by a grant from Russian Science Foundation №22-73-10038.

1. Low J., Yu J., Jaroniec M., Wageh S., Al-Ghamdi, A. A.: Adv. Mater. **29**, 1601694 (2017)
2. Gavrilin I., Dronov A., Volkov R., Savchuk T., Dronova D., Borgardt N., Pavlikov A., Gavrilov S., Gromov D.: Appl. Surf. Sci. **516**, 146120 (2020)
3. Savchuk T., Gavrilin I., Konstantinova E., Dronov A., Volkov R., Borgardt N., Maniecki T., Gavrilov S., Zaitsev V.: Nanotechnology **33**, 55706 (2022)
4. Lu B., Zheng Y., Yuan L.: Materials **12**, 1525 (2019)

O23

Superoxide generated in alkaline TiO_2 powder

R.I. Samoilova[1], S.A. Dikanov[2]

[1]Voevodsky Institute of Chemical Kinetics and Combustion, Russian Academy of Sciences, Novosibirsk, Russia
[2]Department of Veterinary Clinical Medicine, University of Illinois at Urbana-Champaign, Urbana, Illinois, USA

The properties of a superoxide anion depend on the local positive charge, near which it is usually stabilized on a solid surface [1]. In this work, to generate the superoxide radical, we used a catalyst obtained by treating $Ti(OR)_4$ (R = iPr, nBu) with hydrogen peroxide H_2O_2, which is used as a selective heterogeneous catalyst for the oxidation of organic compounds [2]. Our experiments with $TO_2…O_2^{\bullet-}$ catalyst obtained with the joint addition of peroxide and KOH solution of alcohol show the formation of the superoxide radical with the atypical g_{zz} = 2.10 [3]. Similar EPR signal was previously observed in various systems containing alkaline ions that allowed us to suggest the special role of K^+ ions in the $O_2^{\bullet-}$ stabilization. However, ^{39}K nucleus(i) did not produce any resolved features in reported EPR spectra. Therefore, we applied 2D HYSCORE spectroscopy to characterize hyperfine interactions between $O_2^{\bullet-}$ and the ^{39}K and ^{1}H nuclei in its environment. Q-band HYSCORE spectra have shown the presence of ^{39}K near the superoxide. Comparison of the magnetic characteristics and electronic configuration defining isotropic coupling of ^{39}K with ^{23}Na in Na coated MgO [4] allowed us to predict significantly smaller ^{39}K hyperfine couplings for the similar structural MO_2 motifs. Estimated values give reasonable agreement between calculated and experimental ^{39}K HYSCORE spectra. Other finding for this superoxide is the existence of a strongly coupled ^{1}H with the anisotropic coupling $T \sim 7$ MHz, which suggests the formation of a H-bond with O-H distance < 2 Å. So far, the interaction with closely located alkaline ion and strongly coupled proton $T \sim 10$ MHz has been reported for $O_2^{\bullet-}$ on Na/MgO only. However, two different $O_2^{\bullet-}$ species with g_{zz} = 2.014 and 2.091 were present in this sample and strongly coupled ^{23}Na with a = 15 MHz and the ^{1}H with anisotropic coupling T = 9.8 MHz were assigned to different species $O_2^{\bullet-}$/NaMgO and $O_2^{\bullet-}$/HMgO, respectively. Only one type of $O_2^{\bullet-}$/$KTiO_2$ species with g_{zz} = 2.10 was found in our work. It means that signals from ^{39}K and a strongly coupled proton with $T \sim 7$ MHz in HYSCORE spectra are produced by interactions with this $O_2^{\bullet-}$ and should be considered as the elements of its structure. Therefore, independent data to support the hypothesis that the presence of a stable superoxide in systems containing alkali metals requires the simultaneous proximity of M+ ion(s) and the formation of a hydrogen bond with its environment still needed [5].

1. Anpo M., Che M., Fubini B., Garrone E., Giamello E., Paganini M.C.: Topics in Catalysis **8**, 189–198 (1999)
2. Dewkar G.K., Nikalje M.D., Sayyed Ali I., Paraskar A.S., Jagtap H.S., Sudalai A.: Angew. Chem. Int. Ed. Engl. **40**, 405–408 (2001)
3. Samoilova R.I.: Dikanov S.A.: Appl. Magn. Reson. **53**, 1089–1104 (2022)
4. Napoli F., Chiesa M., Giamello E., Preda G., Di Valentin C., Pacchioni G.: Chem. Eur. J. **16**, 6776–6785 (2010)
5. Samoilova R.I., Dikanov S.A.: Inorganics **11**, 274 (2023)

O24

Phase transitions in Sr_2FeNbO_6 double perovskites

R.M. Eremina[1,2], D.V. Popov[1], R.G. Batulin[2], I.V. Yatsyk[1], F.G. Vagizov[2], A.L. Zinatullin[2], M.A. Cherosov[2], T.I. Chupakhina[3], Yu.A. Deeva[3], T. Maiti[4]

[1]Zavoisky Physical-Technical Institute, FRC Kazan Scientific Center of RAS, Kazan, Russia, e-mail: REremina@yandex.ru
[2]Kazan (Volga Region) Federal University, Kazan, Russia
[3]Institute of Solid State Chemistry of the Russian Academy of Sciences (UB), Ekaterinburg, Russia
[4]Department of Materials Science and Engineering Indian Institute of Technology Kanpur, Kanpur, India

Perovskites are oxides with formula ABO_3, where A is alkaline earth metal ion, B is transition metal ion. Perovskites have octahedral oxygen framework built around B ions. Those frameworks surround A ions in hexagonal (cubic) formation [1]. Double perovskites are a type of perovskites that simultaneously consist of two of the above formulas. The ions in double perovskites usually have a mixed valence. The magnetic properties of perovskites strongly depend on their composition. Their major difference double perovskites $A_2B'B''O_6$ from complex single perovskites is an ordering in the arrangement of B′ and B″ ions, B′ or B″ ions can be form chains or plane.

The aim of this work is investigation of magnetic, transport and ESR properties of Sr_2FeNbO_6 double perovskite. Polycrystalline powders of $Sr_2FeNbO_{6-\delta}$ perovskite were synthesized via the solution combustion precursor method. Temperature dependencies of specific heat were measured for the $Sr_2FeNbO_{6-\delta}$ ceramic in the temperature range of 4–300 K at 0 and 9 T. The Mössbauer spectra of $Sr_2FeNbO_{6-\delta}$ were measured in the temperature range from 7 K to room temperature. It follows from low-temperature Mössbauer measurements (at T = 7 K) that the sample contains two types of magnetic structures that differ in the length and strength of magnetic antiferromagnetic correlations. The observed asymmetry of the Mössbauer spectra at room temperature can be associated with the presence in the sample of centers of iron atoms Fe_1^{3+} and Fe_2^{3+} with different local environments. The isomer shift and the average value of the quadrupole shift at room temperature for Fe_1^{3+} are IS = 0.35(6) mm/s and $\langle\varepsilon\rangle$ = 0.19(8) mm/s, respectively. The Fe_1^{3+} contributes to the 61% of the total spectrum area. It was found that the hyperfine parameters for the Fe_2^{3+} center are IS = 0.37(4) mm/s and $\langle\varepsilon\rangle$ = 0.32(0) mm/s. The two-peak structure of the magnetic contribution to the specific heat and an asymmetric doublet in the Mössbauer spectra indicate the phase separation in two subsystems.

The Curie-Weiss temperature Θ_{CW} = 60 K was determined from the approximation of the temperature dependence of the inverse susceptibility by Curie-Weiss low. The exchange integral calculated from the temperature dependence of the integral intensity and the Curie-Weiss temperature agree and equal J/k_B = 10 K. The negative Curie-Weiss temperature indicates the antiferromagnetic nature of the exchange interactions between the iron spins. The phase separation is confirmed by the observation of two EPR lines in ceramics. The observation of peaks in the real part of AC magnetization and the absence of peaks in the imaginary part and hysteresis loops confirm the canted antiferromagnetic ordering to quasi one-dimensional states in two subsystems at ~29 K and ~10 K.

This research was supported by the RSF (Project No. 22-42-02014).

1. Bhalla A., Guo R., Roy R.: Materials Research Innovations **4**, 3–26 (2000)

O25

Mobility of polar liquids intercalated into the inter-plane space of graphite oxide as revealed by EPR spin probe technique

D.A. Astvatsaturov[1,2], N.A. Chumakova[1,2]

[1]N.N. Semenov Federal Research Center for Chemical Physics, Russian Academy of Science, Moscow, Russia, e-mail: ASTVaaaa@yandex.ru
[2]M.V. Lomonosov Moscow State University, Chemistry Department, Moscow, Russia

Graphite oxide (GO) – a layered non-stoichiometric derivative of graphite – easily swells in polar liquids. Swelling leads to the intercalation of liquids into the inter-plane space of the material. GO/water suspensions are used to obtain graphene oxide membranes (GOMs) – thin layered films, which are perspective materials for filtering and separation of polar liquids mixtures. It is known that GOMs possess unique separation selectivity: the permeability for water is much higher than for ethanol, methanol and other polar liquids. The key to this phenomenon seems to be an understanding of properties of liquids inside GO. The goal of this contribution is to study the mobility of polar liquids of different nature (acetonitrile, methanol, ethanol, and water) inside GO, and to reveal the correlation between the intercalated liquids mobility and their ability to permeate through GO membranes. The mobility of intercalated liquids was estimated on the basis of the mobility of TEMPO radicals inserted in between the GO planes.

We found out that all liquids under study form inside GO two fractions with different mobility – solid-like and liquid-like. The relative amount of these fractions depends on temperature and amount of intercalated substance. The liquid-like fraction possesses much lower mobility if to compare with the corresponding bulk liquid. The rotational mobility of methanol and ethanol was found to be is nearly the same but it is higher than for acetonitrile. This is intriguing due to the fact that viscosity of the bulk methanol and ethanol is higher than viscosity of acetonitrile. The mobility of intercalated water was found to be close to the mobility of intercalated ethanol and methanol in wide temperature range.

This work was supported by Russian Scientific Foundation (grant No. 23-23-00016).

O26

Study of helium-3 nuclear relaxation mechanisms in contact with DyF_3 nanoparticles

A.M. Garaeva, E.M. Alakshin, E.I. Boltenkova, K.R. Safiullin, I.V. Romanova

Kazan Federal University, Kazan, Russia

Helium-3, due to its small molecular size, non-zero spin, and the ability to remain liquid at sufficiently low temperatures, is of great interest. This compound can be used as a model system in the study of relaxation mechanisms due to the large opportunities for changing the parameters and experimental conditions. Thus, rather long relaxation times of liquid helium-3 begin to shorten due to wall relaxation [1] or fast diffusion [2].

Of particular interest is the relaxation of helium-3 near paramagnetic centers, which create local magnetic fields, thereby affecting the rate of relaxation of the system. When considering a helium-3 system in contact with paramagnetic particles, relaxation will also depend on the concentration of paramagnetic particles and on the particle size. The study of these processes is extremely important for understanding the mechanisms of liquid relaxation near paramagnetic particles, which can later be used for a more detailed study of the magnetic properties of magnetic particles, as well as for the development of MRI contrast agents.

Dysprosium fluoride is a dipole ferromagnet with an easy magnetization axis along the [010] axis of the crystal lattice; the Curie temperature is 2.55 K along the [010] axis for a single crystal [3]. The compound has unique properties due to which it can be used as a high-field MRI contrast agent [4] and as an additive to Nd-Fe-B magnets to increase the coercive force [5].

In this work, we measured the rates of longitudinal and transverse relaxation of helium-3 nuclei in contact with 20 nm DyF_3 (99.67%) and LaF_3 (0.33%) powder in the adsorbed layer, in the liquid bulk, and in the case of coating particles with a helium-4 layer depending on the temperature in the range 1.5–3 K in the fields of 173 and 505 mT. In the case of liquid helium-3, in the absence of helium-4 coating of particles, a two-component relaxation of the longitudinal and transverse magnetization is observed.

For explanation this phenomenon theoretical model was proposed. Calculations of longitudinal and transverse relaxation times were made based on the Hamiltonian of the dipole-dipole interaction between a ^3He nucleus and Dy^{3+} ions. Theoretical values are in good agreement with the experimental ones.

This work was supported by the Russian Science Foundation (Project No. 23-72-10039).

1. Lefevre V.: Contribution à l'étude de l'hélium-3 polarisé gazeux. I. Relaxation à la surface de H_2 solide. II. Relaxation en volume: effets quantiques d'indiscernabilité : diss. Université Pierre et Marie Curie-Paris VI, 1984.
2. Lusher C.P., Secca M.F., Richards M.G.: Journal of low temperature physics **72**, 71–97 (1988)
3. Savinkov A.V., Korableva S.L. et al.: Journal of Physics: Condensed Matter **48** (20), 485220 (2008)
4. González-Mancebo D., Becerro A.I., Rojas T.C. et al.: Particle & Particle Systems Characterization **10** (34), 1700116 (2017)
5. Xu F., Zhang L., Dong X. et al.: Scripta Materialia **12**(64), 1137–1140 (2011)

O27

Application of a pH-sensitive spin label in the EPR study of the ionized state of the active site in the Fpg-DNA complex

I.A. Litvinov[1,3], S.S. Ovcherenko[1,3], N.A. Bulgakov[2,3], I.A. Kirilyuk[1], D.O. Zharkov[2,3], E.G. Bagryanskaya[1]

[1]N.N. Vorozhtsov Novosibirsk Institute of Organic Chemistry, Novosibirsk, Russia
[2]SB RAS Institute of Chemical Biology and Fundamental Medicine, Novosibirsk, Russia
[3]Novosibirsk State University, Novosibirsk, Russia

DNA-formamidopyrimidine glycosylase – Fpg is an enzyme recognizing and excising oxidized purine bases of bacterial DNA as a base excision repair step. The amino acid region Pro1-Glu2 is known to be important for Fpg glycosylase activity. Any mutation of the amino acid fragment leads to loss of the protein activity. Interestingly, molecular dynamics simulations have shown significant changes in electrostatic interactions in the active site of the Fpg-DNA complex when Glu2 is replaced by Gln2 (E2Q mutation) [1]. However, it has not yet been proven by experimental methods. One possible way to study such a local phenomenon is the application of pH-sensitive spin labels combined with EPR [2]. Taking into account the property of Fpg to form specific complexes with DNA with a single strand gap we have designed DNA duplexes with a gap in one of the strands and covalently bound a pH-sensitive spin label to 5′ or 3′ ends surrounding the gap. According to our expectations in one of the options the spin label could get in the gap and turn out inside the active site of Fpg during the complex formation. As soon as the label is inside the active site any differences in local electrostatics in the wild-type Fpg and in inactivated mutant – E2Q would be visible in the EPR spectra.

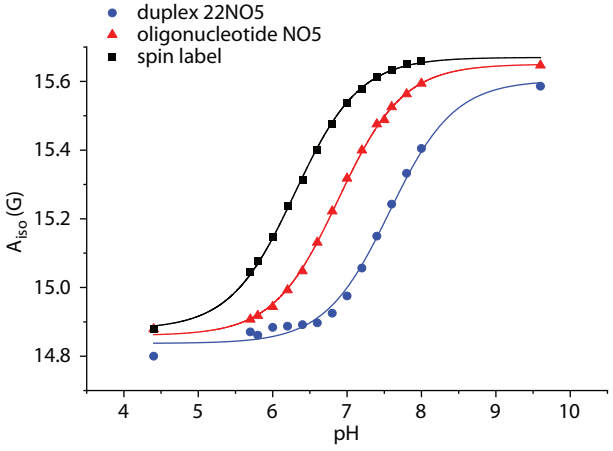

Fig. 1. Comparison of pH calibration curves for samples of spin label, oligonucleotide with spin label and duplex with spin label.

O27

We examined the applicability of the method for determining the local electrostatic differences in the active site of the wild-type Fpg and E2Q. The spin label applied has demonstrated pH-sensitivity in the physiological pH range. The range shifts towards higher pH values when the spin label is attached to the oligonucleotides and DNA duplexes (Fig. 1). The EPR spectra have shown the appearance of the spectral component corresponding to an immobile spin label when Fpg or E2Q are added to the spin labeled DNA duplexes. Thus, we have established the fact of the complexes formation. Unfortunately, the results of EPR measurements at pH = 7.5 do not provide unambiguous conclusion about the electrostatic difference in the active sites of Fpg and E2Q.

1. Perlow-Poehnelt R.A. et al.: Biochemistry **43** (51) 16092–16105 (2004)
2. Voinov M., Smirnov A.: Electron Paramagnetic Resonance **22**, 71–106 (2011)

O28

Inner structure and sorption properties of graphene oxide membranes according to EPR and sorption experiments

A.V. Kaplin[1,2], N.A. Chumakova[1,2], E.A. Eremina[2], A.T. Rebrikova[2], M.V. Matveev[2], M.V. Korobov[2]

[1]N.N. Semenov Federal Research Center for Chemical Physics, Russian Academy of Science, Moscow, Russia
[2]M.V. Lomonosov Moscow State University, Chemistry Department, Moscow, Russia

Graphite oxide is a layered material obtained by oxidation of graphite in an acidic environment. There are two main ways to obtain graphite oxide – Hammers' and Brodie's methods. The materials obtained by these methods (HGO and BGO) differ in degree of oxidation, composition of the oxygen-containing groups as well as ability to swell in polar liquids; HGO swells more compared to BGO. The membranes prepared from graphite oxide are capable of retaining gases and sorbing, separating, and purifying many polar liquids.

At present work, the data on sorption of acetonitrile and water by HGO and BGO, as well as by membranes manufactured from these powders by vacuum filtration method, was obtained, and compared with the orientational order of the membranes. Ordering of the graphene oxide layers in the membranes was determined using spin probe technique. The orientational order parameters of spin probes in various membranes were found to be significantly different and were in the range of P_{20} = 0.2–0.5. Also it was shown that the equilibrium sorption values for acetonitrile at room temperature were different as for different membranes and for membranes and corresponding powders. In contrast, the equilibrium sorption values for water were the same for graphite oxide powders and all membranes formed from these powders.

The experimental data obtained [1] indicate that the sorption properties of graphene oxide membranes depend on their internal structure; however, this dependence is complex and requires further study.

This work was supported by RSF (grants 22-29-00544 and 23-23-00016).

1. Kaplin A.V. et al.: Membranes **13** (2023)

O29

Application of ^{13}C isotopomers of triarylmethyl radicals in the study of penetration of the unstructured RL2 protein into cancer cells

A.E. Raizvikh[1,3], S.S. Ovcherenko[1,3], O.A. Chinak[2], K.A. Lomanovich[1], O.Yu. Rogozhnikova[1], D.V. Trukhin[1], V.M. Tormyshev[1], E.G. Bagryanskaya[1]

[1]N.N. Vorozhtsov Novosibirsk Institute of Organic Chemistry, SB RAS, Novosibirsk, Russia
[2]SB RAS Institute of Chemical Biology and Fundamental Medicine, Novosibirsk, Russia
[3]Novosibirsk State University, Novosibirsk, Russia

Stable nitroxyl and triarylmethyl radicals occupy a special place among the objects studied by the EPR method, due to which the EPR method has been widely used in biophysical studies. Stable nytroxyl radicals are widely being used as mediators of controlled radical polymerization, redox catalysis, magnetochemistry and spintronics. Other important uses of nitroxyl radicals have been their application as spin probes and spin labels to study the structure and functions of biopolymers. Nitroxyl radicals (NR) are stable with respect to oxygen and heating. The main areas of their application as spin probes are works on the study of pH and oxidation processes.

At the same time a new type of radicals (triarylmethyl type) (TAM) was synthesized in 1998. Triarylmethyl radicals were created with the purpose of using them as polarizing contrast agents for magnetic resonance imaging [1]. The study of their properties, including high stability in living organisms, long electron spin relaxation time, very narrow lines in the EPR spectrum, led to their use as probes for oximetry and measurement of distances in biopolymers [2, 3]. A number of new radicals representing isotopomers of Finnish trityl (Finland, FT) and OX063 have been synthesized in recent works of Benoit et al. and in NIOC SB RAS [4, 5]. The obtained triarylmethyl radicals not only have the properties of their precursors, but are also sensitive to the changes in the nature of the mobility of the molecule (rotational correlation time). Therefore, new radicals are promising compounds in the study of the viscosity of various media.

This work is devoted to the study of the isotopomers FT and OX063 and their applications in the viscosity measurement of media, as well as investigating their stability under intracellular conditions. EPR spectroscopy was used to study the mobility of TAM isotopomers and the mechanism of penetration of a spin label based on TAM and disordered RL2 protein into A549 human lung cancer cells. The stability of FT and OX063 isotopomers with nitroxy stereosubstituted radicals was compared in living cells.

1. Ardenkjaer-Larsen J.H., Laursen I., Leunbach I., Ehnholm G., Wistrand L.-G., Petersson J.S., Golman K.: JMR **133**, 1–12 (1998)
2. Liu Y, Villamena FA, Sun J, Wang T, Zweier JL.: Free Rad. Biol. Med. **46**, 876–883 (2009)
3. Reginsson GW, Kunjir NC, Sigurdsson ST, Schiemann O.: Chem. Eur. J. **18**, 13580–13584 (2012)
4. Poncelet M, Driesschaert B.: Angew. Chem. **132**, 16593–16596 (2020)
5. Poncelet M., Ngendahimana T., Gluth T.D., Hoblitzell E.H., Eubank T.D., Eaton G.R., Eaton S.S., Driesschaert B.: Analyst **147**, 5643–5648 (2022)

O30

Obtaining high-resolution NMR spectra inside a working heterogeneous reactor

E.S. Kononenko[1,2], I.V. Koptyug[2]

[1]Novosibirsk State University, Novosibirsk, Russia
[2]International Tomography Center SB RAS, Novosibirsk, Russia

Nuclear magnetic resonance (NMR) has established itself as a highly informative method not only in biomedical research, but also for the catalytic reactors study. The state of the art in this area is the study of heterogeneous catalytic processes in the gas phase during reactor operation. To obtain a signal of sufficient intensity in the study of a gas, spin hyperpolarization methods are used, for example, parahydrogen-induced polarization (PHIP). This method increases the signal intensity and greatly facilitates the experiments in the gas phase [1].

However, in order to study an operating reactor, for example, to determine the areas of overheating of the catalytic pellets, or to obtain product distribution maps, it is necessary to place the reactor directly inside an NMR spectrometer. This mode of obtaining a hyperpolarized signal by the PHIP method is called PASADENA. It is distinguished by an antiphase line shape (i.e., each group of signals has an absorption and an emission parts). It is important to point out that heterogeneous catalyst granules placed in a magnetic field distort its uniformity. In turn, the magnetic field inhomogeneity leads to line broadening in the NMR spectra, which, in addition to a major loss of spectral resolution, results in a dramatic drop in intensity of antiphase spectra due to the mutual compensation of the positive and negative components of the NMR signals. Therefore, for the studies of gas-phase catalytic processes by NMR methods with the

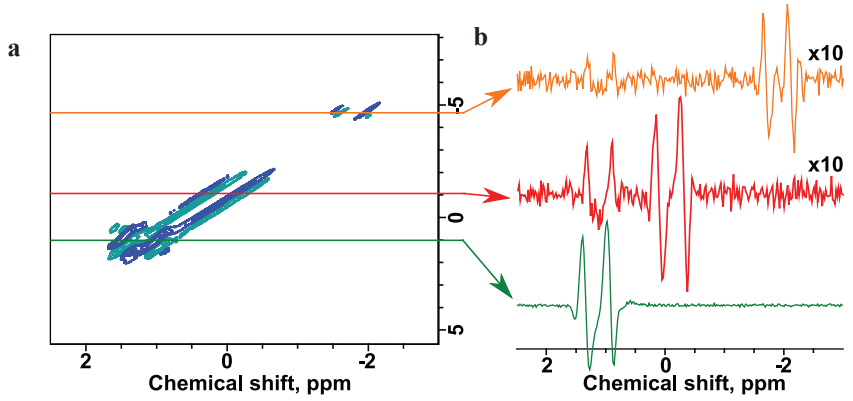

Fig. 1. a 2D NMR spectrum of hyperpolarized propane obtained using the COSY pulse sequence (blue corresponds to the positive part of the signal, light blue – negative). **b** One-dimensional slices of the 2D NMR spectrum of hyperpolarized propane in an inhomogeneous magnetic field.

involvement of PHIP, it is necessary to develop a technique for obtaining well-resolved NMR spectra independent of magnetic field inhomogeneity.

A possible solution to this problem is the use of pulse sequences that generate multi-quantum coherences. A combined use of the COSY pulse sequence with phase cycling makes it possible to obtain a signal that originates from a double-quantum coherence only. Theoretical simulations demonstrate that such signals with different offsets from the resonance frequency are distributed along the sloping line in the two-dimensional (2D) spectrum. Thus, each slice taken along the second direction of the 2D spectrum gives a one-dimensional (1D) high-resolution spectrum, in which the line broadening due to magnetic field inhomogeneity is dramatically reduced.

To verify this experimentally, a model reactor with a layer of catalytically active granules was placed inside an RF probe. It created a chaotic inhomogeneous magnetic field, which cannot be compensated by shimming coils. Despite this, we obtained a 2D spectrum by selecting a double-quantum coherence only, which made it possible to obtain high-resolution 1D spectrum of hyperpolarized propane inside the working heterogeneous reactor (Fig. 1) with the antiphase structure of the multiplets preserved. Thus, the results obtained show the possibility to use this approach for operando studies of heterogeneous gas-phase hydrogenation reactors.

This work was supported by the Russian Science Foundation (grant # 23-23-00394).

1. Kononenko E.S., Svyatova A.I. et al.: J. Phys. Chem. C. **126**, 14914–14921 (2022)

O31

Behavior of TAM-radicals with a piperazine linker as a 5′-label for distance measurements in DNA duplexes by ^{19}F-ENDOR and MD

N.B. Asanbaeva[1], D.S. Novopashina[2], O.Yu. Rogozhnikova[1], V.M. Tormyshev[1], A. Kehl[4], A.A. Sukhanov[3], A.V. Shernyukov[1], A.M. Genaev[1], A.A. Lomzov[2], M. Bennati[4,5], A. Meyer[4,5], E.G. Bagryanskaya[1]

[1]N.N. Vorozhtsov Novosibirsk Institute of Organic Chemistry SB RAS, Novosibirsk, Russia
[2]Institute of Chemical Biology and Fundamental Medicine SB RAS, Novosibirsk, Russia
[3]Zavoisky Physical-Technical Institute, FRC Kazan Scientific Center of RAS, Kazan, Russia
[4]Research Group EPR Spectroscopy, Max Planck Institute for Multidisciplinary Sciences, Göttingen, Germany
[5]Institute of Physical Chemistry, Department of Chemistry, Georg August University of Göttingen, Göttingen, Germany

Stable organic radicals are widely used as labels for studying the structure and properties of biological molecules. Electron paramagnetic resonance (EPR) based pulsed dipolar spectroscopy has become an effective tool for measurement of nanometer distances in the range 1.8–16.0 nm in biomolecules. Nonetheless, shorter distances are less accessible due to addition of a substantial spin exchange interaction to the dipole–dipole interaction, and because a rather strong microwave field is required to attain proper modulation depth. Shorter distances can be obtained using ^{19}F ENDOR. In this case [1], TAM-radicals have an advantage as spin-labels due to narrow EPR lines, their long electron-spin relaxation times and a small *g*-anisotropy.

The interaction of TAM and a terminal base pair generally could affect the real distance distribution in DNA. In this work, we explore the application of ^{19}F ENDOR experiments to study TAM and 19F spin-labeled DNA duplexes. We use a combination of an oligonucleotide spin-labeled with TAM-based radicals 5′ ends (Finland trityl and OX063 as labels with the same piperazine linker) and a complementary oligonucleotide mono-fluorine spin-labeled at two positions.

For all labeled DNA duplexes, we obtained resolved Mims ENDOR spectra. This allowed us to compare the experimental results and molecular dynamic simulation-based (MD)-results for labels of different types with each other (Example see Fig. 1). It turned out that the influence of the linker's configuration on the trajectory of the MD simulation is much stronger than that of the chiral configuration of the trityl core. Overall, the comparison showed good agreement between the spectra based only on MD simulations and the experimental spectra. Regardless of the type of TAM radical (hydrophobic Finland and hydrophilic OX063), a similar pattern in the ENDOR-spectra are obtained, which agrees well with their similar behavior in MD simulations. The formation of flexible capping structures is observed in MD simulations for both type of TAM radicals. These structures make the major contribution to the "experimental doublet" of the Mims ENDOR-spectra.

The stabilizing interactions between TAM and the terminal base pair in such structures work effectively only in the case of the cis-configuration of the piperazine linker. The nature of such interactions for considering types of radicals is different.

O31

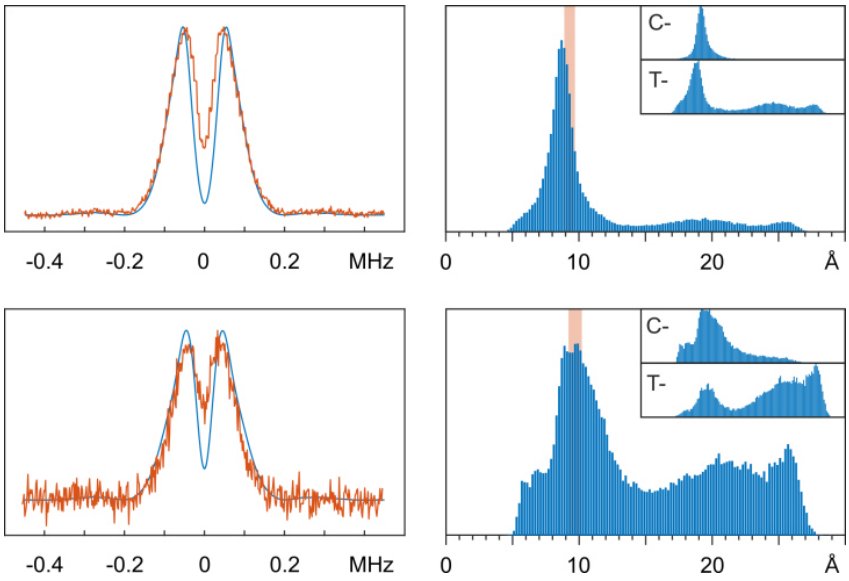

Fig. 1. Left: Example of a comparison of the simulated Mims ENDOR spectra (blue curve) with experiments (orange curve); Right: the corresponding pair distance distributions between the F atom and a central carbon atom of the trityl group used for the simulations. DNA part is the same, but TAM part is different (Top: Finland trityl; Bottom: OX063). The insets present the distributions for the cis- ("C-") and trans-("T-") linker configuration separately. The orange region in a distribution marks the interval determined from the difference between the peaks of the experimental "doublet".

For Finland trityl, this can be explained by hydrophobic interactions, while this is not possible for hydrophilic OX063. In the latter case, the analysis of trajectories shows that in flexible capping structures there is a successive relay-race formation-breaking a few of weak hydrogen bonds between OX063 and of terminal duplex base pairs. This phenomenon could explain the stabilization in the case of OX063. The observed hydrogen bonding patterns are radically different for the cis-configuration from the trans-configuration and show interactions leading to greater stabilization of the capping structures for the former.

More information can be found in the published article [2].

1. Asanbaeva N.B. et al. : Phys. Chem. Chem. Phys. **24**, 5982–6001 (2002)
2. Asanbaeva N.B. et al. : Phys. Chem. Chem. Phys. doi:10.1039/D3CP02969G (2023)

O32

Helium-3 nuclear magnetic resonance in contact with rare-earth trifluoride particles

E.M. Alakshin, A.M. Garaeva, E.I. Boltenkova, V.V. Kuzmin, K.R. Safiullin, I.V. Romanova

Kazan Federal University, Kazan, Russia

Helium-3 has unique properties such as good permeability, liquid state at low temperatures, and non-zero nuclear spin, which make it of great interest, especially when considering nuclear magnetic relaxation. In this work, the relaxation of helium-3 nuclei in contact with different rare-earth trifluoride particles will be considered.

For LaF_3 particles, the relaxation of helium-3 on the surface of these particles, in the gaseous and liquid state of helium-3 in contact with these particles, was considered. In all these states the dominant contribution to relaxation is made by relaxation in the adsorbed layer due to the modulation of dipole-dipole interaction by the quantum motion in the adsorbed two-dimensional film. The times of longitudinal and transverse relaxation depend differently on the external magnetic field. For example, the longitudinal relaxation time depends linearly on the field, while the transverse relaxation time does not depend on the external magnetic field at all.

The presence of close frequencies of transitions between energy levels in the ^{141}Pr nuclei of PrF_3 and ^3He particles makes it possible to exist cross-relaxation in nuclear spin-lattice relaxation. The analysis of obtained data for PrF_3 nanoparticles testifies in favor of cross-relaxation presence in the nuclear spin-lattice relaxation data, which takes place between ^3He and ^{141}Pr nuclei. It was shown that relaxation of the longitudinal magnetization of ^3He nuclei in contact with PrF_3 in external magnetic field occurs through two channels: a high-field relaxation due to the ^3He atoms motion in local field inhomogeneities and low-field relaxation via adsorbed layer.

In case helium-3 nuclei in contact with DyF_3 particles a ferromagnetic phase transition can be observed in the solid matrix. Near the phase transition, fluctuations of the magnetic field induced by Dy^{3+} ions in DyF_3 particles increase, which affects the spin kinetics of helium-3 nuclei. The magnetic relaxation of powders of a mixture of DyF_3 and LaF_3 of different sizes (5 nm–3 μm) was studied at temperatures of 1.5–3 K in different magnetic fields. The phase transition can only be detected for sufficiently large particles, and no anomalies have been found for small particles near the temperature of ferromagnetic ordering. This agrees with the study that with a decrease in the particle size, the phase transition temperature shifts according to a power law, and for sufficiently small particles the Curie temperature goes beyond the region of the measured temperatures. The maximum in the temperature dependence of the relaxation rate shifts with a change in external magnetic fields. The relaxation rate also changes when the particles are covered with nitrogen layers. A possible explanation for these phenomena is proposed.

This work was supported by the Russian Science Foundation (Project No. 23-72-10039).

O33

Submillisecond charge-carrier spin relaxation in $CsPb(Cl,Br)_3$ perovskite nanocrystals in a glass matrix measured by hybrid radiooptical technique

M.L. Skorikov[1], V.V. Belykh[1], E.V. Kulebyakina[1], E.V. Kolobkova[2,3], M.S. Kuznetsova[4], M.M. Glazov[5], D.R. Yakovlev[1,5,6]

[1]P.N. Lebedev Physical Institute, Russian Academy of Sciences, Moscow, Russia
[2]St. Petersburg State Institute of Technology (Technical University), St. Petersburg, Russia
[3]Research Center for Optical Materials Science, ITMO University, St. Petersburg, Russia
[4]Spin Optics Laboratory, St. Petersburg State University, St. Petersburg, Russia
[5]Ioffe Institute, Russian Academy of Sciences, St. Petersburg, Russia
[6]Experimentelle Physik 2, Technische Universität Dortmund, Dortmund, Germany

Lead halide perovskite (LHP) nanocrystals (NCs) have emerged in the past years as a material platform offering much promise in light-emission and other optoelectronic applications (see, e.g., [1]). The spin properties of charge carriers in LHPs and LHP NCs have recently also attracted much interest (see [2] and references therein).

Here, we investigated the charge-carrier spin states and spin relaxation in $CsPb(Cl,Br)_3$ NCs embedded in a fluorophosphate glass matrix [3]. We found that a state with an unusually small g factor ($|g| = 0$–0.07) exists in this system, and the longitudinal spin relaxation time T_1 for this state is unusually long (hundreds of μs).

The hybrid radiooptical technique described in [4] was used to investigate the spin properties of charge carriers in the material under study. An elliptically polarized laser beam, tuned into optical resonance with the NC exciton transition, was passed through the sample. The circular and linear polarization components of this beam served, respectively, to pump the nonequilibrium spin polarization in NCs and to probe it by measuring the Faraday rotation angle. The sample was placed in an optical helium-flow cryostat where its temperature T could be varied between 5 and 300 K. A constant magnetic field was applied to the sample at an angle (typically 45°) to the light beam using a permanent magnet outside the cryostat. A miniature coil (1 mm inner diameter) placed next to the sample inside the cryostat was used to apply a radiofrequency (rf) magnetic field ($f_{rf} = 0.1$–150 MHz) oriented along the laser beam direction. If f_{rf} is close to the Larmor frequency f_L of the charge carriers in NCs, the rf magnetic field effectively destroys the optically induced spin polarization. The rf field amplitude was modulated in the kHz frequency range, and the resulting differential Faraday rotation signal was measured by a lock-in amplifier. An important additional advantage of the described technique is that the relaxation times T_1 characterizing the observed rf resonances can be determined in a spectrally-selective manner using the spin inertia effect (see below).

The optically detected magnetic resonance (ODMR) curves at different values of the constant magnetic field B can now be recorded by measuring the Faraday signal as a function of f_{rf} for different distances between the magnet and the sample. A typical curve thus obtained represents a broad asymmetric peak that shifts to higher frequencies and becomes broader and lower with increasing B. The magnetic-field dependence of the ODMR curve peak position is shown in Fig. 1. Two features of this plot are noteworthy: (i) the g factor obtained in this way is very small (the apparent $g \approx 0.07$,

O33

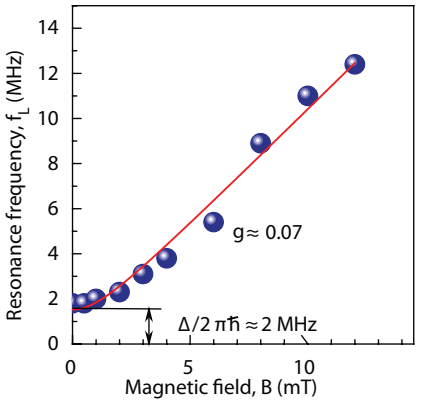

Fig. 1. Magnetic-field dependence of the ODMR peak position (T = 5 K). The line shows the fit to the experimental data by the equation $f_L = \sqrt{\Delta^2 + (g\mu_B B)^2}/2\pi\hbar$.

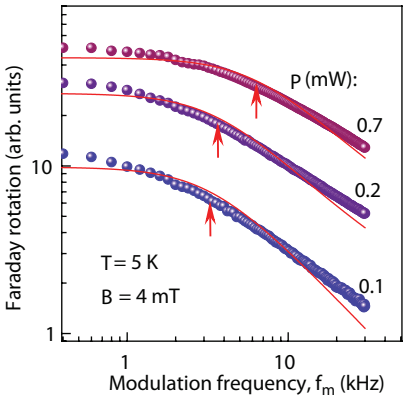

Fig. 2. Faraday rotation signal versus the rf field modulation frequency (spin inertia curves) for different laser powers (T = 5 K). Lines show fits of the experimental data by $S = A/\sqrt{1+(2\pi T_1 f_m)^2}$.

while the electron and hole g factors in LHPs are typically on the order of 1) and (ii) there is a frequency offset of about 2 MHz at zero magnetic field.

The above results can be understood if we assume that the observed resonance corresponds to transitions between NC exciton states with zero component of the total momentum along the magnetic field. Then, the observed g factor is actually the difference between those of the electron and hole, which can be quite small. Meanwhile, the frequency offset equals the exchange splitting Δ between the exciton states with total momentum J = 1 and J = 0. A model based on this picture describes the experimental data (i.e., the shape of ODMR curves at different magnetic fields B) reasonably well if the significant inhomogeneous broadening is taken into account. In particular, the latter is responsible for a considerable deviation between the value of the g factor seen in Fig. 1 and the average value obtained from the fit ($g \approx 0.01$).

The longitudinal relaxation time T_1 corresponding to the observed spin transitions can be determined by taking measurements for different frequencies f_m of the rf field amplitude modulation: the signal is maximum when $f_m \ll 1/T_1$ and starts to decrease (and acquires a phase shift) owing to the spin inertia effect [5] when $f_m \geq 1/T_1$ (Fig. 2). The behavior of the signal amplitude and phase as a function of the modulation frequency depends on the character of level broadening [4]. The fits shown in Fig. 2 correspond to the simplest case and are reasonably good. The relaxation times obtained in this way vary greatly across the inhomogeneous ensemble of NCs. At T = 5 K, T_1 equals tens of μs at the ODMR curve peak, but increases to as long as 700 μs for smaller values of the effective g factor. At elevated temperatures, T_1 decreases quite rapidly (an order of magnitude at T = 20 K).

1. Akkerman Q.A., Rainò G., Kovalenko M.V., Manna L.: Nature materials **17**, 394–405 (2018)
2. Kirstein E., Kopteva N.E., Yakovlev D.R., Zhukov E.A., Kolobkova E.V., Kuznetsova M.S., Belykh V.V., Yugova I.A., Glazov M.M., Bayer M., Greilich A.: Nature Communications **14**, 699 (2023)
3. Kolobkova E.V., Kuznetsova M.S., Nikonorov N.V.: J. Non-Cryst. Solid **563**, 120811 (2021)
4. Belykh V.V., Melyakov S.R.: Phys. Rev. B **105**, 205129 (2022)
5. Heisterkamp F., Zhukov E. A., Greilich A., Yakovlev D. R., Korenev V. L., Pawlis A., Bayer M.: Phys. Rev. B **91**, 235432 (2015)

O34

Numerical and analytical averaging of the free induction decay signals from small spin clusters

K.B. Tsiberkin, V.K. Henner, E.I. Kovycheva

Perm State University, Perm, Russia

Using the numerical algorithm and analytical estimates, we describe the scaling of Abragam trial function for the low-dimensional spin cluster and consider the ways to evaluate the average signal from large number of clusters have different sizes. That permits to simulate realistic FID signals using the low-dimensional numerical modeling avoiding huge simulation [1–3].

Here, we consider a system consisting of a number of cubic-shaped spin clusters (Fig. 1). The study gives analytical and numerical realization of the FID averaging. An analytical method is based on approximate scaling of the trial function with the system volume. The scaling is determined by spatial dependence of dipolar interaction. It is proportional to the cube of distance between spins, therefore we assume that here exists a scaling of dipolar Hamiltonian by the volume of spin cluster. Since the empirical parameters of trial function a and b are given by the FID spectrum moments, they also will have the same scaling. Finally, we set

$$F(t;V) \approx \exp\left(-\frac{a^2t^2}{2V^2}\right)\frac{\sin bt/V}{bt/V},$$

where V is the dimensionless cluster volume is referred to some characteristic spatial scale. Introducing the volume distribution function, one may build a summary signal which will be the model of total observable FID:

$$F_\Sigma(t) \approx \frac{1}{bt}\int dV\,\rho(V)V\exp\left(-\frac{a^2t^2}{2V^2}\right)\sin\frac{bt}{V}.$$

The numerical method uses a quantum-based approach for low-dimensional spin cluster of given configuration [4]. The algorithm evaluates the energy spectrum and

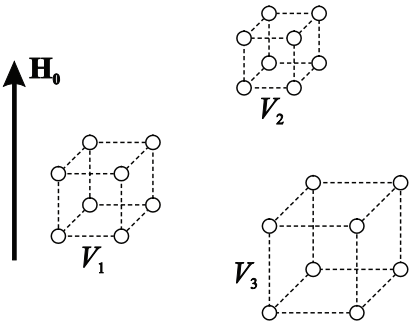

Fig. 1. Schematic image of spin clusters configuration used in simulations; it is an ensemble of independent cubic cells of different size under constant magnetic field.

O34

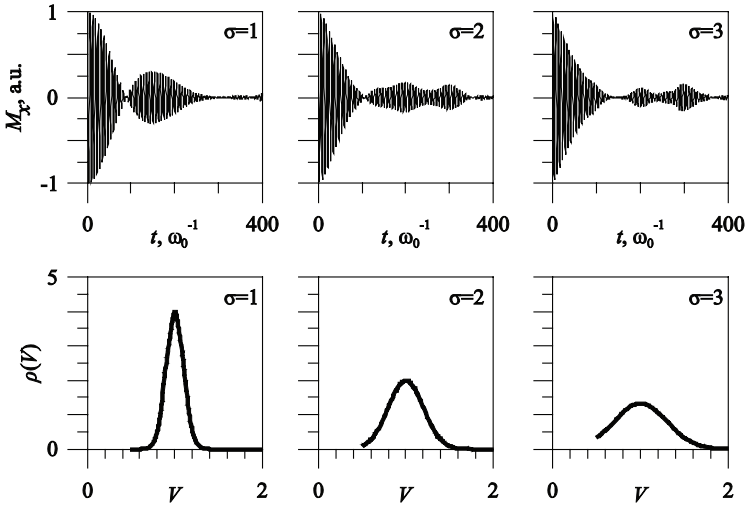

Fig. 2. The simulated total FID evaluated with the Gaussian distribution for varying standard deviation; the bottom row shows the shape of the applied distribution functions.

eigenvectors of spin cluster. Then, a dynamics of observable variables is calculated using the superposition of single-state evolution operators.

If the distribution of cluster size is well-localized, the total signal is determined by FIDs from spin clusters of similar size. Therefore, the observable transversal magnetization should have a typical envelope oscillation with the decay time given by dipole energy. That has a simple analytical estimate using the Laplace's formula for small dispersion of cluster size. The left column at Fig. 2 shows that the numerically simulated signal with localized distribution also closes the typical shape of envelope.

The opposite case has the almost uniform cluster size distribution. The average signal decay in numerical simulation close to the exponential law (see Fig. 2, right column). Unfortunately, there is no simple analytical result for general case. The exact formula for the FID is given by series of special functions. Nevertheless, the upper estimate of averaged FID is the power dependence t^{-1}.

It should be noted that the analysis and simulations are given for the ensemble of geometrically similar clusters. Only their size varies, while the shape and orientation to the external field are the same for all elements. The effect of possible variations in their structure is omitted here, and it requires additional analysis. Despite this, we assume that the averaging method can be a good instrument for simulation of superlattice magnetic structures. Finally, that opens a way to determine the parameters of the magnetic cluster distribution in the diluted material with a regular inner structure using experimental measurements of the free-induction decay signal.

1. Henner E.K., Schaposhnikov I.G.: Radiospectroscopy **10**, 74–81 (1976)
2. Kovycheva E.I., Tsiberkin K.B.: Bull Perm Univ. Physics **2**, 26–35 (2022)
3. Tsiberkin K.B.: Eur. Phys. J. B **96**, 70 (2023)
4. Henner V.K., Klots A., Nepomnyashchy A.A., Belozerova T.S.: Appl. Magn. Reson., **52**, 859–866 (2021)

O35

Features of superparamagnetic resonance of iron clusters in nanocrystalline sodium titanate

D.A. Saritsky, A.I. Neumoin, D.P. Opra, A.M. Ziatdinov

Institute of Chemistry, Far Eastern Branch of the RAS, Vladivostok, Russia,
e-mail: denissaricki@mail.ru

Nanostructured materials based on sodium titanate ($Na_2Ti_3O_7$) attract attention due to their unique hierarchical two-level (micro/nano) architecture composed of thin-walled nanotubes [1]. Doping with impurity ions allows to modify the physicochemical properties of sodium titanate [2]. These materials have potential for applications in energy, catalysis, electronics, and sensing.

This paper presents the results of electron magnetic resonance (EMR) studies of spin characteristics of nanosized sodium titanate particles doped with iron ions. The EMR spectra were recorded on a JEOL-X330 spectrometer.

Fig. 1 shows the first derivatives of the microwave field energy absorption of $Na_2Ti_3O_7$ powders doped with different amounts of iron ions at –160 °C. At high temperatures, the shape of the resonance line is close to the Lorentzian (Fig. 2). As the temperature decreases, the line broadens and shifts towards low magnetic fields. Simultaneously, the shape of the line acquires a form characteristic of the EMR of superparamagnetic particles (Fig. 2). Consequently, impurity iron ions form small single-domain ferromagnetic clusters in the samples. The resonance with $g \sim 4.3$ belongs to single Fe^{3+} ions ($3d^5$, $S = 5/2$) in strongly distorted octahedral crystal fields [3].

Theoretical modelling of the EMR spectrum of iron-doped sodium titanate was performed under the assumption that the broad resonance belongs to superparamagnetic iron oxides. The calculations assumed the presence of magneto-crystalline anisotropy and demagnetization fields in them. The shape of the particles was assumed to be

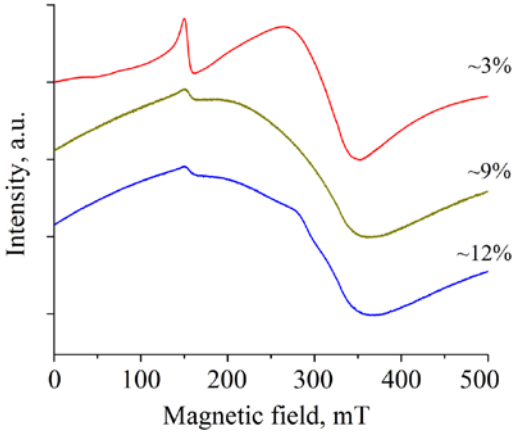

Fig. 1. EMR spectra of $Na_2Ti_3O_7$ powder doped with different amounts of iron ions; $T = –160$ °C.

O35

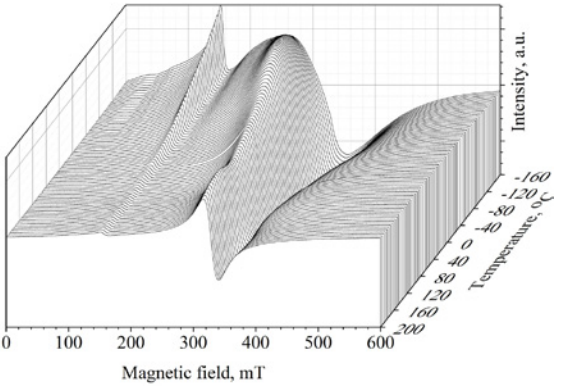

Fig. 2. Temperature dependence of the EMR spectrum of $Na_2Ti_3O_7$ powder doped with ~3% of iron ions.

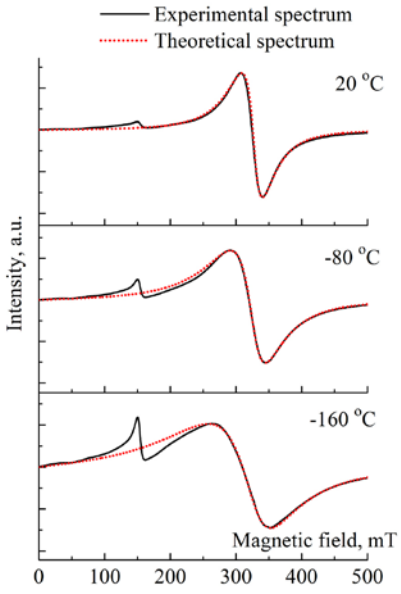

Fig. 3. Experimental and theoretical EMR spectra of $Na_2Ti_3O_7$ powder doped with ~3% Fe ions at different temperatures.

spherical with a slight ellipsoidal distortion. The particle size distribution was assumed to be lognormal. Fig. 3 shows the results of the approximation of the EMR line shape of sodium titanate powder doped with ~3% Fe at different temperatures, performed under the above assumptions.

1. Opra D.P., Sinebryukhov A.I., Neumoin A.I., Podgorbunsky A.B., Gnedenkov S.V.: ChemChemTech. **65,** 37–41 (2022)
2. Chandel S., Wang Ch., Singh S. P., Wang N., Rai A. K.: ACS Appl. Nano Mater. **5**, 18591–18602 (2022)
3. Castner T., Newell S., Holton W.C., Slichter C.P.: J. Chem. Phys. **32**, 668–673 (1960)

O36

T_m relaxation time study of $Sc_2@C_{80}CH_2Ph$

R.B. Zaripov, Yu.E. Kandrashkin

Zavoisky Physical-Technical Institute, FRC Kazan Scientific Center of RAS, Kazan, Russia

At present, the search for magnetic molecules with long spin coherence times and understanding of decoherence mechanisms remain the focus of research. One of the approaches for isolating the paramagnetic center from the influence of the environment is the encapsulation it into a molecular container. One of the effective containers is the fullerene cage. In this regard, the spin coherence was studied using the dimetallofullerene $Sc_2@C_{80}CH_2Ph$ as an example [1, 2].

Phase relaxation time was measured using the primary echo protocol for various resonant transitions corresponding to several magnetic quantum numbers m (0, ±1, ±2, ±3) for a given total nuclear spin j (3, 4, 5). The maximum relaxation time is observed for $m = -1$. By going from $m = -1$ to $m = +1$ and $m = -3$ phase relaxation time is decreased. These results are related with the inhomogeneous broadening of these transitions. The line corresponding to $m = -1$ has the narrowest width. In both directions from this point, the width of the lines increases. In this case, the widths of the lines at $m = 0, -2$ and at $m = 1, -3$ are approximately equal. The dependence of the phase memory time on the linewidth is observed at temperature ranges of 60–120 K. With decreasing temperature, it becomes less pronounced. The results are explained in terms of rotational diffusion of an endohedral fragment in a fullerene cage.

Acknowledgments: The research was supported financially by Russian Science Foundation (project #22-43-04424). The scandium dimetallofullerene was provided by Dr. A. Popov, IFW Dresden, Germany.

1. Zaripov R.B., Kandrashkin Yu.E., Salikhov K.M., Büchner B., Liu F., Rosenkranz M., Popov A.A., Kataev V.: Nanoscale **12**, 20513–20521 (2020)
2. Kandrashkin Yu.E., Zaripov R.B., Liu F., Büchner B., Kataev V., Popov A.A.: PCCP **23** (33), 18206–20 (2021); Schafer A., Horn H., Ahlrichs R.: J. Chem. Phys. **97**, 2571–2577 (1992)

O37

Critical behavior of the $EuFe_2As_2$ crystal as revealed by magnetic and microwave measurements

D.E. Zhelezniakova[1,2], I.I. Gimazov[1], Y.I. Talanov[1]

[1]Zavoisky Physical-Technical Institute, FRC Kazan Scientific Center of RAS, Kazan, Russia
[2]Institute of Physics, Kazan Federal University, Kazan, Russia

The superconductivity formation mechanism in high-temperature superconductors is not finally established till now. There is an assumption that the Cooper pair formation is mediated by magnetic fluctuations. That's why materials in which superconductivity and magnetism coexist are of interest for research. $EuFe_2As_2$ is one of parent compounds for some superconductors. It has a layered structure and is ordered antiferromagnetically at T_N = 19 K. Eu^{2+} ions have a large magnetic moment 7.9 μ_B and they interact strongly with conduction electrons in Fe-As layers. The compound is not superconducting at ambient pressure, but superconductivity is emerged with applying an external pressure and with replacing Eu by Na, K, Rb or As by P and Fe by Co [1].

It is known that in relatively weak magnetic fields, superconductivity in the $EuFe_2As_2$ compound (under pressure) coexists with the ferromagnetic state. The problem of the coexistence of superconductivity and magnetism is of particular interest.

To understand whether magnetism affects the formation of superconductivity, it is necessary to determine the dimensions of magnetic correlations. If the interaction is two-dimensional, then magnetic ordering occurs only in Eu layers and does not affect the formation of superconductivity in Fe-As layers. Otherwise, in the case of a three-dimensional interaction, the fluctuations also exist out of the plane, which means that they can contribute to the Cooper pair formation. The dimension of interaction can be deduced from the analysis of the critical behavior of magnetic system in the vicinity of the ordering temperature.

To determine the dimensionality of magnetic correlations, we performed a joint analysis of data obtained from transport, magnetic, and radiospectroscopic measurements. The dependence of the magnetic susceptibility near the phase transition temperature is well described by the power law:

$$\chi(T) \propto \chi_0 \left(\frac{T - T_N}{T_N} \right)^{-\gamma} .$$

Thus, one can obtain the value of the critical susceptibility exponent γ. The impact of critical fluctuations on microwave absorption is described by equation:

$$A_{\mathrm{cr}}(T) \propto A_0 \left(\frac{T - T_N}{T_N} \right)^{-z\nu} .$$

This allows us to estimate the critical index of the correlation length ν and the dynamic critical index z. Note that the dynamic index z most clearly reflects the dimension of the interaction. However, its value can be obtained only from an analysis

of high-frequency measurements, which include the method used by us for recording nonresonant microwave absorption.

Using the obtained values of critical parameters, we can choose the theoretical model that best describes the critical behavior, and thus to determine the dimension of interaction. Comparison of obtained parameters with the models of Ising, Heisenberg and XY (see review [2] and references therein) suggests that the interaction of spins near the magnetic ordering temperature is described by the 3D XY model. According to this model the spins are strongly bound in the Eu ion plane, while planes are weakly connected with each other and, therefore, can affect the superconducting state.

The authors are acknowledge to Pervakov K.S. and Vlasenko V.A. from P.N. Lebedev Physical Institute of the Russian Academy of Sciences for synthesis of crystals and measurements of magnetic susceptibility in the framework of RSF grant No 21-72-20153.

1. Ikeda M., Hagiwara M., Kobayashi T. et al.: J. Korean Phys. Soc. **62**, 2007 (2013)
2. Hohenberg P.C., Halperin B.I.: Rev. Mod. Phys. **49**, 435 (1977)

O38

Relaxation of multiple-quantum NMR coherences in dipolar coupled spin pair

E.B. Fel'dman, E.I. Kuznetsova, K.V. Panicheva, S.G. Vasil'ev, A.I. Zenchuk

Federal Research Center of Problems of Chemical Physics and Medicinal Chemistry of RAS, Chernogolovka, Russia

With currently increasing interest among researchers in the field of magnetic resonance to the systems prepared in exotic states, which are far from equilibrium or with large amounts of spin order, the foundations of the relaxation theory are being reinvestigated [1]. The novelty of the approach is associated with the application of the Lindblad equation, which is commonly used in the theory of open quantum systems . In practice, the interaction of the particular system of interest with the environment is inevitable. The goal of the theory is to include the influence of the environment on system of interest without explicit consideration of the complete system. The stochastic interactions with the environment on the timescales relevant in NMR can be well described as a Markovian process [1]. The Lindblad equation is of fundamental importance in this case since it describes the quantum dynamics in the most general way [2].

In the present article, we consider a system consisting of two spins coupled by the dipole-dipole interaction. We use the XY dipolar Hamiltonian that describes the spin dynamics in the homonuclear multiple-quantum (MQ) NMR experiments [3]:

$$H_{\mathrm{MQ}} = -\frac{D}{2}(I_1^+ I_2^+ + I_1^- I_2^-), \tag{1}$$

where D is the dipolar coupling and $I^{\pm}$ are rising/lowering spin angular momentum operators. The result of the developed theory based on the Lindblad equation predict oscillatory exchange between intensities of the zeroth (J_0) and second ($J_{\pm 2}$) order MQ coherences accompanied by the exponential decay of both with characteristic time T_{r} on the preparation time t of MQ NMR experiment:

$$\begin{aligned} J_0(t) &= e^{-t/T_{\mathrm{r}}}\cos^2(Dt) \\ J_2(t) &= J_{-2}(t) = \frac{1}{2}e^{-t/T_{\mathrm{r}}}\sin^2(Dt)\,. \end{aligned} \tag{2}$$

The experimental examination of the theory was accomplished in a single crystal of hambergite on a Bruker Avance III spectrometer operating at 400.2 MHz proton resonance frequency. The protons in the hambergite (Be_2BO_3OH) form well-isolated zigzag spin chains [4]. The planes of different zigzags are parallel. The zigzag arrangement allow manipulating the strength of the dipolar couplings for the spins by orienting the spin chain in the external magnetic field. One special orientation can be obtained when we set the direction of the field in the plain of the zigzag at the magic angle with respect to one of the vectors connecting the neighbors in the chain. The coupling

O38

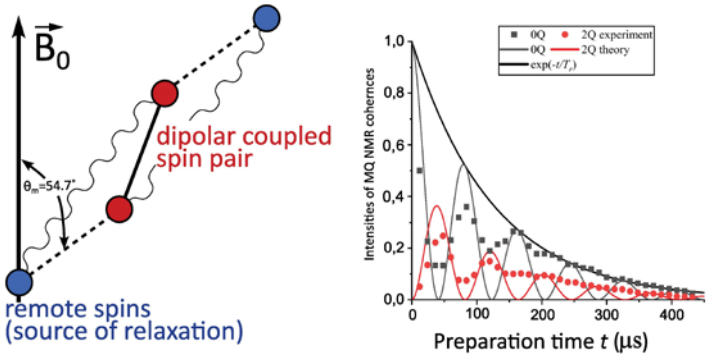

Fig. 1. The isolated spin pairs of protons obtained in hambergite at a special orientation in the external magnetic field (left). The dependence of the intensities of MQ NMR coherences on the duration of the preparation time (right): the dots correspond to experimental data, solid lines – theoretical predictions.

with one of two nearest partners vanish and the second take large value resulting in a set of well-isolated spin pairs. This situation is illustrated on the left part of Fig. 1.

The ^{1}H spectra in considered orientation show the doublet expected for the isolated pair of spins, from which the strength of the dipolar coupling is easily extracted. The right part of Fig .1 demonstrates the intensities of MQ NMR coherences as a function of preparation time. The experimental data shown with dots agree well with the theoretical predictions. The frequency of oscillations correspond well to the to the dipolar coupling determined from single-quantum spectrum. The decay of the coherences is exponential in agreement with the theory. The constant of the exponential decay T_r was found to be 125 μs. Relaxation of MQ coherences occurs due to the dipole-dipole interactions of the spins giving rise to MQ NMR coherences with other surrounding spins. The estimation of the relaxation time using the Fermi's golden rule for next nearest neighbors gives a close value of 277 μs, giving a strong support to the dipole-dipole character of the relaxation due to the spins of the pairs belonging to the same chain.

The work was performed as a part of a state task, State Registration No. AAAA-A19-119071190017-7.

1. Levitt M.H., Bengs C.: Magn. Reson. **2**, 395–407 (2021)
2. Manzano D.: AIP Advances **10**, 025106 (2020)
3. Baum J., Munowitz M., Garroway A.N.: A. Pines, J. Chem. Phys. **83**, 2015–2025 (1985)
4. Bochkin G.A., Fel'dman E.B., Kiryukhin D.P., Kushch P.P., Vasil'ev S.G. : Journal of Magnetic Resonance, **350**, 107415 (2023)

O39

Thermoresponsive polymers from spin probe and spin label EPR spectroscopy point of view

E.N. Golubeva[1,2], E.M. Zubanova[1]

[1]Faculty of Chemistry, Lomonosov Moscow State University, Moscow, Russia
[2]Sechenov University, Moscow, Russia

Thermoresponsive polymers are a class of "smart" materials that have the ability to respond to a change in temperature; a property that makes them useful materials in a wide range of applications and consequently attracts much scientific interest [1]. Some thermoresponsive polymers exhibit lower critical solution temperature (LCS). Below LCST, these polymers are soluble in water due to the formation of hydrogen bonds between water molecules and hydrophilic amide groups in the polymer chains. Upon heating above LCST, hydrogen bonds degrade, and hydrophobic interactions prevail leading to the collapse of the polymer coil into a dense low-polar globule. This effect determines the widespread use of thermoresponsive polymers in various fields of biomedicine, including cell engineering and the development of drug delivery systems. Thermoresponsive polymer solutions and gels have been studied extensively in the literature; the macroscopic swelling behavior was primarily of interest. On the contrary, microstructure of inhomogeneities forming during coil-to globule transition is under the question.

Electron paramagnetic resonance spectroscopy is a perspective approach to obtain information from a guest molecule's point of view about the processes at micro- and nanoscale level. EPR spectroscopy with its high sensitivity and selectivity opens the way to probe the specific characteristics of responsive polymers by adding paramagnetic tracer molecules (spin probes), or grafting them to the polymer chains (spin labels) to provide a picture of the collapse process at the molecular level, based on variations of the rotational dynamics and chemical environment.

In the presentation, the results of the adaptation of spin-probe and spin-label approach to study collapse processes in aqueous solutions of one of the most known thermoresponsive polymers – poly(N-isopropylacrylamide) (PNIPAM) and corresponding copolymers will be presented. Small amphiphilic radical (2,2,6,6-tetramethylpiperidin-1-yl)oxyl (TEMPO) (ca. 6.7 Å in diameter) is a powerful tool to detect and control the formation of nanoscopic polymer globules [3–6]. A lower polarity and higher viscosity of the globules result in changes of spin Hamiltonian parameters and line widths of TEMPO spectra compared with those for TEMPO aqueous solutions, reflecting a decrease of the amplitudes of the spectral lines belonging to the radicals in the solution and the appearance of broader components of the TEMPO spectrum corresponding to probes localized in the globules (Fig. 1). Broadening of the spectra of the fast-moving radicals in water by spin-exchange with Cu^{2+} ions allows obtaining individual spectra of the spin probe in polymer globule after collapsing and getting reliable Spin-Hamiltonian parameters of both types of probes localization in solutions. This "quenching" approach has shown the formation of inhomogeneities in PNIPAM aqueous solution at 2-3 degrees below the critical temperature measured by microscopic methods.

O39

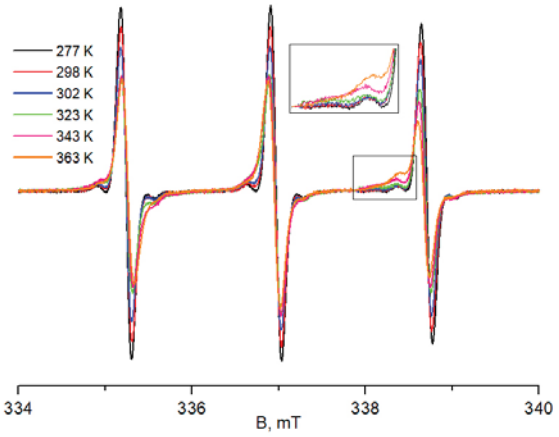

Fig. 1. EPR spectra of TEMPO in aqueous solutions of graft copolymers of N-Isopropylacrylamide with oligolactide.

The collapse mechanism depends crucially on the hydrophobicity/hydrophilicity of the comonomers. A small amount of strongly hydrophilic comonomers leads to the exclusive occurrence of static inhomogeneities, because of a strong tendency to intermolecular aggregation and hence to the formation of large aggregates already at the onset of the nanoscale collapse of the polymers. On the contrary, a small amount of very hydrophobic comonomers like oligolactides leads to the occurrence of dynamic inhomogeneities, featuring guest exchange at temperatures above the macroscopic LCST.

The localization of spin probes in aqueous solutions of PNIPAM during the collapse is determined by the hydrophobicity of the probe and its size. A small amphiphilic or hydrophobic probes up to 1–10 nm (TEMPO or 4-hydroxybenzoato-TEMPO) is almost completely (up to 95% of the total amount) are captured by the globules formed during the phase transition, while a large probe containing a long alkyl tail (methyl-5-doxyl stearate) does not enter the polymer globule.

The information obtained by spin-probe and spin-label EPR spectroscopy should be taken into account when designing medical systems based on thermoresponsive polymers and other stimuli responsive materials.

The research was financially supported by a grant from the Russian Science Foundation (project no. 22-73-00062).

1. Ward M.A., Georgiou Th.K.: Polymers **3**, 1215–1242 (2011)
2. Zubanova E.M., Ivanova T.A., Ksendzov E.A. et al.: Polymers **14**, 4746 (2022)

O40

Structural investigations of fibril-forming peptide fragments of semenogelin1 protein

D.A. Osetrina, A.G. Bikmullin, A.R. Yulmetov, T.A. Mukhametzyanov, V.V. Klochkov, D.S. Blokhin

Kazan Federal University, Kazan, Russia

It is known that four peptide fragments of the semenogelin1 (SEM1) protein (SEM1(45-107), SEM1(49-107), SEM1(68-107), SEM1(86-107)) form amyloid fibrils in seminal fluid. These peptides play an important physiological role in the fertilisation process and increase the infectivity of the human immunodeficiency virus (HIV) [1]. The amyloid fibrils of SEM1 act as cationic bridges, reducing electrostatic repulsion between negatively charged surfaces such as oocytes and spermatozoa, as well as HIV virions and target cells. To understand the processes of SEM1 peptide fibril formation, it is necessary to study the native structures of these peptides, as well as the mechanisms of transforming native structure into fibrils.

In this work, spatial structures of all four peptides in monomeric form (SEM1(45-107), SEM1(49-107), SEM1(68-107), SEM1(86-107)) and the N-domains structures of SEM1(45-107), SEM1(49-107), SEM1(68-107) peptides (SEM1(45-67), SEM1(49-67), SEM1(68-85)), were found for the first time. High-resolution nuclear magnetic resonance spectroscopy (NMR) and molecular modeling were used as research methods. Circular dichroism (CD) spectroscopy was also conducted for N-domains and the peptide SEM1(86-107) to determine the secondary structure of peptides. The obtained data from NMR experiments and structure calculations are consistent with CD spectroscopy data. The investigated peptide fragments of semenogelin1 protein have a disordered secondary structure but contain small helical regions (α,3_{10}–helices). We hypothesize that these helical regions may participate in fibril formation. And the lack of rigid structuring of peptides favours the adaptation of peptides to different conditions of fibril formation.

In addition, in this work, the dimer SEM1(68-107) was simulated using molecular dynamics in the GROMACS package and metadynamics using the PLUMED library for GROMACS [2]. The construction of the free energy profile using metadynamics was performed to search for the most probable conformation of the SEM1(68-107) dimer. Furthermore, molecular dynamics simulations were conducted for 1μs for one structure from the most probable conformation of the dimer to test the stability of the structure.

Throughout the entire simulation, the dimer structure remained stable, but there were conformational changes in the structure of each peptide compared to the initial structure of the monomer SEM1(68-107). Both peptides in the dimer have stable helical regions: 72Asp-77Asp and 90Leu-93Thr; there is a bend in the main peptide chain – β-loop (81K82S83Q84Q85Y), held together by a hydrogen bond between residues 81K and 85Y.

The above-described conformational changes in the structure of the SEM1(68-107) dimer are characteristic of the formation of the nucleation core during the lag phase

of amyloid peptide oligomerization [3]. Additionally, the obtained results in this study demonstrate that we observe an intermediate state before beta-sheet aggregation. Indeed, the formation of an amyloidogenic assembly containing helical fragments is a key step in fibril formation [4].

This work is supported by the Russian Science Foundation (D.S. Blokhin, project no. 20-73-10034)

1. Roan N., Muller J., Liu H. et al.: Cell Host Microbe **10**, 541–550 (2011)
2. Bonomi M., Branduardi D., Bussi G. et al.: Comput. Phys. Commun. **180**, 1961–1972 (2010)
3. Liu G., Prabhakar A., Aucoin D. et al.: J. Am. Chem. Soc. **132**, 18223–18232 (2010)
4. Kirkitadze M., Condron M., Teplow D.: JMB **312**, 1103–1119 (2001)

O41

Assessing neurotransmitter levels using magnetic resonance spectroscopy during short visual stimulation

A.N. Yakovlev[1,2], A.V. Gritskova[1], A.V. Manzhurtsev[1,2], M.V. Ublinskii[1,2], P.E. Menschchikov[3], T.A. Akhadov[1]

[1]Clinical and Research Institute of Emergency Paediatric Surgery and Traumatology, Moscow, Russia
[2] Emanuel Institute of Biochemical Physics, Russian Academy of Sciences, Moscow, Russia
[3]Philips Healthcare, Moscow, Russia

The human brain relies on key neurometabolites, glutamate (Glu) and gamma-aminobutyric acid (GABA), as excitatory and inhibitory neurotransmitters, respectively. Understanding their dynamics in response to stimuli is crucial for unraveling brain function. In studies involving single stimuli, changes in [Glu] over short periods (up to 5 s) have been attributed to neurotransmitter release from vesicles, primarily due to the low rate of metabolic processes [1]. The metabolic changes of neurotransmitters typically exhibit characteristic times of at least one minute, whereas vesicle cycle processes occur with characteristic times ranging from 1 to 20 seconds [2]. We expect that short visual stimulation leads to increased GABA and Glu levels, given their release from vesicles. This work aims to measure GABA and Glu levels in response to a brief visual stimulus lasting three seconds, shedding light on their kinetics after neuronal activation.

MRI and single voxel ^{1}H-MRS were performed using the Philips Achieva dStream 3T MRI System (Eindhoven, Netherlands) using the 20 coil SENSE Head coil. The study involved 33 and 25 healthy volunteers to measure GABA and Glx, respectively. The 8/4 Hz flashing checkerboard was used for stimulation in similar blocks (3 s – stimulus, 13.5/21 s – black screen, GABA/Glx respectively). FMRI images were acquired using gradient-echo echo-planar imaging (GE EPI) sequence with T_R/T_E = 3000/40 ms, flip angle = 90°, in-plane resolution = 2.4×2.4 mm, slice thickness = 4 mm, number of slices =30 and 83 transients. An activation map was obtained using SPM12 in response to visual stimulation. The spectra for GABA measurement were obtained using the MEGA-PRESS sequence without macromolecules suppression (T_R = 1500 ms, T_E = 68 ms, NSA = 802, voxel size – 30×40×25 mm, ON: 1.89 ppm, OFF: 7.46 ppm), for Glx-PRESS (T_R/T_E = 2000/35 ms, NSA = 432, 20×30×20 mm). All spectra were localized in the activated region of the visual cortex.

To obtain GABA-dynamics with a temporal resolution of 1.5 s and reliable SNR, five adjacent transients were averaged (the middle one corresponding to the particular time point was chosen with weight of 2). Spectra for GABA were preprocessed in Gannet. PRESS spectra were preprocessed using FID-A (frequency and phase aligning, water removal). Quantitative processing of the spectra was performed using LCmodel.

The impact of BOLD effect was assessed in metabolite spectra by estimating the differences in total creatine (Cr) singlet (3.03 ppm) linewidth between each time point and the value at –1.5 s (1.5 s before the start of the stimulus presentation). Cr linewidth was determined as model estimation parameter subtracted by 3 Hz (default line-broadening in GannetPreInitialise). The difference between the obtained values (GABA/Cr, Cr, and linewidth of tCr) corresponding to individual time points were

O41

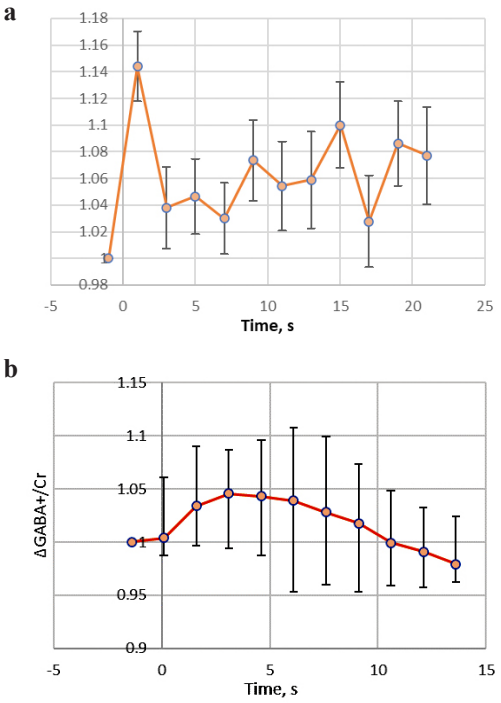

Fig. 1. Mean intensities ratio Glx/Cr (**a**) and GABA/Cr (**b**, ± standard error of the mean, SEM) values normalized to the baseline value of each volunteer.

tested for normality by the Shapiro-Wilk test. In the case of a normal distribution, Fisher's least significant difference (LSD) test was performed; otherwise, uncorrected Dunn's test was used. Multiple comparisons were adjusted by the Benjamini-Hoschberg method (FDR-adjusted), the significance level was set at $q < 0.05$.

An increase in the level of Glx/Cr was found at the 1 (+14%, $q = 0.006$) and 15 (+10%, $q = 0.04$) second after the presentation of the stimulus and a rapid decrease to the initial level. The level of GABA also increases for 1.6–3.1 s (+3–5%, $q < 0.05$), after which it decreases to its initial level. The maximum changes (mean ± s.d.) in the line widths and heights for Cr were –1.4 ± 0.3%, and +1.3 ± 0.2%, respectively, and for NAA –1.6 ± 0.2%, and +1.2 ± 0.1%, respectively.

The use of a short stimulus made it possible to observe rapid changes in the level, which cannot be associated with metabolic processes. Therefore, statistically significant change in GABA/Cr and Glx/Cr may indicate that there is a change in the MR-"visible" pool of GABA and Glu upon release from the vesicles (keeping in mind the relatively large $T_E = 68/35$ ms and relatively short T_2 of GABA and Glu).

The change in the width of the creatine and NAA lines are most likely due to the BOLD effect[3], since the resulting curve reaches a maximum at about 6 seconds, similar to the standard hemodynamic response observed with fMRI.

1. Mullins P.G.: Scandinavian Journal of Psychology **59**, no. 1, 91–103 (2018)
2. Südhof T.C.: Annual Review of Neuroscience **27**, 509–547 (2004)
3. Zhu X.H., Chen W.: Magnetic Resonance in Medicine **46**, no. 5, 841–847 (2001)

Po1

Experimental low-field DNP setup with switchable magnetic fields

A.S. Alexandrov, I.M. Shafigullin, V.D. Skirda

Institute of Physics, Kazan Federal University, Kazan, Russia

Earlier we reported [1] on the development of a setup for DNP in weak magnetic fields of 10 mT. Now we have improved the setup for operation in various switchable fields. We have changed the magnetic system for single layer solenoid coil with low inductance of 2.47 mH to achieve minimal switching time. A new controlled current source with PID feedback has been designed and fabricated to drive the new magnetic system at maximum speed. The time to establish a current of 25 A in a circuit with solenoid coil was no more than 4 ms. The new system of magnetic field generation allows to freely select the frequencies of EPR saturation and NMR registration in a certain area.

Based on this an experimental setup for dynamic polarization of nuclei with the possibility of switching the magnetic field in the range of 1–75 mT was set up. NMR signal amplification of a Cr^{5+} complex sample in ethylene glycol was obtained by the DNP method; saturation of the EPR line was carried out at a frequency of 65 MHz in a field of 2.4 mT, and the NMR signal was registered at a frequency of 3 MHz in a field of 71.6 mT. The maximum enhancement e of the NMR signal using DNP at optimal saturation parameters was 30.1, which is close to the enhancement values (e = 50) in a 330 mT magnetic field given in the literature for the used paramagnetic center Cr^{5+} in ethylene glycol [2]. Thus, an original result was obtained, i.e., DNP in a magnetic field of 2 mT, and the operability of the created experimental setup for the dynamic polarization of nuclei was demonstrated.

1. Alexandrov A., Ivanov A., Archipov R., Gafurov M., Tagirov M.: Magn. Res. in Sol. **21**(2), 3–3 (2019)
2. Fedotov V.: Zh. Eksp. Teor. Fiz. **53**, 1982–1986 (1967)

Po2

Elementary operations of quantum computation by using high spin ions and phase-modulated microwave pulses

M. Arifullin

Orenburg University, Orenburg, Russia, e-mail: arifullinm@mail.ru

Novel and highly promising quantum computing schemes based on solid-state systems have been proposed, utilizing high-spin paramagnetic ions with a total spin (S) greater than 1 in the absence of external magnetic fields [1–3]. In such high-spin systems, qubits and qutrits are manipulated using high-frequency pulses with varying phases. The zero-field splitting of the ground state in high-spin ($S > 1$) paramagnetic ions embedded in crystals is caused by spin-orbit interactions [4]. Without any external magnetic field, the ground state of the ion (e.g., Cr^{3+}) consists of four spin states: $|3/2, +1/2\rangle$ and $|3/2, +1/2\rangle$ and two excited states, $|B\rangle = 2^{-1/2}|\alpha_i\alpha_j\alpha_k - \beta_i\beta_j\beta_k\rangle$ and $|D\rangle = 2^{-1/2}|\alpha_i\alpha_j\alpha_k + \beta_i\beta_j\beta_k\rangle$ of which are naturally entangled GHZ states [1].

By employing radio frequency or microwave pulses, it is possible to manipulate the populations and coherencies of these states, and alter their magnetic properties even at zero magnetic field [1]. Thus, all four spin states $|3/2, +1/2\rangle$ and $|3/2, +1/2\rangle$, $|B\rangle$ and $|D\rangle$ can be utilized as qubits. However, the degenerate pair of states $|A\rangle$ and $|B\rangle$ is more preferable due to the absence of magnetic decoherence mechanisms. The practical use of paramagnetic crystals with embedded high-spin ions does not require strong magnetic fields or vacuum/laser equipment.

Resonant radiofrequency or microwave pulses with different polarizations and phases can produce spin manipulations similar to CNOT, Phase Shift, Quantum Fourier Transformations, and other quantum gates. For spin paramagnetic sublevels, the first transition from alignment to polarization induced by radio frequency pulses should be accompanied by the appearance of macroscopic magnetization, even in zero magnetic fields [4, 5].

The work was funded by RFBR according to the research project № 18-37-00374.

1. Abragam A., Bleaney B.: Electron Paramagnetic Resonance of Transition Ions. Oxford: Clarendon press 1970.
2. Nielsen M., Chuang I.: Quantum Computation and Quantum Information. Cambridge: Cambridge University Press 2010.
3. Pileio G.: Progress in Nuclear Magnetic Resonance Spectroscopy, **56**, 217–231 (2010)
4. Arifullin M.R., Berdinskiy V.L.: Physics of the Solid State **62**, 440–444 (2020)
5. Arifullin M.R., Berdinskiy V.L.: Russ. Phys. J. **63**, 888–893 (2020)

Po3

Relationship between the molecular structure and the triplet state properties of the bodipy dimers

H. Cao[1], A.A. Sukhanov[2], M.M. Bakirov[2], J. Zhao[1], Yu.E. Kandrashkin[2]

[1]State Key Laboratory of Fine Chemicals, Frontiers Science Center for Smart Materials, School of Chemical Engineering, Dalian 116024, China
[2]Zavoisky Physical-Technical Institute, FRC Kazan Scientific Center of Russian Academy of Sciences, Kazan, Russia, e-mail: pinas1@yandex.ru

Study the intersystem crossing in heavy atom-free organic compounds are highly desired to get longer T_1 state lifetimes of a triplet photosensitizers. A series of Bodipy dimers (B1, B2, B3) with different mutual orientations were investigated by transient X-band EPR (TREPR) spectroscopy. TREPR measurements were performed at 80 K (B1, B2, B3) and at 40 K (B2) in frozen small polar solvent mixture (Tol:2MeTGF, 1:1 used). The TREPR spectra of Bodipy dimers has essentially different polarization of the triplet sublevels. The excited states of the molecules B1, B2, B3 are predominately populated along the axes *y*, *x* and *z*, respectively, in the molecular frame of the Bodipy. Thus, the electron spin selectivity of the intersystem crossing is highly sensitive to the molecular structure of these dimers. The spectra were simulated by the spin Hamiltonian including the Zeeman interaction and zero-field splitting. All three spectra demonstrate a significant reduction of the zero-field splitting (ZFS) parameters compared to the (iodinated) monomers or to other dimers with the orthogonal chromophores. The additional measurements at a lower temperature (40 K) don't detect any changes in the spectral properties of the dimer B-2. Overall, the results obtained reveal the delocalization of the excited state of the triplet over two subunits [1].

1. Sukhanov A.A., Cao H., Zhang X., Zhao J., Kandrashkin Yu.E: PCCP **25**, 209 (2023)

Po4

Accounting material imperfections in the design of Halbach magnet arrays

A.V. Bogaychuk

Institute of Physics, Kazan Federal University, Kazan, Russia;
Tatarstan Academy of Sciences, Kazan, Russia

Portable low-field systems for nuclear magnetic resonance (NMR) have a lavish history of their development and nowadays are widely used in various fields of industry, chemistry, biology, physics, geology, medicine and etc. [1, 2]

The homogeneity of the static magnetic field is the crucial parameter which determines the NMR sensitivity and resolution. Therefore, considerable work has been devoted to design a permanent magnets assembly with sufficient strength and homogeneity that may be scaled to arbitrary size. Significant progress was achieved thanks to Halbach magnet array [3].

The performance of permanent magnets is limited not only by their design [4], but also by their high sensitivity to temperature and imperfections of magnetic materials. Whereas the first issue can be solved by temperature stabilization of environment or temperature compensating magnet design, the issue of material imperfection will always be an individual problem in each magnet construction.

The use of new modern methods and approaches [5, 6] for the experimental evaluation of the imperfection of magnetic materials is proposed in this work. As well as the application of the results obtained in the design of the Halbach magnet arrays.

This work was supported by the Russian Science Foundation (Project No. 23-22-00135).

1. Blumich B.: J. Magn. Reson. **306**, 27–35 (2019)
2. Yao Y., Liu D., Che Y., Tang D., Tang S., Huang W.: Fuel **89**, 1371–1380 (2010)
3. Halbach K.: Nuclear Instruments and Methods in Physics Research **169**, 1–10 (1980)
4. Müller K.-H., Krabbes G., Fink J., Gruß S., Kirchner A., Fuchs G., Schultz L.: J. Magn. Magn. Mat. **226-230**, 1370–1376 (2001)
5. Ortner M., Bandeira L.: SoftwareX **11**, 100466 (2020)
6. Hugon C., D'Amico F., Aubert G., Sakellariou D.: J. Magn. Reson. **205**, 75–85 (2010)

Po5

A study of self-assembly process of DyF_3 nanoparticles using ^1H NMR

E.I. Boltenkova, A.M. Garaeva, A.V. Bogaychuk, E.M. Alakshin

Kazan Federal University, Kazan, Russia

The study of the self-assembly processes remains an urgent task of science, since the knowledge gained about these processes in real time can later be used to create contrast agents for high-field MRI and CT, targeted drug delivery, and to create multifunctional nanocomplexes. For example, [1] describes a method for quantifying changes in the size of nanoparticles, their concentration, and consumption of reagents in real time at subnanometer resolution.

Dysprosium trifluoride can be used as a high field contrast agent for magnetic resonance imaging [2]. Dysprosium trifluoride nanoparticles tend to self-assembly [3]. Particles with a size of 5 nm are collected into microsized agglomerates with a size of 1×0.3 μm. Each agglomerate consists of 5 nm thick chains. Yet, the mechanisms and roles of nanoparticle clustering are largely unexplored.

In this work DyF_3 samples were successfully synthesized using the colloidal chemistry method without treatment (5 nm), with their subsequent microwave treatment (20 nm) and hydrothermal treatment (28×16 nm.). The DyF_3 nanoparticles colloidal solutions with different concentrations were studied by ^1H NMR to measure the T_1 and T_2 relaxation times. The self-assembly processes of DyF_3 nanoparticles without treatment and with different types of treatment and using different chemical reactions were also studied using ^1H NMR.

The influence of the treatment method on the self-assembly rate of DyF_3 nanoparticles in a colloidal solution will be discussed.

This work was supported by the Russian Science Foundation (Project No. 23-72-01084).

1. Mashiach R., Weissman H., Avram L. et al.: Nature Communications **12**, 229 (2021)
2. Gonzalez-Mancebo D., Becerro A.I., Rojas T.C. et al.: Part. Part. Syst. Charact. **34**, 1700116 (2017)
3. Alakshin E.M., Kondratyeva E.I., Nuzhina D.S. et al.: J. Nanopart. Res. **20**, 332 (2018)

Po6

A simple way to experimentally determine the correlation time by the double quantum resonance method in the case of exponential decay of the magnetic dipole-dipole correlation function

I.V. Brekotkin[1], N.F. Fatkullin[2], K. Saalwächter[2]

[1]Institute of Physics, Kazan Federal University, Kazan, Russia
[2]Institut für Physik–NMR, Martin-Luther-Universität Halle-Wittenberg, Halle (Saale), Germany

In a recent publication [1] the influence of the effects of spins spatial displacements between RF pulses in Baum-Pains sequence [2, 3] on the normalized Double Quantum (DQ) build up function has been researched. We derived expression for this build up function for the exponentially decaying magnetic dipole-dipole correlation function using the results of [1]. This exponentially decaying correlation function in this case looks as the following:

$$\frac{1}{N_s}\sum_{i\neq j}\left\langle \omega_{ij}(t)\omega_{ij}(0)\right\rangle = \left\langle \Omega^2\right\rangle \exp\left\{-\frac{|t|}{\tau_0}\right\}, \tag{1}$$

where N_s – number of spins in system, $\langle\Omega^2\rangle = (1/N_s)\sum_{i\neq j}<\omega_{ij}{}^2>$, τ_0 – correlation time and $\omega_{ij}(t)$ – the parameter describing in frequency units the effective strength of the dipole-dipole coupling of spins with numbers i and j at time moment t. In this case, if the Anderson-Weiss approximation is applied, the dependence of normalized DQ build up function on half of experimental time τ_{DQ} and time between RF pulses in Baum-Pains sequence Δ is:

$$I_{n\mathrm{DQ}}(\tau_{\mathrm{DQ}};\Delta) = \frac{1}{2}\left(1-\exp\left\{-2\tilde{I}^{(0)}_{n\mathrm{DQ}}(\tau_{\mathrm{DQ}})(1-p)\right\}\right), \tag{2}$$

where

$$\tilde{I}^{(0)}_{n\mathrm{DQ}}(\tau_{\mathrm{DQ}}) = \left\langle \Omega^2\right\rangle \tau_0^2\left(1-\exp\left\{-\frac{\tau_{\mathrm{DQ}}}{\tau_0}\right\}\right)^2, \tag{3}$$

and

$$p = \frac{1-\frac{1}{4}\left(e^{-\frac{\Delta}{\tau_0}}+6e^{-2\frac{\Delta}{\tau_0}}+e^{-\frac{3\Delta}{\tau_0}}-4e^{-\frac{4\Delta}{\tau_0}}\right)}{\left(1+e^{-\frac{\Delta}{\tau_0}}+e^{-2\frac{\Delta}{\tau_0}}\right)^2}. \tag{4}$$

Quantity p is connected with the contribution of spin movement to the normalized DQ build up signal. An important circumstance is that p does not depend on τ_{DQ} as, for example, it is in case with correlation function which is modelled by a power-law decay [1]. The expressions (2–4) can also be derived from the results of [4], which is based on a more phenomenological approach than this one.

The quantity p only depends on ratio Δ/τ_0. This fact allows us to propose a fairly simple way to experimentally determine the correlation time τ_0. If one fixes time τ_{DQ} and measures quantity $I_{nDQ}(\tau_{DQ}; \Delta)$ for two different times Δ_1 and Δ_2 then one can find correlation time from the following equation, which is consequent of the expressions (2)–(4):

$$\frac{1-p(\Delta_1/\tau_0)}{1-p(\Delta_2/\tau_0)}=\frac{\ln\left(1-2I_{n\mathrm{DQ}}(\tau_{\mathrm{DQ}};\Delta_1)\right)}{\ln\left(1-2I_{n\mathrm{DQ}}(\tau_{\mathrm{DQ}};\Delta_2)\right)}. \tag{5}$$

This expression could be simplified with the following approximation:

$$p(\Delta/\tau_0)\simeq\frac{\frac{5}{12}(\Delta/\tau_0)^2}{1+\frac{5}{12}(\Delta/\tau_0)^2}. \tag{6}$$

Taking in account the approximation (6) one can derive from expression (5) simple formula for correlation time:

$$\tau_0=\left(\frac{5}{12}\frac{\Delta_1^2\ln\left(1-2I_{n\mathrm{DQ}}(\tau_{\mathrm{DQ}};\Delta_1)\right)-\Delta_2^2\ln\left(1-2I_{n\mathrm{DQ}}(\tau_{\mathrm{DQ}};\Delta_2)\right)}{\ln\left(\frac{1-2I_{n\mathrm{DQ}}(\tau_{\mathrm{DQ}};\Delta_2)}{1-2I_{n\mathrm{DQ}}(\tau_{\mathrm{DQ}};\Delta_1)}\right)}\right)^{1/2}. \tag{7}$$

We thank the German Research Foundation (DFG) for funding a guest professorship for N.F. in the framework of the SFB-TRR 102 (project A01, project-ID 189853844).

1. Brekotkin I.V., Fatkullin N.F., Lindt K., Mattea C., Stapf S.: J. Chem. Phys. **157**, 224108 (2022)
2. Baum J., Munowitz M., Garroway A.N., Pines A.: J. Chem. Phys. **83**, 2015 (1985)
3. Baum J., Pines A.: J. Am. Chem. Soc. **108**, 7447(1986)
4. Saalwächter K., Zeigler P., Spyckerelle O., Haidar B., Vidal A., Sommer J.-U.: Macromolecules **119**, 3468 (2003)

Po7

Application of neural networks for estimating magnetic parameters of EPR spectra of pH-sensitive nitroxide radicals

D.R. Davydov, D.O. Antonov, E.G. Kovaleva

Institute of Chemical Technology, Ural Federal University, Ekaterinburg, Russia

This study is devoted to the development and application of neural networks for estimating the hyperfine interaction constant of the EPR spectra of pH-sensitive nitroxide radicals introduced into various solid-phase systems. In the course of testing the efficiency of the developed algorithms, it was determined that the relative error of the prediction of the hyperfine interaction constant of experimental EPR spectra without taking into account the anomalous increase in error in case of EPR spectra is $\delta = \pm 10\%$.

Currently, machine learning methods, including various types of neural network algorithms, are increasingly attracting the attention of researchers in various fields of spectroscopy [1] with their unique features, which allow to accelerate and simplify the processing of the obtained experimental data.

However, in EPR spectroscopy, research on the application of neural networks in data processing has not yet shown significant progress compared to other types of spectroscopy. This statement also applies to the processing of EPR spectra of pH-sensitive nitroxide radicals, which can be used to determine the electrical properties of substances by determining the pH-sensitive parameter of EPR spectra – the hyperfine interaction constant (HPI) of the EPR spectra of these radicals introduced into the analyzed systems [2].

In order to determine the feasibility of using machine learning techniques, this study developed several multilayer perceptron-type neural networks for predicting the HPI of pH-sensitive nitroxide radicals, and validated the performance of the developed algorithms on experimental EPR spectra.

The results obtained show that the relative error (δ) of the developed algorithms for EPR prediction is of the order of $\delta = \pm 10\%$ relative to the results obtained during EPR determination using specialized software. However, the speed of HPI prediction is about 10–60 seconds for the whole series of spectra (depending on the computing power of the computer), which makes the application of neural networks an extremely effective tool for estimating the magnetic parameters of EPR spectra. This work is an extension of the published research on the application of neural networks to analyze the EPR spectra of pH-sensitive nitroxide radicals [3].

The work was carried out with the financial support of the Ministry of Science and Higher Education of the Russian Federation under Agreement No. 075-15-2022-1251 dated 13.12.2022 (registration No. 13.2251.21.0176).

1. Meza Ramirez C.A., Greenop M., Ashton L., Rehman I.: u Applications: Appl. Spectrosc. Rev. **56**, 733–763 (2021)
2. Kovaleva E.G., Molochnikov L.S., Venkatesan U., Marek A., Stepanova D.P., Kozhikhova K.V., Mironov M.A., Smirnov A.I.: J. Phys. Chem. C. **120**, 5, 2703–2711 (2016)
3. Davydov D.R., Antonov D.O., Kovaleva E.G.: Appl. Magn. Reson. **54**, 595–612 (2023)

Po8

Formation of a nutation signal in the flowing liquid at the noise level in the entire flow measurement range

I.D. Kochetkov[1], V.V. Davydov[1], R.V. Davydov[1,2]

[1]Peter the Great St. Petersburg Polytechnic University, St. Petersburg, Russia
[2]Department of Bioinformatics and Mathematical Biology, Alferov University, St. Petersburg, Russia

The development of scientific and technological progress, the use of new liquid media in the technical cycles of industrial production and electrical energy (nuclear power plants) [1, 2], as well as increased requirements for the control of hydrocarbons in the pipeline system [3] required the development of new devices or the modernization of those in operation. Devices based on the phenomenon of nuclear magnetic resonance (NMR) are one of the promising directions in solving new problems of monitoring the parameters of current media [2–4]. It is because they eliminate the contact of the measuring elements with the flowing medium, and the measurements carried out using NMR do not change the medium's physical structure and chemical composition.

At present, many different models of NMR flowmeters – relaxometers – have been developed in the world, in which pulse methods (Hann spin echo and Carr–Purcell sequence) [3] or a nutation line with a modulation technique for recording the NMR signal [4] are used to measure the liquid flow rate and relaxation times T_1 and T_2. Using the nutation line and the modulation technique makes it possible to measure the liquid flow q, and the range is 6–10 times greater than when using the pulse technique with an error of 0.5–1.0%. All these models of devices have one drawback, which is associated with an increase in the measurement error q with rapid changes in fluid flow. The method proposed earlier by us using the effect of parametric resonance of the magnetic field in the area where the nutation coil is located [2] has several difficulties when it is implemented at rapidly changing flow rates. Especially in the case of placing the nutation coil in an area with strong electromagnetic interference, which is possible when controlling the flow parameters of various media in nuclear power plants. The formation of satellites in the nutation line is disturbed, which interferes with the formation of the q measurement mode at the noise level [2]. The automatic

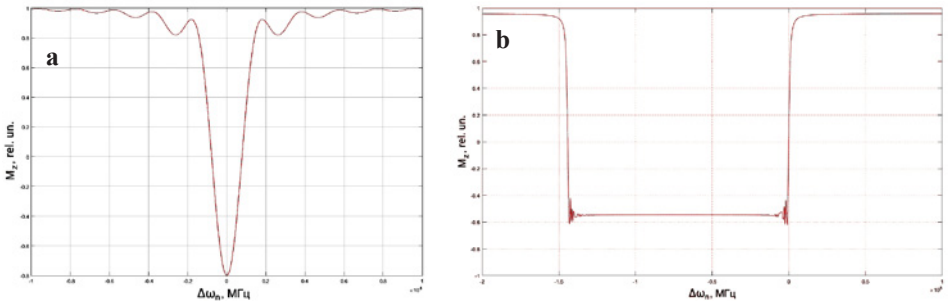

Fig. 1. The dependence of the change in the magnetization M_z on $\Delta\omega_n$. Graphs (**a**) and (**b**) corresponds the following values: $H_1 = 4.21$ A/m, $\Delta H_0 = 11.12$ A/m and $H_1 = 5.66$ A/m, $\Delta H_0 = 2698.21$ A/m.

Po11

Development of tests to increase the specificity of diagnostics using dynamic MRI of patients with voice function disorder

M.Ya. Fattakhova[1], V.L. Odivanov[1], Ya.V. Fattakhov[1], V.N. Krasnozhen[2], V.V. Fedorova[2], A.F. Akhatov[3], E.S. Bekmacheva[3], A.D. Lukashov[3]

[1]Zavoisky Physical-Technical Institute, FRC Kazan Scientific Center of RAS, Kazan, Russia
[2]Kazan State Medical Academy, Kazan, Russia
[3]Diagnostic Center BarsMed, Kazan, Russia

New voice tests have been developed to increase the specificity of the diagnosis of patients with voice function disorder using dynamic magnetic resonance imaging. Functional and organic pathologies of vocal organs are widespread among university teachers, school teachers, vocalists, employees of enterprises with noise, chemical and dust pollution [1]. Previously, tests for use in conjunction with the method of spectral analysis of voice were used to diagnose diseases

Our preliminary investigations were performed on magnetic resonance imaging system Siemens Verio with magnetic field induction 3.0 T in the mode of dynamic tomography. Using dynamic MRI it is shown that the some tests are especially effective for diagnostics of vocalist patients [1].

The aim of the study is to develop new specialized tests for a comprehensive method of diagnosing patients with voice function disorder using both dynamic MRI and clinical techniques, as well as computer spectral analysis of the patient's voice. This provides patients with a faster and more accurate diagnosis.

A number of voice tests are used to diagnose speech patients. In addition to the well-known tests, new original ones have been developed. These are the tests: “Extended tone A”, “Extended tone I”, “Glissando up”, “Glissando down”, “Whisper-speech”, “Stro-bass”. With the help of the hardware and software complex, the test was recorded and further processing, including the Fourier transform, took place.

The tests are designed in such a way that when they are pronounced, various organs or parts of organs are connected to the sound formation, which makes it possible to increase the specificity and sensitivity of MRI diagnostic techniques.

We investigated the diagnostic capabilities of voice samples in the examination of various voice disorders, both in speech patients and in vocal patients. The instability of the sound amplitude during the pronunciation of the test is clearly visible on the spectra. Also, numerous non-periodic small peaks are detected on the record. A number of patients have an unstable pattern of voice formants. Each of the formants is affected by all sections of the sound production path, but to varying degrees. This allows, in combination with dynamic MRI, to obtain unique diagnostic information about the state of all organs of voice formation.

1. Fattakhova M., Khabipov R., Krasnozhon V., Fedorova V., Bekmacheva E., Akhatov A.: International Conference “Modern Development of Magnetic Resonance”, October 3–7, 2022. Abstracts. Kazan, Russia. P. 107.

system for adjusting the parameters of the modulation field does not have time to respond to a rapid change in the value of q. Measurements of q either stop or occur with large errors. Therefore, it is necessary to find a new solution to this problem. We propose implementing one of the possible options for solving this complex problem using a strong inhomogeneous magnetic field in the area where the nutation coil is located. Let us consider the system of Bloch equations for describing the formation of a nutation line in a flowing fluid. Let us introduce new coefficients into the Bloch equations, which allow us to consider the change in the inhomogeneity of the magnetic field ΔH_0 in the zone of the nutation coil. The shape of the nutation line is calculated from the change in the component of the magnetization vector M_z (the amplitude of the registered NMR signal is proportional to M_z, since the relation $T_1 > t_c \geq T_2$ is satisfied, where t_c is the time of liquid movement from the nutation coil to the registration coil).

$$\begin{aligned} &dM_x/dt + M_x/T_2 + [\Delta\omega_n + (\Delta H_0/t_n)\gamma t + \gamma H_m \sin(\omega_m t)]M_y = 0\ , \\ &dM_y/dt + M_y/T_2 - [\Delta\omega_n + (\Delta H_0/t_n)\gamma t + \gamma H_m \sin(\omega_m t)]M_x + \gamma H_1 M_z = 0, \\ &dM_z/dt + M_z/T_1 - \gamma H_1 M_y - M_0/T_1 = 0\ , \end{aligned} \quad (1)$$

where $t_n = V_n/q$ is the time spent by the liquid segment under the action of magnetic fields in the nutation coil, H_m and ω_m are the amplitude and frequency of the modulating field, $M_p = \chi_0 H_p \gg M_0 = \chi_0 \cdot H_0$.

Fig. 1 shows, as an example, the nutation lines obtained based on solution (1) for various values of the inhomogeneity of the magnetic field ΔH_0, the flow rate of the flowing liquid q, and the field H_1.

The obtained results of the calculation of the nutation line show its broadening and decrease in the value of M_z to the zero level. Controlling the values of H_1 and ΔH_0 makes it possible to ensure the NMR signal registration at the noise level, which was previously achieved only with satellite lines (parametric resonance) [2]. It should also be noted that the method of controlling the shape of the nutation line proposed by us makes it possible with higher stability to ensure the fulfillment of the following relation $T_1 > t_c \geq T_2$ (where t_c is the time of liquid movement from the nutation coil to the registration coil), which ensures that the amplitude of the registered NMR signal is proportional to the value of M_z.

Comparison of the previously obtained results of the nutation line broadening in [2] with the calculations using (1) shows that in this NMR mode, the flowmeter-relaxometer will work more stably with a rapid change in the value of q. The margin for a rapid change in q for stable operation of the device is at least an order of magnitude greater than when using satellite lines. It should also be noted that in (1), a linear dependence of the change in the magnetic field inhomogeneity along the length of the nutation coil is presented. This dependence can be quadratic or cubic; modern designs of electromagnetic systems make it possible to do this. Therefore, it is necessary to continue these studies to determine the optimal variant for controlling the magnetic field inhomogeneity along the length of the nutation coil.

1. Sadovnikova M.A., Murzakhanov F.F., Mamin G.V., Gafurov M.R.: Energies **15**, 6204–6218 (2022)
2. Davydov V.V., Dudkin V.I., Vysoczkiy M.G., Myazin N.S., Rud' V.Y.: Applied Magnetic Resonance **49**, 665–678 (2018)
3. Kashaev R.S., Kien N.C., Tung T.V., Kozelkov O.V.: Journal of Applied Spectroscopy. **86**, 890–895 (2019)
4. Davydov V.V., Dudkin V.I., Karseev A.Y.: Russian Physics Journal **58**, 146–152 (2015)

Po10

Modification of the implanted silicon surface by a powerful light pulse

B.F. Farrakhov, Ya.V. Fattakhov

Zavoisky Physical-Technical Institute, FRC Kazan Scientific Center of RAS, Kazan, Russia, e-mail: bulat_f@mail.ru

During processing with light pulses of various durations and power densities on the surface implanted layer of semiconductor wafers, the process of solid-phase recrystallization and anisotropic local melting occurs [1], and the effect of formation of nanofilaments can also be observed [2], depending on the semiconductor and the implanted ion. Solid-phase recrystallization is the process of restoring the crystal structure with the electrical activation of ions after ion implantation. Anisotropic local melting is the process of melting the near–surface layer of a semiconductor, with rapid heating of the surface by light pulses of various physical principles of radiation.

The possibility of modifying the relief of the surface layer of the p-n junction implanted with silicon under the influence of a powerful light pulse due to the formation of local melting regions is shown. Several modifications of the surface relief for silicon with surface orientation (111) have been obtained. With the help of such surface modification, it is possible to increase the surface area in solar panels.

A sample of KDB-1 grade silicon with a surface orientation (111) was selected for the study, as one of the most widely used materials in the field of solar energy. Implantation was carried out with P^+ ions with an energy of 50 keV and a dose of $3.12 \cdot 10^{15}$ cm^{-2}. The surface of the implanted silicon samples was modified under the influence of powerful light pulses of millisecond and second durations, before the formation of relief structures of various shapes, on the installation of the UOL.P.-1 by the emission of three xenon flash lamps. Visual inspection of the surface and photo registration were carried out on an optical microscope MBS-9 with 100x magnification. Some of the results are shown in Fig. 1.

1. Farrakhov B., Fattakhov Ya.: Instrum. Exp. Tech. **62**, 226–231 (2019)
2. Stepanov A, Farrakhov B, Fattakhov Ya. et al.: Vacuum **186**, 110060–110063 (2021)

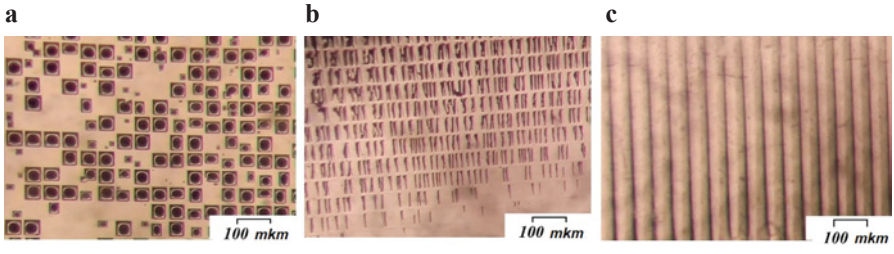

Fig. 1. Photos of the silicon surface implanted with phosphorus ions P^+ with an energy of 50 keV and a dose of $3.12 \cdot 10^{15}$ cm^{-2}, after pulsed light annealing with a power density of 60 W $\cdot$ cm^{-2} (**a**), 240 W $\cdot$ cm^{-2} (**b**), 900 W $\cdot$ cm^{-2} (**c**) and durations of 3.5 sec (**a**), 750 ms (**b**), 120 ms (**c**), respectively.

Po9

ESR of the rare-earth ions in $CsCaF_3$ single crystals

M.L. Falin[1], V.A. Latypov[1], S.L. Korableva[2]

[1]Zavoisky Physical-Technical Institute, FRC Kazan Scientific Center of RAS, Kazan, Russia, e-mai: falin@kfti.knc.ru
[2]Kazan (Volga Region) Federal University, Kazan, Russia

Double fluoride crystals with perovskite structure ABF_3 are very interesting because they are convenient model systems for studying the magneto-optical properties of impurity dopant ions. In principle, in these matrices it is possible to substitute two various cations being inequivalent positions. This enables one to carry out investigations of impurity dopant ions in sixfold or uncommon twelvefold coordinations. The physical properties of rare-earth ions in these compounds are not sufficiently studied. The introduction of three-charge rare-earth ions is hampered because of heterovalent substitution and the essential difference in the ionic radii of rare-earth ions and lattice cations. Previously we presented results on the study of Yb^{3+} ions in $CsCaF_3$ crystals [1–4]. This report is devoted to the further study of impurity paramagnetic centers formed by Ce^{3+}, Nd^{3+}, and Dy^{3+} ions in $CsCaF_3$ single crystals.

The crystals were grown using the Bridgman-Stockbarger method. The concentration of the impurity ions was 0.1–1.0 w%. The EPR experiments were carried out using an X-band spectrometer ERS-231 (Germany) at $T = 4.2$ K.

In the doped crystals different types of impurity paramagnetic centers were discovered. The parameters of the corresponding spin Hamiltonians, the ground states and their wave functions were determined. Structural models of the observed complexes were proposed. The obtained results were analyzed in comparison with the results for the same paramagnetic ions in other hosts.

1. Bespalov V.F., Falin M.L., Kazakov B.N. et al: Appl. Magn. Reson. **11**, 125–133 (1996)
2. Falin M.L., Anikeenok O.A., Latypov V.A. et al: Phys. Rev. B **80**, 174110 1–11 (2009)
3. Falin M.L, Gerasimov K.I., Latypov V.A. et al: Appl. Magn. Reson. **40**, 65–73 (2011)
4. Falin M.L, Gerasimov K.I., Latypov V.A.: Appl. Magn. Reson. **45**, 707–714 (2014)

Po12

Peculiarities of transient nutation in biradicals

R.T. Galeev, R.B. Zaripov, K.M. Salikhov

Zavoisky Physical-Technical Institute, FRC Kazan Scientific Center of RAS, Kazan, Russia,
e-mail: galeev_rt@rambler.ru

The transient nutation method was applied to the study of biradicals. This method allows one to determine the spin state of the system. It was expected that biradicals would exhibit the properties of either weakly coupled systems ($S = 1/2$) or strongly coupled systems ($S = 1$). In fact, it was found that nutation can contain signals that can be attributed to both systems. However, the obtained nutation frequencies differed from those expected for the respective systems. Our study showed that the features of the studied compounds can be explained if we assume that the interaction between spins is of the order of magnitude of spin frequencies difference. For the case of weak amplitudes of the microwave field, equations for the expected nutation frequencies were found. The resulting equations made it possible to estimate the interaction between the radicals.

Po13

Magnetic properties of $Ln_{0.5}Sr_{1.5}Ti_{0.75}Cu_{0.25}O_4$ (Ln = Pr, Nd) layered perovskite

T.P. Gavrilova[1,2], A.R. Yagfarova[1], I.V. Yatsyk[1], M.A. Cherosov[2], R.G. Batulin[2], Yu.A. Deeva[3], T.I. Chupakhina[3], R.M. Eremina[1]

[1]Zavoisky Physical-Technical Institute, FRC Kazan Scientific Center of RAS, Kazan, Russia
[2]Institute of Physics, Kazan Federal University, Kazan, Russia
[3]Institute of Solid State Chemistry of RAS (UB), Ekaterinburg, Russia

Layered perovskite structures with the chemical formula A_2BO_4 (where A is a rare earth or alkaline earth element, and B is d-metals of the IV period of the periodic table) belong to the Ruddlesden-Popper phases and they are widely known and intensively studied due to their multifunctional set of properties and promising practical applications. The scientific interest in $Ln_{0.5}Sr_{1.5}Ti_{0.75}Cu_{0.25}O_4$ (Ln = Pr, Nd) compounds is caused by the following experimental fact. It is known form literature that the dielectric properties of these compounds differ significantly, although they have a similar crystal structure and morphology [1]. In this context, the study of magnetic properties is of particular interest. Here we present the detailed magnetometry and electron spin resonance measurements of $Ln_{0.5}Sr_{1.5}Ti_{0.75}Cu_{0.25}O_4$ (Ln = Pr, Nd) oxides to investigate the possible realization of a complex magnetic structure due to the presence of two magnetic ions and the strong competition of different types of magnetic interactions.

$Ln_{0.5}Sr_{1.5}Ti_{0.75}Cu_{0.25}O_4$ (Ln = Pr, Nd) complex oxides with a layered perovskite structure were synthesized using the precursor method by the pyrolysis of metal-organic compositions. Magnetic properties were investigated using the magnetometry and electron

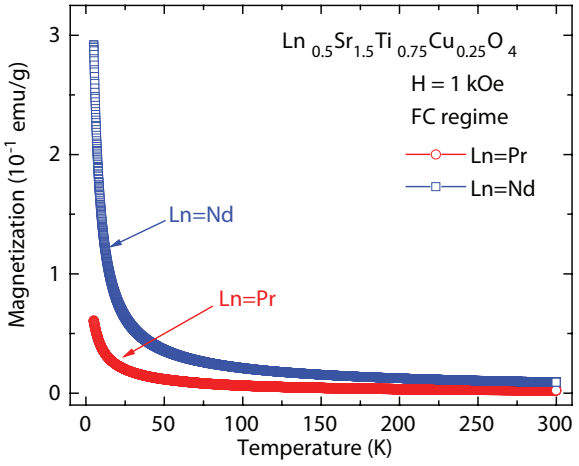

Fig. 1. Temperature dependence of magnetization for $Ln_{0.5}Sr_{1.5}Ti_{0.75}Cu_{0.25}O_4$ (Ln = Pr, Nd) layered perovskites measured in FC regime in the external magnetic field H = 1 kOe.

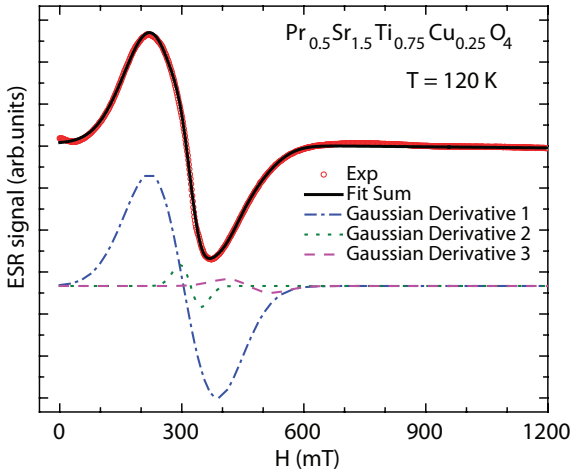

Fig. 2. Typical electron spin resonance spectra in $Pr_{0.5}Sr_{1.5}Ti_{0.75}Cu_{0.25}O_4$ at T = 120 K. Symbols show the experimental data, solid line shows the best fit using the sum of three derivative of the Gaussian line shape; dashed, dotted and dashed-dotted lines show the contributions to the ESR line separately.

spin resonance (ESR) methods. Magnetization measurements showed that the absolute value of the magnetization and effective magnetic moment for $Ln_{0.5}Sr_{1.5}Ti_{0.75}Cu_{0.25}O_4$ (Ln = Nd) compound is much higher than in the case Ln = Pr (Fig. 1); a significant difference was also observed in the magnetization dependences on the external magnetic field. The electron spin resonance spectra have the complicated lineshape and it can be decomposed into three components for both $Ln_{0.5}Sr_{1.5}Ti_{0.75}Cu_{0.25}O_4$ (Ln = Pr, Nd) complex oxides (Fig. 2). The complex inhomogeneous internal magnetic structure may arise due to the presence of two type of magnetic ions: Nd^{3+} ($4f^3$, S = 3/2) and Cu^{2+} ($3d^9$, S = 1/2) in $Nd_{0.5}Sr_{1.5}Ti_{0.75}Cu_{0.25}O_4$, and Pr^{3+} ($4f^2$, S = 1) and Cu^{2+} ($3d^9$, S = 1/2) in $Pr_{0.5}Sr_{1.5}Ti_{0.75}Cu_{0.25}O_4$, respectively.

Finally, one can conclude that despite of the similar crystal structure these two compounds can exhibit various magnetic properties and the previously observed difference in dielectric properties for these two compounds may be related to the difference in their magnetic properties.

1. Chupakhina T.I. et al.: Mendeleev Commun. **29**, 349 (2019)

Po14

Interplay of the d-impurities electrons and band electrons in the 3D Dirac semimetal Cd_3As_2

Yu. Goryunov[1], A. Nateprov[2]

[1]Zavoisky Physical-Technical Institute, FRC Kazan Scientific Center of RAS, Kazan, Russia
[2]Institut of Applied Physics, Moldova State University, Chisinau, Moldova

Topological materials are characterized by a strong spin-orbit coupling of the spin and orbital degrees of freedom of Dirac electrons, which leads, in particular, to the fact that the direction of their spins is strongly related to the direction of their motion. This obviously refers to the parent electrons of the topological material. But, in view of the fact that the modification of the electronic properties of semiconductors or semimetals is carried out by introducing impurity centers into the material, the study of the interaction of donor electrons in localized and band states is of particular importance. In this case, it would be logical to study the mutual influence of Dirac electrons and localized electronic states, which, along with the spin angular momentum, also have an orbital one.

As follows from a comparison of the concentration of conduction electrons in pure stoichiometric Cd_3As_2 with the number of electrons in the s-shells of metal atoms, electrons from the outer s-shells almost completely enter the valence band and do not participate in conduction. For example, resistivity measurements gave [1] temperature-independent electron concentrations $n_e = 2.2 \cdot 10^{19}$ cm^{-3} versus $n_e = 6 \cdot 10^{17}$ cm^{-3} for a pure sample. The unit cell α-Cd_3As_2 has a volume of $3.9 \cdot 10^{-21}$ cm^3 and contains 192 s-electrons of cadmium. Those, in a pure sample, less than 0.01% of the available s-electrons enter the conduction band. When doped at a level of ~1%, the concentration of conduction electrons increases by 2 orders of magnitude. This, however, indicates that only about 1% of the s-electrons coming from impurities enter the conduction band. Thus, electrons enter the conduction band only due to local events leading to the ionization of divalent ions of d-impurities or divalent cadmium ions.

The EPR experiments carried out on magnetic impurities of d-metals in (Fe, Mn, Cr) confirmed this version. These elements, having ionic radii somewhat smaller than the divalent cadmium ion, quite easily enter the crystal structure of cadmium arsenide. This is supported by X-ray diffraction and EDX data. Thus, in the case of doping with iron, despite its noticeable concentration in the sample, the EPR signal from Fe^{2+} is not observed. In the experiment, only a weak signal is observed from the Fe^{3+} ion with a g-factor slightly higher than the g-factor of a free electron, which is characteristic of an ion in a pure spin state $3d^5$ with $S = 5/2$, $L = 0$, $g = 2.0036$ versus $g = 2.0023$ for a free electron. Due to this nature of the entry of a magnetic ion into a topological semimetal, the weak anti-localization regime, which is evidenced by a positive magnetoresistance, is preserved at achievable doping levels.

In the case of doping with manganese [2], an intense signal is observed from the Mn^{2+} ion, which has the same pure spin state $3d^5$ with $S = 5/2$, $L = 0$ and $g = 2.0024$, which almost coincides with the g factor of a free electron. This also indicates the absence of a density of s-electrons at the crystal lattice sites at the locations of cad-

mium ions. Those, the conduction electrons do not interact with the localized magnetic moments located in these positions. The spectrum also shows a slight admixture of a signal with a slightly different *g*-factor from ions in tetrahedral vacancies. This shift indicates the presence in this position of the crystal lattice of the density of s-electrons, the polarization of which changes sign with increasing impurity concentration. At a manganese concentration of about 10 at.%, the positive magnetoresistance is suppressed, which is a sign of the termination of the weak anti-localization regime.

When doped with chromium ions, the EPR signal from divalent chromium ions is also not observed in the X-band. There is a noticeable presence of Cr^{3+} ions, which have a $3d^3$ state with $S = 3/2$ and $L = 3$. For this state, signals with anisotropic *g*-factors in the range of 1.95-1.98 are usually observed. In the case of Cd_3As_2, a signal with an anisotropic and anomalously large *g* factor in the range of 2.13–2.18 is observed in the powder sample. The anomalous value of the *g* factor is associated with the influence of band electrons, which have giant values of *g* factors, through the orbital angular momenta of the localized magnetic states of the Cr^{3+} ion.

1. Goryunov Yu.V., Nateprov A.N.: Phys. Sol. St. **60**, 68 (2018)
2. Goryunov Yu.V., Nateprov A.N.: Phys. Sol. St. **63**, 223 (2021)

Po15

Two-dimensional normal distribution of zero field splitting parameters for EPR spectra of transferrin

G.G. Gumarov*, M.I. Ibragimova, A.I. Chushnikov, I.V. Yatsyk

Zavoisky Physical-Technical Institute, FRC Kazan Scientific Center of RAS, Kazan, Russia,
*e-mail: ifoggg@gmail.com

EPR spectroscopy on transition metal ions is a powerful tool for studying the structure and structural-functional relationships. In particular, the conformational heterogeneity of iron ions in transferrin (TF) leads to an inhomogeneous and non-isotropic distribution of zero field splitting parameters (ZFS). A method based on the "error grid" method is proposed for modeling EPR spectra with a distribution of splitting parameters in the zero field [1]. In this work it is proposed to approximate such distribution by two-dimensional normal distributions. This approach makes it possible to avoid the "redescription" of spectra, which can arise for the "grid of errors" method. The technique was used for numerical processing of EPR spectra recorded in the X-band at a temperature of 80 K from standard blood serum samples containing the paramagnetic iron transport protein transferrin. It was found that the spectra are well described by two two-dimensional normal distributions with different coordinates of their centers (see Fig. 1). However, it is difficult to find a solution exclusively within the normal distribution (which, apparently, is the only one). The error grid method is convenient for preliminary analysis, determination of trends in the distribution.

Calculations have shown that the desired distribution of ZFS parameters consists of two components. The first one shows a high degree of correlation between D and E (≈ 0.8–0.95) and characterized by a ratio of E/D = 0.3 (coordinates of distribution centers). For the second component, E/D = 0.23 and $\rho \sim 0 \div 0.8$. Such regularity was

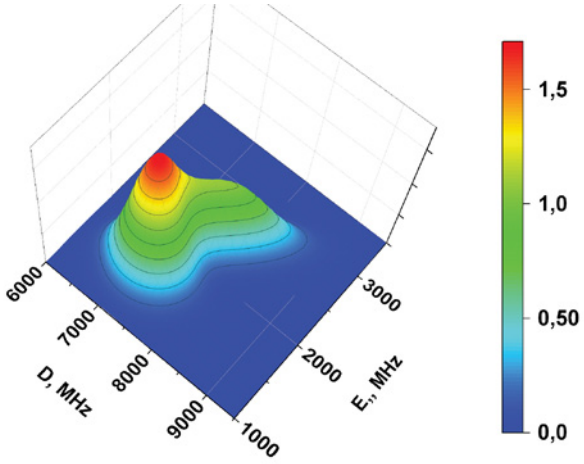

Fig. 1. Normal distribution of ZFS parameters for the EPR spectrum of TF.

found for all human blood samples studied since the coordinates of the distribution centers practically do not change. This allows us to hope that our hypothesis about the two-dimensional normal distribution of ZFS parameters is correct. The variability of the correlation of ZFS parameters requires further analysis. In addition, the problem under consideration is an inverse problem associated with an incorrect formulation [2]. Regularization methods, which are being intensively developed at the present time, are applicable to such problems. Further systematic analysis is required, including methods of quantum chemistry and molecular dynamics.

1. Azarkh M. et al.: Phys. Chem. Chem. Phys. **21**, 16937–16948 (2019)
2. Tikhonov A., Arsenin V.: M.: Nauka, 1974.

Po16

Axial symmetry line in X-band EPR spectra of human serum transferrin at helium temperatures

M.I. Ibragimova, A.I. Chushnikov, G.G. Gumarov, I.V. Yatsyk

Zavoisky Physical-Technical Institute, FRC Kazan Scientific Center of RAS,
e-mail: ibragimova@kfti.knc.ru

One of the paramagnetic proteins of blood serum is the iron transport protein – transferrin (Tf), which consists of two homologous lobes, termed the N- and C-lobe. Each lobe is divided into two subdomains, between which there is a deep cleft with a distorted octahedral geometry for the reversible binding of iron ions (Fe^N or Fe^C) in the high-spin ferric form (S = 5/2). A great contribution to the study of Tf in human blood serum was made by J-band EPR [1, 2]. These investigations made possible to determine, in particular, the presence in Fe^N of a second conformation iron site with practically axial electronic structure that differs significantly from the main conformation. At a frequency of 9.38 GHz at T ~ 80 K in the EPR spectrum of blood serum from iron ions in Tf, two absorption lines with effective g-factors ~4.3 and ~9.0 are assigned to transitions within Kramers doublets. At the same time, in the X-band EPR spectra of blood serum recorded at T = 5 K, we registered one more new signal with an effective g-factor of ~6.0 (see Fig. 1). The intensity of this signal depends on temperature and drops to zero at ~40 K.

To simulate the EPR spectra of frozen human Tf samples, the EasySpin software package [3] was used, in particular, the "pepper" utility, designed to calculate the EPR spectra of powdered solid samples. In this case, the temperature dependence of the EPR signal was taken into account, which made it possible to better describe the features of the experimental spectra. The dotted lines in Fig. 1 show the simulation of X-band spectrum recorded at a temperature of 5 K. Our simulation made possible to describe

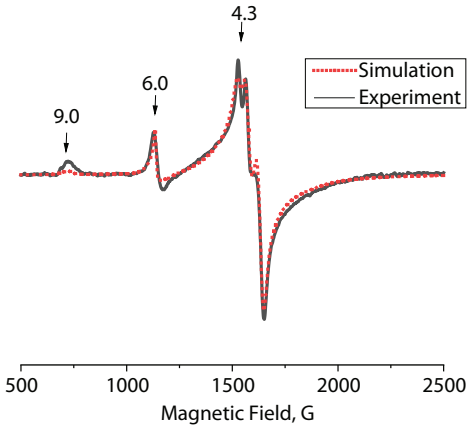

Fig. 1. X-band EPR spectrum of Tf recorded at 5 K.

quite well all the features of the experimental spectrum: characteristic three-component EPR signal (a double peak and a shoulder) near $g' \sim 4.3$, flanked by exceptionally broad tails near $g' \sim 4.3$, weak line with $g' \sim 9.0$ and, most importantly, signal with $g' \sim 6.0$. The signal with $g' \sim 6.0$ in frozen solution X-band spectra are with the help of the rhombograms for $S = 5/2$ readily assigned to transitions within the $|\pm 1/2\rangle$ and $|\pm 3/2\rangle$ doublets [1]. This signal we associated with the second iron conformation of the iron bound to N-lobe, which has a complete zero-field axial symmetry with $E/D \sim 0$. E and D are principal values of **D**-tensor and expressed in just two parameters $D = 3/2D_z$ and $E = 1/2(D_x - D_y)$ [1]. This conclusion contradicts the findings of J.M. Kolesar et al. [4, 5], who associated the signal with $g' \sim 6.0$ with high-spin heme and suggested with a certain degree of doubt that this signal comes from the oxidized state of heme in cytochrome *c* released from mitochondria.

Despite all the numerous studies, the X-band EPR spectrum of transferrin and its variations baffled researchers for decades and still remain a mystery.

1. Azarkh M. et al.: Phys.Chem.Chem.Phys. **21**, 16937–16948 (2019)
2. Mathies G. et al.: Biol Inorg Chem. **20**, 487–496 (2015)
3. Stoll S., Schweiger A.: J. Magn. Reson. **178**(1), 42–55 (2006)
4. Kolesar J. et al.: J. Inorg. Biochem. **102** (4), 693–698 (2008)
5. Kolesar J. et al.: Exper. Therap. Med. **2**, 119–123 (2011)

Po17

Correlation of NMR signal parameters with the supramolecular structure of oil

D.S. Ivanov, V.D. Skirda, D.L. Melnikova, T.A. Kazbaev

Institute of Physics, Kazan Federal University, Kazan, Russia

The development of methods and techniques of non-destructive control is of significant importance in ensuring technological progress in many sectors of the Russian economy. At the same time for the transition to the so-called digital economy it is necessary to develop methods of express analysis with a sufficiently high level of informativity. These requirements can be achieved by using and/or developing achievements in the field of nuclear magnetic resonance.

As the focus of interest is naturally shifting to heavy oil and natural bitumen, the situation with respect to the established approaches and capabilities of NMR is becoming more and more complex. In particular, in these objects, the correlation between oil viscosity and nuclear magnetic relaxation times is no longer as clearly observed as for light oils, and the use of high-resolution NMR (HR NMR) techniques is becoming increasingly problematic [1, 2].

In this regard, it seems possible to allow that the arising problems are related to the complexity of the molecular composition. In particular, heavy and high-viscosity oils have a significant content of paramagnetic admixtures [3]. This factor should also be taken into account in high-field NMR studies, as it is possible to form internal nonlinear gradients of the magnetic field directly inside the sample, which will distort the obtained data. In this regard, studies using low-field NMR equipment may be relevant. The results obtained allow us to establish correlations between NMR parameters and physicochemical properties of oil.

This work was funded by the subsidy allocated to Kazan Federal University for the state assignment in the sphere of scientific activities number FZSM-2023-0016.

1. Sandor M., Cheng Y., Chen S.: J. Petr. Sci. and Eng. **147**, 416–426 (2016)
2. Gizatullin B. et al.: Energy & Fuels **32**, 11261–11268 (2018)
3. Korb J. et al.: J. Phys. Chem. **119**, 24439–24446 (2015)

Po18

Electron and nuclear magnetic properties near ZEFOZ region

Yu.E. Kandrashkin

Zavoisky Physical-Technical Institute, FRC Kazan Scientific Center of RAS, Kazan, Russia

In the vicinity of spin level anti-crossing the properties of the electron-nuclear spin system depend considerably on the difference, ΔB, between the magnetic field and the critical field at which the zero first-order Zeeman shift (ZEFOZ) occurs. The theoretical analysis shows that the influence of hyperfine interactions (HFI) decreases linearly when approaching the ZEFOZ point, the HFI splitting of the EPR lines is essentially independent of ΔB.

Electron spin echo envelope modulation (ESEEM) characterizes the degree of spin coherence transfer to the nuclear subsystem. The modulation depth of ESEEM depends directly on the quantization axes of the nuclear spin (at a given states of the electron spin) and in the vicinity of ZEFOZ point has an approximately quadratic dependence on ΔB with a small cubic asymmetry due to the Zeeman interaction of the nuclear spin.

Figure 1 shows a sketch of how the quantization axes vary with magnetic field detuning from the ZEFOZ point. At this point, the quantization axis of the spin states is maximally deviated from the direction of the external magnetic field and the wavefunctions of the Zeeman interaction are maximally mixed (blue line). The independence of the energy on the magnetic field at $B = B_0$ reduces the efficiency of the HFI. As a result, the quantization axes of the nuclear spin subspaces are controlled only by the Zeeman interaction. Detuning from the ZEFOZ point increases the contribution of the HFI and removes the collinearity of the quantization axes of the nuclear spin subspaces. The modulation depth, $k = \sin^2 2\Delta\varphi$, dependent on the mutual deviation of these quantization axes is shown in red. The deviation is maximal when the impacts of the Zeeman and hyperfine interactions are equal.

1. Kandrashkin Yu.E.: Journal of Magnetic Resonance **350,** 107433 (2023)

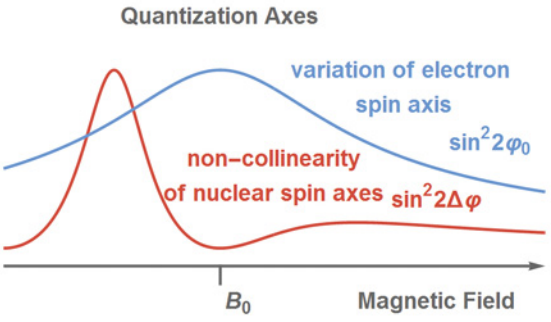

Fig. 1. Variation of the quantization axes in the vicinity of ZEFOZ point.

Po19

^{51}V NMR study of electronic structure and hyperfine interaction in chalcogenides Cr_xVSe_2 ($x \leq 0.5$)

M.E. Kashnikova[1], N.A. Utkin[1], A.G. Smolnikov[2], V.V. Ogloblichev[2], Y.V. Piskunov[2], A.F. Sadykov[2], D.F. Akramov[1,2]

[1]Institute of Physics and Technology, Ural Federal University, Ekaterinburg, Russia
[2]M.N. Mikheev Institute of Metal Physics of the Ural Branch of the Russian Academy of Sciences, Ekaterinburg, Russia

At present, layered dichalcogenides of transition elements are the subject of numerous scientific studies due to the variety of physical and physicochemical properties of materials based on these compounds. The most studied representatives of the family of layered dichalcogenides of transition elements are molybdenum, tungsten, and titanium dichalcogenides. Compounds such as VX_2 and ZrX_2 (X – Se, Te), which are of no less interest from scientific and technological points of view, have been studied in less detail in the scientific literature. Vanadium dichalcogenides are interesting because of the presence of phase transitions at low temperatures, leading to the appearance of charge density waves in the crystal structure of the sample.

In this work, an NMR study and a study of the magnetic properties of vanadium dichalcogenide intercalated with chromium Cr_xVSe_2 ($x \leq 0.5$) were carried out. The

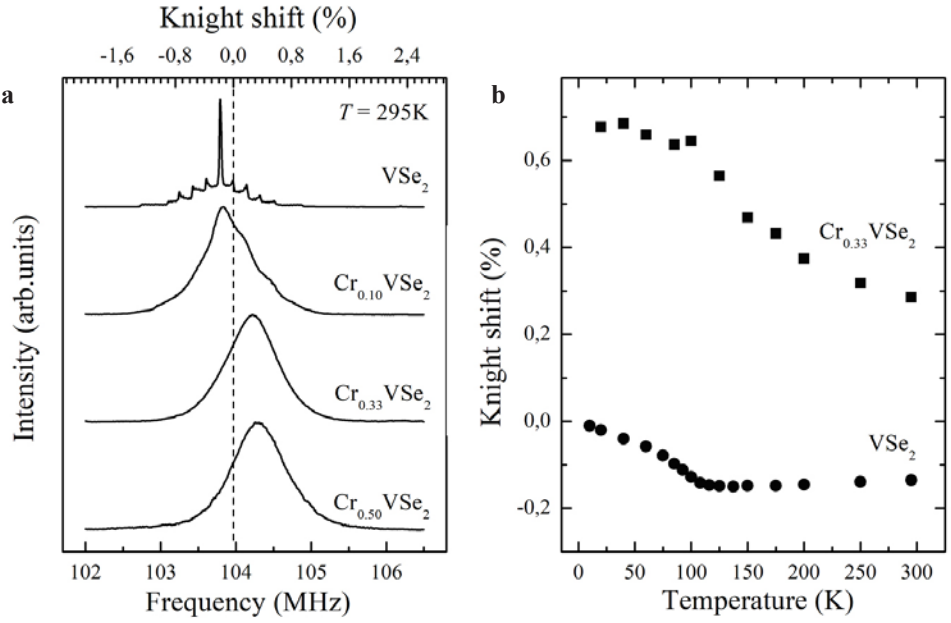

Fig. 1. a ^{51}V NMR spectra in Cr_xVSe_2 (x = 0, 0.1, 0.33, 0.5) in an external magnetic field of 92.8 kOe at a temperature of T = 295 K. The NMR spectra were recorded using a resonant silver coil. **b** Temperature dependence of the Knight shift of ^{51}V nuclei for VSe_2 and $Cr_{0.33}VSe_2$.

NMR spectrum of ^{51}V nuclei in the initial VSe_2 (Fig. 1a) is a narrow symmetrical line located on a wide pedestal of satellite lines. Such a characteristic structure is due to the interaction of the quadrupole moment of the nucleus with the electric field gradient created at the location of the nuclei by their charge environment. The NMR spectrum of ^{51}V nuclei in VSe_2 is well processed under the assumption that all vanadium atoms are equivalent and are in good agreement with the literature data [1, 2]. Upon intercalation of chromium ions into the VSe_2 structure, the NMR spectrum broadens, the fine structure disappears, and the average line shift increases. In $Cr_{0.33}VSe_2$, when the temperature decreases, the shift increases and the NMR line widens (Fig. 1b).

A significant broadening of the spectra shows a significant local inhomogeneity, both charge and magnetic, of the Cr_xVSe_2 ($x \leq 0.5$) compounds. From the temperature dependences of the shift and susceptibility, an estimate was made of the hyperfine interaction constant in vanadium ions. Analyzing the obtained dependences $\chi(T)$, it can be noted that there is no long-range magnetic order in the entire concentration range of chromium, and below the critical temperature, a state of the spin or cluster glass type is formed. The absence of long-range magnetic order in Cr_xVSe_2 compounds differs from the behavior of a number of other M_xTX_2 systems intercalated with chromium, in particular, such as Cr_xTiSe_2, in which, as established at $x > 0.33$, antiferromagnetic order is realized, as well as $Cr_{0.33}NbSe_2$ and $Cr_{0.65}TiTe_2$ compounds with ferromagnetic ordering of the magnetic moments of chromium [3–5].

This work was supported by the Russian Science Foundation (project no. 22-12-00220).

1. Tsuda T., Kitaoka Y., Yasuoka H.: Physica **105B**, 414 (1981)
2. Skripov A.V., Stepanov A.P., Shevchenko A.D., Kovalyuk Z.D.: Phys. stat. sol. (b) **119**, 401 (1983)
3. Hu W.Z., Wang G.T.: Physical review B **78**, 085120 (2008)
4. Inoue M., Hughes H.P., Yoffe A.D.: Adv. Phys. **38**, 565 (1989)
5. Pleschov V.G. et al.: J. Alloys Compd. **320**, 13 (2001)

Po20

Synthesis and EPR study of nitroxide radical single crystal

R.B. Zaripov[1], I.T. Khairutdinov[1], M.M. Bakirov[1], A.I. Kokorin[2], T. Kálai[3], M. Balog[3]

[1]Zavoisky Kazan Physical-Technical Institute, Russian Academy of Sciences, Kazan, Russia, e-mail: semak-olic@mail.ru
[2]N. N. Semenov Institute of Chemical Physics, Russian Academy of Sciences, Moscow, Russia
[3]Institute of Organic and Medicinal Chemistry, Faculty of Pharmacy, University of Pécs, Pecs, Hungary

Currently, there is a continuing increase in the use of the magnetic moments of electrons and nuclei as qubits. Biradicals containing stable radicals can be of great importance for quantum technologies. Since they seem to be promising elements for the implementation of two-qubit logical operations [1, 2]. It is important that stabilized organic biradicals are characterized by relatively long spin decoherence times for unpaired electrons in their radical fragments. We also note that the study of biradicals by EPR

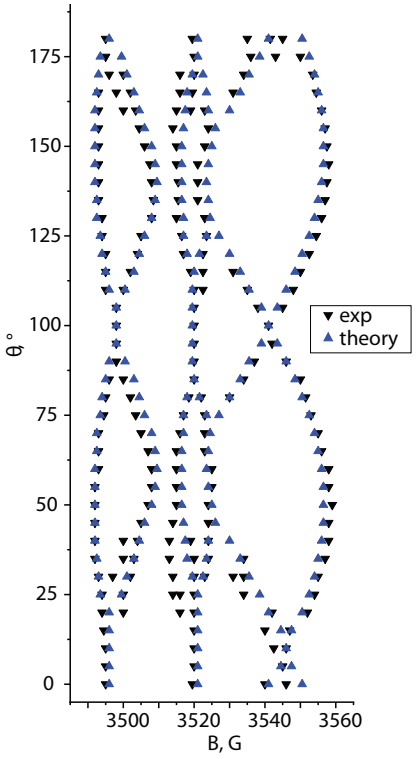

Fig. 1. Angular dependences of the resonance components of the EPR spectra of diluted nitroxide single crystal in the X-band.

spectroscopy makes it possible to obtain unique information on the exchange interaction between radical centers bound by a system of covalent bonds in order to study the effect of bond conjugation on spin exchange. Moreover, by changing the length of the chain connecting two paramagnetic centers, one can obtain the desired values of the exchange interaction between them. In addition, the study of the spin density distribution in the biradical structure is of particular interest [3].

In our work, we tested several methods for the synthesis of a high-quality single crystal of the nitroxide radical. The quality of the synthesis was assessed using EPR spectroscopy. It is no secret that the successful application of EPR spectroscopy requires the synthesis of magnetically dilute systems. Otherwise, due to the strong exchange interaction in the EPR spectrum, one will get only one uniformly broadened line. For quantum computing operations, it is very important to selective excitation of the desired spins by electromagnetic field pulses. The spins of a given paramagnetic center should have their own resonance lines in the EPR spectrum that do not overlap with the lines of another. Single crystals of nitroxide radicals satisfy this requirement well. The EPR spectrum of these single crystals in one given orientation has a simple form. It is not necessary to average the spectrum over all possible orientations as in the case of a powder sample. The powder spectrum of nitroxide radicals is quite complex due to the anisotropy of the hyperfine interaction. Selective excitation of the centers in this case is impossible, since each line of the powder spectrum is a superposition of signals of different orientations.

We have shown that two synthesis methods give single crystal with the enough properties. Modeling of EPR spectra in the X and Q bands shows the presence of 2 non-equivalent centers in the unit cell. Figure 1 shows orientation dependence of resonance lines of the spectrum of nitroxide single crystal in the X band. This dependence can be explained only by two nonequivalent centers.

The reported study was funded by RSF according to the research project № 22-72-10063.

1. Nakazawa Sh., Nishida Sh., Ise T., Yoshino T., Mori N., Rahimi R.D., Sato K., Morita Y., Toyota K., Shiomi D., Kitagawa M., Hara H., Carl P., Hofer P., Takui T.: Angew. Chem. Int. Ed. **51**, 1–6 (2012)
2. Volkov M.Yu., Salikhov K.M.: Appl. Magn. Reson. **41**, 145 (2011)
3. Kokorin A.I., Gromov O.I., Kálai T., Hideg K.: Appl. Magn. Reson. **47**, 1283 (2016)

Po21

Development of pulse sequences to improve the information of surveys of specialized magnetic resonance imaging system with 0.4 T magnetic field induction

A. Kolesova[1], T. Islamov[1], I. Sidorov[1], Ya. Fattakhov[2], V. Odivanov[2]

[1]Institute of Physics, Kazan (Volga Region) Federal University, Kazan, Russia, e-mail: akolesova0707@mail.ru
[2]Medical Physics Methods Laboratory, Zavoisky Physical-Technical Institute, FRC Kazan Scientific Center of RAS, Kazan, Russia

Nowadays, magnetic resonance imaging (MRI) is one of the most effective non-invasive diagnostic methods in medicine. This method does not use ionizing radiation, which makes it safe to use. It is based on the detection of relaxation changes in the structural component of tissues during pathological processes in organs.

All over the world there is an increasing interest in medium- and low-field MRI systems. Mid-field MRI is significantly cheaper when purchased and during operation. This will allow them to be used in emergency rooms and medical institutions in small towns. Due to some limitations, medium and low field MRI do not allow the use of all methods used in high field installations. This makes the development of new measurement methods for mid-field MRI systems topical.

The presented project makes it possible to raise the quality of diagnostics of mid-field MRI to the level of MRI with 1.5 T. New methods of magnetic resonance imaging can increase sensitivity and reduce the time of examination of patients on medium- and low-field devices.

A method has been developed to obtain more information in standard time. The method is based on the Carr-Purcell and Meibum-Gill sequences. It allows you to get

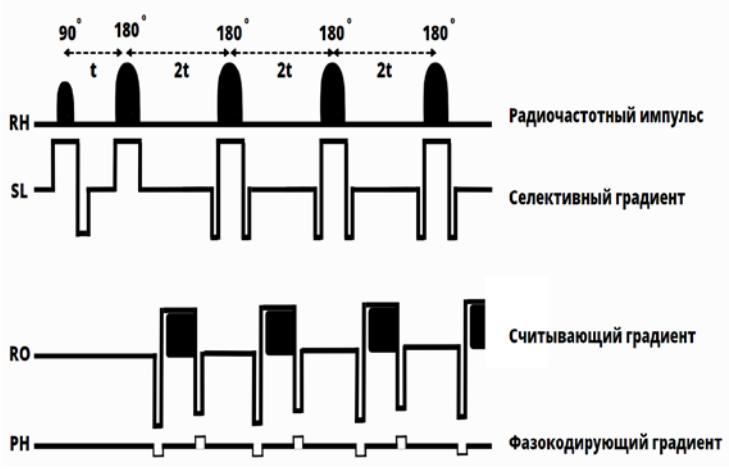

Fig. 1. Schematic representation of the developed sequence.

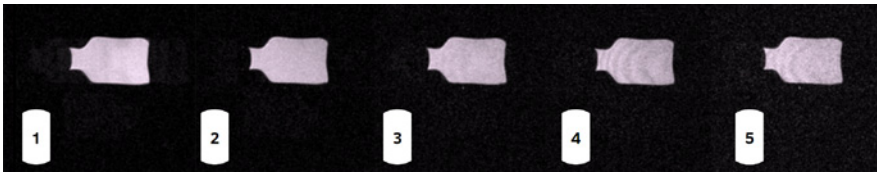

Fig. 2. Images of the phantom obtained using the developed sequence on a MRI system with a magnetic field induction of 0.4 T. The numbers in the figure indicate the serial numbers of the echo in one cycle of the sequence.

a complete relaxation decay in T_2 in one measurement cycle. In this case, the spin echo signal is recorded several times in one run. The number of echoes is selected by the MRI operator. As a result, an image is formed for each signal. A schematic representation of the sequence is shown in Fig. 1.

To test the consistency of the sequence, we used a phantom. The results of the implementation of the sequence are shown in Fig. 2.

In the future, this sequence will be tested on more complex phantoms with substances with different relaxation times T_2, as well as on tissues of a living person. The project is an example of an import substitution program being implemented in the Russian Federation.

Po22

Modeling the magnetic response of a functionalized carbon sphere

E.I. Kovycheva, K.B. Tsiberkin, V.K. Henner

Perm State University, Perm, Russia

The properties of highly porous carbon materials can be controlled by inserting metal cores into shells or by depositing magnetic ions on the carbon surface. For example, adding an impurity in a high concentration leads to the opening of a band gap in the energy spectrum of carbon, and the material becomes close to a semiconductor in its properties. In addition, the described materials can find applications in the development of new systems for storing, processing and transmitting information using spin magnetic moments [1]. The study of composites with properties that are controlled by an applied magnetic field, is an urgent task. In this work, we analyze the dynamics of the spin clusters magnetization with a ring structure in different states, as well as their combination in the form of a spherical carbon nanoshell formed by rings of different numbers of spins.

There are series of calculations of the evolution of the transverse magnetization of spin systems, including from 6 to 12 particles with spin 1/2, grouped into ring structures of various radii.

The calculated magnetization signals from individual rings were summed to simulate the dynamics of a spherical structure (Fig. 1) according to the technique described in [2, 3]. The total signal shows monotonic decay, but the exact dependence requires additional analysis.

One may see that an increase in the number of spins in the cluster makes the transversal magnetization signal at long times weaker (Fig. 2a). It gives more precise the experimental picture even without taking into account thermodynamic effects in the model. The relaxation time with a change in the number of spins (and the radius of the ring, respectively) practically does not change, which confirms the reliability of the simulation at short times with a small number of particles in the system.

In addition, the contribution of the exchange interaction to the system was considered (Fig. 2b). A positive exchange interaction leads to a significant increase in the relaxation time, while the negative exchange decreases it.

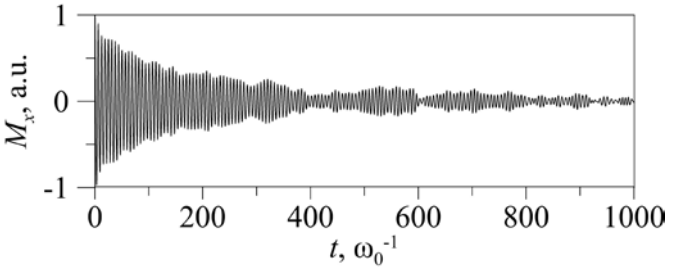

Fig. 1. The total magnetization of the spherical shell model is the superposition of signals from noninteracting ring spin clusters with radii from 0.50 to 2.0.

Po22

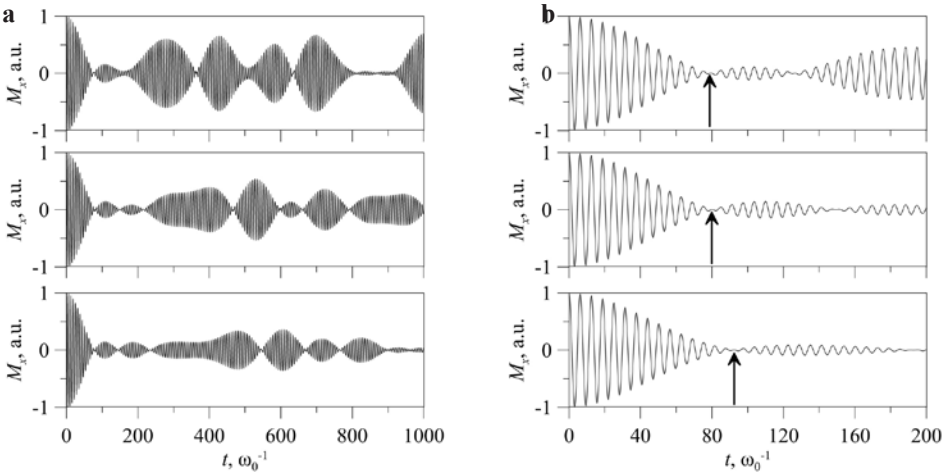

Fig. 2. Magnetization of a single ring spin cluster: **a** with a different particle number, from top to bottom: 6, 8 and 10 particles; **b** effect of exchange interaction, from top to bottom: $J = -10^{-2}$, 0 and $+10^{-2}$, dipole energy is 10^{-2} for all cases, ring includes of 8 particles; the arrows mark the first zero of the magnetization envelope.

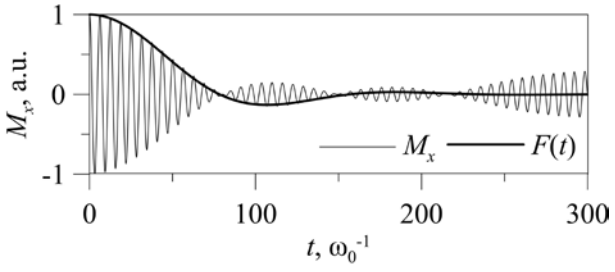

Fig. 3. Comparison of the Abraham function with the signal of transverse magnetization from single ring of 8 particles.

In addition, an analytical calculation was made for the moments of the of magnetization signal spectrum, and the Abraham functions were calculated for a ring system of 8 spins [4]. An example of its comparison with the numerical simulation of the signal is shown in Fig. 3. Combination of these approaches makes us possible to estimate the analytical dependence of $M_x(t)$ on the ring radius [5].

1. Rudakov G.A., Sosunov A.V., Ponomarev R.S., Khenner V.K., Reza M.S., Sumanasekera G.: Phys. Solid State **60** (1), 167 (2018)
2. Henner E.K., Schaposhnikov I.G.: Radiospectroscopy **10**, 74–81 (1976)
3. Henner V.K., Klots A., Nepomnyashchy A.A., Belozerova T.S.: Applied Magnetic Resonance **52**, 859–866 (2021)
4. Abragam A.: The principles of nuclear magnetism, p. 599. Oxford: Clarendon Press 1961.
5. Kovycheva E.I., Tsiberkin K.B.: Bull. Perm Univ. Phys. **2**, 26–35 (2022)

Po23

^{1}H NMR method for monitoring aspirin intake at therapeutic doses

G. Kupriyanova[1], I. Mershiev[1], E. Moiseeva[2], V. Rafalskiy[2]

[1]Institute of Physics, Mathematics and Information Technology, e-mail: galkupr@yandex.ru
[2]Center of Clinical Trials, Immanuel Kant Baltic Federal University, Kaliningrad, Russia

Introduction. Cardiovascular disease (CVD) is the leading cause of morbidity and mortality among individuals worldwide [1]. High adherence to pharmacotherapy, especially antithrombotic drugs, in patients with CVD is essential to prevent fatal complications. In this regard, it is very important for the physician to have a tool for objective assessment of adherence to therapy. One of the most important components of antiplatelet therapy is aspirin, so this drug is of the greatest interest in the development of adherence monitoring methods [2]. The high-resolution NMR method is becoming more and more widespread in urine metabolomics. It has been shown that slightly more than 200 metabolites can be routinely identified with NMR spectroscopy techniques. Research shows that of all platforms and technologies, NMR is proving to be the best, both in terms of coverage and quantification of metabolites, as a diagnostic tool for various diseases [3]. In this regard, prevention of CVD is of particular importance, namely, a simple and effective method of taking low doses of aspirin. In

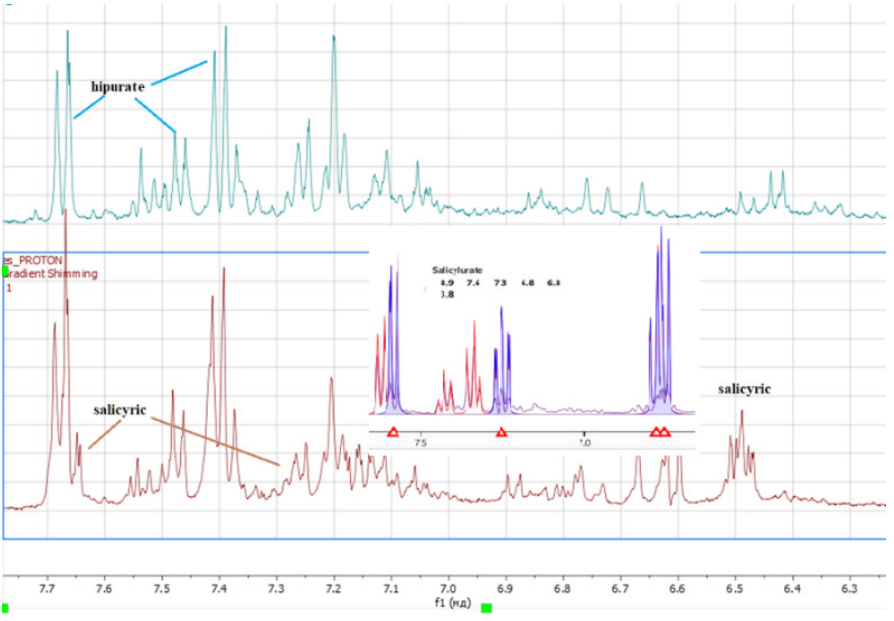

Fig. 1. Fragments of the ^{1}H NMR spectra of urine of the volunteer (N2) before taking 100 mg of aspirin (top picture) and 4 hours after taking the drug (bottom picture). The inset shows a fragment of the spectrum (red) processed in the Genome program, which makes it possible to identify salicyluric acid (blue spectrum).

Po23

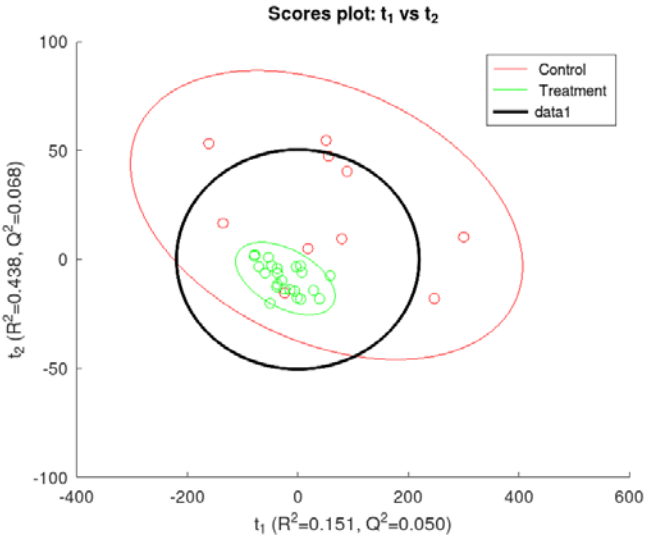

Fig. 2. Results of principal component analysis (PCA) of a dataset of urine samples from 33 healthy volunteers and patients. Data points from the ASA treatment group appear to be highly localized.

this work, we investigated the problem of reliable detection of aspirin metabolites by NMR after taking the drug in small doses both in healthy volunteers and in patients with signs of cardiovascular disease. The study assessed urinary salicyluric acid (SU) levels as a function of the time between drug administration and urine collection. In order to study the variability of the metabolomic profile, urine studies of volunteers were carried out at different times of the year.

Human subject research. The investigation used a panel of 14 healthy volunteers, drawn from the students and staff of Immanuel Kant Baltic Federal University, ages 19–50 years, body weight 55–85 kg and 8 patients with cardiovascular disease. The subjects had taken no drugs for at least seven days before their participation in the study; no other exclusion criteria were applied. Urine of different healthy volunteers was collected in December, July, October. There were no restrictions on the diet of the volunteers. Urine samples were collected from healthy volunteers and patients with cardiovascular disease after signing informed consent. Urine samples of healthy volunteers were collected before and after administration of 75, 100 and, 300 mg ASA. Urine samples of patients with cardiovascular disease were collected after administration of 75 or 100 mg ASA. The time between administration the drug and collecting urine from patients with cardiovascular disease ranged from 2 hours to 21 hours. The urine pH was adjusted to 7.2–7.4 by adding phosphorus buffer solution (K_2HPO_4) to the urine sample.

Urine samples were examined by ^{1}H NMR on a VARIAN 400 spectrometer with 9 T magnetic field. All spectra were acquired at 25°C. For ^{1}H NMR experiments, 540 µl of the sample was placed in a standard 5 mm tube. The total sample volume was brought to 600 µl by adding 60 µl of a 0.1% solution of DSS (4,4-dimethyl-4-silapentane-1-sulfonic acid) in D_2O.

Results. A urine study of 14 healthy volunteers before and after taking various doses of Aspirin (75 mg, 100 mg, 300 mg and 3 g) revealed the following important

result. In all volunteer urine samples, SU signals of varying intensity were detected in three characteristic regions of the ^{1}H NMR spectrum, namely, a doublet at 7.78 ppm, overlapping triplet and doublet 6.8–6.89 ppm (specify) due to the protons of the aromatic ring (Fig. 1), and at 3.92 ppm referred to CH_2, in cases where the time intervals between taking the drug and the time of urine collection varied from 2 hours to 18 hours. However, we were able to reliably detect SU signals in the urine only in one healthy volunteer 24 hours after taking the drug. It should be noted that there were marked differences in the metabolic profile of healthy volunteers and patients with signs of cardiovascular disease. In addition, slight variations in the metabolomic profile were found in healthy volunteers during the winter and summer months. However, changes in the spectra of urine samples caused by the appearance of aspirin metabolites after a single dose of various doses of the drug were observed in all volunteers. In those cases, when the time between taking the drug and collecting urine reaches 20–21 hours, the intensity of the SU signals was observed to decrease and it became problematic to distinguish them against the background of more intense hippurate signals. In this case, the presence of the metabolite was determined by the change in the integrated intensity of the region of the spectrum, exciting the lines of the hippurate doublet and the putative doublet of salicyluric acid in the range from 7.86 to 7.75 ppm. A more reliable result of the presence of the salicyluric acid metabolite is given by estimates of the signal level of the CH_2 group in the region of 3.82–3.84 ppm., which does not overlap with the hyppurate signal. However, it was found that the intensity of the signal of the CH_2 group decreased somewhat when a buffer solution was added. The spectra of prepared urine samples from patients with signs of CVD and taking the drug at a dose of 100 mg were studied. In all samples, except for one sample, ^{1}H NMR signals of SU were unambiguously determined in the characteristic regions of 7.61–7.65 ppm, 6.89–6.92 ppm and 3.82–3.84 ppm. In a patient whose urine collection was carried out after 21 hours, signals in the areas of 7.61–7.63 ppm and 6.87–6.91 ppm were not clearly visible, which overlapped with the signals of other metabolites, but a signal from CH_2 groups (3.82–3.84 ppm) of saliciluric acid was clearly observed.

Thus, monitoring is proposed to be carried out according to the group of salicyluric acid signals in the areas of 7.61–7.65 ppm, 6.89–6.92 ppm and 3.82–3.84 ppm in the spectra of urine samples collected in the morning after taking the drug in the evening hours of the previous day. Diagnosis of the presence of other lines of the aromatic part of SU is problematic, since the triplet lines in the region of 7.5 ppm SU overlap with hippurate and other metabolites, the level of which depends on many factors. Considering that the time of taking the drug by the patient remains unknown, some monitoring difficulties may arise when taking small doses of AS and the time between taking the drug and collecting urine exceeds 20 hours. Due to the specificity of metabolic processes, only some volunteers reliably recorded SU signals after 24 hours after taking the drug (refer), while in most patients the intensity of SU signals, especially the doublet at 7.78, sharply decreased.

1. Virani SS, Alonso A, Aparicio H.J., Benjamin E.J., Bittencourt M.S., Callaway C.W. et al.: Circulation. **143**, e254– e743 (2021)
2. Duffy D, Kelly E, Trang A, Whellan D, Mills G.: Postgrad Med. **126**(1), 18–28 (2014)
3. Pulido N., Guevara-Morales J.M., Rodriguez-López A., Pulido Á., Díaz J., Edrada-Ebel R.A., Echeverri-Peña O.Y.: Metabolites **11**, 891 (2021)

Po24

Out-of-phase electron spin echo in photovoltaic composite of P3HT and single-walled carbon nanotubes

L.V. Kulik, E.S. Kobeleva, A.V. Kulikova

Voevodsky Institute of Chemical Kinetics and Combustion SB RAS, Novosibirsk Russia,
e-mail: a.kulikova1@g.nsu.ru

Despite the promising photovoltaic performance of the composite of poly-3-hexylthiophene (P3HT) with semiconducting single-walled carbon nanotubes (s-SWCNT), the short-circuit current density jsc for this composite is low in comparison with jsc of typical polymer/fullerene composites. To clarify the origin of the poor photogeneration of free charges, out-of-phase electron spin echo (ESE) technique was used with laser excitation of the P3HT/s-SWCNT composite. The presence of out-of-phase ESE signal is a valid proof that the charge-transfer state of $P3HT^+$/s-$SWCNT^-$ is formed upon photoexcitation and the spins of $P3HT^+$ and s-$SWCNT^-$ are correlated. In the same experiment with pristine P3HT film the out-of-phase ESE signal was not detected.

The out-of-phase ESE envelope modulation trace for P3HT/s-SWCNT composite was similar to that of the polymer/fullerene photovoltaic composite PCDTBT/$PC_{70}BM$, which implies the same distance of initial charge separation in the range 2–4 nm. However, out-of-phase ESE signal decay with delay after laser flash increase for P3HT/s-SWCNT composite was much faster, with a characteristic time of 10 μs at 30 K. That result shows the higher geminate recombination rate for the P3HT/s-SWCNT composite, which may be one of the reasons for the relatively poor photovoltaic performance of this system.

Moreover, no out-of-phase ESE signal was observed in a composite of P3HT and fluorinated SWCNT which correlates with its extremely low photovoltaic performance

This work was supported by RSF (project №23-73-00072)

Po25

On the difficulties of classical MRI techniques application in porous media

D.L. Melnikova, V.D. Skirda, A.S. Alexandrov, D.S. Ivanov, R.V. Archipov, O.I. Gnezdilov, A.A. Ivanov, M.M. Doroginitsky, T.A. Kazbaev, A.L. Valiullin

Institute of Physics, Kazan Federal University, Kazan, Russia

MRI methods are less frequently used to study various materials, firstly, due to their higher degree of heterogeneity, including heterogeneity in magnetic susceptibility. As a result, internal magnetic field gradients are formed in such objects when they are introduced into an external magnetic field, which critically reduces the resolution of MRI techniques.

This negative effect is most pronounced in composite and porous materials, which are promising for many areas of applied science and technology (mechanics, engineering, hydrogeology, petroleum geology, geophysics, biology and biophysics) [1]. Due to the difference of magnetic susceptibilities at the pore boundaries, the internal magnetic field gradients in them can reach several T/m [2, 3], which can be comparable or even exceed the external gradient amplitudes used for spatial coding in MRI. Unlike static inhomogeneities of the magnetic field, the internal gradients arising in porous materials are unique, depend on the structure, composition, and state of the material [4], and their influence on the image obtained in MRI cannot be compensated by software tools during processing. It is possible to apply phase-phase encoding techniques for such objects, however, this requires a significant increase in the time required to perform the study [5].

As a result, for a whole class of materials, which include many natural substances such as rocks and soil, zeolites, biological tissues, many artificial materials such as glass, polymer composites, cement, ceramics, the possibility of studying by MRI methods using frequency coding is actually lost.

This work was funded by the subsidy allocated to Kazan Federal University for the state assignment in the sphere of scientific activities number FZSM-2023-0016.

1. Gitis V., Rothenberg G.: Handbook of Porous Materials: Synthesis, Properties, Modeling and Key Applications. World Scientific (2020), 1492 p.
2. Seland J., Washburn K., Anthonsen H., Krane J.: Phys. Rev. E **70**(5), 051305 (2004)
3. Mitchell J., Chandrasekera T., Johns M., Gladden L., Fordham, E.: Phys. Rev. E **81**(2), 026101 (2010)
4. Hürlimann M.: J. Magn. Res. **131**(2), 232–240 (1998)
5. Callaghan P., Forde L., Rofe C.: J. Magn. Res., Series B **104**(1), 34–52 (1994)

Po26

Spin dynamics in domain walls with adiabatic pulse NMR excitation

I. Mershiev, G. Kupriyanova

The Institute of Physical and Mathematical Sciences and Information Technology,
Immanuel Kant Baltic Federal University, Kaliningrad, Russia

Adiabatic pulses are used in NMR to provide broadband excitation and inversion in inhomogeneous B1 field [1]. Other uses of adiabatic pulses include sensitivity enhancements in solid state NMR and pulsed EPR excitation.

NMR in magnetic materials is another field of magnetic resonance spectroscopy that deals with very broad spectra up to hundreds of MHz. Because of the intrinsic properties of magnetic materials, spin dynamics of nuclei in domain walls is complex and include multiple effects [2] such as dispersion of enhancement factor in domain walls, boundary effects at domain wall intersections, directional averaging effects in isotropic samples, etc. In this work, we explore possibilities of using adiabatic pulses for NMR spin-echo experiments in magnetic materials.

Calculations based on the solution of Bloch-Ricatti equations for hyperbolic secant adiabatic pulses [3] and spin magnetization calculations considering domain wall dynamics in ferromagnetic [4] show that broadband adiabatic pulses are capable of creating greater inverted magnetization than regular pulse at some critical field strength, or adiabatic condition [5]. The effect can be used to increase sensitivity of spin-echo experiments in soft magnetic materials.

1. Baum J., Tycko R., Pines A.: Phys. Rev. A **32**, 3435 (1985)
2. Oliveira I.S. Guimarães A.P.: J. Magn. Magn. Mater. **170**, 277 (1997)
3. Silver M.S., Joseph R.I., Hoult D.I.: Phys. Rev. A **31**, 2753 (1985)
4. Stearns M.B.: Phys. Rev. **162**, 496 (1967)
5. Tannús A., Garwood M.: NMR Biomed. **10**, 423 (1997)

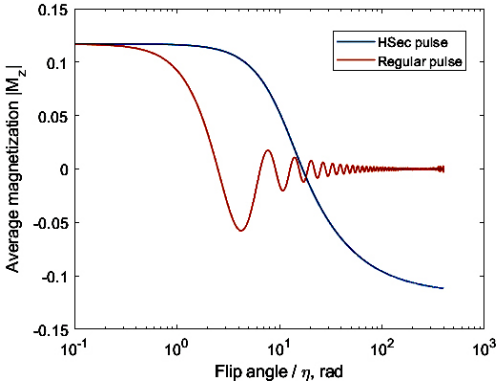

Fig. 1. Comparison of calculated inverted spin magnetization values for hyperbolic secant and regular constant frequency pulse in isotropic ferromagnetic sample.

Po27

Exploring the properties of the V_B defect in hBN: optical spin polarization, Rabi oscillations, and coherent nuclei modulation

F.F. Murzakhanov, G.V. Mamin, M.A. Sadovnikova, I.N. Gracheva, M.R. Gafurov

Institute of Physics, Kazan Federal University, Kazan, Russia

Today, point defects in solid state have acquired particular interest in condensed matter physics through their new opportunities and current unsolved problems. Structural disorders of the crystal lattice, called color centers, can lead to significant changes in the optical and spin properties of the material. Comprehensive studies of optically polarized high-spin states ($S \geq 1$) of defects in wide-gap semiconductors have revealed a new scientific and technical direction for the development of quantum technologies [1, 2]. Hexagonal boron nitride, with an ultra-wide band gap E_g = 6 eV, containing a negatively charged boron vacancy (V_B) with unique spin, optical, and coherent properties presents a new two-dimensional platform for the implementation of quantum technologies.

This work establishes the value of V_B spin polarization under optical pumping with λ_{ext} = 532 nm laser using high-frequency (ν_{mw} = 94 GHz) electron paramagnetic resonance (EPR) spectroscopy. In optimal conditions polarization was found to be $P \approx 38.4\%$. Our study reveals that Rabi oscillations (Fig. 1) induced on polarized spin states persist for up to 30–40 μs, which is nearly two orders of magnitude longer than what was previously reported [2]. Analysis of the coherent electron-nuclear interaction through the observed electron spin echo envelope modulation (ESEEM) made it possible to detect signals from remote nitrogen and boron nuclei, and to establish a corresponding quadrupole coupling constant C_q = 180 kHz related to nuclear quadrupole moment of ^{14}N. These results have fundamental importance for understanding the spin properties of boron vacancy.

1. Pezzagna S, Meijer J.: Applied Physics Reviews **8**, 011308 (2021)
2. Kagan C.R., Bassett L.C., Murray C.B., Thompson S.M.: Chem. Rev. **121**, 3186–233 (2021)

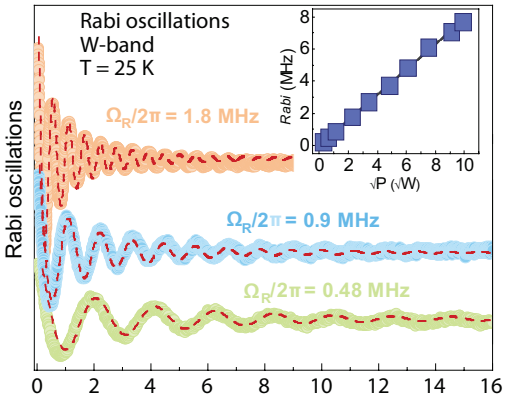

Fig. 1. Rabi oscillations between the states M_S = 0 and M_S = +1 of the boron vacancies at different microwave powers, $B_0 \parallel c$. The linear dependence of Rabi frequency on the square root of microwave power (which is proportional to B_1) is demonstrated in the inset.

Po28

FMR investigation of magnetic properties of planar Ni microparticles with square shape

N.I. Nurgazizov[1], A.P. Chuklanov[1], D.A. Bizyaev[1], A.A. Bukharaev[1], L.V. Bazan[1], V.Ya. Shur[2], A.R. Akhmatkhanov[2]

[1]Zavoisky Physical-Technical Institute, FRC Kazan Scientific Center of RAS, Kazan, Russia
[2]School of Natural Sciences and Mathematics, Ural Federal University, Ekaterinburg, Russia

Recently, the control of microparticle magnetic properties by uniaxial stress has been intensively studied [1, 2]. The stress in such microparticles can be created by various ways, for example, by using of the difference in the thermal expansion coefficients of the single crystal substrate where particles are formed. Here, changing in the magnetic properties of planar Ni microparticles formed on the $LiNbO_3$ (CLN) and on the $KTiOPO_4$ (KTP) single crystal surfaces was studied. Ni microparticles formed on the glass surface were used as a control sample. The microparticles had a square shape and lateral dimensions of 7.5 μm. The height of the microparticles was 0.03 μm. The electron beam evaporation was used for microparticles forming. The material was deposited under ultrahigh vacuum conditions through a metal mesh tightly pressed to the substrate surface at the room temperature. It was carrying out by Multiprobe P (Omicron) device.

For FMR measurements, the Bruker EMX Plus with a field (Hex) up to 1.4 T and a microwave field at a frequency of 9.8 GHz was used. FMR specters were taken for all samples at orientation angles [0°; 180°] in the temperature range [–10; 60] °C. Based on the data obtained, the angular dependence of the resonant field (H_{res}) was plotted for various temperatures. The dependences on temperature for the direction of the anisotropy axis on temperature and for the dependence of the eccentricity ($e = H_{res,max} - H_{res,min}$) were found. It was found that on single-crystal substrates the anisotropy axis of Ni microparticles rotates on approximately 90° when the sample is heated from –10 to +60 °C with step 10 °C. The eccentricity decreases from 0.6 to 0.25 as the temperature rises from –10 °C to +30 °C, then increases to 0.5 as the temperature rises to 60 °C. On a glass substrate with an isotropic coefficient of thermal expansion was observed that the anisotropy axis is related to the shape of the microparticles and, as expected, no change in its direction with temperature variation. The value of the eccentricity on this sample also practically does not change and is approximately 0.3. The results of the studies performed are in good agreement with the data of changes in the domain structure of Ni microparticles obtained earlier by magnetic force microscopy [3].

The research was supported by RSF (project № 22-29-00352).

1. Bukharaev A.A., Zvezdin A.K., Pyatakov A.P., Fetisov Yu.K.: Phys. Usp. **61**, 1175 (2018)
2. Bandyopadhyay S., Atulasimha J., Barman A.: Appl. Phys. Rev. **8**, 041323 (2021)
3. Nurgazizov N.I., Bizyaev D.A., Bukharaev A.A., Chuklanov A.P., Shur V.Ya., Akhmatkhanov A.R.: Phys. Solid State **64**, no. 9, 1305 (2022)

Po29

Investigation of the features of the interaction of water molecules and saccharides in aqueous solutions by NMR

D.A. Parfenova, D.L. Melnikova, V.D. Skirda

Department of Molecular Physics, Institute of Physics, Kazan Federal University, Kazan, Russia, e-mail: daryaparfenova@mail.ru

In the field of scientific research, of particular interest is the study of aqueous solutions of saccharides. A large list of works is devoted to the possibilities of using saccharides in medicine and pharmacology to create new drugs and improve treatment methods [1], in the food industry as substitutes and additives [2], in the chemical industry to obtain other demanded compounds and materials [3]. The study of the characteristics of saccharides during their dissolution plays an important role in determining their structural and functional properties, which will improve the efficiency of their use. Currently, the mechanisms of interaction of water molecules and saccharides remain poorly studied [4].

The purpose of current work was to study the features of the interaction of water molecules and saccharides in aqueous solutions using nuclear magnetic resonance method. The monosaccharide D-xylose and the disaccharide sucrose were chosen as the objects of study in this work. It was found that the spin-spin relaxation of water molecule protons is characterized by an anomalously strong concentration dependence for both studied saccharide solutions. As additional results, the fulfillment of the condition for rapid exchange between the protons of water molecules and the protons of the hydroxyl groups of saccharides is shown for all experimental data and in the entire studied concentration range.

The work was carried out on the equipment of the Federal Center of Shared Facilities for physical and chemical research of substances and materials (FCSF) KFU Bruker AVANCE 400 MHz spectrometer optimized for microtomography, solid state and self-diffusion.

1. Yu W., Zhang N., Li C.: Curr. Pharm. Des. **15**, 3826–3836 (2009)
2. Röhrig C.H., Choi S.S., Baldwin N.: Crit. Rev. Food Sci. Nutr. **57**, 1017–1038 (2017)
3. Hengtao T., Zheng Z., Zhi C., Xin J., Liangzhi L.: Mol. Catal. **531**, 112672 (2022)
4. Heugen U., Schwaab G., Bründermann E., Havenith M.: PNAS **103**, 12301–12306 (2006)

Po30

Studies of Sr_2MnNbO_6 double perovskites

D.V. Popov[1], R.G. Batulin[2], I.V. Yatsyk[1], V.A. Shustov[1], T. Maiti[3], R.M. Eremina[1]

[1]Zavoisky Physical-Technical Institute, FRC Kazan Scientific Center of RAS, Kazan, Russia, e-mail: kazan-city.dvpopoff@yandex.ru
[2]Kazan (Volga Region) Federal University, Kazan, Russian Federation
[3]Department of Materials Science and Engineering, Indian Institute of Technology Kanpur, Kanpur, India

Perovskites are oxides with formula ABO_3, where A is alkaline earth metal ion, B is transition metal ion. Perovskites have octahedral oxygen framework built around B ions. Those frameworks surround A ions in hexagonal (cubic) formation [1]. Double perovskites are the type of perovskites, that consist of two aforementioned formulas at once. Their major difference from complex single perovskites is an ordering in the arrangement of B ions – in double perovskite, B ions can form chains.

The aim of this work is investigation of Sr_2MnNbO_6 double perovskite through magnetic, calorimetric, ESR and neutron diffraction measurements. To achieve this, AC and DC magnetization dependences from temperature and external magnetic field were measured. Temperature dependencies of magnetization were measured in zero field cooling (ZFC) and field cooling (FC) modes at range 2–300 K. The hysteresis loops were observed at T = 5, 15, 30, 40 and 42 K and external magnetic field up to 9 T. The compound exhibits four magnetic transitions in AC data: at T = 42.5, 38.9, 12.7, and 6.7 K. In addition, specific heat measurements were made on Sr_2MnNbO_6.

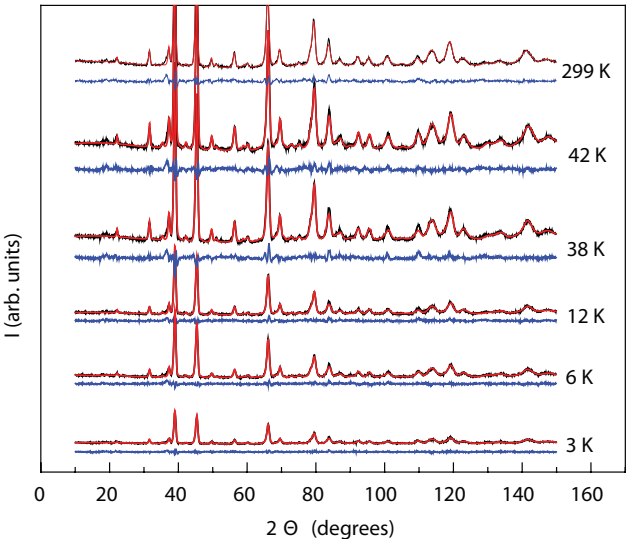

Fig. 1. ESR spectra of Sr_2MnNbO_6 at temperature range of T = 38–42 K.

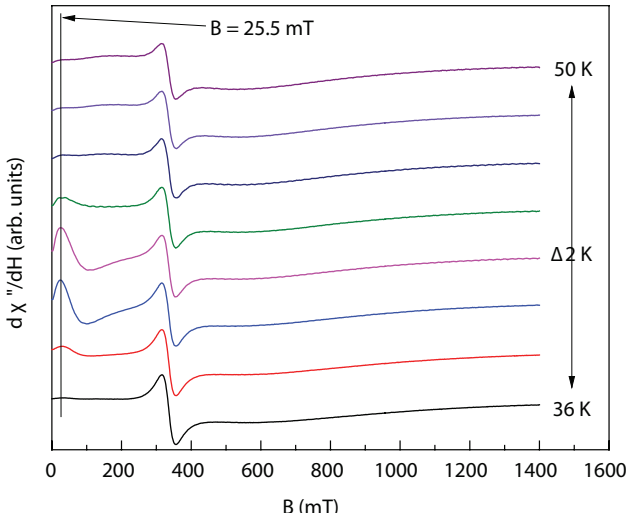

Fig. 2. Neutron diffraction patterns of Sr_2MnNbO_6. Red is a Rietveld method approximation. Blue is a difference between the experiment and the fit.

Neutron diffraction patterns of Sr_2MnNbO_6 ceramics were measured at temperatures of 3, 6, 12, 38, 42, and 299 K. Structural peaks were approximated by the Rietveld method.

EPR spectra were also measured using a Bruker spectrometer at temperature range from 10 to 340 K. An unusual ESR line was observed for Sr_2MnNbO_6 at $H_{res} \approx 500$ Oe at 38–42 K.

This research was supported by the Russian Science Foundation (Project No. 22–42-02014) and DST Project number DST/INT/RUS/RSF/P-55/2021.

1. Bhalla A., Guo R., Roy R.: Materials Research Innovations **4**, 3–26 (2000)

Po31

Kinetics of spin probe release from graphene oxide membranes

A.A. Potapova[1], T.S. Yankova[1], N.A. Chumakova[1,2]

[1]Lomonosov Moscow State University, Faculty of Chemistry, Moscow, Russia
[2]N.N. Semenov Federal Research Center for Chemical Physics, Russian Academy of Science, Moscow, Russia

Graphite oxide is a layered non-stoichiometric material consisting of partially oxidized graphene layers. Graphene oxide membranes are of great research interest due to their unique selective permeability to liquids and gases. The graphene oxide membranes can be used for separation of polar liquids and gases, as well as for water purification [1]. The detailed mechanism of selective permeability of graphene oxide membranes is currently unknown. In the work, we present a first attempt of kinetic study of water and acetonitrile passage through membranes using the spin probe method.

Nitroxide spin probes (TEMPO, TEMPOL) were introduced into graphene oxide membranes from the solutions in acetonitrile, water or by using of supercritical carbon dioxide. The membrane samples were placed into liquids (acetonitrile, water). The samples of the solutions were analysed using EPR-spectroscopy to count number of spins released at certain time moment. The solution under the membrane was replaced to pure solvent every time to provide a differential kinetic data.

Through the analysis of the spin probe release for membrane samples of different geometric sizes, it was found that there is no influence of sample shape on the release kinetics, so the release of the spin probe molecules occurs generally through the main surface of the membrane. It was shown that the release kinetics obeys Fick's law. It

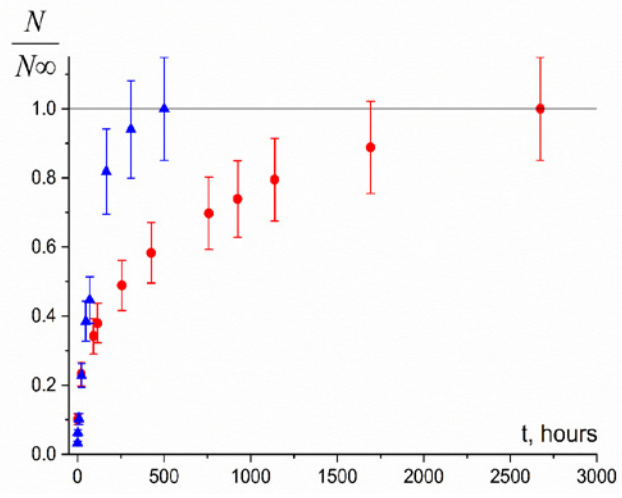

Fig. 1. Kinetic curves of the release of TEMPOL spin probes from a graphene oxide membrane into acetonitrile (circles) and into water (triangles), number of spins is normalized on total released number of spins.

turned out that the release of probe molecules in water is much faster than in acetonitrile (see Fig. 1). This fact, apparently, reflects the higher speed of movement of water molecules inside the membrane, compared with acetonitrile. It was found that prolonged interaction of the membrane with water leads to a change in the characteristics of the probe molecules release. It was shown that the way of spin probes introduction into membrane using a supercritical carbon dioxide significantly affects the degree of probe molecules agglomeration in membranes.

The work was supported by the Russian Science Foundation grant № 23-23-00016.

1. Nair R.R., Wu H.A, Jayaram P.N., Grigorieva V., Geim A.K.: Science **335**, 442–444 (2012)

Po32

Structural, magnetic and fluorescence characterization of Eu (III) Schiff base complexes with asymmetric ligands

A.V. Pyataev[1], Kh.R. Khayarov[2], I.V. Galkina[2]

[1]Department of Solid State Physics, Institute of Physics, Kazan Federal University, Kazan, Russia
[2]A.M. Butlerov Institute of Chemistry, Kazan Federal University, Kazan, Russia

In this work, two complexes of europium (III) based on β-naphthol and phenol were synthesized and investigated by the methods of ^{151}Eu Mössbauer spectroscopy, NMR spectroscopy, thermogravimetry, mass spectroscopy. It was found that the structure of the studied complexes (Fig. 1) determines the spin state of the central ion. The β-naphthol-based complex exhibits diamagnetic properties (S = 0), and the complex, where the ligand is phenol-based azomethine, is paramagnetic (S = 3) (Fig. 2). It was shown that the studied complexes exhibit a broad spectral response upon excitation in the ultraviolet part of the spectrum [1].

1. Khayarov K. et al.: Polyhedron **199**, 115092 (2021)

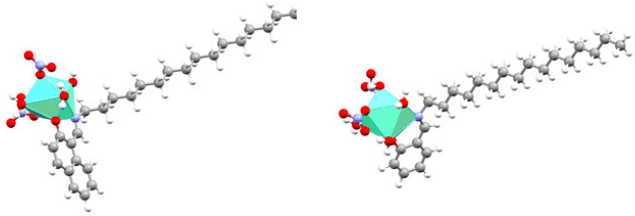

Fig. 1. Coordination polyhedral of the Eu (III) ions in complex I (left) and complex II (right).

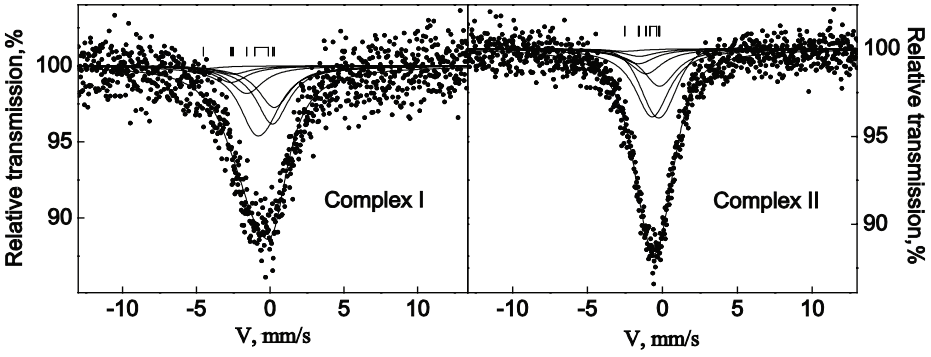

Fig. 2. ^{151}Eu Mössbauer transmission spectra complex I (left) and complex II (right).

Po33

High-frequency dielectric anomaly in a quasi-2D square kagomé lattice nabokoite family compounds

Y.V. Rebrov[1,2], V.N. Glazkov[1], P.S. Berdonosov[3,4], A.F. Murtazoev[3], V.A. Dolgikh[3]

[1]P.L. Kapitza Institute for Physical Problems, Moscow, Russia, e-mail: yavrebrov@edu.hse.ru
[2]HSE University, Moscow, Russia
[3]M.V. Lomonosov Moscow State University, Moscow, Russia
[4]National University of Science and Technology "MISiS", Moscow, Russia

Relatively recently model of the Heisenberg antiferromagnetic lattice has been proposed, which is a two-dimensional network of corner-sharing triangles with alternative square and octagonal voids [1]. This model has been called the square kagomé lattice (SKL). There are two non-equivalent positions for the magnetic ions with antiferromagnetic exchange bounds between nearest neighbors. Numeric simulations [2] predicts formation of the spin-liquid state for a Heisenberg magnet on SKL lattice with gapped triplet excitations and a continuum of singlet excitations filling the triplet gap.

Nabokoite family compounds $ACu_7(TeO_4)(SO_4)_5Cl$ (A = K, Na, Cs, Rb) are among the few systems in which a frustrated magnetic subsystem of the SKL type is formed [3,4]. These compounds have a layered structure (Fig. 1). Quasi-two-dimensional layers are formed by copper ions in Cu1 and Cu3 positions, while ions in Cu2 position 'decorates' SKL layers. Ions in Cu2 position could provide a link between the quasi-two-dimensional layers, but the presence of four identical exchange bonds with Cu1 ions also leads to frustration, and in the mean-field approximation these interactions compensate for each other. Curie-Weiss temperature for nabokoites is 100–200 K, but traces of magnetic order are observed for some of these compounds only below 4.5 K [4], indicating broad temperature range for spin-liquid physics. Earlier studies of

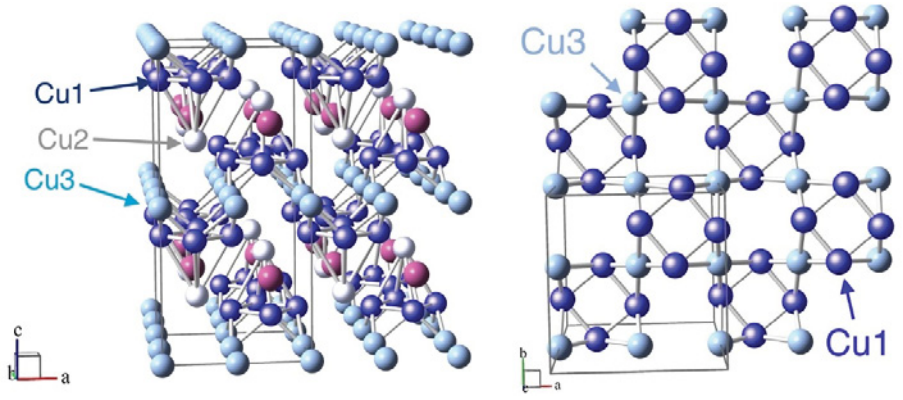

Fig. 1. Structure of the nabokoite family compounds. Blue, white, and cyan balls indicate 3 non-equivalent positions of copper ions; pink balls indicate the positions of alkaline ions. Left side – general view of the structure, right side – view of the layer in which the square kagomé lattice is formed.

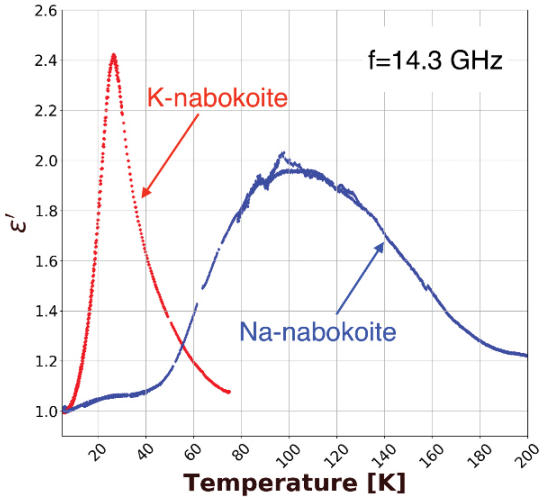

Fig. 2. Temperature dependence real part of the dielectric permittivity of potassium (red) and sodium (blue) compounds of the nabokoite family.

K-nabokoite [3] revealed dielectric anomaly at 24 K. The change in dielectric properties can be related to a rearrangement of the crystal structure of the sample leading to a change of exchange bonds. This rearrangement could lift the frustration of the Cu1–Cu3 or Cu1–Cu2 exchange bonds thus leading to the freezing of the spin liquid into a Néel ordered state.

We have studied ultra-high-frequency (9–14 GHz) dielectric properties of the nabokoite family compounds in the temperature range 1.7–300 K. Nabokoite sample was placed in the electric field beam in microwave cavity, variation of the cavity eigen-

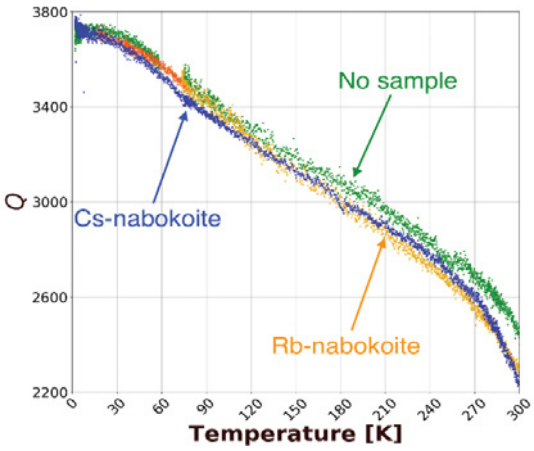

Fig. 3. Temperature dependence of the Q-factor in experiments with cesium (blue), rubidium (orange) compounds of the nabokoite family and reference experiment without sample (green).

frequency and Q-factor with temperature allowed to determine ε' and ε'' temperature dependences. We have observed dielectric anomalies (both in real and imaginary parts of dielectric permittivity) for K- and Na-nabokoites at ≈25 and ≈105 K, correspondingly (Fig. 2). No dielectric anomaly of comparable amplitude was observed for Rb- and Cs-nabokoites over the studied temperature range. E.g., the temperature evolution of the cavity Q-factor in the experiments with Rb- and Cs-nabokoites coincides with the results of the reference experiment without sample (Fig. 3).

The nature of this dielectric anomaly is unknown, but high-accuracy X-ray diffraction measurements on potassium nabokoite show that the thermal ellipsoid for potassium ions located between the layers of the SKL as shown in Fig. 1 is anomalously elongated in the (*ab*) plane at room temperature. This may suggest the existence of alkali metal positions close in space and equivalent in energy. This further suggests that the dielectric anomaly could be related to the localization of alkali ions in one of the positions, which practically does not affect the frustrated spin subsystem Cu1-Cu3, but can lift frustration of the Cu1-Cu2 bounds. This could lead to coupling between the quasi-dimensional layers and eventually to the formation of a 2D magnetic ordering at low temperatures.

The work was supported by Russia Science Foundation Grants 22-12-00259 (ultra-high-frequency measurements) and 23-23-00205 (samples preparation).

1. Siddharthan R. et al.: Phys. Rev. B **65**, 014417 (2001)
2. Richter J. et al.: Phys. Rev. B **105**, 144427 (2022)
3. Markina M.M. et al.: arXiv:2212.11623 (2022)
4. Murtazoev A.F. et al.: ChemPhysChem e202300111 (2023)

Po34

Rare-earth-doped calcium phosphates for biomedical applications

M.A. Sadovnikova[1], G.V. Mamin[1], F.F. Murzakhanov[1], M.R. Gafurov[1], N.V. Petrakova[2], M.A. Goldberg[2], V.S. Komlev[2]

[1]Kazan Federal University, Kazan, Russia
[2]A.A. Baikov Institute of Metallurgy and Material Science, Russian Academy of Sciences, Moscow, Russia

The development of calcium phosphate (CP) based biomaterials for the repair and healing of damaged bones is caused by the constant need to improve the quality of life. Despite significant progress in the design of implants based on titanium and tantalum alloys, zirconium dioxide or polymer compounds, CP ceramics remains the most at-

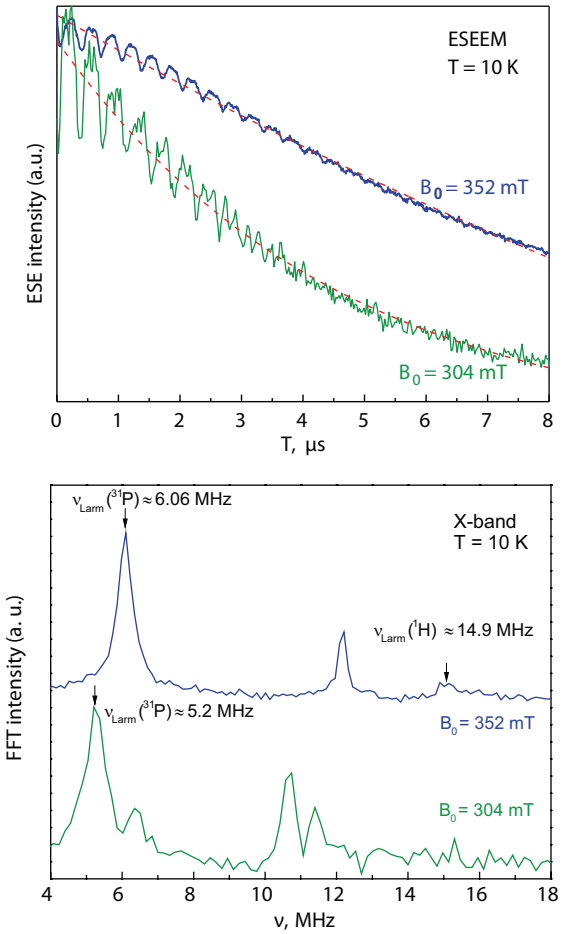

Fig. 1. Electron Spin Echo Envelope Modulation (ESEEM) experiment for tricalcium phosphate-0.25Ce for different values of B_0 (top); Fourier transformed ESEEM spectrum in the frequency range for different values of B_0 (bottom).

tractive bioactive inorganic material. Due to its chemical and mechanical similarity to bone mineral, as well as its excellent biocompatibility, biological activity, and osteogenic properties, CPs are used to replace and repair diseased or damaged parts of the musculoskeletal system, for drug and gene delivery systems, as a coating for titanium bone implants, and as a filler for biocomposites. However, some disadvantages such as unpredictable resorption rate and limited osteoinduction, don't fully satisfy all clinical requirements. An important feature of CPs is that their structure makes it possible to include a wide range of different ions to improve its properties [1]. Replacing Ca^{2+} in CPs with other ions strongly affects the characteristics of CPs particles, including size, crystallinity, solubility, thermal stability, surface characteristics, and adsorption activity. Therefore, to develop multifunctional materials, CPs is alloyed with various cations and anions (magnesium Mg^{2+}, copper Cu^{2+}, cobalt Co^{2+}, manganese Mn^{2+}, iron Fe^{3+}, etc.).

Recently, rare earth ions have been used in various materials such as phosphors, laser technology, magnetic materials, catalysts, superconducting materials, fuel cells, sensors, medical materials and dental materials, which are used in various fields of science, technology and medicine. Thus, gadolinium ions (Gd^{3+}) in the CP structure can act as contrast agents for magnetic resonance imaging, and the substitution of calcium ions in the CP lattice for cerium ions (Ce^{3+} and/or Ce^{4+}) is an interesting subject, since compounds containing Ce ions have been used in medicine as antibacterial agents.

Electron paramagnetic resonance (EPR) is known as a sensitive non-destructive method for studying the magnetic properties and symmetry of the crystal field, analysis of electron-nuclear interaction, local nuclear environment (Fig. 1). In our study, we demonstrate the possibilities of various continuous-wave (CW) and pulsed EPR methods for the comprehensive study of CPs with rare-earth (Gd, Ce) elements. The spectra show a ^{31}P signal centered at the Larmor frequency for the field B_0 = 352 mT, the frequency $\nu_{Larm}(^{31}P)$ = 6.06 MHz, and for B_0 = 304 mT, respectively, $\nu_{Larm}(^{31}P)$ = 5.2 MHz. The relaxation times of Ce ions were measured for two different magnetic fields (B_0 = 352 mT, B_0 = 304 mT) differing by about 10 times (T_2 = 31.0(5) μs, T_2 = 3.0(1) μs, respectively), which most likely indicates that the Ce ion occupies two Ca^{2+} positions.

The procedure of chemical synthesis of rare earth elements into the structure of calcium phosphates, is a rather complicated task, because ions with different charge state and ionic radius are substituted. The successful realization of the CP material as biocompatible implies the absence of side phases of synthesis and the non-destruction of the local position of the surrounding ions in the crystal lattice. EPR makes it possible to study the electronic transitions of paramagnetic particles, and its high spectroscopic resolution makes it possible to determine the position of an impurity center, valence, and the presence of side phases. The obtained results can be used for qualitative and quantitative control of rare-earth elements inclusion in the structure of CPs and can serve as a basis for quantum-chemical modeling of the crystal lattice and physical and chemical properties in the creation of materials with the desired functionality.

The research was funded by the Russian Science Foundation, grant number 23-63-10056

1. Jeong J. et al.: Bioactive calcium phosphate materials and applications in bone regeneration: Biomaterials research **23**, no. 1, 1–11 (2019)

Po35

Low-cost ODMR attachment for commercial EPR spectrometers

M.A. Sadovnikova, F.F. Murzakhanov, B.V. Yavkin, D.G. Zverev

Kazan Federal University, Kazan, Russia

The Optically Detected Magnetic Resonance (ODMR) technique combines the properties of electron paramagnetic resonance (EPR) with high sensitivity and selectivity of photoluminescence signal detection. ODMR experiment is a realization of double resonance, in which electronic transitions between different orbital states are controlled by laser radiation and magnetic transitions by microwave (mw) radiation [1]. The ODMR technique routinely allows to register signals down to single emitter even at room temperature, confirming its high sensitivity. However, it should also be noticed that ODMR is characterized by some limitations in its application for the structure under study: system must be compliant to the optical excitation, it is crucial to have effective spin-dependent channels leading to a change in the optical properties of the system when the magnetic resonance condition is fulfilled [2].

In our work the low cost device for ODMR has been developed for use with commercial EPR spectrometers. The equipment is based on a scheme (Fig. 1) with coaxial optical fibers, where the excitation is transmitted through a central fiber with a diameter of 400 μm, and the luminescence signal is collected using seven optical fibers with diameter of 200 μm. The device has the ability to modulate the excitation radiation, mw frequency and magnetic field. The ODMR attachment has been successfully tested on standard and well-known NV^- centers in diamonds.

The assembled ODMR attachment has the ability to modulate the excitation radiation, mw frequency and magnetic field that may be necessary for further experiments on different crystals to increase the signal-to-noise ratio. It has been tested on standard and well-known NV^- paramagnetic centers in diamonds. The best signal-to-noise ratio was obtained when the modulation of the magnetic field was used.

The work is financially supported by Russian Science Foundation (grant No. 23-22-00271).

1. Suter D.: Magnetic Resonance **1**, 115 (2020
2. Carbonera D.: Photosynthesis research **102**, 403–414 (2009)

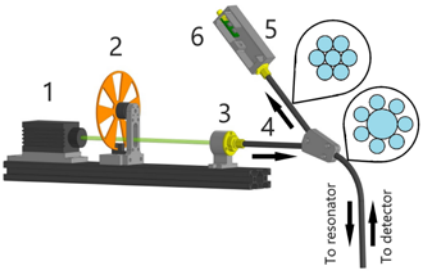

Fig. 1. Optical part of the ODMR attachment (1) A 532 nm diode-pumped laser, (2) an optical obturator (3) 1064 nm filter and collimator, (4) optical fiber 400 μm, (5) silicon photodiode, (6) preamplifier.

Po36

Magnetic resonance spectra of inhomogeneous conductors $La_{1-x}K_xMnO_3$

N.S. Saenko, N.I. Steblevskaya, M.V. Belobeletskaya, A.M. Ziatdinov

Institute of Chemistry, Far Eastern Branch of the RAS, Vladivostok, Russia,
e-mail: saenko@ich.dvo.ru

In stoichiometric $LaMnO_3$ at Neel temperature T_N = 140 K, a transition occurs from the paramagnetic to the antiferromagnetic state [1]. The T_N and magnetic properties of this compound can be changed by creating vacancies in it or by doping with metal ions [2–5]. However, the degree of change in the properties of this compound is very sensitive to the method of synthesis, as well as to the nature and concentration of the impurity. The aim of this work is to study some magnetic properties of the extraction-pyrolytic lanthanum manganite $LaMnO_3$ and its potassium-doped derivatives $La_{1-x}K_xMnO_3$ (x = 0.1, 0.15) using the methods of electron paramagnetic and ferromagnetic resonances (further, united under the general name: electronic magnetic resonance – EMR). All spectra were recorded on a JEOL-X330 spectro-meter equipped with standard variable temperature unit DVT5 (ES-13060).

The EMR spectra of the initial $LaMnO_3$ and its potassium-doped derivatives at different temperatures are shown in Fig. 1. All samples at high temperatures have line shape close to Lorentzian. As the temperature decreases, the shapes of the considered lines are transformed, and in such a way that their approximations by the Lorentzian become less and less satisfactory. Moreover, there is a gradual rise in both the integral intensity of the resonance (Fig. 2a) and the effective value of its g-factor (Fig. 2b), determined from the value of the magnetic field at the point of intersection of the resonance contour with the zero line. An increase in the peak-to-peak width (ΔB) of the line with decreasing temperature becomes noticeable below ~25°C (Fig. 2c). At low temperatures, there is a small but reliably measured absorption of microwave power at zero magnetic field (Fig. 1).

Quasi Lorentzian forms of resonance lines of $La_{1-x}K_xMnO_3$ (with x = 0.0, 0.1, 0.15) at high temperatures prove them to be observed mainly on paramagnetic particles. On the other side, lowering the temperature causes broadening of the lines by a factor of 4-6 and an increase in the effective values of the g-factors of the resonances and transformation of the line shapes to the form (Fig. 2c), which is typical for the line shape of ferromagnetic resonance [6–7]. In addition, the presence of microwave power absorption at low temperatures at zero external magnetic fields (Fig. 1) is a characteristic feature of the EMR spectra of ferromagnetic materials with residual magnetization [6–7]. All the above points to the existence of ferromagnetic clusters in samples, the amount of which increases with decreasing temperature. The transition temperatures of $La_{1-x}K_xMnO_3$ into the ferromagnetic phase (Curie temperatures, T_C), determined by the point at which the continuation of the linear section of the temperature dependence of inverse integral intensity of the resonance $1/I$ crosses the temperature axis (Fig. 3), are equal to –17.4, –13.7 and –4.8 °C for x = 0.0, 0.1, 0.15, respectively. The observation of EMR in the initial lanthanum manganite at $T < T_N$ is obviously a consequence of its nonstoichiometric structure (Fig. 1a).

The report discusses the degree of influence of Dyson distortions in the EMR line shape of the $La_{1-x}K_xMnO_3$ on base of the theoretical analysis of experimental data.

Po36

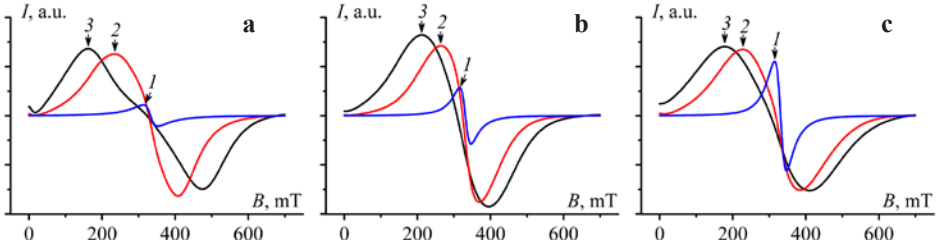

Fig. 1. EMR spectra of the compounds $LaMnO_3$ (**a**), $La_{0.9}K_{0.1}MnO_3$ (**b**) и $La_{0.85}K_{0.15}MnO_3$ (**c**) at different temperatures. Spectra 1, 2 and 3 were measured at temperatures +20, –80 and –160 °C, respectively.

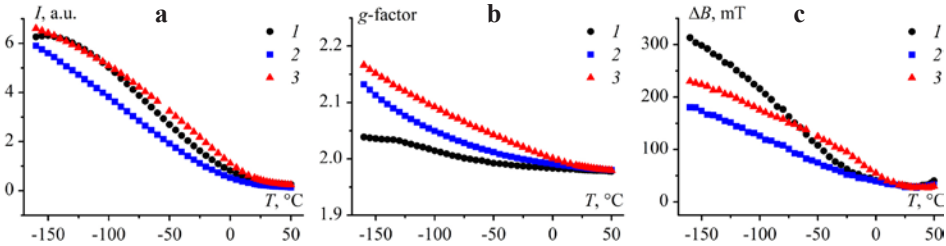

Fig. 2. The temperature dependences of the double integral of the EMR line (**a**), the effective value of the *g*-factor (**b**) and the peak-to-peak width (**c**) of the EMR line of the compounds $La_{1-x}K_xMnO_3$. Curves 1, 2 and 3 correspond to x = 0.0, 0.1, 0.15, respectively.

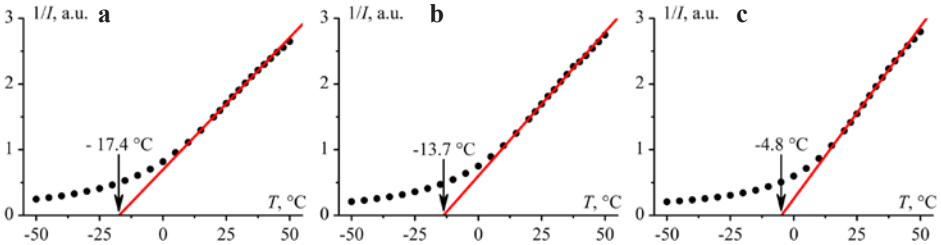

Fig. 3. The temperature dependences of the reciprocal double integral (1/*I*) of the EMR line of the compounds $La_{1-x}K_xMnO_3$ with x = 0.0 (**a**), 0.1 (**b**), 0.15 (**c**), respectively. The arrows indicate the temperature of the phase transition to the ferromagnetic phase (T_C).

The research results were compared with the corresponding literature data on the $La_{1-x}K_xMnO_3$ synthesized by other methods.

The work was carried out under a state assignment of the Institute of Chemistry, Far Eastern Branch of the Russian Academy of Sciences, Vladivostok, Russia (project FWFN(0205)-2022-0003).

1. Wollan E.O., Koehler W.C.: Phys. Rev. **100**, no. 2, 545–563 (1955)
2. Gluchowski P. et al.: Materials **13**, no. 7, 1788 (2020)
3. Eremina R.M. et al.: Phys. Rev. B **84**, no. 6, 064410 (2011)
4. Bouzid S.A. et al.: J. Alloys Compd. **839**, 155546 (2020)
5. Deisenhofer J. et al.: Phys. Rev. B **66**, no. 5, 054414 (2002)
6. Castel V., Youssef J.B., Brosseau C.: J. Nanomaterials **2007**, 27437 (2007)
7. Guskos N. et al.: Nanotechnol. Secur. Syst. **2015**, 33–47.

Po37

Electron paramagnetic resonance and charge compensation in nanocrystalline sodium titanate doped with copper ions

D.A. Saritsky, V.V. Zheleznov, D.P. Opra, A.M. Ziatdinov

Institute of Chemistry, Far Eastern Branch of the RAS, Vladivostok, Russia,
e-mail: denissaricki@mail.ru

In this work we report the results of determination by EPR of the magnetic nonequivalent states of impurity copper ions and the nature of charge compensation in sodium titanate ($Na_2Ti_3O_7$), which has a two-level micro/nano architecture [1]. The EPR spectra were recorded on a JEOL-X330 spectrometer.

Computer analysis of the second derivative of microwave field absorption by sodium titanate powder doped with copper ions (Fig. 1) shows that impurity copper ions are in it in three magnetically non-equivalent states (Table 1). Two of them are Cu^{2+} ions in the substitution positions of the matrix ion Ti^{4+} in the crystal field of the tetragonal-extended oxygen octahedron, which stabilizes the unpaired hole predominantly in the atomic orbital $d_{x^2-y^2}$. Some difference in the distortion of the oxygen environment of these types of Cu^{2+} centers can be explained by the fact that they are in different regions of the particle. For example, centers of smaller and larger abundance can be distributed in its volume and concentrated in regions predominantly near the particle surface, respectively. A significant difference in the resonance widths of magnetically nonequivalent Cu^{2+} centers also speak in favor of their preferential localization in different regions of the particle.

Analysis of the parameters of EPR spectra of Cu^{2+} centers located in the positions of substitution of Ti^{4+} ions by the methods of molecular orbital theory shows that the

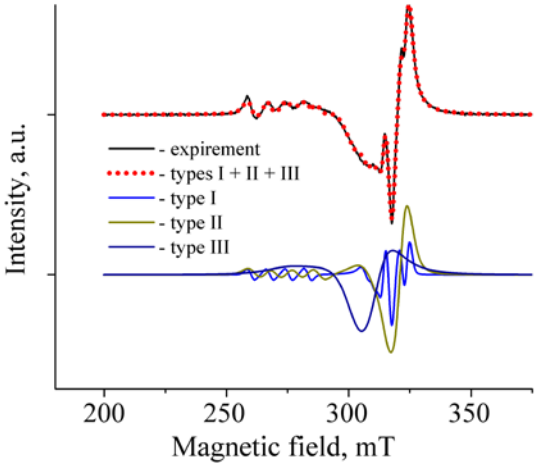

Fig. 1. Second derivatives of theoretical and experimental EPR spectra of $Na_2Ti_3O_7$ powder doped with copper ions; T = –160 °C, the X-band.

Table 1. Parameters of the spin Hamiltonian of rhombic symmetry (g_i, A_i, $P_{\|}/h$, η), electric field gradient in the region of the nucleus of copper ions (eq), the widths of the Lorentz (ΔB_L) and Gaussian (ΔB_{Gi}) components of the Voigt resonance contours and contributions of different types of Cu^{2+} centers to the integral intensity of the theoretical spectrum presented in Fig. 1.

Type of center	g_i	A_i, mT	$P_{\|}/h$, MHz (η)	$eq \cdot 10^{21}$, V/m^2	ΔB_L, mT	ΔB_{Gi}, mT	Contribution,%
I	g_x = 2.088 g_y = 2.070 g_z = 2.407	A_x = 3.88 A_y = 3.17 A_z = 10.82	45.5 (0.2)	36.5	1.17	ΔB_{Gx} = 3.45 ΔB_{Gy} = 2.70 ΔB_{Gz} = 3.78	5.27
II	g_x = 2.095 g_y = 2.066 g_z = 2.369	A_x = 3.46 A_y = 1.41 A_z = 11.60	41.9 (0.32)	33.6	4.22	ΔB_{Gx} = 3.33 ΔB_{Gy} = 3.06 ΔB_{Gz} = 4.54	25.02
III	g_x = 2.146 g_y = 2.146 g_z = 2.264	A_x = 1.60 A_y = 1.60 A_z = 7.02	–	–	12.3	ΔB_{Gx} = 2.14 ΔB_{Gy} = 2.14 ΔB_{Gz} = 2.61	69.71

delocalization of the hole (spin density) from the $d_{x^2-y^2}$ orbital to four s-orbitals of equatorial oxygen ions is ≈24%. The admixture of the excited d_z^2-orbital to the ground state of the hole is negligibly small, which indicates the absence of vibronic coupling between them.

The absence in the EPR spectra of copper-doped sodium titanate samples of resonance absorption at electrons captured by oxygen vacancies indicates that the charge imbalance resulting from the replacement of the matrix ion Ti^{4+} by the impurity ion Cu^{2+} is compensated not by the formation of new oxygen vacancies. A comparative analysis of the values of the parameters of the EPR spectra of all three types of Cu^{2+} impurity centers shows that the charge neutrality of the sample is provided by type III copper centers located in the interlayer spaces of the sample. The main part of these ions (~90%) is in the positions of substitution of lattice Na^+ ions. A much smaller part of them (~10%) is in the interstitial spaces.

The authors are grateful to N.S. Saenko for help in recording the EPR spectra. The work was carried out within the framework of state assignments to the Institute of Chemistry, Far Eastern Branch of the Russian Academy of Sciences (projects: No. FWFN(0205)-2022-0002 and FWFN(0205)-2022-0003.

1. Chen H., Wy Y., Duan J. et al.: ACS Appl. Mater. Interfaces **11**, 42197–42205 (2019)

Po38

Cr^{4+} centers in yttrium orthosilicate Y_2SiO_5

G.S. Shakurov[1], R.B. Zaripov[1], A.P. Potapov[2], V.A. Vazhenin[2], M.Yu. Artyomov[2], K.A. Subbotin[3,4], A.V. Shestakov[5]

[1]Zavoisky Physical-Technical Institute, FRC Kazan Scientific Center of RAS, Kazan, Russia
[2]Ural Federal University, Ekaterinburg, Russia
[3]Prokhorov General Physics Institute, Russian Academy of Sciences, Moscow, Russia
[4]Mendeleev University of Chemical Technology of Russia, Moscow, Russia
[5]POLYUS Research Institute of M.F. Stelmakh Joint Stock Company, Moscow, Russia

Yttrium orthosilicate Y_2SiO_5 (YSO) single crystals doped with rare earth and transition 3d ions are promising materials for quantum memory elements. In recent years, they have been actively studied, including the studies by electron paramagnetic resonance (EPR) spectroscopy. Chromium-doped YSO crystals are also known as the promising active media and saturable absorbers of near-IR lasers. In this case, the optically active center responsible for the near-IR luminescence is believed to be tetrahedrally coordinated Cr^{4+}. However, this conclusion has been made based only on the optical spectroscopy data. We carried out a special search for the EPR signals of Cr^{4+} ions in YSO:Cr crystal using a broadband EPR spectrometer. The EPR spectra of Czochralski grown Y_2SiO_5:Cr and Y_2SiO_5:^{53}Cr crystals have been studied. After the detection of the resonant signals, we have continued the investigations with use of a Q-band spectrometer. The EPR spectra of Cr^{3+} and Cr^{4+} ions were recorded. Within the framework of the existing theory of EPR spectra, the set of spin Hamiltonian parameters was obtained. It allowed to describe the experimental angular and frequency-field dependences of tetravalent chromium in YSO:Cr crystal in non-contradictory manner. Weak repulsion of the energy levels of Cr^{4+} centers in the magnetic field directed near the principal axis of the local coordinate system made it possible to detect the EPR spectrum of Cr^{4+} in YSO:Cr crystal in the X-band. The fine structure parameters of tetravalent chromium in Y_2SiO_5 host were obtained based on the analysis of the angular and frequency-field dependences of the EPR spectra. The conclusion about tetrahedral coordination of Cr^{4+} ion in this host was made. Based on the comparison of integral intensities of the EPR signals of Cr^{4+} and Cr^{3+} ions, their concentrations ratio in the crystal was estimated to be ~1:3.

The research work of the authors from Ural Federal University was supported by the Ministry of Science and Higher Education of Russia Federation (grant FEUZ-2023-0017) using the equipment of the Ural Center of Shared Facilities “Modern Nanotechnologies”. The authors from Zavoisky Physical-Technical Institute acknowledge the financial support from the government assignment for FRC Kazan Scientific Center of RAS.

Po39

Spin fluctuation transition in the conical phase of MnSi

A.V. Shestakov[1], I.V. Yatsyk[2], R.M. Eremina[2], S.V. Demishev[1]

[1]Prokhorov General Physics Institute of RAS, Moscow, Russia
[2]Zavoisky Physical-Technical Institute, FRC Kazan Scientific Center of RAS, Kazan, Russia

Studies of manganese monsilicide, MnSi, by the electron paramagnetic resonance (EPR) method made it possible to significantly refine the physical picture of the magnetic properties of this metal with helical magnetic ordering. Recent work has been mainly concentrated in the region of high-frequency (60 GHz) EPR, where the paramagnetic and spin-polarized phases have been studied in detail in the magnetic field range $H \sim$ 20 kOe [1, 2]. At the same time, for the conical phase existing in the range $H \leq 6$ kOe, the only work is known in which the EPR spectrum in the region of 9.6–34.5 GHz, consisting of several lines, was recorded [3]. Additional interest in the study of the conical phase of MnSi is related to the spin fluctuation transition (SFT) expected at $T_L \sim 15$ K [1] due to the crossover between quantum and classical fluctuations [4]. SFT is a kind of special magnetic transition, at which characteristics of spin fluctuations change, but either onset or change of magnetic ordering is not necessarily occurs [5, 6]. Therefore, an SFT may be expected inside magnetic phase with long-range magnetic order far from the phase transition boundary [6]. For studying the SFT, electron paramagnetic resonance is a convenient method, since the EPR linewidth W provides direct information on the amplitude of spin fluctuations [5, 6].

We report on the study of the conical phase of a MnSi single crystal in the range of 9 GHz in the temperature interval $T < 30$ K. The steady magnetic field was aligned along the [001] crystallographic direction. During the analysis, the experimental spectrum was decomposed into several components in accordance with the previous results [3]. It is found that in the range $26 < T < 30$ K the EPR spectrum is formed by one main line with a weak satellite. A decrease in temperature in the region $T < 26$ K leads to the splitting of the spectrum into two main most intense lines (line 1 and line 2) and several lines of lower amplitude, observed in the range of magnetic fields below 3 kOe. The resonant fields for lines 1 and 2 increase with decreasing temperature and cross the phase boundary between the conical and spin-polarized phases at $T \sim 16$ K and $T \sim 6$ K, respectively. Temperature dependences of the width of the main lines $W(T)$ in the spectrum are shown in Fig. 1. It can be seen that in the vicinity of possible SFT $T \sim 15$ K, line 1 is already in the spin-polarized phase and its width increases with decreasing temperature, in accordance with the results of high-frequency measurements [2]. At the same time, the position of line 2 corresponds to the region of existence of the conical phase up to ~6 K, and this feature in the EPR spectrum can be used to identify the spin fluctuation transition. As follows from the experimental data, the width of line 2 exhibits a maximum at $T \sim 15$–17 K, corresponding to a 2.7 time change in $W(T)$ magnitude. Thus, we can conclude that this feature at $T \approx T_L$ is due to the SFT predicted in [1, 4].

It should be marked that the characteristic temperatures found earlier in [2], which reflect the change in the regime of spin fluctuations, are in good agreement with the

Po39

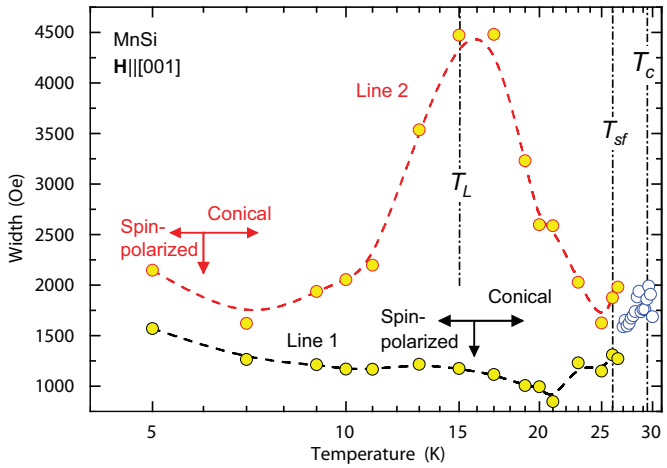

Fig. 1. Temperature dependence of the widths $W(T)$ of the main EPR lines in MnSi. Vertical arrows mark temperatures, where a transition from conical to spin-polarized phase occurs for each line. Dash-dotted lines correspond to characteristic temperatures obtained in [2]. Maximum of $W(T)$ for line 2 at $T \sim T_L$ is a fingerprint of spin fluctuation transition.

data obtained in the present work. Not only the temperature of SFT T_L, but also the temperature T_{sf} = 26 K, which corresponds to the ordering of spin fluctuations in spin-polaron states [2] is clearly manifested in the EPR spectra in the 9 GHz region. Indeed, at this temperature, the spectrum splits into several lines (Fig. 1). This result shows that the reduced magnetic moments ~0.3 μ_B/Mn, which form the conical phase of MnSi, arise as a result of screening of the localized Mn magnetic moments by band electrons with the formation of quasi-bound states of the spin-polaron type in agreement with earlier suppositions [1, 4, 5].

We thank V.A. Shustov (Zavoisky Physical-Technical Institute, FRC Kazan Scientific Center of RAS, Kazan, Russia) for determining the crystallographic axes of the crystal by X-ray diffraction analysis. Financial support from the government assignment for FRC Kazan Scientific Center of RAS is acknowledged.

1. Demishev S.V. et al.: Phys. Rev. B **85**, 045131 (2012)
2. Demishev S.V. et al.: JETP Lett. **115**, 673–678 (2022)
3. Date M., Okuda K., Kadowaki K.: J. Phys. Soc. Jpn. **42**, 1555–1561 (1977)
4. Demishev S.V. et al.: JETP Lett. **98**, 829–833 (2014)
5. Demishev S.V.: Applied Magnetic Resonance, **51**, 473–522 (2020)
6. Demishev S.V.: Physics-Uspekhi, in press. DOI: 10.3367/UFNr.2023.05.039363

Po40

Magnetic properties of $La_{0.7}Sr_{0.3}Mn_{0.9}Fe_{0.1-x}Zn_xO_3$ (x = 0.05, 0.075 and 0.1)

Z.Y. Seidov[1,6], R.M. Eremina[2], I.V. Yatsyk[2], A.V. Shestakov[3], F.G. Vagizov[4], V.A. Shustov[2], A.G. Badelin[5], V.K. Karpasyuk[5], H.-A. Krug von Nidda[6]

[1]Institute of Physics, Ministry of Science and Education, Baku, Azerbaijan
[2]Zavoisky Physical-Technical Institute, FRC Kazan Scientific Center of RAS, Kazan, Russia
[3]Prokhorov General Physics Institute of the RAS, Moscow, Russia
[4]Institute of Physics, Kazan Federal University, Kazan, Russia
[5]Astrakhan State University, Astrakhan, 414056, Russia
[6]Experimental Physics V, EKM, Institute of Physics, University of Augsburg, Augsburg, Germany

Magnetic properties of polycrystalline $La_{0.7}Sr_{0.3}Mn_{0.9}Fe_{0.1-x}Zn_xO_3$ (x = 0.05, 0.075 and 0.1) have been investigated by means of electron spin resonance, magnetic susceptibility, and Mössbauer measurements. All samples show a clear ferromagnetic transition. The Curie temperature T_C decreases on increasing Zn content T_C = 278, 193 and 166 K for x = 0.05, 0.075 and 0.1, respectively. For all three samples, an anomalous downturn of the inverse susceptibility significantly above T_C and the concomitant observation of ferromagnetic resonance signals coexisting with the paramagnetic resonance up to approximately room temperature, indicates a Griffiths-like behavior [1, 2]. This regime is characterized by the coexistence of ferromagnetic entities within the globally paramagnetic phase. We also observed a magnetocaloric effect with a maximum magnetic entropy change ($|\Delta S_{max}|$) value occurring close to the Curie temperature T_C, corresponding to $|\Delta S_{max}|$ = 2.9, 2.6 and 2.61 J/(kg · K) under magnetic field change (ΔH) of 50 kOe for x = 0.05, 0.075 and 0.1, respectively. The relative cooling power (RCP) values were found to vary between 250 and 310 J/kg. Mössbauer studies for x = 0.05 indicate that Fe is in the trivalent high-spin state. The temperature evolution of the Mössbauer spectra at low temperatures ($T < T_C$) is typical for ferromagnetic clusters with a wide distribution in size and magnetic correlation length.

1. Seidov Z.Y., Yatsyk I.V., Vagizov F.G., Shustov V.A., Badelin A.G., Karpasyuk V.K., Najafzade M.J., Ibrahimov I.N., Estemirova S.Kh., Krug von Nidda H.-A., Eremina R.M.: J. Magn. Magn. Mater. **552**, 169190 (2022)
2. Eremina R.M., Yatsyk I.V., Seidov Z.Y., Vagizov F.G., Shustov V.A., Badelin A.G., Karpasyuk V.K., Abdinov D.S., Tagiev M.M., Estemirova S.Kh., Krug von Nidda H.-A.: Appl. Magn. Reson. **54**, 449 (2023)

Po41

Plant cell dehydration models – monitoring by NMR relaxometry on subcellular level

T.A. Sibgatullin, O.V. Sautkina, P.V. Mikshina

Kazan Institute of Biochemistry and Biophysics, FRC Kazan Scientific Center of RAS, Kazan, Russia

The relaxation rate of the water magnetization in plant cells is mainly determined by its interaction with the surrounding non-aqueous components (mainly, cell wall polymers). Depending on the geometry of the cell (shape and size), structural features of the cell wall (thickness and density), as well as the membrane integrity and its water permeability, the rate of diffusional exchange between the water compartments of the cell and so the measured T_2 relaxation will vary.

Celery collenchyma strands were chosen to demonstrate the possibilities of monitoring of dehydration processes within the plant tissue sample of uninjured homogeneous cells.

The report proposes a methodological approach (based on NMR-relaxometry) to determine the mode of dehydration of plant tissues at the cellular level at certain conditions. Whether it goes through the free shrinkage of cells or plasmolysis, lysis, combination of abovementioned processes. The portion of damaged cells can be reported when NMR-relaxometry is applied in combination with extracellular MRI contrast agents. The effect of membrane destruction (freeze-thaw) on the dynamics of plant tissue dehydration is demonstrated. The change of the portion of the cell wall associated water upon the freeze-thaw cycle was reviled.

The reported study is a preliminary step for the transition to a completely non-invasive monitoring of dehydration processes. In combination with MRI technique the proposed approach can be applied to a complex plant objects.

The proposed method of monitoring of water status in biological tissues will facilitate the improvement of food storage technologies like the convective dehydrofreezing of vegetables evolved for reducing cell damage.

Po42

Inhomogeneities in PNIPAM-albumin aqueous solutions: spin probe and spin label study

G.A. Simenido[1], E.M. Zubanova[1], E.N. Golubeva[1,2]

[1]Lomonosov Moscow State University, Faculty of Chemistry, Moscow, Russia
[2]Sechenov University, Moscow, Russia

Poly-*N*-isopropylacrylamide (PNIPAM) is one of the stimuli-responsive polymers that undergo changes in physical and/or chemical properties in solutions in response to external stimuli, such as changes in temperature, pH, ionic strength, light irradiation. PNIPAM and its copolymers exhibit thermal sensitivity due to the coil to globule transition in aqueous solutions in the physiological temperature range, and therefore these polymers are used in biomedicine. In particular, matrices of thermoresponsive polymers are used to obtain cell layers and three-dimensional cell structures. Complexation of polymers with proteins of cell culture and extracellular matrix can lead to a change in the temperature interval of the coil to globule transition due to the formation of microheterogeneities in solution and the penetration of polymer chains into the extracellular matrix, which can hinder the subsequent process of detachment of cell layers. The purpose of this work was to establish the effect of proteins on the coil to globule transition temperature, microstructure and microdynamics of aqueous solutions of PNIPAM. The turbidimetry method was used to determine the phase transition temperature, and electron paramagnetic resonance spectroscopy within the framework of spin probe and spin label techniques was used to establish the microstructure and microdynamics of inhomogeneities in polymer solutions.

The objects of study were 1% and 10% aqueous solutions of PNIPAM in the presence of 2.5, 5 and 10% bovine serum albumin (BSA), BSA free solutions with the same concentration were also studied. Using the TEMPO radical as a spin probe, it was shown that nanoscale inhomogeneities exist in solutions of PNIPAM and albumin. The structure of these inhomogeneities in protein and polymer solutions is different. At protein concentrations of ~10%, the formation of inhomogeneities in solution was observed already at 273–295 K. Addition of BSA to a PNIPAM solution leads to an increase in the proportion of probe molecules located in polymer-protein inhomogeneities along compared to a protein-free solution. The use of a paramagnetic label covalently attached to the polymer chain makes it possible to determine the dynamics of the polymer chain itself. It was shown that the EPR signal of spin-labeled PNIPAM is close to the hard limit of rotation of the nitroxide radical with an average rotational correlation time of about 0.1 μs. It was also shown by EPR spectroscopy using spin-labeled PNIPAM that the collapse of the polymer chain at 305 K occurs faster when BSA is added: the fraction of slowly rotating label particles in the globule increases with increasing protein concentration. Apparently, albumin contributes to the formation of inhomogeneities in PNIPAM solutions during the coil to globule phase transition, but does not affect the structure of the globule core.

This research was supported by the Russian Science Foundation (Grant 22-73-00062).

Po43

NMR study of acetonitrile intercalated into graphite oxide

Yu. Slesareva[1], M. Volkov[1], E. Vavilova[1], N. Chumakova[2], D.A. Astvatsaturov[2]

[1]Zavoisky Physical-Technical Institute, FRC Kazan Scientific Center of RAS, Kazan, Russia
[2]M.V. Lomonosov Moscow State University, Chemistry Department, Moscow, Russia

The study of the mobility of molecules of polar liquids intercalated into the interplanar space of graphite oxide is of considerable interest due to the potential opportunity of creating inexpensive filtering membranes. It has previously been shown that dry graphite oxide membranes are completely impermeable to ethanol, propanol and acetone, but are surprisingly permeable to water. It was later found that the permeability of such a membrane depends on the water content in it.

In this work, two samples containing acetonitrile intercalated into graphite oxide have been prepared and studied by NMR spectroscopy. These samples differ from each other in the content of the intercalated acetonitrile (77% and 95% of acetonitrile relative to the equilibrium sorption value).

The temperature dependences of the ^{1}H NMR spectra of the samples showed that in the NMR spectrum of the B-GO–CH_3CN (95%) sample, a single wide line is observed in the range from 200 to 310 K, whereas in the spectrum of the B-GO–CH_3CN (77%) sample, side bands begin to appear more and more noticeably with increasing temperature (Fig. 1). The observed difference may be related to the different ratio of high and low mobile fractions of intercalated acetonitrile in the studied GO samples.

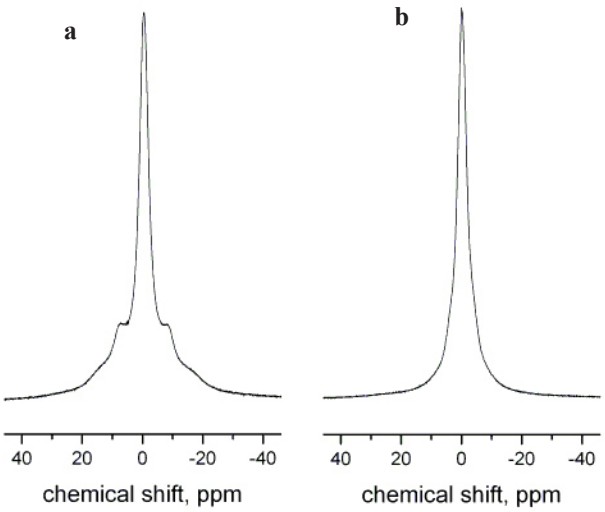

Fig. 1. ^{1}H NMR spectum of the sample containing 77% acetonitrile intercalated into graphite oxide (**a**). ^{1}H NMR spectum of the sample containing 95% acetonitrile intercalated into graphite oxide (**b**). The NMR spectra shown here were recorded at room temperature.

Po44

Dynamics of the spin-liquid phase of the frustrated antiferromagnet Cs_2CoBr_4

T.A. Soldatov[1], A.I. Smirnov[1], A.V. Syromyatnikov[2]

[1]P.L. Kapitza Institute for Physical Problems of RAS, Moscow, Russia
[2]Petersburg Nuclear Physics Institute named by B.P. Konstantinov of National Research Center "Kurchatov Institute", Gatchina, Russia

Frustration mechanism plays a significant role in formation of the ground state in magnetic crystals. A conventional case implies geometrical frustration of antiferromagnetic exchange interactions between magnetic ions which are placed on the lattice of very special type such as triangular, kagome, square-kagome or pyrochlore. In more exotic cases like in quantum spin ices and Kitaev magnets frustration arises from crystal anisotropy with axes directed differently for neighbor spins.

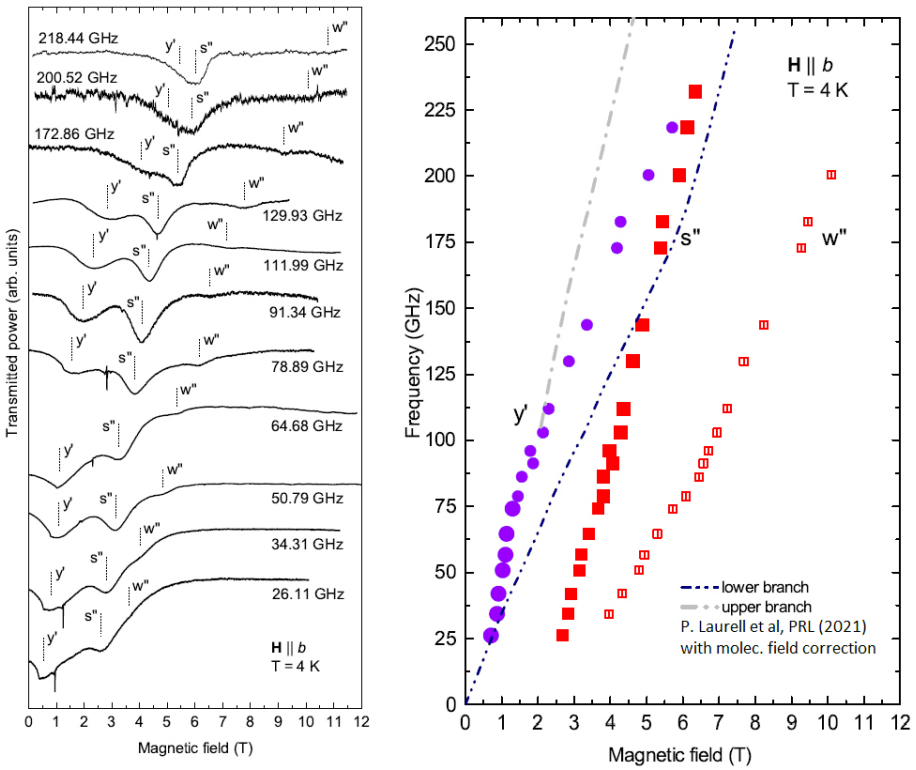

Fig. 1. Left panel: ESR lines of Cs_2CoBr_4 at $H \| b$ and various frequencies taken at 4.0 K. Letters indicate the observed modes which frequencies are displayed on the frequency-field diagram on the right panel. Right panel: Frequency-field diagram of Cs_2CoBr_4 at $H \| b$ and T = 4.0 K. Intensive lines are marked by closed symbols, a weak line – by open symbols. Dashed lines present calculations of ref. [3] corrected for molecular-field of adjacent chains. Light grey line corresponds to excitations with zero intensity at k = 0.

In this work we represent the electron spin resonance (ESR) investigation of magnetic crystal Cs_2CoBr_4 with presence of both frustration mechanisms mentioned above which result in a complicated interplay. Dielectric crystal of Cs_2CoBr_4 is a quasi two dimensional antiferromagnet with magnetic layers of isosceles triangles. The significant single ion anisotropy energy $D = 12$ K is large compared to the main exchange integral $J = 2$ K at the bases of triangles. The exchange along the lateral sides of triangles is frustrated and hence the magnetic system may be considered as weakly interacting spin chains. At low temperatures the magnetic ions may be taken as pseudospins $s = 1/2$ coupled with an anisotropic exchange. This provides an analogy with a well known quasi two-dimensional triangular system of Cs_2CuCl_4, demonstrating spinon continuum of excitations, which is conventional for Heisenberg $S = 1/2$ chain [1].

In this work we study spin dynamics in the spin-liquid phase, i.e. above the Neèl temperature 1.3 K but below the temperature of the onset of exchange correlations of pseudospins. Our experiments reveal several branches of excitations which strongly differ both from the excitations in the low-temperature ordered phase and from high-temperature paramagnetic resonance of uncorrelated pseudospins and spins. Examples of ESR records for different frequencies in the range 25–250 GHz taken for 4 K and corresponding frequency-field diagram are shown on Fig. 1.

We suppose that the transition through the Neèl point results in the transformation of the spectrum in the ordered phase to a spectrum of spinon-like continuum in a qualitative correspondence with DMRG theory of Refs. [2, 3] and the spinon continuum modified by uniform Dzyaloshinsky-Moriya interaction [4, 5]. Additionally, we observe spinon-type mode w" which is conserved in the high-energy range of the low temperature spectrum, demonstrating the coexistence of spin-liquid excitations and magnons of the ordered phase.

We acknowledge the support by the Russian Science Foundation: Grant No. 22-12-00259 for experiment and Grant No. 22-22-00028 for theory.

1. Coldea R., Tennant D.A., Tylczynski Z.: Phys. Rev. B **68**, 134424 (2003)
2. Bruognolo B., Weichselbaum A., Jan von Delft, Garst M.: Phys. Rev. B **94**, 085136 (2016)
3. Laurell P., Scheie A., Mukherjee Ch. J., Koza M.M., Enderle M., Tylczynski Z., Okamoto S., Coldea R., Tennant D. A., Alvarez G.: Phys. Rev. Lett. **127**, 037201 (2021)
4. Povarov K., Smirnov A., Starykh O., Petrov S., Shapiro A.: Phys. Rev. Lett. **107**, 037204 (2011)
5. Smirnov A., Soldatov T., Povarov K., Hälg M., Lorenz W.E.A., Zheludev A.: Phys. Rev. B **92**, 134417 (2015)

Po45

ESEEM study of electron transfer in menB complexes of photosystem I embedded into dry trehalose matrix

A.A. Sukhanov[1], M.D. Mamedov[2], A.Y. Semenov[2], K.M. Salikhov[1]

[1]Zavoisky Physical-Technical Institute, FRC Kazan Scientific Center of RAS, Kazan, Russia
[2]N. Belozersky Institute of Physical–Chemical Biology, Lomonosov Moscow State University, Moscow, Russia

The study of the stabilizing and cryoprotective effect of trehalose at different degrees of humidity on photoinduced charge separation in photosynthetic pigment-protein complexes of photosystems (PS) I and II is important for the creation of drought-resistant varieties of agricultural crops and for long-term preservation of proteins at room temperature without loss of their activity, and can be widely used for application in biotechnology. Therefore, the study of molecular dynamics and mechanisms of the stabilizing and cryoprotective effect of trehalose on photoinduced charge separation in photosynthesis reaction centers remains an urgent task.

In the present work, we used the ESEEM (electron spin echo envelope modulation) signal of the charge-separated cofactor spins, to determine the distance between the spins of P_{700}^{+} (chlorophyll dimer) and A^{-} (phylloquinone acceptor) in the PS I complexes from MenB mutant, which contain plastoquinone in the quinone-binding A_1-site embedded in dry trehalose matrix at different temperatures. These distances were also determined in PS I complexes from MenB lacking the terminal 4Fe-4S F_A/F_B clusters and complexes lacking all three 4Fe-4S clusters, F_X, F_A, and F_B. It was shown that the ESEEM frequency for these complexes does not change as the temperature rises from 150 K to room temperature.

The obtained results allow us to suggest a model [1, 2] of the protective effect of trehalose matrix on the electron transfer in the reaction center of PS I that is based on different hydrogen-bond networks between trehalose, local water, and protein.

The study was financially supported by the RSF and the Cabinet of Ministers of the Republic of Tatarstan within the framework of the scientific project No. 22-23-20165, https://rscf.ru/project/22-23-20165.

1. Sukhanov A.A., Mamedov M.D., Möbius K., Semenov A.Y., Salikhov K.M.: Applied Magnetic Resonance, **49**, 1011 (2018)
2. Sukhanov A.A., Mamedov M.D., Milanovsky G.E., Salikhov K.M., Semenov A.Y.: Biochemistry (Moscow), **87**, 1109 (2022)

Po46

Magnetic properties of quasi-two-dimensional $LiCu_3O_3$, an example of quasi-two-dimensional solid Li^+-Cu^{2+} solution

A.A. Bush[1], S.K. Gotovko[2,3], V.Yu. Ivanov[4], V.I. Kozlov[1,2], P.S. Kudimkina[2,3], E.G. Nikolaev[2], L.E. Svistov[2]

[1]MIREA – Russian Technological University, Moscow, Russia
[2]P.L. Kapitza Institute for Physical Problems, RAS, Moscow, Russia,
e-mails: nikolaev@kapitza.ras.ru, svistov@kapitza.ras.ru
[3]National Research University Higher School of Economics, Moscow, Russia
[4]Prokhorov General Physics Institute, Russian Academy of Sciences, Moscow, Russia

$LiCu_3O_3$ is an example of the cuprate with mixed valency of copper: the number of magnetic Cu^{2+} (S = 1/2) ions is twice as much as the number of nonmagnetic Cu^+ ions. The X-ray diffraction experiments on micro crystals of $LiCu_3O_3$ [1] show that the crystal structure consists of four stacked alternating square planes. One square plane consists of Cu^+ ions and other three square planes consist of $(Li^+,Cu^{2+})O^{2-}$ complexes. The nodes of these three square planes are occupied by the nonmagnetic lithium ions and magnetic copper ions statistically with proportion 1 to 2 to ensure electrical neutrality. Single-phase samples of $LiCu_3O_3$ crystals of millimeter size were grown recently [2]. Here we discuss the study of magnetic state of $LiCu_3O_3$ with magnetometry, NMR and ESR techniques. The crystallographic structure of $LiCu_3O_3$ allows to consider the magnetic material as an example of highly diluted quasi two-dimensional S = 1/2 magnet on a square lattice. Two magnetic transitions were observed at T_{c1} ~ 25 K and T_{c2} ~120 K. In our report we suggest the model of magnetic states of $LiCu_3O_3$ which can qualitatively describe the set of obtained experimental data.

The work was supported by the Russian Science Foundation Grant No. 22-12-00259.

1. Hibble S.J., Köhler J., Simon A.: Journal of solid state chemistry **88**, 534 (1990)
2. Bush A.A., Kamentsev K.E., Tishchenko E.A.: Inorganic Materials **55**(4), 374 (2019)

Po47

^{1}H and ^{19}F MRI for recognizing RF coil circuits and constructing their sensitivity maps

A.A. Tarasova[1], N.V. Anisimov[2], Yu.A. Pirogov[1]

[1]Faculty of Physics, Lomonosov Moscow State University, Moscow, Russia
[2]Faculty of Fundamental Medicine, Lomonosov Moscow State University, Moscow, Russia

MRI methods can be used to study a wide range of objects, which leads to a variety of types of RF coils used as NMR signal sensors. In our practice, we also used various types of coils, including wireless ones – Fig. 1 [1, 2]. In some cases, existing branded coils can be adapted to solve special MRI problems by making changes to the circuit [3]. Therefore, it is relevant to obtain information about the scheme and design of the coils, if possible, in a non-invasive way. The aim of this work is to visualize the structure of the coils of a clinical 0.5 T MR scanner (Bruker Tomokon S50), as well as to build their sensitivity maps.

We noticed that the coil itself can be an object of MRI imaging due to the presence of hydrogen-containing parts in its design – in particular, plastic cladding elements. Conductors placed next to them affect the distribution of magnetic fields, and, consequently, the contrast of the image. It allows identifying the conductors on it. Contrast variations are more pronounced if the signal is received by the coil itself. This approach

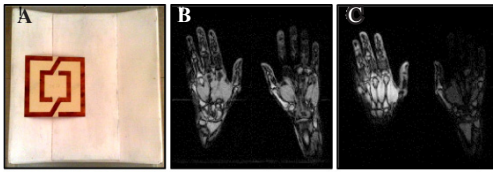

Fig. 1. A – wireless square-shaped transmission line resonator (20×20 cm^2) placed on the branded spinal coil. B and C – ^{1}H MRI of hands without and with a wireless resonator, respectively.

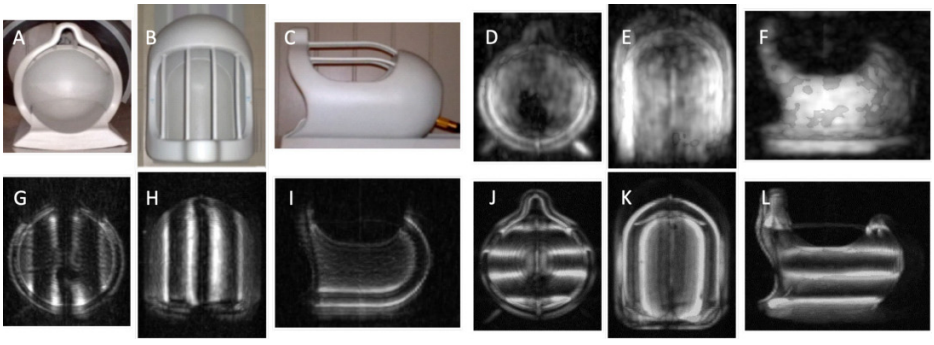

Fig. 2. Images of a branded coil for head MRI in three projections. A–C – photos; ^{1}H MRI: D–F – coil used in passive mode. In the active mode, only one of the channels works – G–I – channel 1, J–L – channel 2.

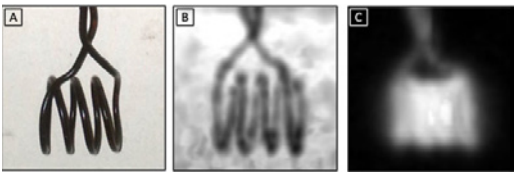

Fig. 3. 4-turn solenoid in "dry water": A – photo; B and C – ^{19}F MRI (19.8 MHz) – passive and active (TR) modes, respectively.

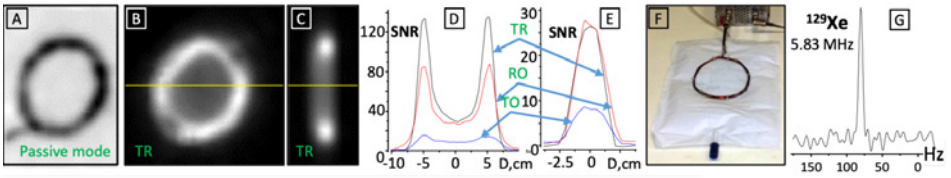

Fig. 4. A–C – ^{19}F MRI of 4-turn loop in "dry water". A – passive mode, B and C – two projections in active (TR) mode. D and C – SNR graphs for different variants of the active mode for the directions indicated by light lines on B and C, respectively. F – photo of a loop coil placed over a ^{129}Xe gas-filled plastic balloon. G – ^{29}Xe NMR spectrum at 0.5 Tesla, T_1~1 min, scan time = 10 minutes.

is especially productive for multi-channel coils – if only one of the channels is used to receive a signal, then the image can reveal conductors related only to this channel. Fig. 2 shows proton images (21.1 MHz) of the head coil (PN 5437) obtained by 3D gradient echo method (GRE).

Additional possibilities for clarifying the design of the coil arise when it is immersed in a medium that gives an NMR signal. Then it is possible to construct an image of the coil from the loss of a signal in the image obtained from the given A B C medium – the signal void imaging (SVI) technique. This method is good for objects from which it is difficult to obtain an NMR signal. For many of them, ordinary water is suitable as a background medium, but a number of objects cannot be immersed in it. Water is not suitable for visualizing coils, not only because of its destructive effect but also its electrical conductivity.

Instead of ordinary water, we used the so-called "dry water" – fluorinecontaining liquid Novec 1230 ($C_6F_{12}O$) from 3M. It does not conduct current, does not penetrate the surface of the poured objects, and therefore does not spoil them, and at the same time, it penetrates well into their pores and cavities. Using this fluid, we applied a ^{19}F MR scan (3D GRE) to visualize a 4-turn solenoid and a 6-turn loop coil. Figures 3B and 4A show images of these coils when they were operated in passive mode – RF excitation and response from "dry water" was produced by external coils.

Additional possibilities arise when using coils in the active mode, when they work as either receiving (RO), or transmitting (TO), or transmitting-receiving (TR) – Figures 3C, 4B, 4C. In this case, volumetric images of the medium in which these coils are immersed are obtained, and they display coil sensitivity maps. Graphs of SNR along the diameter and axis of the coil are shown in Figures 4E and 4F, respectively. We used these maps to estimate the effective volume of ^{129}Xe gas (thermal polarization)

producing an NMR signal (5.8 MHz) that was detected by a loop coil placed over a gas-filled plastic balloon – Figures 4F, 4G.

Thus, ^{1}H and ^{19}F MRI can give information about RF coils – construction, conductors and sensitivity map. The coils themselves can be used to receive signals from both their own body elements and the environment in which they are immersed. Fluorine-containing "dry water" is well suited as such a medium. This research was supported by the Russian Foundation for Basic Research grant No. 19-29-10015, the Interdisciplinary Scientific and Educational Schools of Moscow University "Molecular Technologies of the Living Systems and Synthetic Biology" and "Photonic and quantum technologies. Digital medicine".

1. Anisimov N.V., Gulyaev M.V., Volkov D.V. et al.: Phys.Wave Phenomena **23** (4), 304–310 (2015)
2. Gulyaev M.V., Protopopov A., Pavlova O.S. et al.: J. Magn. Reson. **339**, 107216 (2022)
3. Anisimov N.V., Tarasova A.A., Pavlova O.S. et al.: Appl. Magn. Reson. **52**, 221–233 (2021)

Po48

Multinuclear ^{1}H, ^{13}C, ^{27}Al and ^{31}P NMR spectroscopy in the study of the structure of the 3-spiro-substituted polycyclic borolanes, alumolanes and phospholanes

T.V. Tyumkina[1], S.M. Idrisova[2], R.R. Nurislamova[2], L.I. Tullyabaeva[3]

[1]Institute of Petrochemistry and Catalysis, FRC Ufa Scientific Center of RAS, Ufa, Russia
[2]Laboratory of structural chemistry
[3]Laboratory catalytic synthesis

Terpenes and their derivatives are widely used in medicine, food and perfume industry, and as intermediates in total syntheses of natural biologically active products [1]. Therefore, it is important not only to develop functionalization methods in terpenes chemistry, but also to study stereochemical features of novel compounds that may possess useful properties. Earlier the new polycyclic organoalumimum compounds were synthesized [2] by catalytic cycloalumination of methylenecyclobutane derivatives of terpenes with Et_3Al in the presence of Cp_2ZrCl_2, which served as reactants in the one-pot synthesis of appropriate heterocyclic compounds (Fig. 1). The new polycyclic borolanes and phospholane oxides have been obtained by the reaction of replacement of aluminum atom in 1-ethyl-3-*spiro* polycyclic alumolanes by boron and phosphorus atoms with $PhBCl_2$ and $PhPCl_2$ respectively [3, 4].

Comparative conformational analysis of the metal and elemental organic compounds was performed by quantum chemical approach [Priroda 6.0, 5]. The stereochemistry of compounds was determined.

1. Ardashov O., Pavlova A., Il'ina I., Morozova E., Korchagina D., Karpova E., Volcho K., Tolstikova T., Salakhutdinov N.: J. Med. Chem. **54**, 3866–3879 (2011)
2. D'yakonov V., Tuktarova R., Islamov I., Tyumkina T., Dzhemilev U.: Journal of Heterocyclic Chemistry, **53**, 6, 1750–1760 (2016)
3. Тюмкина Т., Нурисламова Р., Махаматханова А., Халилов Л., Джемилев У.: Изв. АН. Сер. хим. **6**, 1143–1150 (2022)
4. Tyumkina T., Tulyabaeva L., Idrisova S., Islamov D., Khalilov L., Dzhemilev U.: Phys. Chem. Chem. Phys. **25**, 13104–13115 (2023)
5. Laikov D., Chem. Phys. Lett. **281**, 151–156 (1997)

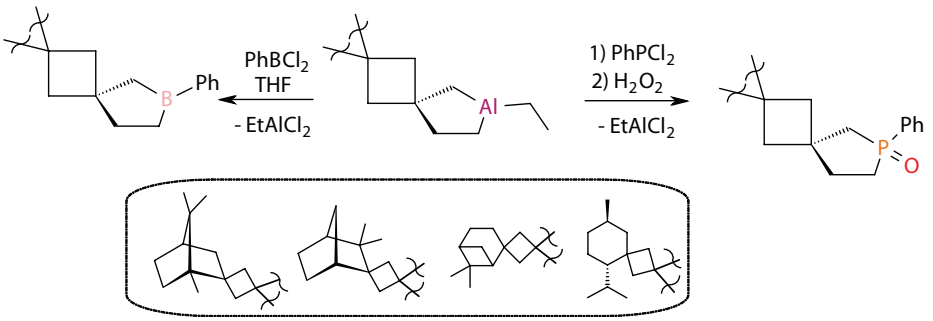

Fig. 1. Synthesis of new polycyclic B,Al,P-containing compounds.

Po49

Features of the iron charge states in semi-insulating β-Ga_2O_3:Fe identified by high-frequency electron paramagnetic resonance

Yu.A. Uspenskaya, R.A. Babunts, A.S. Gurin, E.V. Edinach, P.G. Baranov

Ioffe Institute, Saint Petersburg, Russia

Both single crystals and thin films of beta-gallium oxide (β-Ga_2O_3) can be used in various fields: from power electronics to solar-blind UV detectors. One of the attractive features of the Ga_2O_3 system is its high radiation resistance, making it suitable for use in space applications.

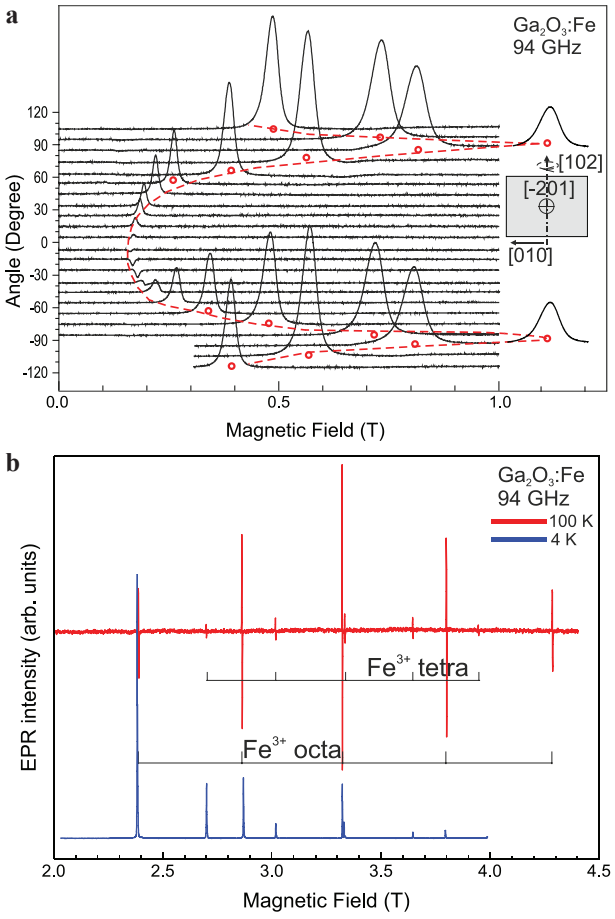

Fig. 1. EPR spectra of semi-insulating Ga_2O_3:Fe crystal recorded at 94 GHz: **a** Fe^{2+} ions measured at temperature of 2 K; **b** Fe^{3+} ions measured at temperatures of 4 K and 100 K.

Recently, the results of electron paramagnetic resonance (EPR) research of nominally undoped β-Ga_2O_3 bulk crystals were published [1]. The study demonstrate that the Fermi level position, varied by means of electron irradiation, is one of the critical parameters that determines the charge and spin states of transition elements.

The charge states of non-Kramers Fe^{2+} ions (S = 2) and Fe^{3+} ions (S = 5/2) in the octahedral and tetrahedral positions of the crystal lattice in a commercial substrate of semi-insulating gallium oxide β-Ga_2O_3 before and after proton irradiation with an energy of 15 MeV have been identified by high-frequency EPR (Fig. 1). It has determined unambiguously that there are two charge states for iron, Fe^{2+} and Fe^{3+}, in the semi-insulating material. Protons irradiation with an energy of 15 MeV and a dose of ~10^{16} cm^{-2} does not lead to any change in intensity or shape of the EPR spectra, that indicates a high radiation resistance of semi-insulating β-Ga_2O_3.

This work was supported by the Russian Science Foundation № 22-12-00003, https://rscf.ru/project/22-12-00003.

1. Babunts R.A., Gurin A.S., Edinach E.V., Drouhin H.-J., Safarov V.I., Baranov P.G.: J. Appl. Phys. **132**, 155703 (2022)

Po50

Design of a gradient coil system for nuclear magnetic resonance equipment

A.L. Valiullin, V.D. Skirda, D.S. Ivanov, A.S. Alexandrov, O.I. Gnezdilov, M.M. Doroginitsky, T.A. Kazbaev

Institute of Physics, Kazan Federal University, Kazan, Russia

Gradient systems are an important part of nuclear magnetic resonance (NMR) equipment. The main part of any gradient system are gradient coils. They create magnetic fields that change in space according to a certain law, which allows spatial encoding of the NMR signal. So, the magnetic field, changing according to a linear law (linear gradient), provides definite encoding of the signal. Such gradients are used in the study of diffusion and in classical magnetic resonance imaging techniques [1]. However, it is also important to create nonlinear gradients that can be used in such MRI aspects as Patlock [2]. The purpose of this work is to calculate and optimize the parameters of gradient coils based on Golay coils, measuring the field created by coil models made according to certain parameters.

Computer modeling in the MATLAB software package was chosen as the main research method. To measure the cross component of the field generated by the coil, a Gaussmeter based on a Hall sensor (sensitivity 0.1 Gs) was used, the axial part was performing numerical calculations, a program was developed based on the use of the Bio-Savard-Laplace law and the finite element method. At each point of the region of interest (ROI), the magnetic field generated by current conductors is calculated, which allows selecting optimal coil configurations. The parameters for modeling coils are: number of turns, winding pitch, coil radius, central angle, coil length, position in space, smoothing of angles, current value and its direction, angle of rotation of coils around the axis of the cylinder, winding function (step change depending on the coil). Thus, the parameters of linear (G_x, G_y, G_z) and quadratic (G_{xy}, G_{yz}, G_{xz}) gradient coils were determined. Figure 1 shows the configurations of the gradient coils G_x and G_{yz}.

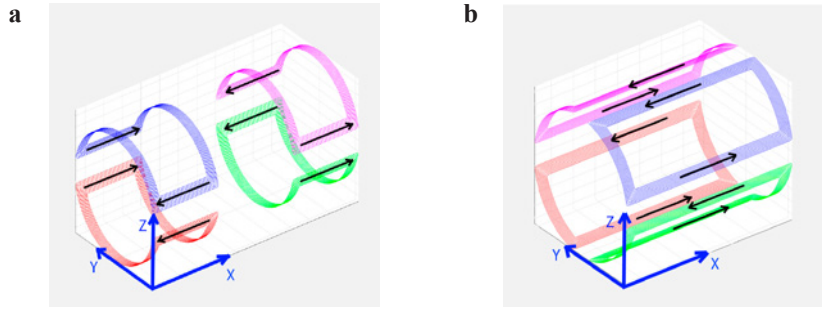

Fig. 1. Configurations of gradient coils: **a** G_x, **b** G_{yz}. The blue arrows show the selected coordinate system. The black arrows show the direction of the current in the coils.

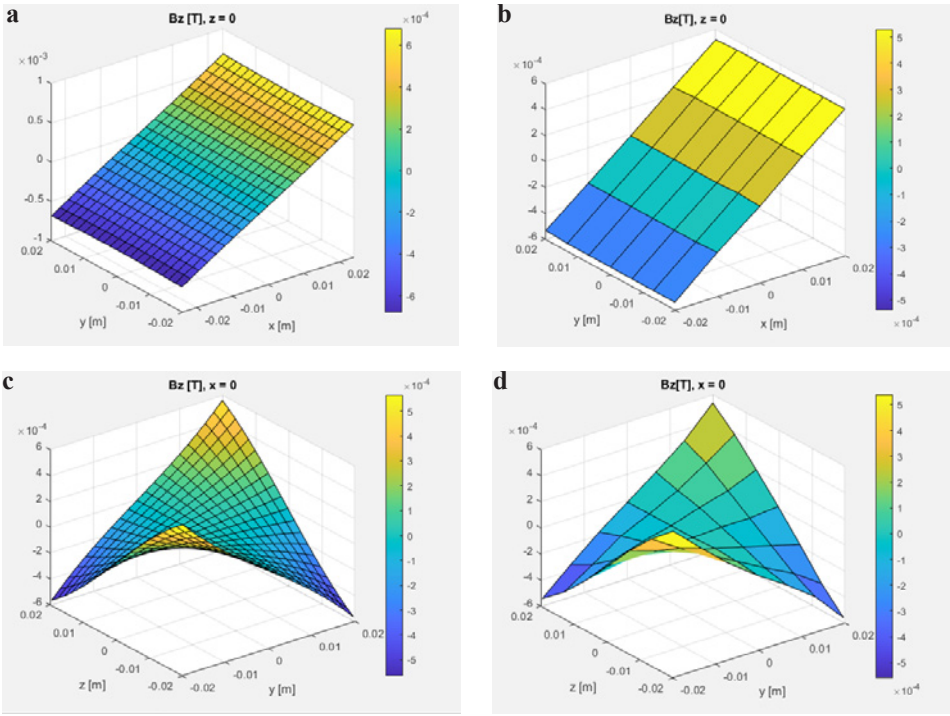

Fig. 2. Maps of magnetic fields: **a** calculated G_x; **b** measured G_x; **c** calculated G_{yz}; **d** measured G_{yz}. The field with gradient G_x is measured in the XY plane at $Z = 0$. The field with gradient G_{yz} is measured in the YZ plane at $X = 0$.

According to certain parameters, models were made for which magnetic fields were measured. For comparison, Fig. 2 shows the results of calculations and measurements of the magnetic field generated by the coils G_x and G_{yz}. The size of the ROI in which the measurements and calculations were carried out are 48 mm×39.6 mm×39.6 mm.

It can be seen from the figures that the calculated fields coincide with the measured ones, deviating by no more than 5%. This correspondence makes it possible to use the developed program in the future when creating gradient systems. Also, from the results obtained by their program, it can be concluded that the disadvantage of the Golay coils used is the small relative size of the ROI region, in which the field inhomogeneity does not exceed 5%. According to the results obtained, this size is approximately 0.6 of the coil radius.

This work was funded by the subsidy allocated to Kazan Federal University for the state assignment in the sphere of scientific activities number FZSM-2023-0016.

1. Ernst R., Bodenhausen D., Vocaun A.: NMR in one and two dimensions / trans. from English (Salikhov K.M., ed.), 1990.
2. Polonskij N.B.: Konstruirovanie elektromagnitnyh ekranov dlya radioelektronnoj apparatury. M.: Sovetskoe radio (1979), 216 p. (In Russian)

Po51

Study of conformations of 1-phenyl-3-(quinolin-8-ylamino)prop-2-en-1-one by NMR, UV-spectroscopy and DFT calculations

M.Yu. Volkov[1], A.R. Sharipova[1], A.F. Shaidullina[2], L.I. Savostina[1,2], O.A. Turanova[1], A.N. Turanov[1]

[1]Zavoisky Physical-Technical Institute, FRC Kazan Scientific Center of RAS, Kazan, Russia
[2]Kazan Federal University, Kazan, Russia

Due to their high reactivity, enaminones are a large class of organic compounds that play an important role in organic synthesis. They are also widely used for the synthesis of biologically active molecular candidates – antibacterial, anti-inflammatory, anticonvulsant and anticancer agents. Enaminones can serve as promising ligands for the synthesis of metal complexes. The study of the tautomerism of the enaminone molecules and the determination of their conformations is important because the various conformations of the enaminones have different reactivity in the synthesis of metal complexes. Enaminon molecules also contain double bonds, which determine the possibility of their E-Z photoisomerization. In order to determine the presence or absence of photoisomerization of molecules of various chemical compounds, NMR and UV spectroscopy are usually used.

This work is aimed at the synthesis and study of the structure and tautomeric transformations of 1-phenyl-3-(quinolin-8-ylamino)prop-2-en-1-one molecules. The molecules of this enaminone can exist in three conformations – isomer E, isomer Z and enol-tautomer (Fig. 1). 1D and 2D NMR, as well as UV-spectroscopy allowed us to establish that almost all molecules of the studied substance, regardless of the polarity of the solvent (hexane, carbon tetrachloride, chloroform, acetone, acetonitrile, dimethyl sulfoxide), are the Z-isomer. It agrees with the results of the calculations performed by the DFT method with CAM-B3LYP functional and the def2-TZVP basis set. Exposure to UV radiation with $\lambda = 365$ nm or heating a solution of the enaminone in dimethyl sulfoxide transforms some part of the enaminone molecules into the E-isomer (about 10%).

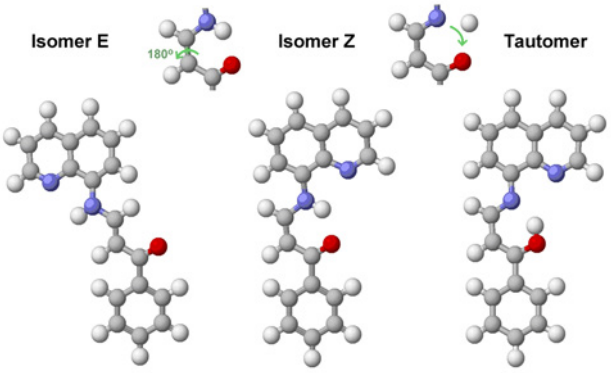

Fig. 1. The possible conformations of 1-phenyl-3-(quinolin-8-ylamino)prop-2-en-1-one.

Po52

Long-lived charge separated states in compact electron donor-acceptor dyads: study of the photophysical property by using transient optical and magnetic resonance spectroscopies

H. Wang[1], X. Xiao[1], Y. Yan[1], A.A. Sukhanov[2], A. Iagatti[3], S. Doria[3], L. Bussotti[3], X. Zhao[1], J. Zhao[1], V.K. Voronkova[2], M. Di Donato[3]

[1]State Key Laboratory of Fine Chemicals School of Chemical Engineering
Dalian University of Technology E-208 West Campus
[2]Zavoisky Physical-Technical Institute, FRC Kazan Scientific Center of Russian Academy of Sciences, Kazan, Russia, e-mail: vor18@yandex.ru
[3]LENS (European Laboratory for Non-Linear Spectroscopy), Sesto Fiorentino, Firenze, Italy

Photoinduced charge separation is important in fundamental photochemistry studies, as well as in applications such as photocatalysis, molecular probes, electroluminescence materials, and photovoltaics. One of the major challenges in this area is to attain charge separated (CS) states showing long lifetimes

To study the charge separation (CS) and long-lived CS state, we prepared a series of dyads based on naphthalimide (NI, electron acceptor) and phenothiazine (PTZ, electron donor), with an intervening phenyl linker attached on the N-position of both moieties and a series of anthraquinone (AQ)-PTZ dyads, with adamantane as the linker. The purpose is to exploit the electron spin control effect to prolong the CS state lifetime by formation of the 3CS state.

The photophysical property of these dyads are studied by transient optical and magnetic resonance spectroscopies.

A study by the time-resolved EPR (TREPR) method showed that spectra from radical ion pairs, charge-separated triplet states, triplet states localized on one of the fragments, or simultaneously localized triplet state and 3CS state are observed upon photoexcitation depending on the structure of the dyads and the polarity of the solvent. So it is shown by TREPR that a radical ion pair was observed for AQ-PTZ and AQ-PTZ-M, whereas in the dyads with the PTZ unit oxidized, only the 3AQ state was observed. Effect of molecular conformation restriction and solvent polarity on the long-lived CS states are discussed.

Po53

Spin-wave resonance in gallium iron oxide

I.V. Yatsyk[1], R.M. Eremina[1], E.M. Moshkina[2]

[1]Zavoisky Physical-Technical Institute, FRC Kazan Scientific Center of RAS, Kazan, Russia,
e-mail: I.Yatsyk@gmail.com
[2]Kirensky Institute of Physics, Federal Research Center KSC SB RAS,
Krasnoyarsk, Russia

The multiferroic materials, which exhibit coexistence and coupling of magnetic and electric orders, have emerged as promising candidates for basic understanding of the coupling between magnetic and electronic properties and uses of the materials in magnetoelectric devices, such as memory, logic devices, sensors, and voltage-driven magnetic

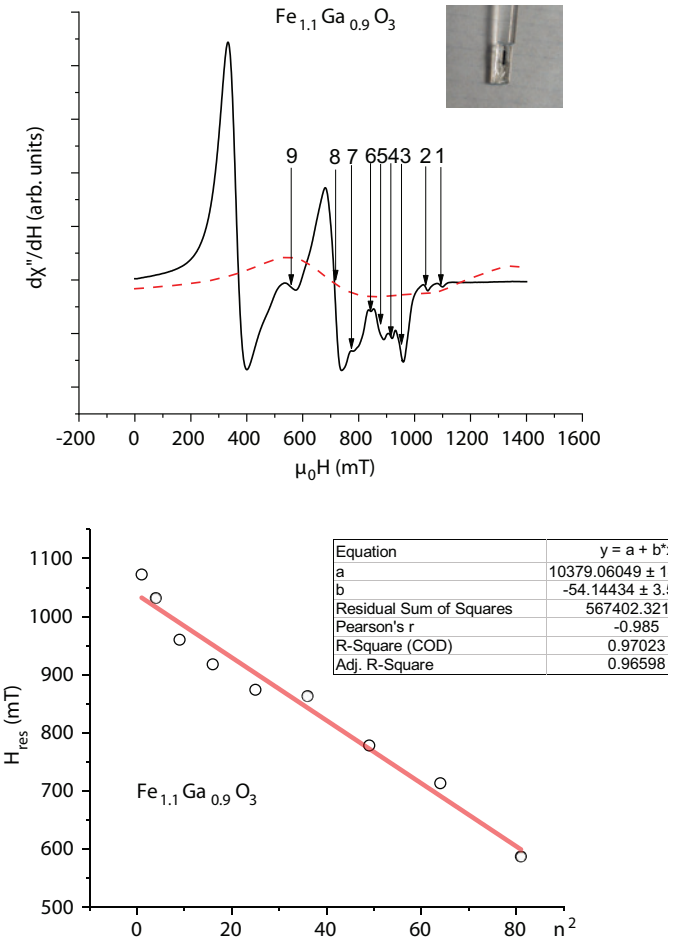

Fig. 1. Spin-wave resonance spectrum (top) and dependence of the magnetic field on the square of the mode number (bottom) $H_{res}(n^2)$ in (*ab*) plane.

tunnel junctions [1–6]. The integration of naturally existing or artificially designed multiferroic materials into devices opens up a new field to achieve the energy-saving and miniaturization of the devices [7]. Some transition metal oxides ($BiFeO_3$, $TbMnO_3$, $BiMnO_3$, $HoMnO_3$, $DyFeO_3$, and $GaFeO_3$) have shown multiferroic properties [1–7] and majority of these oxides showed magnetic order at low temperatures.

The aim of this work is to detect spin-wave resonance in a single crystal of $Fe_{1.1}Ga_{0.9}O_3$. The figure shows two spectra in a mutually perpendicular orientation. The solid line shows a series of peaks, while the dotted line shows only one peak. The dependence of the resonant field for a given series of peaks and the square of the mode number are presented in the right figure. The resulting dependence is linear, which makes it possible to hope for the observation of spin-wave resonance.

I.V.Y. and R.M.E. acknowledge the financial support from the government assignment for FRC Kazan Scientific Center of RAS.

1. Lone A.G., Bhowmik R.N.: Journal of Alloys and Compounds **905**, 164164 (2022)
2. Fiebig M., Lottermoser T., Meier D., Trassin M.: Nat. Rev. Mater. **1**, 16046 (2016)
3. Lu C., Wu M., Lin L., Liu J.M.: Natl. Sci. Rev. **6**, 4 (2019)
4. Spaldin N.A.: Proc. R. Soc. A **476**, 20190542 (2020)
5. Catalan G., Scott J.F.: Adv. Mater. **21**, 2463–2485 (2009)
6. Wang Y.J., Li J.F., Viehland D.: Mater. Today **17**, 269–275(2014)
7. Pyatakov A.P., Zvezdin A.K.: Phys. Usp. **55**, 557–581 (2012)

Po54

The study of EPR spectra in fast-growing buckwheat callus at different phases of its growth

S.V. Yurtaeva[1], I.V. Yatsyk[1], A.I. Valieva[2], A.N. Akulov[2], N.I. Rumyantseva[2]

[1]Zavoisky Physical-Technical Institute, FRC Kazan Scientific Center of RAS, Kazan, Russia, e-mail: S.Yurtaeva@kfti.knc.ru
[2]Kazan Institute of Biochemistry and Biophysics, FRC Kazan Scientific Center of RAS, Kazan, Russia

In this study, the phenomenon of "wide EPR signals" found in fast-growing yeast cells [1–3] was detected in intensively dividing plant cells for the first time. This phenomenon manifests itself in the appearance of broad lines in the EPR spectra in the region g = 2.2–2.3 and a simultaneous change in their static magnetic susceptibility at a certain stage of cell culture growth. The nature of these magnetic changes is not completely understood at the moment, but is of interest. A culture of intensively dividing cells of non-morphogenic callus of Fagopyrum tataricum was used as an object of study. The aim of the research was to study the magnetic resonance characteristics of signals, define their origin (physical nature), and explore if they are connected with cell division.

Frozen and freeze-dried samples of cells were studied by EPR spectroscopy. Cell culture samples were taken every day after transfer to a fresh nutrient medium during its growth for 14 days. It was found that the EPR spectra of cell culture samples depend on the phase of growth. The results of the EPR study showed that during the growth of the cell culture, a strong change in the magnetic properties occurs. It resulted in the appearance of additional intense EMR (FMR) signals depending on the orientation of the magnetic field on 3-4 days of culture growth. The integral intensity of the EPR spectra had a maximum on the 3rd or 4th day of passage. About 20 series of independent experiments were made. The increase in the signal was due to the appearance of the EMR signal in the region of g-value 2.1÷2.2. The temperature and angular dependences of EMR signals were studied.

As a result of the study, it was found that the characteristics of EMR signals ($H_{res}(T)$, $\Delta H(T)$ and integral intensity) in the temperature range 100K–260 K corresponded to the behavior of magnetite nanocrystallites (Fe_3O_4) described earlier in [4] with a characteristic Verwey phase transition. The presence of an angular dependence indicates the ferrimagnetic properties of Fe_3O_4.

The dependence of integral intensity of the EPR spectrum on the time of cultivation was plotted. Simultaneously with EPR data, the characteristics of callus growth, as well as a dependence of the mitotic index on the phases of callus growth were studied.. It has been shown that the moment of appearance of the maximum EMR signal correlated with the moment of registration of the maximum values in mitotic index (characterizing the percent of dividing cells in culture), which points to the relationship between magnetic properties and the process of cell division.

The possibility of a relationship between various contributions in the EPR spectra of cell culture at different stages of growth and different phases of cell division is discussed.

The dependence of EPR spectra on the growth phase and mitotic activity of Tartary buckwheat callus is discussed.

EPR spectroscopic studies of the samples were carried out at KPTI FRC KazSC RAS as a part of the government assignment.

The cultivation of callus and the study of callus growth were performed at KIBB FRC KazSC RAS as a part of the government assignment.

1. Samoilova O.P., Blumenfeld L.A.: Biofizika (in Russian), **6**, iss. 1, 15–19 (1961)
2. Tsapin A.I., Samoilova O.P., Blumenfeld L.A.: Biofizika (in Russian), **34**, iss. 4, 15–19 (1989)
3. Samoilova O.P., Tsapin A.I., Blumenfeld L.A.: Biofizika (in Russian), **40**, iss. 2, 383–388 (1995)
4. Yurtaeva S.V., Efimov V.N., Yafarova G.G. et al.: Appl. Magn. Reson. **47**, 555–565 (2016)

SPIN PHYSICS, SPIN CHEMISTRY, AND SPIN TECHNOLOGY

Magnetic Josephson junctions for superconducting electronics and spintronics

V.V. Ryazanov[1,2,3], T.E. Golikova[1], L.N. Karelina[1], V.V. Bol'ginov[1]

[1]Institute of Solid State Physics, Russian Academy of Sciences, Chernogolovka, Russia
[2]Moscow Institute of Physics and Technology, Dolgoprudny, Russia
[3]National University of Science and Technology MISIS, Moscow, Russia

Our recent investigations are related to superconducting spintronics in Josephson ferromagnet/superconductor (SF) structures. Fundamentally new structures and approaches for applications in superconducting electronics and spintronics are proposed. Among them Josephson SFS structures c π-periodic current-phase relation [1], S-N/F-S devices with spin diffusion and spin injection [2], memory elements on the basis of SFS contacts [3]. We have repeated also well-known experiment by J.J.A. Baselmans et al [4] using the spin-polarized injection to Josephson barrier of SNS junction [5] (see Fig. 1). We have observed two clearly distinct transitions: both from conventional (0-) to π-state (with inversion of superconducting phase difference) and back π-0 transition. We suppose that the "Baselmans effect" mechanism related to energy electron redistribution is significantly complemented by influence of "induced magnetism" due to spin-diffusion [2].

1. Stoutimore M.J.A. et al.: Phys. Rev. Lett. **121**, 177702 (2018)
2. Golikova T.E. et al.: Phys. Rev. B **86**, 064416 (2012)
3. Karelina L.N. et al.: J. Appl. Phys. **130**, 173901 (2021)
4. Baselmans J.J.A. et al.: Nature **43**, 397 (1999)
5. Golikova T.E. et al.: Supercond. Sci. Tech. **34**, 095001 (2021)

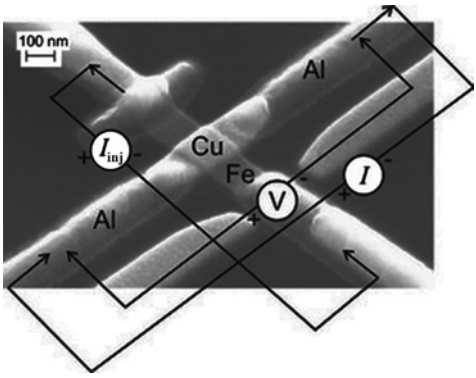

Fig. 1. S-N/F-S nanostructure with spin-injection.

The reduction of metal oxides in the external magnetic field

P.A. Chernavskii[1,2], N.S. Perov[3]

[1]Department of Chemistry, Lomonosov Moscow State University, Moscow, Russia
[2]Institute of Organic Chemistry N.D. Zelinsky, RAS, Moscow, Russia
[3]Faculty of Physics, Lomonosov Moscow State University, Moscow, Russia

Nanotechnology and its products are playing an increasingly important role in the new century. The prospect of large quantities of nanoparticles in a wide variety of materials is opening the way to new types of industrial production based on them. Therefore, nanoparticles play an essential role not only in nature and modern science, but also in advanced technologies.

Intensive research is carried out both in the field of synthesis of magnetic nanoparticles and in the discovery of possibilities of their practical application [1, 2]. At the same time, some reactions involving reagents with magnetic order and a significant magnetic moment allow to follow the course of the reaction, registering changes in the magnetic properties of the corresponding reagents in real time [3].

Previously, the influence of an external magnetic field on the kinetics of hydrogen reduction of metal oxides was studied. The first study of the reaction kinetics of hydrogen reduction of magnetite in magnetic fields of different intensities showed that the reaction mechanism strongly depends on the external magnetic field strength [4]. In [5], the effect of a magnetic field on the kinetic parameters of hydrogen reduction of cobalt oxide Co_3O_4 under isothermal conditions was studied.

The effect of the magnetic field on the reduction rate even in weak fields and the dependence of the oxides conversion degree on the strength of an external magnetic field have been shown.

1. Descamps L., Le Roy D., Tomba C., Deman A.L.: Magnetochemistry **7**, 100 (2021)
2. Darwish M.S., Mostafa M.H., Al-Harbi L.M.: Int. J. Mol. Sci. **23**, 1023 (2022)
3. Chernavskii P., Lunin B., Zakharyan R., Pankina G., Perov N.: Instrum. Exp. Tech. **57**, 78–81 (2014)
4. Chernavsky P.A., Kim N.V., Andrianov V.A., Perfiliev Y.D., Novakova A.A., Perov N.S.: RSC Adv. **11**, 15422–15427 (2021)
5. Chernavskii P., Kazak V., Pankina G., Perov N.: Kinet. Catal. **55**, 117–120 (2014)

Dzyaloshinskii-Moriya interaction origin in Co/Pt symmetric multilayers

D.A. Tatarskiy[1,2], N.S. Gusev[1], O.L. Ermolaeva[1], A.N. Orlova[1], V.L. Mironov[1], S.A. Gusev[1]

[1]Institute for physics of microstructures RAS, Nizhny Novgorod, Russia
[2]Lobachevsky University, Nizhny Novgorod, Russia

The interface between heavy metal or oxides and ferromagnets in thin multilayered films leads to the absence of σ_h mirror symmetry. This give rise to the induced Dzyaloshinskii-Moriya interaction (DMI) and existence of Neel domain walls and skyrmions in films with perpendicular magnetic anisotropy. Recently it has been shown the presence of skyrmions in symmetrical Pt/Co/Pt structures [1]. The reason of the absence of mirror symmetry in such film is unknown. In this work we investigate periodical [Co(0.5 nm)/Pt(1.0 nm)]×N (N = 2÷18) multilayered films trying to find out the asymmetry in their structures. We use Lorentz and analytical transmission electron microscopy (AEM, L-TEM), magneto-optical measurements and magnetic force microscopy (MFM) as complementary methods to obtain comprehensive information about magnetism in our films. L-TEM shows a typical Fresnel contrast of Neel domain walls (Fig. 1a). The domain sizes in demagnetized state are measured by MFM. Their dependence of film thickness is described by analytical homogeneous film model with magnetostatic interaction (Fig. 1b) [3]. Thus proves the assumption that all periods of [Co(0.5 nm)/Pt(1.0 nm)] have a very similar magnetic and structural parameters. The cross section view of the thickest film is shown on Fig. 1c. One can see grain boundaries have very close inclination of grain boundaries. The further analisys of plane specimens shows the monotonical increase of grain sizes vs. total film thickness. Our conclusion is that grains in films grows as inverted truncated pyramids. This peculiarity give rise to the

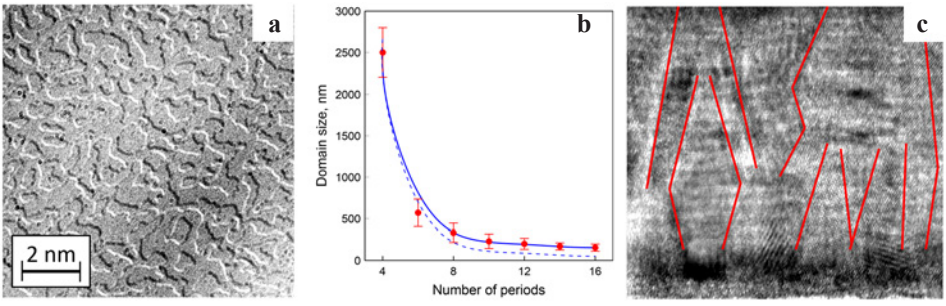

Fig. 1. a Fresnel image of domain walls (a); **b** Domain size in demagnetized state vs. total film thickness; **c** cross section micrograph of [Co/Pt]×18 with guide for eyes lines of grain boundaries.

absence of σ_h mirror symmetry and presence of large DMI. This study is supported by the Russian Science Foundation (Project no. 21-72-10176). The facilities of Center "Physics and technology of micro- and nanostructures" at IPM RAS were used for the analysis of the samples.

1. He M., Xu T., Gao Y., Hu Ch., Cai J., Zhan Y.: Materitals **15**, 8272 (2022)
2. Benitez M.J., Hrabec A., Mihai A.P., Moore T.A., Burnell G., McGrouther D., Marrows C.H., McVitie S.: Nature Communications **6**, 8957 (2015)
3. Meier T.N.G., Kronseder M., Back C.H.: Phys. Rev. B **96**, 144408 (2017)

Cooper pair splitting in magnetic SQUIDs

Ya. Fominov

L. D. Landau Institute for Theoretical Physics RAS, Chernogolovka, Russia,
Moscow Institute of Physics and Technology, Dolgoprudny, Russia,
Laboratory for Condensed Matter Physics, HSE University, Moscow, Russia

We consider SQUIDs with magnetic spin-filtering insets inside the interferometer arms. Coherent transport due to split Cooper pairs becomes pronounced in this case, with two electrons of a pair going through different interferometer arms. The problem is considered both in the ballistic [1] and diffusive [2] limit. While physics in the two limits is essentially different, they share some common properties: the flux periodicity is doubled in comparison with conventional SQUIDs and the system can be controlled by relative direction of magnetizations of the spin filters. At the same time, average current is extremely suppressed in the diffusive limit, and the Josephson effect in this case is due to mesoscopic fluctuations.

1. Stroganov P.L., Fominov Ya.V.: Phys. Rev. B **96**, 174508 (2017)
2. Ioselevich P.A., Ostrovsky P.M., Fominov Ya.V., Feigel'man M.V.: Phys. Rev. B **95**, 094508 (2017)

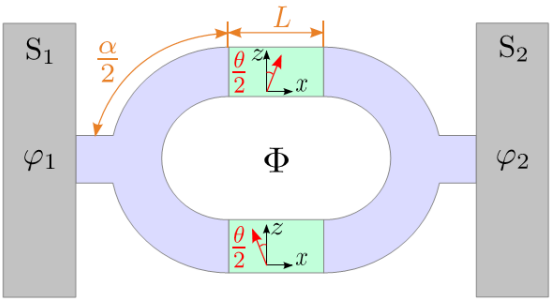

Fig. 1. SQUID with ferromagnetic spin filters inside the arms, producing splitting of Cooper pairs. Gray regions $S_{1,2}$ are singlet superconducting reservoirs, blue regions – three-terminal beam splitters, green insets – half-metallic ferromagnets (spin filters). Angle between the magnetizations of the filters is θ, the SQUID flux is Φ. By α/2 and L we denote phases acquired by quasiparticles in the ballistic regime of transport.

Optical conductivity of quantum spin liquids

V.R. Shaginyan

Petersburg Nuclear Physics Institute, NRC Kurchatov Institute, Gatchina, Russia,
e-mail: vrshag@thd.pnpi.spb.ru

We analyze optical conductivity of the herbertsmithite. Our analysis is in agreement with the corresponding measurements [1], which provide important experimental evidence of the nature of quantum spin liquid (QSL) composed of spinons. Our theoretical consideration of the optical conductivity allows us to reveal the physical mechanisms responsible for its temperature and magnetic field dependences. We show that at elevated temperatures the low-frequency optical conductivity is a decreasing function of T. This observation is consistent with the experimental data [1]. We also demonstrate that the optical conductivity diminishes under the application of magnetic fields. This observation seems to contradict the experimental results since no systematic magnetic field dependence is observed [1]. To elucidate the magnetic field dependence, we note that the measurements of the optical conductivity have been taken at 6 K and the magnetic fields $B = 7$ T [1]. In such a case the system is still in the transition regime and the magnetic field dependence cannot be observed [2–4]. We predict that the B-dependence of optical conductivity can be observed at $B = 7$ T provided that T is less or equal to 1 K. Thus, we predict that the optical conductivity diminishes at growing magnetic fields. Since the contribution coming from phonons does not depend on magnetic fields, we suggest that measurements under the application of different magnetic fields. In our report we expose a state of the art in the investigations of physical properties of 2D geometrically quantum frustrated magnets. As QSL excitations are fermions, the most appropriate description of observed phenomena is based on some spinon formalism. Our analysis permits to describe the multitude of experimental results obtained in measurements on frustrated magnets including inelastic neutron scattering

1. Pilon D.V., Lui C.H., Han T.-H., Shrekenhamer D., Frenzel A.J., Padilla W.J., Lee Y.S., Gedik N.: Phys. Rev. Lett. **111**, 127401 (2013)
2. Shaginyan V.R., Amusia M.Ya., Msezane A.Z., Popov K.G.: Phys. Rep. **492**, 31 (2010)
3. Amusia M.Ya., Popov K.G., Shaginyan V.R., Stephanovich V.A.: Theory of Heavy-Fermion Compounds. Springer Series in Solid-State Sciences Vol. 182, 2014.
4. Amusia M.Ya., Shaginyan V.R.: Strongly Correlated Fermi Systems: A New State of Matter. Springer Tracts in Modern Physics Vol. 283 (Springer Nature: Switzerland AG, Cham), 2020.

BEC based qubits

Yu.M. Bunkov

Russian Quantum Center, Skolkovo, Moscow, Russia

There are two different types of multiparticle coherent states. The coherent states of photons can be observed in optical systems. Another type of coherent states is the Bose Einstein condensation of identical quantum particles [1]. The main difference between these two types of coherent states is that optical coherent states do not have a definite number of particles. Meanwhile, many-particle coherent states in the ideal case have a fixed number of particles [2]. The use of the quantum nature of atomic Bose condensates as a basis for qubits has been theoretically considered for quite a long time [3]. In particular, attention has been paid to the possibility of constructing qubits using the spin component of atomic Bose condensates [4].

Great interest arises when considering analogies between coherent photonic and atomic systems, on the one hand, and their magnon counterparts in magnetically ordered systems. In particular, a large number of studies have been carried out on Yttrium Iron Garnet (YIG) films. A remarkable feature of this system is that the minimum energy and, accordingly, the states of the magnon Bose condensate are formed both in films magnetized longitudinally and transversely to the film plane. In the case of longitudinal magnetization, the magnon Bose condensate is formed by traveling magnons with a nonzero wave vector **k** [5]. That is, this condensate has an analogy with a photon condensate in matter. On the contrary, in the case of transverse magnetization, the energy minimum corresponds to magnons with zero wave vector, which is analogous to the formation of an atomic Bose condensate [6].

In the latter case, it is possible to construct a magnon qubit using analogies with the spinor atomic qubit, the theory of which was developed in [7]. In the presentation, we will consider the possibilities of using this analogy.

This work was supported by the Russian Science Foundation (project no. 22-12-00322).

1. Combescure M., Robert D., Combescure M., Robert D.: Coherent States and Applications in Mathematical Physics, pp. 183–223, 2012.
2. Gross C.: J. Phys. B: Atomic, Molecular and Optical Physics **45**, 103001 (2012)
3. Deutsch C. et al.: Phys. Rev. Lett. **105**, 020401 (2010)
4. Chaudhary M. et al.: Phys. Rev. A **105**, 022443 (2022)
5. Serga A.A. et al.: Nat. Commun. **5**, 3452–3458 (2014)
6. Petrov P.E. et al.: Optics Express **31**, 8335 (2023)
7. Byrns T.: arXiv:2307.00875 (2023)

Phase diagram and Kitaev-like behavior of the quasi-two-dimensional compound $Na_3Co_2SbO_6$

E. Vavilova[1], T. Vasilchikova[2], A. Vasiliev[2], D. Mikhailova[3], V. Nalbandyan[4], S. Streltsov[5]

[1]Zavoisky Physical-Technical Institute, FRC Kazan Scientific Center of RAS, Kazan, Russia
[2]Faculty of Physics. Moscow State University, Moscow, Russia
[3]Institute for Complex Materials, IFW-Dresden, Dresden, Germany
[4]Faculty of Chemistry, Southern Federal University, Rostov-on-Don, Russia
[5]Institute of Metal Physics, Ural Branch of the RAS, Ekaterinburg, Russia

The honeycomb lattice compound $Na_3Co_2SbO_6$ is a material that has been suggested to potentially realize a Kitaev quantum spin liquid ground state. We report the results of the combined study of magnetization, heat capacity and ^{23}Na nuclear magnetic resonance of the powder sample in an extended region of magnetic fields and temperatures. Complex phase diagram includes suppression of AFM order in the magnetic field and demonstrates the importance of anisotropy for switching from 2D to 3D regime. Appearance of field-induced gap behavior give evidence of the formation of a spin-liquid-like phase and possible realizing the Kitaev-Heisenberg scenario.

E.V. would like to thank financial support from the government assignment for FRC Kazan scientific Center of RAS.

Controlling the switching field of a submicron particle by means of thermally induced magnetoelastic effect

D.A. Bizyaev, A.A. Bukharaev, N.I. Nurgazizov, A.P. Chuklanov

Zavoisky Physical-Technical Institute, FRC Kazan Scientific Center of RAS, Kazan, Russia

One of the topics of modern straintronics is magnetization switching in single-domain particles by using the magnetoelastic effect. The switching (or rotation) of the magnetization in particles is usually take place by applying an external magnetic field. The magnitude of the external magnetic field, at which magnetization of particles rotates by 180°, is the Switching Field (SF). The reducing of SF is important for purposes of recording and storing information and for designing logical elements [1, 2]. As was shown in our previous studies, the SF decreasing is possible due to the thermally induced magnetoelastic effect [3].

In this work, the effect of thermally induced mechanical deformations on SF of rectangular particles was considered. The particles were 0.9×0.3×0.03 μm in size and were made form patterned Ni film that was deposited on a lithium triborate single-crystal surface (LiB_3O_5, hereinafter LBO). The particles were engraved in Ni by a tip of Scanning Probe Microscope (SPM) by scratching. The mechanical deformations in particles were induced due to sufficient differences of thermal expansion coefficients of LBO along different crystallographic axes, for the first time. The orientation of rectangular Ni particles relative to crystallographic axes was set during engraving. The engraving and Magnetic Force Microscopy (MFM) measurements were performed on SPM Ntegra. The setup allows to create constant in-plane magnetic field up to ±0.08 T for MFM and to heat sample from room temperature to 150 °C. At every MFM-measurement it was possible to observe the magnetization of 15 particles simultaneously. The Fig. 1a shows SPM image of five out of fifteen submicron Ni particles. The MFM of these particles at their initial state were shown on Fig. 2b. Each particle has a characteristic MFM-image, which corresponds to a state with a quasi-homogeneous magnetization directed along the long side of the particle. The dark region corresponds to one pole of the particle, and the light one to the other.

The goal of the work was to find such an orientation of the particles with respect to magnetic field and deformation axis, at which the maximum change of SF will be observed. And, in addition, after cooling to room temperature and decreasing external magnetic field to zero, the magnetization must rotate by 180° respect to the initial state.

The experiments in temperature range from 25 to 45 °C showed that both an increase and a decrease of SF are possible, depending on direction of thermally induced deformation axis and external magnetic field relative to the particle axes. The SF increases from 17 to 29 mT when angle between the magnetic field and the easy axis (EA, directed along long side of particle) was 20°. In this case, the deformation is directed at 90° relative to magnetic field. The SF decreases from 20 to 13 mT when the angle between the magnetic field and EA was 65° and the angle between the deformation axis (induced by heating) and EA was 25°. In the latter case the magnetization rotates by 180° relative to the initial state when the external magnetic field is turned off and

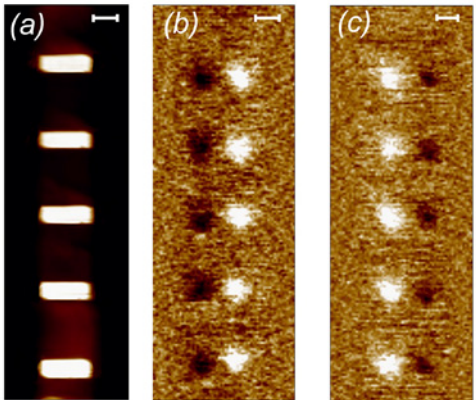

Fig. 1. The switching of magnetization in submicron Ni particles. (a) – topographic image of five particles, obtained by SPM; (b) – the initial MFM image of particles (before magnetization reversal); (c) – MFM image of the same particles after the magnetization was rotated by 180° under applying external magnetic field and the deformation. The length of the dimension bar is 500 nm.

the sample was cooled to room temperature. Figure 1c shows the MFM image of such particles after magnetization rotation. This rotation occurs because of applying external field and deformation from the substrate.

Thus, the obtained experimental results show that it is possible to control SF of submicron Ni particles deposited on LiB_3O_5 single-crystal substrate due to the thermally induced magnetoelastic effect.

The work supported by RSF (grant № 23-29-00085).

1. Kryder M.H., Gage E.C., McDaniel T.W. et al.: Proceedings of the IEEE **96**, 1810–1835 (2008)
2. Bukharaev A.A., Zvezdin A.K., Pyatakov A.P. et al.: Physics – Uspekhi **61**, 1175–1212 (2018)
3. Bizyaev D.A., Bukharaev A.A., Nurgazizov N.I. et al.: Phys. Status Solidi RRL, 2000256 (2020)

O1

Magnetic Josephson junctions for superconducting memory

V.V. Bol'ginov

Institute of Solid State Physics, RAS, Chernogolovka, Russia

The spin antagonism of superconductivity and ferromagnetism gives rise to a number of unusual phenomena of practical importance. For example, the appearance of spatially inhomogeneous superconducting states in the vicinity of the SF interface allows implementation of Josephson superconductor–ferromagnet–superconductor (SFS) junctions with a negative sign of the current–phase relation (pi-junctions) [1]. For the implementation of pi-junctions, the most convenient materials are weakly ferromagnetic alloys with cryogenic Curie temperatures, in which the low exchange energy ensures large spatial scales of the damping of superconductivity and oscillations of the superconducting order parameter [2]. It is known that lowest Curie temperatures can be obtained using alloys based on Pt and Pd with a concentration of magnetic atoms (Fe, Ni, Co) of several atomic percent or less. The use of dilute alloys of Pd with nickel and iron made it possible to realize Josephson junctions with unusual and practically important properties [3, 4].

Over the past 15 years, research has been carried out at the Institute of Solid State Physics RAS on multilayer hybrids based on superconducting niobium and a diluted PdFe alloy with a magnetic atom content of about 1% at. Josephson junctions with a magnetic memory effect suitable for use in digital superconducting electronics [5], as well as magnetic memory elements based on PdFe-Nb-PdFe layered bridge structures [6], were implemented. The report will present the results of experiments on studying the proximity effect in such structures: measuring the dependence of the critical temperature of FS bilayers and the critical current of SFS-junctions on the thickness of the PdFe layer. Difficulties arising in carrying out such experiments will be considered and estimates of the characteristic spatial scales of the superconducting order parameter in the PdFe layer will be given.

1. Golubov A.A., Kupriyanov M.Y., Il'ichev E.: Rev. Modern Phys. **76**(2), 411 (2004)
2. Kupriyanov M.Y., Golubov A.A., Siegel M.: Proc. SPIE **6260**, 62600S (2006)
3. Kontos T., Aprili M., Lesueur J., Genêt F., Stephanidis B., Boursier R.: Phys. Rev. Lett. **89**(13), 137007 (2002)
4. Larkin T.I., Bol'ginov V.V., Stolyarov V.S. et al.: Appl. Phys. Lett. **100**(22) (2012)
5. Bol'ginov V.V., Stolyarov V.S., Sobanin D.S. et al.: JETP Lett. **95**, 366–371 (2012)
6. Karelina L.N., Shuravin N.S., Bolginov V.V. et al.: JETP Lett. **116**(2), 110–116 (2022)

O2

Buzdin, Shapiro and Chimera steps in φ_0 Josephson junctions

K.V. Kulikov[1,2], M. Nashaat[1,3], E. Kovalenko[4], J. Tekić[5], Yu.M. Shukrinov[1,2,6]

[1]BLTP, JINR, Dubna, Moscow region, 141980, Russia, e-mail: kulikov@theor.jinr.ru
[2]Dubna State University, Dubna, Russia
[3]Department of Physics, Faculty of Science, Cairo University, Giza, Egypt
[4]Center for the Development of Digital Technologies, Krasnogorsk, Russia
[5]"Vinča" Institute of Nuclear Sciences, University of Belgrade, Belgrade, Serbia
[6]Moscow Institute of Physics and Technology, Dolgoprudny, Russia

The unique resonance and locking phenomena in the superconductor-ferromagnet-superconductor φ_0 Josephson junction under external electromag-netic radiation are demonstrated when not just the electric but also the magnetic component of external radiation is taken into account. Due to the coupling of superconductivity and magnetism in this system, the magnetic moment precession of the ferromagnetic layer caused by the magnetic component of external radiation can lock the Josephson oscillations, which results in the appearance of a particular type of steps in the current-voltage characteristics, completely different from the well-known Shapiro steps. We call these steps the Buzdin steps in the case when the system is driven only by the magnetic component and the Chimera steps in the case when both magnetic and electric components are present. Unlike the Shapiro steps where the magnetization remains constant along the step, here it changes though the system is locked. The spin-orbit coupling substantially contributes to the amplitude, i.e., the size of these steps. Dramatic changes in their amplitudes are also observed at frequencies near the ferromagnetic resonance. Combinations of the Josephson and Kittel ferromagnetic resonances together with different types of locking pronounced in dynamics and current-voltage characteristics make the physics of this system very interesting and open up a series of new applications.

Numerical simulations were funded by the Russian Science Foundation Project No. 22-71-10022.

Resonant properties of a SQUID consisting of two Phi-0 junctions

I.R. Rahmonov[1,2,3], **Yu.M. Shukrinov**[1,2]

[1]BLTP, Joint Institute for Nuclear Research, Dubna, Moscow Region, Russia
[2]Dubna State University, Dubna, Moscow Region, Russia
[2]Moscow Institute of Physics and Technology, Dolgoprudny, Moscow Region, Russia

The phase dynamics of a SQUID consisting of two Phi-0 junctions has been investigated [1, 2]. The current-phase relation of such junction has a phase shift proportional to the magnetic moment, perpendicular to the gradient of the asymmetric spin-orbital potential. The phase shift allows one to manipulate the internal magnetic moment using the Josephson current. The reverse phenomenon leads to the appearance of the DC component in the superconducting current [3–5].

Based on the numerical solution of the equations of the resistive model for Josephson junctions and the Landau – Lifshitz – Gilbert equations for the magnetic moment of ferromagnetic layer, the current-voltage characteristic and time dependences of the voltage and components of the magnetic moment are calculated. The double resonance in this system is observed, i.e., the simultaneous realization of ferromagnetic resonance and excitation of the SQUID eigenmode. The double resonance in the considered SQUID makes possible the detailed investigation of the resonance properties of Phi-0 junction.

The work is supported by the Russian Science Foundation in the framework of project 22-42-04408.

1. Buzdin A.: Phys. Rev. Lett. **101**, 107005 (2008)
2. Konschelle F., Buzdin A.: Phys. Rev. Lett. **102**, 017001 (2009)
3. Shukrinov Yu.M.: Phys. Usp., DOI: 10.3367/UFNe.2020.11.038894
4. Shukrinov Yu.M., Rahmonov I.R., Sengupta K.: Phys. Rev. B **99**, 224513 (2019)
5. Bobkova I.V., Bobkov A.M., Rahmonov I.R., Mazanik A.A., Sengupta K., Shukrinov Yu.M.: Phys. Rev. B **102**, 134505 (2020)

O4

Magnetism and specific heat of ludwigites

R.M. Eremina[1,2], D.V. Popov[1], T.P. Gavrilova[1], V.A. Shustov[1], M.A. Cherosov[2], E.M. Moshkina[3]

[1]Zavoisky Physical-Technical Institute, Federal Research Center "Kazan Scientific Center of RAS", Kazan, Russia, e-mail: REremina@yandex.ru
[2]Kazan (Volga Region) Federal University, Kazan, Russia
[3]Kirensky Institute of Physics, Federal Research Center KSC SB RAS, Krasnoyarsk, Russia,

Oxyborates with ludwigite-type structures (structural formula $M_2M'BO_5$, where M and M′ being the metallic ions with valence 2+ and 3+ respectively) bears extremely unusual magnetic properties, including, but not limited to random magnetic ions distribution, mixed valence, strong electronic correlations and uncommon charge ordering. These properties are caused by zigzag walls in their crystal structure formed by metal ions of different valence. Another reason is presence of four nonequivalent positions that can be occupied by up to twelve magnetic ions per unit cell. Those positions form two sublattices 3-1-3 and 4-2-4.

The aim of this work is investigation of magnetic, transport properties of $Mn_{1.17}Co_{1.83}BO_5$ and $Mn_{1.39}Co_{1.61}BO_5$. $Mn_{1.17}Co_{1.83}BO_5$ and $Mn_{1.39}Co_{1.61}BO_5$ ludwigites were synthetized by the flux technique and investigated by means of X-ray diffraction, X-ray fluorescence, DC and AC magnetic susceptibility and specific heat analysis. The crystal structure of both ludwigites belongs to the *Pbam* space group with a = 9.25 Å, b = 12.41 Å, and c = 3.05 Å for $Mn_{1.17}Co_{1.83}BO_5$ and a = 9.27 Å, b = 12.45 Å, and c = 3.05 Å for $Mn_{1.39}Co_{1.61}BO_5$. The simultaneously observed negative values of the Curie-Weiss temperatures and ferromagnetic-type hysteresis loops allow us to assume that the ferrimagnetic ordering is realized in $Mn_{1.39}Co_{1.61}BO_5$ below TPhT = 60.8 K, while in $Mn_{1.17}Co_{1.83}BO_5$ in addition to the above mentioned experimental facts the frequency dependence of the real and imaginary parts of the AC magnetization was observed assuming the presence of the canonical spin-glass state below TPhT ≈ 42.3 K. A high value exchange bias was observed in hysteresis loops for $Mn_{1.17}Co_{1.83}BO_5$.

This research was supported by the RSF (Project No. 23-72-00047).

1. Bezmaternykh L., Moshkina E., Eremin E., Molokeev M., Volkov N., Seryotkin Y.: Solid State Phenomena – Trans Tech Publications Ltd **233**, 133–136 (2015)

O5

Electron spin coherence in $CsPbBr_3$ perovskite nanocrystals at room temperature

S.R. Meliakov[1], E.A. Zhukov[1,2], V.V. Belykh[2], E.V. Kulebyakina[1], D.R. Yakovlev[1,2]

[1]P.N. Lebedev Physical Institute of the Russian Academy of Sciences, Moscow, Russia
[2]Experimentelle Physik 2, Technische Universität Dortmund, Dortmund, Germany

Lead halide perovskites have attracted big interest in recent years due to their excellent photovoltaic efficiency and optoelectrical properties. They have a lot of possible applications in different fields: solar cells, light emitting diodes and detectors. Fabrication of perovskite nanostructures further extends the possibility of their application. One of the most popular systems is inorganic $CsPbBr_3$ nanocrystals (NCs).

Spin physics is also addressed to perovskites. Hole spin dynamics have been observed in $CsPbBr_3$ NCs up to room temperature [1, 2]. However, electron spin coherence has not been demonstrated at room temperature so far. Mechanisms of spin relaxation are also poorly investigated. In the present work we investigate electron and hole spin dynamics in $CsPbBr_3$ NCs in the temperature range from 4 to 300 K.

To study spin dynamics we employ time-resolved pump-probe Faraday rotation technique (TRFR). The laser pulse is divided into two parts: circularly polarized pump pulse creates initial spin polarization in the sample and linearly polarized probe pulse, propagating with controlled delay with respect to pump pulse, experiences Faraday rotation of polarization plane by the angle proportional to projection of spin polarization onto optical axis.

Hole or electron spin, placed in the magnetic field **B**, precesses around the magnetic field with Larmor frequency which is determined by the equation $\omega_L = g\mu_B B/\hbar$, where g is the carrier g-factor and μ_B is the Bohr magneton. The loss of the spin precession coherence occurs in time T_2^* (inhomogeneous ensemble spin dephasing time). At room temperature we observe spin precession in the Voigt magnetic field of 400 T, analysis of this signal yields $g_e = 1.68$ and $T_{2,e}^* = 50$ ps. At the temperature of about 50 K and below, an oscillating component with lower Larmor frequency appears. This Larmor frequency gives g-factor $g_h = 0.44$, which corresponds to hole [1]. Evaluation of TRFR traces at helium temperatures also yields $g_e = 1.47$, which we assign to electrons. Thus, we observe electron spin coherence at temperatures from 4 to 300 K. Also, temperature dependence of the electron g-factor is worth highlighting. In Ref. [1] it was shown theoretically and experimentally, that the electron g-factor in perovskites should have inverse dependence on the band gap. However, we observe an increase of the electron g-factor with temperature simultaneously with a growth of the band gap. This work was supported by the Ministry of Science and Higher Education of the Russian Federation (Contract No. 075-15-2021-598 at the P. N. Lebedev Physical Institute).

1. Crane V. et al.: Nano Lett. **20**, 8626–8633 (2020)
2. Lin X. et al.: Nat. Nanotechnol. **18**, 124 (2022)
3. Kirstein E. et al.: Nat. Commun. **13**, 3062 (2022)

O6

Submillimeter optical properties of $Fe_2Mo_3O_8$ antiferromagnet in magnetic fields

K.V. Vasin[1,2], A.R. Nurmukhametov[1], A. Strinic[2], L. Prodan[2], V. Tsurkan[2,3], I. Kézsmárki[2], M.V. Eremin[1], J. Deisenhofer[2]

[1]Institute of Physics, Kazan (Volga region) Federal University, Kazan, Russia
[2]Institute of Physics, Augsburg University, Augsburg, Germany
[3]Institute of Applied Physics, MD-2028 Chisinau, Republic of Moldova

We reinvestigated the optical excitations of $Fe_2Mo_3O_8$ in the THz regime in an external magnetic field [1] for new features and develop a microscopic model that reproduces most properties in THz and MIR range. The material $Fe_2Mo_3O_8$ belongs to the family of polar molybdenum oxides, which has recently come into the focus of research, as different magnetically ordered ground states can be formed and tuned by external magnetic fields [2–8]. Fe^{2+} ions occupy corner-sharing tetrahedral (A) and octahedral (B) sites and are responsible for the magnetism [3, 9, 10]. The focus here is on pairs of 2 magnetic domains from A & B sublattices (see Fig. 1), which are ferrimagnetically ordered in each layer along the *c*-axis. However, the total magnetic moment of

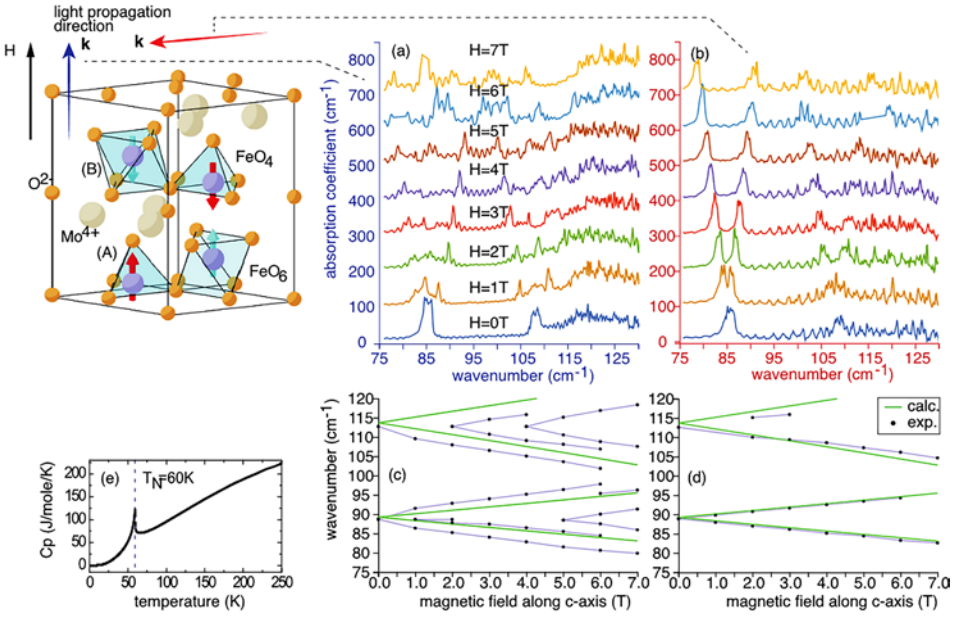

Fig. 1. Crystallographic structure of $Fe_2Mo_3O_8$ (top-left). (a) field dependency of the THz absorption spectra, when the incident light (**k**) is along the *c*-axis (blue), while static magnetic field is applied as **H**||*c*; (b) when **k** is perpendicular to *c*-axis (red); (c) extracted frequencies of the observed modes (black dots) as a function of field *H* and calculated splitting (green lines); (d) the same as (c), but **k** is perpendicular to *c*-axis; (e) measured heat-capacity with an transition to magnetically-ordered state at 60 K.

individual layer is directed opposite to each other, that in the unit-cell effectively shows antiferromagnetic behavior.

Single crystals were grown by the chemical transport reaction method in Augsburg University. The samples were characterized by specific heat (shown in Fig. 1e) and magnetic susceptibility measurements, which clearly show the antiferromagnetic transition at $T_N = 60$ K in agreement with previous results [2, 3].

Observed modes shown on panel (a, b) are both electric and magnetic dipole active and appears below T_N. We describe the observed optical excitations using an single ion approach and a mean-field approximation method. In Figs. 1c and d we show the magnetic field dependence of the eigen energies for two different orientations of the incident light (**k**-vector) with respect to the crystallographic axes. Modes exhibit a V-shaped splitting in magnetic field, yielding effective g-factors of 2 and 2.6 for $\mathbf{k} \perp c$ (see Figs. 1b, d). We believe that this behavior comes from the Zeeman's shift of A and B pairs of domains, since the applied field breaks the symmetry and the up- and down-domains become distinguishable. Our model perfectly fits the results obtained for that case. However when $\mathbf{k} \| c$ (Figs. 1a, c) observed effective g-factors are noticeably larger – 2.35, 3.15 and unknown fan-like features shows up – Fig. 1a. This is very unusual, keeping in mind that the frequency of the mode was expected to be independed with respect to the direction a probing light polarization. Moreover, for the case $\mathbf{k} \| c$ a thickness dependency of g-factors was observed.

The work of K.V., A.N. and M.E. were supported by RNF Grant №. 19-12-00244.

1. Kurumaji T., Takahashi Y. et al.: Phys. Rev. B 95, 020405(R) (2017)
2. Kurumaji T., Ishiwata S., Tokura Y. : Phys. Rev. X 5, 031034 (2015)
3. Wang Y., Pascut G.L. et al.: Sci. Rep. 5, 12268 (2015)
4. Kurumaji T., Ishiwata S., Tokura Y.: Phys. Rev. B 95, 045142 (2017)
5. Tang Y.S., Wang S.M. et al.: Phys. Rev. B 100, 134112 (2019)
6. Csizi B., Reschke S. et al.: Phys. Rev. B 102, 174407 (2020)
7. Tang Y.S., Zhang J.H. et al.: Phys. Rev. B 103, 014112 (2021)
8. Tang Y.S., Zhou G.Z. et al.: Phys. Rev. B 105, 064108 (2022)
9. Varret F., Czeskleba H. et al.: J. Phys. 33, 549 (1972)
10. Cotton F.A.: Inorg. Chem. **3**, 1217 (1964)

Magnetic properties and topology of band structure of rare-earth antimonides

A.V. Lukoyanov[1,2], S.T. Baidak[1,2], Yu.V. Knyazev[1], Yu.I. Kuz'min[1]

[1]M.N. Mikheev Institute of Metal Physics UrB RAS, Ekaterinburg, Russia
[2]Ural Federal University, Ekaterinburg, Russia

Binary and related compounds based on gadolinium (Gd) and antimony (Sb) were found to demonstrate a variety of semimetallic, half-metallic, semiconducting, or metallic properties, as well as topological features in some of them [1] which can be used for spintronic and microelectronic applications. Theoretical band structure and magnetic properties of the binary rare-earth antimonides (Gd, Tb, Dy)Sb were theoretically calculated in this work. First-principles calculations were done within the GGA+U(+SO) method to obtain and analyze the spin-polarized band structure. Strong electron correlations in the 4f shell of rare-earth metals were accounted for in this method. The effect of spin-orbit coupling on the electronic structure was considered. The total magnetic moment of the considered semimetals is determined by magnetic moments of the rare-earth ions, and the calculated effective magnetic moments were compared to the published experimental values for all compounds. The optical conductivity contribution caused by interband transitions was also calculated and used to interpret the energy dependency of experimental optical conductivity spectra obtained by spectroscopic ellipsometry in [2]. In GdSb, TbSb, and DySb, the electron-hole compensated semimetallic states are found to have similar electronic structures and small pseudogaps in the densities of electronic states. The asymmetric electron pocket in the Γ–X–W direction and symmetric hole pockets in the L–Γ–X direction were found being in good agreement with the previous experimental spectral results. The results are published in [2, 3]. This work was supported by the grant of Russian Science Foundation No 22-42-02021.

1. Baidak S.T., Lukoyanov A.V.: Int. J. Mol. Sci. **24**, 8778 (2023)
2. Knyazev Yu.V., Kuzmin Yu.I., Baidak S.T., Lukoyanov A.V.: Solid State Sci. **136**, 107085 (2023)
3. Baidak S.T., Lukoyanov A.V.: Mater. **16**, 242 (2023)

O8

Metallization under pressure in GdNiSb semiconductor

R.D. Mukhachev[1], S.T. Baidak[1,2], A.V. Lukoyanov[1,2]

[1]M.N. Mikheev Institute of Metal Physics UrB RAS, Ekaterinburg, Russia
[2]Ural Federal University, Ekaterinburg, Russia

Gadolinium-based ternary GdTX compounds with *T* standing for a transition metal and X as Si, Al, Ge or Sb, are being investigated due to a variety of interesting properties for efficient, reliable, and environmentally safe spintronic, magnetocaloric, thermoelectric applications [1]. In this work, we report the theoretical results for the electronic structure of GdNiSb at ambient conditions and for the contracted cell volumes corresponding to applied pressure. At ambient conditions, GdNiSb is found to be a narrow gap semiconductor with the indirect band gap equal to 0.38 eV which is close to the gap values reported the other RNiSb compounds [2]. Our calculations for GdNiSb under pressure by reducing its cell volume revealed the broadening of the occupied bands. The band structure changes resulted in a change of the indirect gap along the Γ–X direction into a direct gap at the high-symmetry X point. At $0.65V_0$, where V_0 is the volume of the cell under ambient condition, the band gap is finally closed, the band structure of GdNiSb at this particular volume illustrates the case of (spin) gapless semiconductor with the occupied and empty bands touching exactly at the X point. The band broadening for the smaller volumes led to the closure of the gap at the Fermi energy and increased metallization to some extent with the appearance of Fermi surfaces. At $0.6V_0$, the appearance of a single band crossing along the Γ–X direction was observed, which can be regarded as a Dirac point. Therefore, our theoretical calculations demonstrate a pressure-induced transition from a narrow gap semiconductor to a metal with non-trivial topological states in GdNiSb. This study was supported by the grant of Russian Science Foundation No 22-42-02021.

1. Kuchin A.G., Platonov S.P., Mukhachev R.D., Lukoyanov A.V., Volegov A.S., Gaviko V.S., Yakovleva M.Yu.: Phys. Chem. Chem. Phys. **25**, 15508 (2023)
2. Baidak S.T., Lukoyanov A.V.: Mater. **16**, 242 (2023)

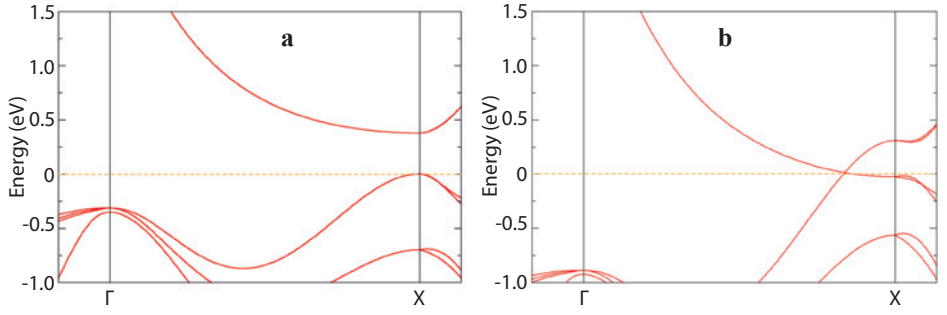

Fig. 1. Band structure of GdNiSb calculated for 0.7 (**a**) and 0.6 of the ambient condition volume V_0 (**b**). The dashed lines indicate the Fermi energy at zero.

Interplay of ferromagnetism and nontrivial topology in triple layers Te-Mn-Te of $MnBi_2Te_4$

V.V. Val'kov, A.O. Zlotnikov, A. Gamov

Kirensky Institute of Physics, FRC Krasnoyarsk Science Center of SB RAS, Krasnoyarsk, Russia

Considering the structure of triple layers Te-Mn-Te, as a part of septuple layers Te-Bi-Te-Mn-Te-Bi-Te of the van der Waals single crystal $MnBi_2Te_4$ [1, 2], the effects of the crystal field, spin-orbit interaction, and covalent mixing between $3d$ orbitals of Mn^{2+} ions and $5p$ orbitals of Te^{2-} ions are studied. We propose the effective tight-binding model with strong electron correlations between d electrons and analyze the topology of the Fermi excitation spectrum in the ferromagnetic state.

In the framework of the formalism of the Zubarev Green's functions and Zwanzig-Mori projection technique the system of equations is obtained in the form

$$\left(\omega - \hat{M}_{k\sigma}\right)\hat{D}_{k\sigma}(\omega) = \hat{P}_{\sigma} ,$$

where $\hat{D}_{k\sigma}$ is the Fourier transform of the matrix Green's function formed by the three-component field operator of p- and d-electrons, $\hat{P}_{k\sigma}$ is the diagonal matrix with elements $(1, N_{0\sigma}, 1)$, and

$$\hat{M}_{k\sigma} = \begin{pmatrix} \varepsilon_{pk\sigma} & -t^{*}_{1k\sigma} & -t_{12k} \\ -N_{0\sigma}t_{1k\sigma} & \varepsilon_{dk\sigma} & -N_{0\sigma}t_{2k\sigma} \\ -t^{*}_{12k} & -t^{*}_{2k\sigma} & \varepsilon_{pk\sigma} \end{pmatrix}.$$

Here $N_{0\sigma} = 1 - n_d/2 + 2\sigma M$ with concentration n_d and magnetization M of d-electrons, $\varepsilon_{pk\sigma}$ and $\varepsilon_{dk\sigma}$ are the bare energies of p- and d-electrons, respectively, renormalized by

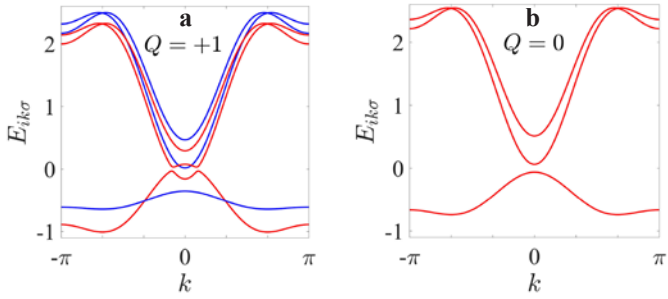

Fig. 1. Fermi excitation spectrum for two phases: **a** unsaturated ferromagnetic phase (red and blue lines correspond to the spin-splitted energy branches); **b** paramagnetic phase with the energy branches which are degenerated with respect to spin projection. In both cases chemical potential is in a gap at zero energy. The Chern number Q is nontrivial ($Q = 1$) in the presence of ferromagnetism and trivial ($Q = 0$) for paramagnetic state.

the p-d exchange interaction and kinematic interaction of Hubbard fermions [3]. The p-d hybridization is described by the functions $t_{1k\sigma}$ and $t_{2k\sigma}$, and t_{12k} is the hopping integral of p-electrons between different Te-layers.

It is crucial that $t_{1k\sigma}$ and $t_{2k\sigma}$ are complex functions depending on spin index. Therefore, nontrivial topology of the energy structure can exist when d- and p-bands are overlapped and long-range magnetic ordering is realized. It is shown that the Chern number Q of the lower filled band has the value +1 in the ferromagnetic phase which is caused by the kinematic interaction. This corresponds to the nontrivial topology of the energy structure of triple layers Te-Mn-Te in $MnBi_2Te_4$. On the contrary, the Chern number is zero and the topology is trivial in the paramagnetic phase.

The reported study was supported by Russian Science Foundation Project No. 23-22-10021 (https://rscf.ru/project/23-22-10021/), and Krasnoyarsk Regional Fund of Science.

1. Otrokov M.M., Klimovskikh I.I., Bentmann H. et al.: Nature **576**, 416–422 (2019)
2. Shikin A.M., Estyunin D.A., Glazkova D.A. et al.: JETP Lett. **115**, 213–225 (2022)
3. Zaitsev R.O.: JETP **96**, 286–300 (2003)
4. Val'kov V.V., Zlotnikov A.O., Gamov A.: JETP Lett. **118**, No. 5 (2023)

O10

Rotation of a magnetic spiral by a spin-polarized current: Slonchevskii's windmill in multilayer structures

A.A. Fraerman

Institute for physics of microstructures RAS, Nizhny Novgorod, Russia

The paper theoretically investigates the coherent rotation of the helical distribution of magnetization under the action of a spin-polarized current, which is known as the Slonchevskii windmill. In contrast to previous works, a magnetic spiral of an exchange nature is considered, which arises as a result of the frustration of interactions between the nearest and next-to-nearest neighbors. It is found that the rotation frequency is proportional to the magnitude of the current, its direction, and the sign of the chirality of the helix. The considered spiral is realized in a system of single-domain ferromagnetic particles due to the magnetostatic interaction between them [1–3]. The frequency of rotation in the simplest case of three ferromagnetic nanoparticles is found and an estimate of the maximum value of the current that can lead to rotation is given (Fig. 1). This work was supported by the Russian Science Foundation grant no. 21-12-00271.

1. Vdovichev S.N. et al. Pis'ma Zh. Eksp. Teor. Fiz. **94**, 418 (2011) [JETP Lett. **94**, 386 (2011)]
2. Mukhamatchin K.R., Fraerman A.A.: Pis'ma Zh. Eksp. Teor. Fiz. **93**, 797 (2011) [JETP Lett. **93**, 716 (2011)]
3. Fraerman A.A. et al.: J. Appl. Phys. **103**, 073916 (2008)

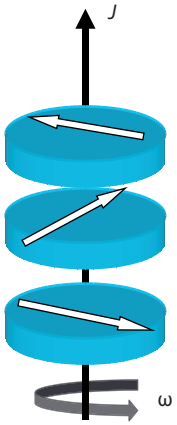

Fig. 1. Magnetic spiral in a system of three single-domain ferromagnetic particles. The spiral is formed as a result of magnetostatic interaction between nearest and farthest particles. It is assumed that particles separated by non-magnetic conductive layers. Then the flow electric current *Jw* leads to the rotation of the magnetic spiral with a frequency ω.

O11

Microscopic theory of Dirac cones splitting in HgTe quantum wells

G.V. Budkin, M.V. Durnev, S.A. Tarasenko

Ioffe Institute, Saint-Petersburg, Russia

Quantum wells based on HgTe are at the forefront of current research due to their outstanding characteristics. Different phases, such as two-dimensional topological insulators, two-dimensional gapless semiconductors, and two-dimensional semiconductors, are implemented depending on the quantum well thickness. The gapless phase with linear spectrum of Dirac fermions that is realized in HgTe quantum wells of critical thickness is of particular interest.

We report on the theoretical study of the the fine structure of Dirac states in HgTe/CdHgTe quantum wells with critical and near-critical thicknesses. We show that the bulk inversion asymmetry caused by the absence of an inversion center in the zinc-blende-type lattice, the interface inversion asymmetry brought on by the anisotropy of chemical bonds at the quantum well interfaces, and the structural inversion asymmetry lifts the spin degeneracy of the Dirac states even at zero wave vector and leads to anticrossing of energy levels.

A microscopic theory of fine structure has been developed for (0*lh*)-oriented HgTe/CdHgTe quantum wells, where *l* and *h* are Miller indices, and an effective Hamiltonian describing the spin splitting of Dirac states has been derived. We demonstrate that effective Hamiltonian contains four parameters which determine spin splitting of the energy spectrum. The energy dispersion of charge carriers was numerically calculated within the framework of the 6-band extended Kane model taking into account the absence of an inversion center and the cubic shape of the crystal lattice, elastic strain in the quantum well, and mixing of the states of light and heavy holes at the interfaces of the quantum well [1]. These calculations made it possible to obtain the parameters of the effective Hamiltonian describing the spin splitting of the spectrum. The spectrum in (0*lh*)-oriented wells has been shown to depend significantly on the crystallographic orientation of the quantum well and the interplay of interface and bulk inversion asymmetry with structure inversion asymmetry, it is generally anisotropic and contains four Weyl points. Analytical expressions are obtained for the energy spectrum of Dirac states as a function of growth directions, and the evolution of the fine structure upon change from the (001) well to the (013) and (011) wells is studied.

This work was supported by the Russian Science Foundation (project 22-12-00211).

1. Durnev M.V., Budkin G.V., Tarasenko S.A.: JETP **135**, 540–548 (2022)

O12

Time-frustrated state of matter

V.E. Valiulin[1,2], A.V. Mikheenkov[1,2], N.M. Chtchelkatchev[1], V.M. Vinokur[3]

[1]Institute for High Pressure Physics, RAS, Troitsk, Moscow, Russia
[2]Moscow Institute of Physics and Technology, Dolgoprudny, Russia
[3]Terra Quantum AG, Rorschach, Switzerland

The exchange interaction is of the quantum mechanical origin and stems from the intertwined effect of the Coulomb interaction and Pauli exclusion principle governing the behavior of indistinguishable fermions with overlapping wave functions. Remarkably, a rich lore narrating how the geometric frustration developing from the exchange effects leads to degeneracies and the emergent frustrated state of matter, neglects the temporal component: local magnetic moments are supposed to instantly interact with each other without delays [1, 2]. However, the flip of electron spin in an atom in a crystal implies a rearrangement of electron density distribution in space, which, in turn, affects the strength of interactions between the atom with its neighbors. The rearrangement of electron clouds occurs at optical frequencies (~500 THz) and so with characteristic time scales ~0.01 ps − 0.1 ps, while the relaxation of the atomic position caused by the spin flip occurs at phonon frequencies (~1 THz) and so picosecond time scales [3]. As a result, the system's temporal evolution is essentially non-Markovian. There are many new functional materials, such as granular multiferroics [4, 5], in which the interaction is not direct but is mediated by an active dielectric or ferroelectric medium. In such materials [6], the time-delay effects are relatively large and should be considered. The superexchange interaction of magnetic moments in granular multiferroic, where electric and magnetic degrees of freedom mutually influence each other, acquires retardation as well. We address a granular multiferroic with time-delayed exchange interaction of magnetic granules in the framework of the quasiclassical Landau-Lifshitz equation. The solution of this equation was considered from analytical and numerical perspective. As the result, we present, that an array of nanomagnets coupled by the real retarded exchange interactions develops a new state of matter, time frustrated matter. The emerging competition between different magnetic orders leads to a new kind of time-core frustration.

1. Balents L.: Nat. **29**, 464 (2010)
2. Kassan-Ogly A.: Phys. Solid State **60**, 1090–1097 (2018)
3. Manipatruni S.: Nat. **565**, 35–42 (2019)
4. Spaldin N., Ramesh R.: Nat. Mater. **18**, 203–212 (2019)
5. Spaldin N.: Nat. Rev. Mater. **2**, 17017 (2017)
6. Dong S., Liu J., Cheong S., Ren Z.: Adv. Phys. **64**, 519–626 (2015)

O13

High spin polarization in full Heusler alloys Mn_2YAl for late 3d transition metals

E.D. Chernov[1], A.V. Lukoyanov[1,2]

[1]M.N. Mikheev Institute of Metal Physics of Ural Branch of Russian Academy of Sciences, Ekaterinburg, Russia
[2]Ural Federal University, Ekaterinburg, Russia

The full Heusler alloys are of great interest because of their unique electronic, magnetic, and multifunctional properties [1] useful for spintronic devices [2]. In particular, the alloys Mn_2YZ with Y – 3d metals and Z – elements of III–V groups, attract the attention of researchers as materials promising for magnetoelectronic and thermoelectric applications [3]. In this work we present the results of first–principles calculations of the electronic structure and magnetic properties of the full Heusler alloys Mn_2YAl for late 3d transition metals Y = Fe, Co, Ni within the framework of GGA(+U) theoretical approaches. These full Heusler alloys were calculated in the reported cubic XA-type crystal structure, in which the alloys under study were found to have a ferro or compensated ferrimagnetic ordering [4]. The electronic structure of Mn_2FeAl and Mn_2CoAl exhibits half-metallic properties. And the electronic structure of Mn_2NiAl is metallic in both spin projections in all computational methods. The total magnetic moment of Mn_2FeAl and Mn_2CoAl is 1.01 and 2.0 Bohr magnetons, respectively, in good agreement with the previous theoretical works [5, 6]. In contrast, the GGA+U calculated total magnetic moment of Mn_2NiAl is about 0.2 Bohr magnetons and agrees well with the results of magnetic measurements [4]. In our calculations, Mn_2FeAl and Mn_2CoAl were found to have the spin polarization as high as 100%, and Mn_2NiAl up to 80%. Thus, the Heusler alloys Mn_2FeAl and Mn_2CoAl are characterized by the half-metallic electronic structure with the maximum spin polarization and have a potential for practical applications.

The state assignment of Minobrnauki of the Russian Federation via theme “Electron” No. 122021000039-4 is acknowledged.

1. Tavares S., Yang K., Meyers M.A.: Prog. Mater. Sci. **132**, 101017 (2023)
2. Elphick K., Frost W., Samiepour M., Kubota T., Takanashi K., Sukegawa H., Mitani S., Hirohata A.: Sci. Technol. Adv. Mater. **22**, 235 (2021)
3. Felser C., Wollmann L., Chadov S., Fecher G.H., Parkin S.S.P.: APL Mater. **3**, 041518 (2015)
4. Marchenkov V.V., Irkhin V.Y., Perevozchikova Y.A., Terent’ev P.B., Semiannikova A.A., Marchenkova E.B., Eisterer M.: JETP **155**, 1083 (2019)
5. Wollmann L., Chadov S., Kübler J., Felser C.: Phys. Rev. B **90**, 214420 (2014)
6. Luo H., Zhu Z., Ma L., Xu S., Zhu X., Jiang C., Xu H., Wu G.: J. Phys. D **41**, 055010 (2008)

O14

Mechanisms of magnetoresistance of the $Bi_{1.1-x}Sn_xSb_{0.9}Te_2S$ topological insulator studied by transport measurements

T.N. Enderova[1,2], V.O. Sakhin[1], Yu.I. Talanov[1]

[1]Zavoisky Physical-Technical Institute, FRC Kazan Scientific Center of RAS, Kazan, Russia
[2]Institute of Physics, Kazan Federal University, Kazan, Russia

Topological insulators (TI) are remarkable novel quantum materials. The surface charge carriers of TI are Dirac fermions with linear dispersion law, hence those carriers are massless and have high mobility. Moreover, surface charge carriers are protected against scattering by non-magnetic impurities owing to time-reversal symmetry and they are characterized by so-called spin-momentum locking, that is rigid bond between the directions of spin and momentum. These peculiar properties make TI promising materials for practical quantum electronics and spintronics devices [1, 2]. It provides numerous ways to manipulate spin or charge state of TI surface via application of magnetic and electric fields due to spin-momentum locking. Therefore, it is crucial to study influence of magnetic field on transport properties of TI.

In this work we used four-probe DC measurements to study temperature and magnetic field dependences of resistance of 3D TI $Bi_{1.1-x}Sn_xSb_{0.9}Te_2S$ (BSSTS). The parent compound, bismuth telluride Bi_2Te_3, has high concentration of current carriers in bulk. High bulk conductivity obscures surface contribution to transport of TI. For this reason, it was suggested to improve compound by introducing Sb, S and Sn dopants [3]. This has proven to effective way to suppress bulk conductivity at low temperatures [4]. It was shown that BSSTS has strong response to applied magnetic field, which in particular includes a weak-antilocalization effect in low magnetic fields. However, more thorough study of various observed phenomena has to be done. Single crystals of BSSTS with Sn concentration $x = 0.02$ and 0.04 were synthesized in the Zavoisky Physical-Technical Institute.

In a low magnetic field ($H < 600$ Oe) the impact of quantum interference on conductivity was detected. This quantum effect corresponds to the case of weak antilocalization, which originates from destructive quantum interference of closed scattering paths of current carriers with strong spin-orbit coupling. Analysis of the magnetoresistance data allowed us to estimate the phase coherence lengths l_ϕ for both samples with Sn content $x = 0.02$ and 0.04. In our samples the l_ϕ magnitude is larger than that of similar bismuth chalcogenide compounds. For crystal with $x = 0.04$ the temperature dependence of l_ϕ value was obtained in wide temperature range (1.5 ÷ 70 K).

Magnetic field destroys fastly the quantum interference, however a positive magnetoresistance continues to be observed in higher magnetic fields. To investigate underlying mechanism of this effect we obtained temperature dependences of resistance with various applied magnetic field. If applied field is relatively high ($H = 5$ kOe) $R(T)$ exhibits activation behavior for both samples. Usually such behavior is associated with gap in energy spectrum. We estimated value of activation energy for samples with different Sn content: E_a equals 60 μeV for $Bi_{1.08}Sn_{0.02}Sb_{0.9}Te_2S$ and 2 meV for $Bi_{1.06}Sn_{0.04}Sb_{0.9}Te_2S$ at $H = 5$ kOe. In magnetic compounds of TI an energy gap emerges in the region close

to the Dirac cone due to magnetic moments [5, 6], but in non-magnetic TI such gap arises under the influence of an external magnetic field. This property of BSSTS can be used to create a topological transistor, where the current flow will be controlled by transferring the topological materials from the conductive state to the non-conductive one through switching on a magnetic field.

The authors acknowledge the financial support from the government assignment for FRC Kazan Scientific Center of RAS.

1. Hsieh D., Xia Y. et al.: Science. **323**, 919–922 (2009)
2. Hasan M.Z., Kane C.L.: RMP. **82**, 3045–3067 (2010)
3. Kushwaha S.K., Pletikosić I. et al.: Nat Commun. **7**, 11456 (2016)
4. Enderova T.N. Sakhin V.O. et al: Memoirs of the Faculty of Physics, Lomonosov Moscow State University. **4**, 2241301 (2022)
5. Yano R., Kudriashov A. et al.: J. Phys. Chem. Lett. **12**, 4180–4186 (2021)
6. Shikin A.M.: Fizika Tverdogo Tela **62**, 8, 1293–1301 (2020) (in Rusian)

O15

Oxygen defects in titanium dioxide crystals. EPR study

A.A. Sukhanov, V.F. Valeev, V.I. Nuzhdin, R.I. Khaibullin

Zavoisky Physical-Technical Institute, FRC Kazan Scientific Center of RAS, Kazan, Russia

Titanium dioxide (TiO_2) is a wide-band-gap oxide semiconductor with many applications ranging, for example, from solar energy conversion and heterogeneous catalysis through the memristor effect to non-volatile random-access memory. Although TiO_2 has been extensively studied, a detailed understanding of the role of point defects in controlling its magnetic, optical and electrical properties still exists [1, 2]. In the given work we have been irradiated single crystalline TiO_2 rutile plate by 40 keV Ar^+ ions at high dose level to modify the magnetic and electrical properties of this oxide material for magnetoelectronic applications. However, the success of the modification requires a complete understanding of the fundamental characteristics of donors and acceptors in TiO_2, including their electronic structure. The electron paramagnetic resonance (EPR) method is well suited for studying point defects in bulk crystals [3, 4]. The information obtained from the bulk crystal can then be used to interpret data observed in various thin-film TiO_2-based electronic devices.

A new paramagnetic center associated with Ti^{3+} ions was recently found in TiO_2 rutile crystal heavily irradiated with argon (Ar) ions [5]. The principal values of the g-tensor and the directions of the principal axes of the g-tensor of this center have not been reported before. In work [5] we proposed a structural model of this center, in which paramagnetic Ti^{3+} ions occupy lattice sites surrounded by an octahedron of six oxygen anions. The high concentration of positively charged oxygen vacancies found in Ar-ion irradiated TiO_2 ensures thermodynamic stability of these Ti^{3+} ions in the rutile lattice due to nonlocal charge compensation. It should be noted that photoexcitation by longer wavelength light in the range of 450-840 nm has no any effect on this center in Ar-ion irradiated TiO_2.

In the present work, we study in details an influence of photoexcitation on EPR-spectra of TiO_2 rutile heavily irradiated with Ar ions. Figure 1 shows an evolution of EPR-spectrum in Ar-ion irradiated TiO_2 crystalline plate under the action of light with two wavelengths of 410 nm and 480 nm, respectively.

A preliminary analysis of the temperature and angular dependences of the spectra presented in Fig. 1 let ones conclude that the observed signals (Fig. 1) can be attributed:

to oxygen vacancies (V_O^+) with $S = 1/2$, which appears under photoexcitation with 410 nm wavelength only;

to $[Ti^{3+}\text{-}V_O]^+$ pair with $S = 1/2$ (center D1), which appears under photoexcitation with 480 nm wavelength;

to ($Ti^{3+}\text{-}V_O^{++}\text{-}Ti^{3+}$) complex with $S = 1$ (center D2), which appears under photoexcitation with both wavelength of 410 and 480 nm;

to Ti^{3+} center with $S = 1/2$, which concentration does not depends on any photoexcitation [5].

It was noted that EPR-signal of V_O^+ disappears after light switch off and ones has not angular dependence in contrast for other centers. On the back side, EPR-signals

O15

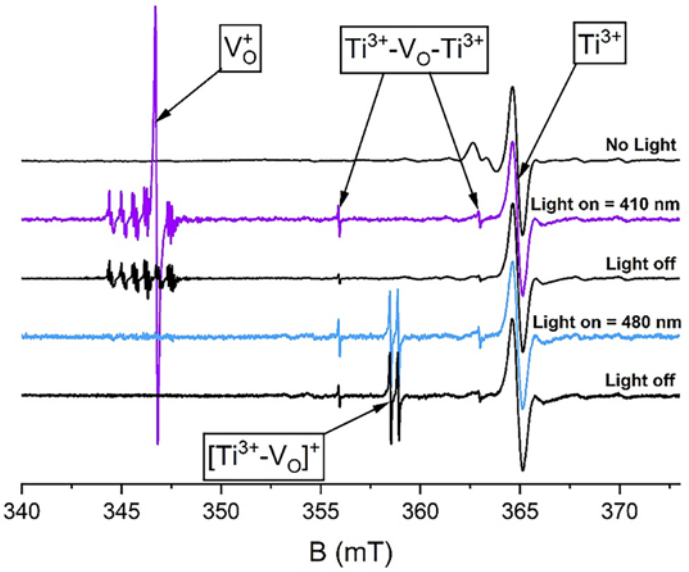

Fig. 1. EPR-spectrum evolution in Ar-ion irradiated TiO_2 crystalline plate under the action of light with different wavelengths. The EPR-spectra have been taken at temperature of 30 K for the magnetic field **B** directed parallel to the [100] axis of TiO_2.

of $[Ti^{3+}$-$V_O]^+$ and (Ti^{3+}-$V_O{}^{++}$-Ti^{3+}) complexes are observed for a considerable time at the temperatures below 30 K.

The study was supported by the Russian Science Foundation (project number 22-19-00712, https://rscf.ru/project/22-19-00712/).

1. Nowotny M.K., Sheppard L.R., Bak T., Nowotny J.: J. Phys. Chem. C **112**, 5275 (2008)
2. Kuznetsov V.N., Serpone N.: J. Phys. Chem. B **110**, 25203 (2006)
3. Al'tshuler S.A., Kozyrev B.M.: Electron Paramagnetic Resonance in Compounds of Transition Elements Moscow: Nauka, 1972. [in Russian]
4. Spaeth J.-M., Niklas J.R., and Bartram R.H.: Structural Analysis of Point Defects in Solids: An Introduction to Multiple Magnetic Resonance Spectroscopy. Berlin, Heidelberg: Springer, 1992.
5. Sukhanov A.A., Valeev V.F., Nuzhdin V.I., Khaibullin R.I.: Magn. Reson. Solids **25**, 23102 (2023)

O16

Kinetics of exciton optical alignment and optical orientation effects in an ensemble of colloidal CdSe/CdS nanoplatelets

O.O. Smirnova, N.V. Kozyrev, S.V. Nekrasov, A.V. Rodina

Ioffe Institute, Saint-Petersburg, Russia

The ensemble of colloidal core-shell CdSe/CdS nanoplatelets (NPLs) allowed the observation of the effects of optical alignment and optical orientation of excitons via the resonant continuous-wave (cw) polarized excitation and detection of the photoluminescence (PL) [1]. By the analysis of the effects dependences on Faraday magnetic field, we have determined the relationships between exciton energy splitting in zero magnetic field, exciton g-factors, exciton relaxation times, and spin lifetimes. However, the analysis of the effects in the cw-regime does not allow the determination of these parameters separately and further experimental and theoretical investigation of time-dependent kinetics of the effects is required.

In this work, we present a theory for the kinetics of the exciton optical alignment and optical orientation in Faraday magnetic field for an ensemble of randomly oriented colloidal CdSe/CdS nanoplatelets with a slight in-plane anisotropy. To describe the studied effects on the timescale of a few nanoseconds as they manifest themselves in the experiment, we consider a pair of bright exciton levels in terms of a pseudospin 1/2. The pseudospin is rotating in the effective magnetic field which accounts for the in-plane anisotropic splitting [2] and external Faraday magnetic field. Its direction distinguishes between longitudinal and transverse spin relaxation in a single NPL. The pseudospin component perpendicular to the effective field provides an oscillating and exponentially decreasing contribution to the kinetics of the effects of optical alignment, optical orientation, and rotation of the linear polarization plane. The non-oscillating exponentially decreasing longitudinal component in zero external magnetic field only contributes to the exciton optical alignment. In an external Faraday magnetic field, longitudinal component contribution to the optical alignment decreases, while to the optical orientation appears and increases.

For the modeling of the experimental kinetics, we perform averaging over the NPLs random in-plane orientation on the substrate, that is typical for the ensemble of colloidal NPLs. In the experiment, the oscillations of the polarization from the NPL ensemble are weakly pronounced. Their damping may be caused by the anisotropy of the spin relaxation time in single NPLs with the exciton dephasing being faster than the longitudinal spin relaxation, or by the dispersion of the parameters (anisotropic splitting and exciton g-factor) in the ensemble. We consider the influence of the ensemble inhomogeneity on the effects kinetics in external magnetic field for different sets of the exciton parameters within the ranges we have determined in [1]. An example for the inhomogeneity influence on the optical alignment and optical orientation effects

O16

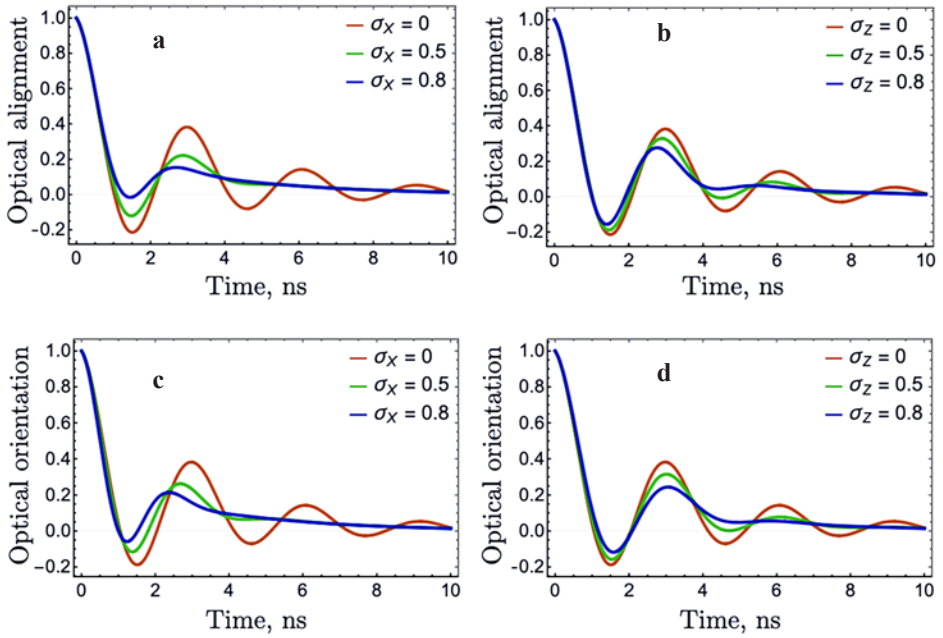

Fig. 1. Theoretical curves of normalized kinetics of the optical alignment and optical orientation effects in Faraday magnetic field of 3 T in the case of the ensemble inhomogeneity of the bright exciton parameters: **a**, **c** anisotropic energy splitting or **b**, **d** exciton g-factor. The Gaussian functions are used to describe the normal distribution of the parameters with the standard deviation 0 (orange curves), 0.5 (green curves) and 0.8 (blue curves). Curves are plotted for a set of the parameters from [1] with bright exciton spin lifetime $T_A = 0.7$ ns.

for a parameter set from [1] with the bright exciton spin lifetime $T_A = 0.7$ ns is shown in Fig. 1. Future analysis of the magnetic field dependences of the time-dependent and time-integrated PL polarizations under polarized pulsed excitation will allow us to determine the exciton spin relaxation and spin dephasing times in the ensemble.

The work is supported by the Russian Science Foundation grant № 23-12-00300

1. Smirnova O.O. et al.: Nanomaterials (2023); Smirnova O.O. et al.: arXiv:2212.06134 (2022)
2. Hu Zh. et al.: Nanoscale **10**, 22861–22870 (2018)

Po1

Ground state magnetic structure, spin dynamics and hyperfine interactions in ternary Fe-Al-B alloys

A.F. Abdullin, E.V. Voronina, E.N. Dulov

Kazan Federal University, Kazan, Russia

Ternary ordered Fe-Al-B alloys based on iron aluminides in a concentration range of Al $x_{Al} > 30$ at.% are of great interest among researchers [1]. In this work, ternary systems $Fe_{65}Al_{30}B_5$ and $Fe_{65}Al_{25}B_{10}$ obtained by mechanosynthesis and subsequent heat treatment were investigated [2].

The $D0_3$ structure and chemical homogeneity of alloys were determined by chemical analysis, X-ray diffraction, Mössbauer spectroscopy and magnetometry [2]. Analysis of the magnetic state of ternary alloys with boron addition showed [3] that the prevailing magnetic phase is ferromagnetic with a small fraction of the spin density wave (SDW). In addition, room temperature ^{57}Fe Mössbauer spectra (MS) of $Fe_{65}Al_{35-x}B_x$ alloys show significant magnetic hyperfine splitting (up to 30.0 T), increased isomer shifts and quadrupole splitting with increasing boron concentration.

To understand the reasons that caused the disappearance of the magnetic order characteristic of SDW and a significant increase in bulk and local magnetic characteristics (the Fe atom magnetic moment in the alloy and the local ^{57}Fe hyperfine magnetic field (HMF) B_{hf}), several variants of the polynomial distribution of Fe, Al and B over bcc supercell atoms positions were simulated. In particular, the distribution of atoms at the positions of the $D0_3$ structure; the chaotic distribution taking into account the near-neighbor chemical order over two and three coordination spheres; taking into account interstitial boron atoms. In each case, the most likely configurations were identified. Using the ^{57}Fe HMF values obtained from DFT calculations (WIEN2k [4]) for the nuclei of iron atoms in the $D0_3$ supercell, the Mössbauer spectra of the ordered $Fe_{65}Al_{30}B_5$ alloy at different temperatures (5–60 K) and external magnetic field (0–50 kOe) were synthesized using SpectrRelax software [5].

Model analysis of the Mössbauer spectra of the ordered $Fe_{65}Al_{30}B_5$ alloy showed that the model of the chaotic distribution of aluminum and boron atoms over Fe1 positions of the $D0_3$ structure best describes the recorded MS and shows consistency over a wide range of temperatures and values of the external magnetic field. Based on the analysis, it was revealed that the alloy under study is magnetically inhomogeneous. In addition to the dominant ferromagnetic component, there is a magnetic phase with a different field and temperature behavior.

1. Bormio-Nunes C., Hubert O.: JMMM **393**, 404–418 (2015)
2. Voronina E.V., Al'Saedi A., Ivanova A.G. et al.: Phys. Met. Metallogr. **120**, 1213–1220 (2019)
3. Voronina E.V., Arzhnikov A.K., Chumakov A.I. et al.: Advances Cond. Mat. Phys. **18**, 1-8 (2018)
4. Blaha P., Schwarz K., Tran F. et al: J. Chem. Phys. **152**, 074101 (2020)
5. Matsnev M.E., Rusakov V.S.: Mössbauer Spectroscopy in Materials Science-2012: Proceedings of the International Conference MSMS-12, Olomouc, Czech Republic **1489**, 178–185 (2012)

Po2

Synthesis, structural and magnetic properties of Ni_2CrBO_5 oxyborate with ludwigite structure

N.A. Belskaya[1], A.A. Krasilin[1], E.V. Eremin[2], D.S. Chikurov[1]

[1]Ioffe Institute, RAS, Saint-Petersburg, Russia
[2]L.V. Kirensky Institute of Physics, SB of RAS, Krasnoyarsk, Russia

The transition metal oxyborates with the ludwigite structure have attracted considerable interest due to their complex magnetic behavior.

In this study, we have investigated the magnetic properties and crystal structure of Ni_2CrBO_5 ludwigite. The ludwigite's crystal structure consists of oxygen octahedra and trigonal BO_3 groups. The divalent metal ions prefer to occupy distinct crystallographic sites, including M1, M2, and M3, corresponding to the 2a, 2b, and 4g Wyckoff positions, respectively. Additionally, the metal site M4 is filled by ions with a higher valence state, Me^{3+}. The magnetic properties of the compound are closely related to the ion filling this site.

The synthesis of Ni_2CrBO_5 was performed via the solid-phase method. Phase composition and sample purity were confirmed using powder X-ray diffraction. After optimizing the heat treatment conditions and oxide ratio (Ni_2O_3, Cr_2O_3, B_2O_3), a single-phase Ni_2CrBO_5 powdered sample was obtained, exhibiting an orthorhombic structure with the *Pbam* (55) space group. The unit cell parameters were determined as follows: a = 9.20195 Å, b = 12.11049 Å, c = 2.98407 Å, and V = 332.545244 Å^3. The compound Ni_2CrBO_5 the sites M1 and M3 occupied by Ni atoms, M2 – Cr atoms, and M4 is occupied by Ni and Cr atoms in the ratio of 0.5/0.5 (Fig. 1.). In Fig. 1, a green color indicates the boron atoms and a red color indicates the oxygen atoms. Ni_2CrBO_5

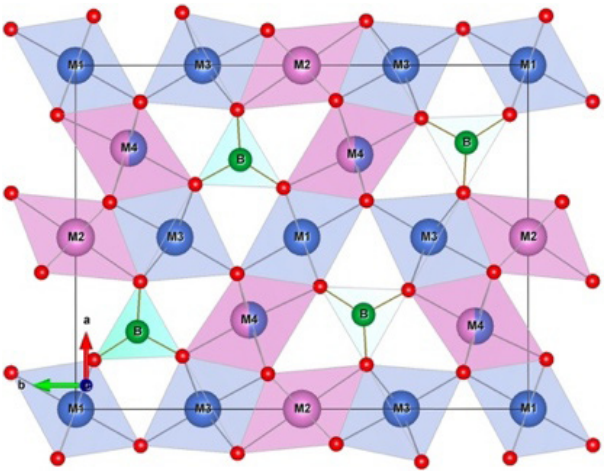

Fig. 1. Visualization of Ni_2CrBO_5 unit cell in *ab*-plane.

Po2

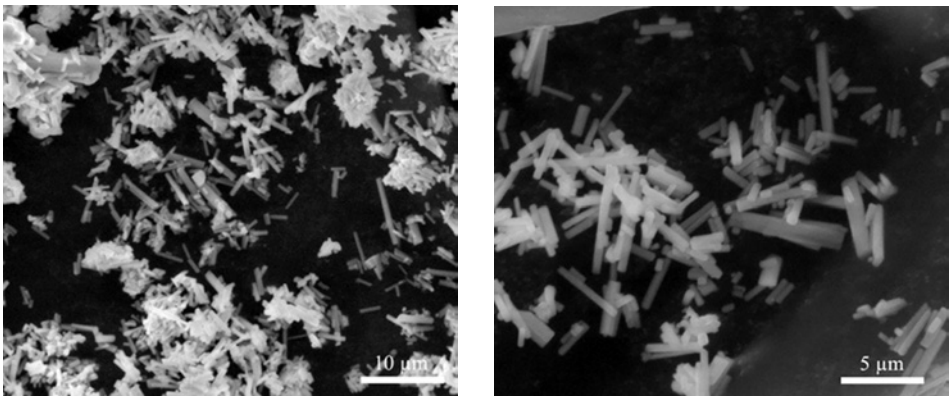

Fig. 2 SEM micrographs of Ni_2CrBO_5 particles.

has an elongated needle-like morphology, growth occurring along the crystallographic *c*-direction (Fig. 2).

The magnetization measurements were performed using a Quantum Design physical property measurement system (PPMS-9) on powder pressed into a tablet, which was placed in a sample holder using an optical microscope. The compound exhibits a magnetic anomaly at $T_N = 133$ K, corresponding to the onset of the antiferromagnetic transition and is in accordance with of ferrimagnetic behavior. Notably, Ni_2CrBO_5 demonstrates a remarkably high T_N compared to other ludwigite systems, for example such as Ni_2MnBO_5 [1], Ni_2FeBO_5 [2] and Ni_2TiBO_5 [3]. Other ludwigites, such as, iron ludwigite Fe_3BO_5 undergoes a cascade of the magnetic transformations: PM-AFM-Ferri, at the critical temperatures $T_{N1} = 112$ K and $T_{N2} = 70$ K [5–7]. At same time, Co_3BO_5 shows only one magnetic transition to the ferrimagnetic state at $T_N = 43$ K [8]. At temperatures ranging from 170 to 300 K, the magnetic susceptibility χ follows the linear

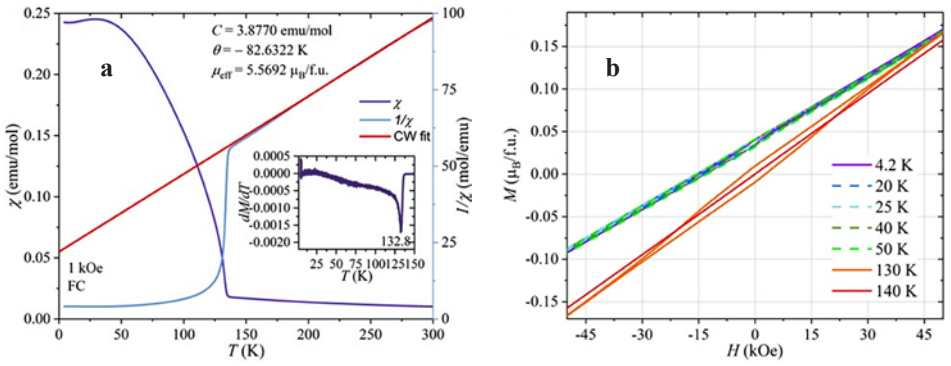

Fig. 3. a Temperature dependence of magnetic susceptibility and reversal susceptibility, obtained upon cooling the sample at H =1 kOe (FC), the inset to the figure shows the first derivative of magnetization. **b** Magnetic field dependencies of magnetization of ludwigite Ni_2CrBO_5, obtained at $T = 4.2$ K, 20 K, 25 K, 40 K, 50 K, 130 K, and 140 K.

Curie-Weiss law (Fig. 3a), with a negative Curie-Weiss temperature $\theta = -82.6$ K, suggesting predominant antiferromagnetic interactions. The effective magnetic moment of around 5.57 μ_B/f.u. was calculated from the value of the Curie constant. At $T = 130$ K, the $M(H)$ curve exhibits a hysteresis loop (Fig. 3b), indicating the presence of permanent magnetization. With decreasing temperature, the hysteresis loop shifts along the ordinate axis, indicating incomplete demagnetization under the applied external field.

In summary, the magnetic properties of Ni_2CrBO_5 ludwigite obtained for the first time have been investigated, and its high T_N and magnetic behavior have been compared to other Ni-containing ludwigites. The obtained results should light on the potential applications and unique properties of this compound.

1. Moshkina E., Sofronova S.: J. Magn. Magn. Mater. **402**, 69–75, (2016)
2. Heringer M.A.V., Freitas D.C.: Phys. Rev. Mater. **3** (9), 094402 (2019)
3. Freitas D.C., Continentino M.A.: Phys. Rev. B **79** (13), 134437 (2009)
4. Sofronova S.N., Veligzhanin A.: Phys. Status Solidi B **260** (5), 2200457 (2023)
5. Larrea J., Sánchez D.R.: Phys. Rev. B **70**, 174452 (2004)
6. Bordet P., Suard E.: Phys. Rev. B **79**, 144408 (2009)
7. Knyazev Yu.V., Kazak N.V.: JMMM **474**, 493–500 (2019)
8. Freitas D.C., Continentino M.A.: Phys. Rev. B **77**, 184422 (2008)

Po3

Phase transitions in the chiral ferromagnetic MnSi

A.A. Povzner, M.A. Chernikova, A.G. Volkov, T.A. Nogovitsyna

Physics Department, Ural Federal University, Ekaterinburg, Russia

The phase transitions were considered in chiral ferromagnetic MnSi with interatomic coulomb correlations caused by Hubbard and Hund interactions. It is shown that due to Berry curvature in strongly correlated d-electrons MnSi [1] phase transition from order parameter region, characterized by chiral spin spiral, leads to appearance of A-phase with skyrmion microregion of the same chirality. The loss of thermodynamic stability of the A-phase is accompanied by transition to paramagnetic phase with skyrmion of left and right chirality.

The thermodynamic stability limits of chiral microstructures are determined by curvature of the density of d-electron states near Fermi-level, derived from DFT+U calculations. It is shown that A-phase appears because of topologically induced first order magnetic transition, and transition to paramagnetic state with segregation of skyrmion microstructures occurs as a result of second-order thermodynamic phase transition. With temperature shift chemical potential beyond topologically induced region of negative DOS curvature, skyrmions in paramagnetic state disappear.

It has been established that topological charges of skyrmions microstructures are defined by spatial fluctuations of the spin and charge electron density, arising from interatomic coulomb interactions in the system of d-electrons. The calculations of the factors of the exchange enhancement of the magnetic susceptibility are consistent with experimental data [1] and correctly determine the temperature region of the existence ferromagnetic A-phase and paramagnetic region of mixed chirality, observed during the scattering of polarized neutrons [2].

1. Bauer A., Pfleiderer C.: Springer Series in Materials Science **228**, 1–28 (2016)
2. Janoschek M., Garst. M., Bauer A., Krautscheid P., Georgii R., Boni P., Pfleiderer C.: Phys. Rev. B **87**, 1–16 (2013)

Po4

$Li_3V_2(PO_4)_3$-based composites as potential cathode materials for lithium-ion batteries: ESR, magnetization and electrochemical measurements

T. Gavrilova[1], Yu. Deeva[2], I. Yatsyk[1], M. Cherosov[3], R. Batulin[3], N. Lyadov[1], S. Khantimerov[1]

[1]Zavoisky Physical-Technical Institute, FRC Kazan Scientific Center of RAS, Kazan, Russia
[2]Institute of Solid State Chemistry of RAS (UB), Ekaterinburg, Russia
[3]Institute of Physics, Kazan Federal University, Kazan, Russia

Compounds based on the lithium-vanadium phosphate $Li_3V_2(PO_4)_3$ (LVPO) can be used as a cathode material in metal-ion batteries due to the stability of their crystal structure with respect to the change in the valence state of transition ion caused by the processes of intercalation/deintercalation of an alkaline element during the charge/discharge process of the electrochemical cell. In this context, the investigation of physical properties of $Li_3V_2(PO_4)_3$-based structures is of great interest. Here we present the magnetic and electrochemical properties investigations of $Li_3V_2(PO_4)_3$-based composites, including $Li_3V_2(PO_4)_3/Li_3PO_4$ (LVPO/LPO) composite with the different Li_3PO_4 salt concentration, $Li_3V_2(PO_4)_3$/C (LVPO/C) composite and three-component heterostructure $Li_3V_2(PO_4)_3/C/Li_3PO_4$ (LVPO/C/LPO).

LVPO/LPO samples were obtained by the thermal hydrolysis method with the subsequent annealing in Ar atmosphere [1, 2]. In comparison, the LVPO/C composite was synthesized by the above-mentioned method and soft-template method [3]. The three-component heterostructure was obtained as a mechanical mixture of LVPO/C composite with Li_3PO_4 salt. Magnetic properties of LVPO-based composites were investigated using magnetometry and electron spin resonance (ESR) methods. Electrochemical property investigations were performed by the galvanostatic method; the electrochemical voltage profiles and the discharge capacity depending on the number of charge-discharge cycles at different C-rates were obtained.

Based on all experimental data, one can suggest that the degree of non-stoichiometry (lithium deficiency) depended on the chemical composition of the sample (including the amount of Li_3PO_4 salt) and has a significant effect on the electrochemical properties. As an example, the increase in the discharge capacity was observed for LVPO/LPO composite with increasing in lithium deficiency. Moreover, using the ESR method the stabilization of the V^{3+} valence state due to the presence of LPO salt was detected and the almost complete reduction of vanadium ions to the valence state V^{3+} after a few charge/discharge cycles for LVPO-based composites was shown that indicates the reversible intercalation of all lithium ions to the structure during the delithiation/lithiation process.

This work is supported by the Russian Science Foundation (grant #19-79-10216).

1. Gavrilova T. et al.: Magnetochemistry **7**, 64 (2021)
2. Gavrilova T. et al.: Magnetochemistry **8**, 105 (2022)
3. Gavrilova T.P. et al.: Solid State Commun. **323**, 114108 (2021)

Po5

Transfer of spin state between the intermediate valence impurities by donor Dirac electrons

Yu.V. Goryunov

Zavoisky Physical-Technical Institute, FRC Kazan Scientific Center of RAS, Kazan, Russia

Since the time when an understanding of the mechanisms [1] of formation of atomic localized magnetic moments in solids arose, there has also been a problem of the mechanisms of transfer of spin state between localized magnetic moments. From this perspective, great interest is aroused by the behaviour of magnetic impurities in the Dirac topological materials. The most interesting properties of Dirac materials are the linear spectrum of electronic excitations in the conduction band and topological protection of the electron spin states from which follows possibility of transfer of the impurity spin states on a long distances. Previously [2] it has been studied the behaviour of magnetic impurities of Eu in a Dirac semimetal α-Cd_3As_2 by means ESR. Recent we found that the valence electrons of the Eu^{2+} ion, like Cd^{2+}, enter in the valence band, and the electrons associated with the partial transition of the Eu^{2+} ion to Eu^{3+} are the source of electrons in the conduction band. However, the energies of removal of the second and third Eu electrons from the crystal are 11.25 and 24.7 eV, respectively. The same values for Cd are 16.908 and 36.48 eV. This energy can be compensated from lattice elastic stress energy at transition Eu^{2+} in Eu^{3+}, which is different for substitutional and interstitial positions. The elastic energy arising from the placement of the Eu^{2+} ion in the tetrahedral coordination position of the Cd^{2+} ion or in the tetrahedral vacancy can be estimated from the sizes of ions and the lattice constants using the data of [3] on the parameters of the Lenard-Jones potential, $U(r) = U_0[(\sigma/r)^{12} - (\sigma/r)^6]$. Those, replacing Cd^{2+} with Eu^{3+} is almost equivalent, and replacing Cd^{2+} with Eu^{2+} transfers the ion system to a position corresponding to strong repulsion. Calculation for the excess repulsion energy of 4 As^{3-} ions for the substitution position gave value 6.285 eV. For the interstitial position we obtain an excess energy 14.8 eV. The analogous values of repulsive energy for the Eu^{3+} ion are: –0.065 eV (substitution) and 0.78 eV (interstitial). I.e. the trivalent state for Eu is energetically unfavourable in any case. Assuming that valence electrons of Cd determine the bottom of the conduction band, we find that an energy about 24.7 – 16.908 ~ 7.792 eV is required to transfer the third electron of europium to this level. This energy slightly exceeds the lattice energy released when the valence state of the europium ion changes in the substitution position and is significantly less than that in the interstitial position. In this regard, the lifetimes of an ion in the magnetic state and its effective magnetizations in these positions differ significantly. Due to the conservation laws and topological protection of spin state, an electron emitted from the corresponding position by the magnetic Eu^{2+} ion transfers energy and angular momentum to the Eu^{3+} ion located in such the same position in crystal lattice and it restores here the spin state of the Eu^{2+} ion.

1. Anderson P.W.: Phys. Rev. **124**, 41 (1961)
2. Goryunov Yu.V., Nateprov A.N.: Phys. Sol. St. **60**, 68 (2018)
3. Maghfiroh C.Y., Arkundato A., Misto, Maulina W.: J. Phys. Conf. Ser. **1491**, 012022 (2020)

Po6

Magnetic properties and spin Hall effects in Py/MnPt heterostructures

A.Kh. Kadikova[1], I.V. Yanilkin[1], A.I. Gumarov[1], B.F. Gabbasov[1], D.G. Zverev[1], L.R. Tagirov[1,2], R.V. Yusupov[1]

[1]Institute of Physics, Kazan Federal University, Kazan, Russia
[2]Zavoisky Physical-Technical Institute, FRC Kazan Scientific Center of RAS, Kazan, Russia

Nowadays, antiferromagnetic spintronics is a rapidly developing field. Technological solutions in this direction are promising for the elements of magnetoresistive random-access memory (MRAM). Traditionally, antiferromagnets in magnetoresistive cells are used to fix the direction of magnetization of one of the two ferromagnetic layers. Recently, an interest in antiferromagnets has gained due to the possibility of their use as active components in spin valves with perpendicular magnetic anisotropy (PMA). For example, in metallic antiferromagnets (AF) containing normal heavy metal, the spin-orbit interaction can convert a charge current into a spin current via the direct spin Hall effect. This means that in AF/F structures, where F is a ferromagnet, spin-charge transformations can be observed, and, accordingly, such heterostructures can be used in magnetoresistive cells switched using the spin Hall effect.

In the talk, we will present the results of the structure and properties of AF/F thin-film structure studies, where the Mn_xPt_{1-x} intermetallic compound serves as an antiferromagnet, and the ferromagnetic layer is made of permalloy ($Ni_{80}Fe_{20}$, or Py). Both the epitaxial samples and a polycrystalline heterostructure were synthesized. It was established that the antiferromagnetic layers in heterostructures crystallize in the tetragonal L10-phase. Magnetization hysteresis loops have been studied, and the magnetocrystalline anisotropy in the Py-film plane has been detected.

The inverse spin Hall effect (ISHE) was studied utilizing the ferromagnetic resonance (FMR) spectroscopy. A broadening of the resonance lines of AF/F heterostructures was found in comparison with similar single F-layers. Spin-pumping-induced ISHE voltage signal generated in the Mn_xPt_{1-x}/Py heterostructure was registered. The spin Hall angles for antiferromagnets containing different amounts of normal heavy metal were estimated.

Po7

Investigation of the features of a superconducting spin valve Fe1/Cu/Fe2/Cu/Pb on a piezoelectric substrate

A.A. Kamashev, N.N. Garif'yanov, A.A. Validov, R.F. Mamin, I.A. Garifullin

Zavoisky Physical-Technical Institute, FRC Kazan Scientific Center of RAS, Kazan, Russia,
e-mail: kamandi@mail.ru

The properties of a superconducting spin valve Fe1/Cu/Fe2/Cu/Pb on a piezoelectric substrate PMN-PT substrate ($[Pb(Mg_{1/3}Nb_{2/3})O_3]_{1-x}$ - $[PbTiO_3]_x$) under the influence of an electric and magnetic field have been studied. The magnitude of the shift of the superconducting transition temperature in the magnetic field H_0 = 1 kOe equal to 150 K was detected, while the full superconducting spin valve effect was demonstrated. Abnormal behavior of superconducting transition temperature was shown, which manifests itself in the maximum values of superconducting transition temperature with orthogonal orientation of the magnetization vectors of ferromagnetic layers, when studying the angular dependence of superconducting transition temperature in an external magnetic field (see Fig. 1). This may indirectly indicate the fixation of the magnetization vector of the Fe1-layer on a PMN-PT piezoelectric substrate. It was found that with an increase in the magnitude of the applied electric field to the PMN-PT substrate, the shift in superconducting transition temperature of the Fe1/Cu/Fe2/Cu/Pb heterostructure increases. The maximum shift was 10 mK when an electric field of 1 kV/cm was applied (see Fig. 2).

The reported study was funded by Russian Science Foundation according to the research project No. 21-72-10178.

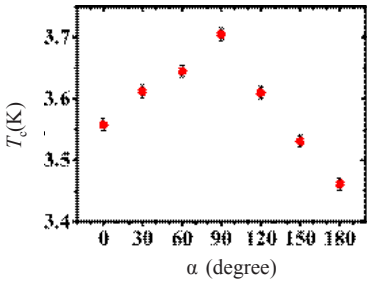

Fig. 1. Dependence of T_c on the angle α between the direction of the cooling field used to fix the direction of the magnetization of the Fe1 layer and the applied magnetic field H = 1 kOe that rotates the magnetization of the Fe2 layer.

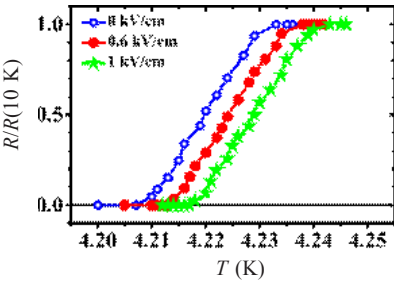

Fig. 2. Superconducting transitions curves for the sample for the sample PMN-PT/Fe1(3 nm)/Cu(4 nm)/Fe2(1 nm)/Cu(1.2 nm)/Pb(60 nm)/Si_3N_4 when applying an electric field to PMN-PT substrate: shift of T_c is 5 mK when applying an electric field 0.6 kV/cm; shift of T_c is 10 mK when applying an electric field 1 kV/cm. The error of the experiment corresponds to the size of the character.

Po8

Features of ferromagnetism in epitaxial SnO_2 films implanted with Co-ions at different temperatures

R.I. Khaibullin[1], A.I. Gumarov[1,2], A.A. Sukhanov[1], A.M. Rogov[3], A.G. Kiiamov[2], I.R. Vakhitov[1,2], V.F. Valeev[1], A.L. Zinatullin[1,2]

[1]Zavoisky Physical-Technical Institute, FRC Kazan Scientific Center of RAS, Kazan, Russia
[2]Institute of Physics, Kazan Federal University, Kazan, Russia
[3]Interdisciplinary Center for Analytical Microscopy, Kazan Federal University, Kazan, Russia

Semiconducting tin dioxide (SnO_2) doped with a magnetic 3d-elements is a promising material for optoelectronic, photovoltaic, spintronic and energy storage applications [1, 2]. Although the room temperature ferromagnetism (FM) in transition metal (TM)-doped SnO_2 had been early reported [2, 3], the origin and the mechanism of long-range ferromagnetic order are still an open question. There are indications that the FM strongly depends on the fabrication method of TM-doped SnO_2. Moreover, the presence of oxygen vacancies was systematically related to the observed ferromagnetic state [4].

In this work, we investigated the possibilities of ion-beam implantation for obtaining cobalt-doped SnO_2-films. This technique allows not only doping any material with any impurities at any concentration, but also generates a large number of oxygen vacancies in oxide structure during the ion irradiation process. Herein, the emphasis was placed on studying the effect of the SnO_2 temperature during the implantation with cobalt ions on the manifestation of ferromagnetism.

The experimental samples have been obtained in two stages. At the first stage, thin $SnO_{2-\delta}$-films with a thickness of 150 nm were grown on R-cut Al_2O_3 single crystalline substrates by the reactive (Ar + O_2) magnetron sputtering of the elemental tin target. The subsequent annealing in air at the temperature of 1273 K for 120 min has been performed to restore the stoichiometric oxygen content in the films. The epitaxial growth on Al_2O_3-substrate and crystal lattice perfection, as well rutile phase of stoichiometric SnO_2-films with (101)-surface orientation have been recognized from the analysis of low energy electron diffraction (LEED) and X-ray diffraction (XRD) patterns taken at different geometries of measurements. Surface morphology and elemental composition of all prepared films have been investigated using high-resolution SEM/EDX element mapping which show that the all the prepared films have an almost flat surface with a roughness below 5 nm and ones are elemental homogeneity along at submicron scale. Then, at second stage, 40 keV Co^+ ions were implanted into epitaxial SnO_2-films with the fluence of 1.5×10^{17} ion/cm^2 at room (300 K) or the elevated (900 K) substrate temperatures during ion irradiation in order to induce ferromagnetism in SnO_2 films. The depth profiles and valence state of cobalt implant have been studied by X-ray photoelectron spectroscopy (XPS) in combination with argon ion etching technique. It was established that the most of Co impurity is in metallic (neutral) Co^0 state and locates in near-surface region of about 30 nm thickness for SnO_2-films implanted at room temperature. At the same time, the cobalt is found in divalent Co^{2+} charge state and ones distribute over all thickness of SnO_2-film in the samples implanted at elevated temperature. Both XPS and EDX analysis showed that oxygen content in Co-implanted SnO_2 is significantly decrease.

Po8

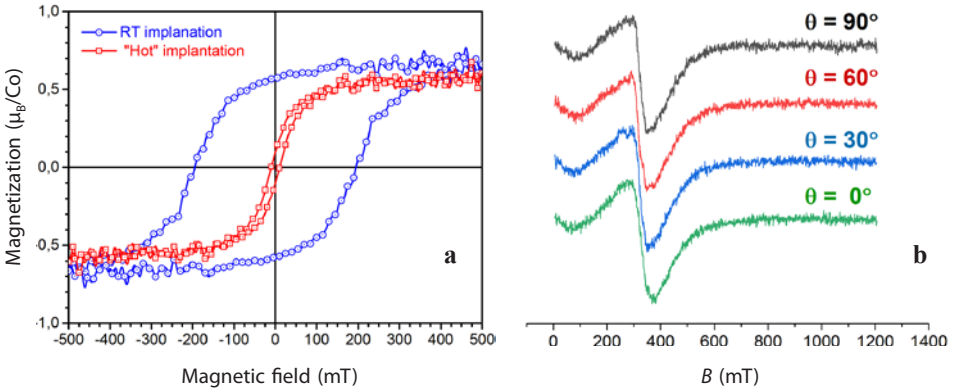

Fig. 1. a In-plane magnetic hysteresis loops for epitaxial SnO_2 films implanted with Co ions at room (RT) or at the elevated ("Hot") temperatures; **b** out-of-plane angular dependence of FMR spectrum for the sample implanted at the elevated temperature, $T_{meas.}$ = 300 K.

The magnetic properties of Co-implanted SnO_2 films have been studied by vibrating sample magnetometry (VSM) and ferromagnetic resonance (FMR) spectroscopy at 9.5 GHz. The magnetic measurements were taken only at room temperature but at different orientations of the applied magnetic field with respect to the film plane. VSM study showed that all Co-implanted SnO_2 films reveal a ferromagnetic response with clearly defined magnetic hysteresis loops in the in-plane geometry (Fig. 1a). It is clearly seen that the samples show almost same values of the saturation magnetization (M_s ~ 0.6-0.7 μB/Co ions). However, the coercive fields are notably different, namely, $B_c \cong$ 200 mT for SnO_2 film implanted at room temperature and $B_c \cong$ 10 mT for the sample implanted at the elevated substrate temperature.

A strong effect of the substrate temperature during Co ion implantation on the FMR-spectra have been established. For SnO_2 film implanted at room temperature FMR-signals are clearly observed only when the magnetic field applied out-of-plane direction. Moreover, two lines can be recognized from the analysis the out-of-plane angular dependence of FMR spectra (not shown). When magnetic field is applied exactly along to the normal of SnO_2 film plane, resonance fields equal approximately 0.73 and 0.97 T for the first and the second lines, respectively. On the other hand, one FMR-signal and a very weak angular dependence of resonance field (0.31 T $\leq B_{res.} \leq$ 0.32 T) are observed in the film implanted at the elevated temperature (Fig. 1b).

The comprehensive analysis of our results indicates the formation of either a dense granular magnetic media consisting of anisotropic cobalt nanoparticles or a magnetically isotropic solid solution of Co^{2+} ions in the SnO_2 films implanted at room or the elevated substrate temperatures, respectively.

The study was supported by the Russian Science Foundation (project number 22-19-00712, https://rscf.ru/project/22-19-00712/).

1. Dalapati G.K., Sharma H., Guchhait A. et al.: J. Mater. Chem. A **9**, 16621–16684 (2021)
2. Worku Y., Sahu D.R., Srinivasu V.V., Ferromagnetism in SnO_2 Doped with Transition Metals (Fe, Mn and Ni) for Spintronics Application: A Review of Experimental Status, Ch. 7 in book: Magnetic Materials and Magnetic Levitation (IntechOpen, March 24, 2021).
3. Fitzgerald C.B., Venkatesan M., Dorneles L.S. et al.: Phys. Rev. B **74**, 115307 (2006)
4. Borges P.D., Scolfaro L.M.R., Alves H.W.L. et al.: Nanoscale Research Lett. **7**, 540 (2012)

Po9

Electron spin resonance study of $La_{0.7-x}Eu_xSr_{0.3}MnO_3$ manganite compounds

D.V. Mamedov[1], R.M. Eremina[1], I.V. Yatsyk[1], S. Vadnala[2], S. Asthana[2], S.I. Andronenko[3], S.K. Misra[4]

[1]Zavoisky Physical-Technical Institute, FRC Kazan Scientific Center of RAS, Kazan, Russia
[2]Physics Department, Indian Institute of Technology, Hyderabad, India
[3]Institute of Physics, Kazan Federal University, Kazan, Russia
[4]Physics Department, Concordia University, Montreal, Canada

The manganites of the general formula $A_{1-y}B_yMnO_3$, where A is a rare-earth ion and B = Ca, Ba, Sr have been extensively studied by the techniques of electron spin resonance (ESR). At the same time, special attention was given to understanding the dynamics of spins near and above the magnetic phase transition, as well as to understand the phase separation, influence of Jahn-Teller effect and Griffiths phase. The transport, magnetic and structural properties of these compounds depend on the presence of the rare-earth ions (A^{3+}), e.g. La^{3+}, Nd^{3+}, Eu^{3+}, together with the divalent ions (B^{2+}), e.g. Sr^{2+}.

Here we have studied the ESR-spectra of the perovskite type manganites $La_{0.7-x}Eu_xSr_{0.3}MnO_3$ (x = 0.1–0.7). The ESR measurements were carried out on an EMX/plus spectrometer (Bruker) in X-band (9.4 GHz) with a nitrogen purge and a temperature controller RS 232 (Bruker) in the temperature range from 100 to 340 K.

The magnetic lines evolution shows that when lanthanum (ionic radius 117 pm) is replaced in the A-position by europium (ionic radius 95 pm), the temperature of the magnetic phase transition decreases.

The increase in structural disorder for samples with x from x = 0.0 to 0.3, causes an increase in the distribution of the cation radius as x increases [1, 2]. On the other hand, the disorder decreases when x increases from 0.3 to 0.7. Therefore, for the sample $Eu_{0.7}Sr_{0.3}MnO_3$, its activation energy became smaller due to its disorder being less.

The minimal linewidth in $La_{0.7-x}Eu_xSr_{0.3}MnO_3$ paramagnetic region corresponds to bottlenecked spin relaxation model, especially at low influence of disorder (x = 0.7, 0.6).

The manganite series, $La_{0.7-x}Eu_xSr_{0.3}MnO_3$ are inhomogeneous and each ferromagnetic component has its own Curie temperature, which was revealed by ESR method.

1. Vadnala S., Rao T.D., Pal P., Asthana S.: Physica B **448**, 277–280 (2014)
2. Vadnala S., Pal P., Asthana S.: J. Rare Earth **33**, 1072–1080 (2015)

Po10

Magnetoelectric properties of magnetic nanostructures

R.F. Mamin, T.S. Shaposhnikova

Zavoisky Physical-Technical Institute, FRC Kazan Scientific Center of RAS, Kazan, Russia

Magnetoelectric properties are very important for various applications and therefore the magnetoelectric effect has long been actively studied. New materials with interesting characteristics have been obtained recently for practical application [1, 2]. This effect is often observed in multiferroics [2], as well as in various inhomogeneous structures consisting of components with different ferroic properties. In this report, within the framework of the phenomenological model, the possibility of the magnetoelectric effect in systems with non-uniform magnetic ordering is considered. The microscopic mechanism of the occurrence of the magnetoelectric effect in such systems is due to the presence of the Dzyaloshinskii-Moriya interaction. The occurrence of electric polarization is considered both for small volumetric spherical magnetic particles in a paramagnetic matrix and for "ordinary" two-dimensional skyrmions. The inhomogeneous distribution of magnetization leads to inhomogeneous electric polarization. As a result, the action of the magnetic field on the magnetic subsystem leads to a change in the inhomogeneous distribution of the electric polarization, and as a result, a magnetoelectric response occurs. The specific form of expressions for the electric polarization and magnetoelectric response is determined by the inhomogeneous distribution of magnetization in the localization regions of such skyrmion-like structures. A non-zero magnetoelectric response to the action of a magnetic field occurs, but it appears only at certain directions of the external magnetic field. The study was carried out within the framework of the state task of the FRC KazSC RAS.

1. Spaldin N.A., Ramesh R.: Nat. Mater. **18**, 203–212 (2019)
2. Fiebig M., Lottermoser T., Meier D., Trassin M.: Nat. Rev. Mater. **1**, 16046 (2016)

Po11

Evidencing of controlled spin state transition in binuclear Fe(III) complex supported calix[4]arene Schiff base

A.V. Pyataev[1], I.V. Strelnikova[2,3], A.S. Ovsyannikov[2], D.R. Islamov[3], P.V. Dorovatovskii[4], S.E. Solovieva[2,3], I.S. Antipin[2,3]

[1]Department of Solid State Physics, Institute of Physics, Kazan Federal University, Kazan, Russia
[2]A. M. Butlerov Institute of Chemistry, Kazan Federal University, Kazan, Russia
[3]A. E. Arbuzov Institute of Organic and Physical Chemistry, FRC Kazan Scientific Center of RAS, Kazan, Russia
[4]National Research Centre "Kurchatov Institute", Moscow, Russian Federation

The effects of the removal of the lattice-solvent molecules on the spin transition process in dinuclear complex $[Fe^{III}_2\text{-}1_2(OMe)_2]$ with two Schiff base units at the lower rim (Fig. 1) according to [1] were investigated by low-temperature Mössbauer spectroscopy. Figure 2 shows the ^{57}Fe Mössbauer spectra recorded at 19 K before (as-prepared sample) and after the annealing at 150° C for 48 hours at 20 K. At 19 K, the spectrum reveals a major area fraction of 90.3% for the HS sites and an area fraction of 9.7% for the LS sites indicating an incomplete spin transition.

This work was supported by the Russian Science Foundation (project no. 22-73-10139).

1. Zhang W.C., Huang Z.T.: Synthesis **09**, 1073–1076 (1997)

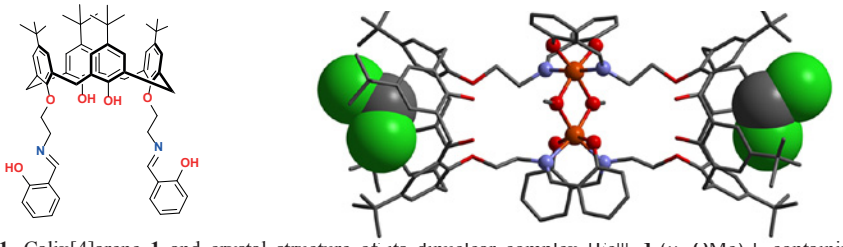

Fig. 1. Calix[4]arene **1** and crystal structure of its dinuclear complex $[Fe^{III}_2\text{-}\mathbf{1}_2(\mu_2\text{-}OMe)_2]$, containing two non-equivalent Fe^{III}-atoms and calix[4]arene cavity with two included CH_2Cl_2 solvent molecules.

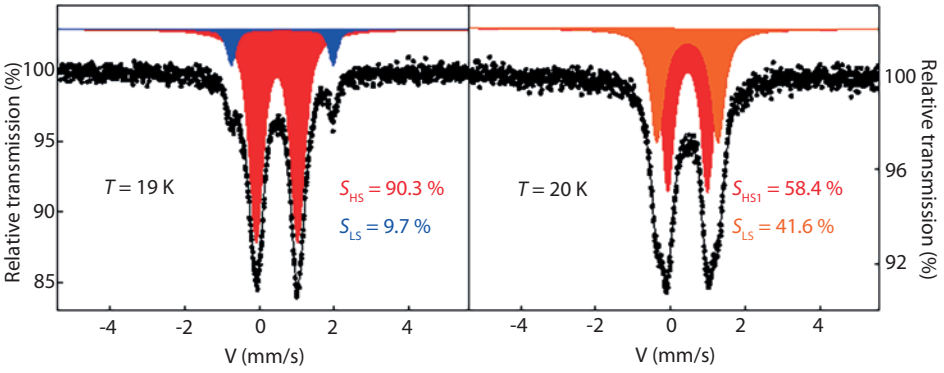

Fig. 2. Mössbauer spectra of dinuclear complexes $[Fe^{III}_2\text{-}\mathbf{1}_2(\mu_2\text{-}OMe)_2]$ taken at low temperatures. The as-prepared sample (left) and after the annealing at 150°C for 48 hours (right).

Po12

Pressure-induced crystal structure transformations in high-pressure prepared $Bi_{1-x}Tb_xFeO_3$ compounds (x = 0.05, 0.1, and 0.3)

D.A. Salamatin[1,3], S.E. Kichanov[2], I.E. Kostyleva[1], L.F. Kulikova[1], A.V. Bokov[1], D.P. Kozlenko[2], A.V. Tsvyashchenko[1]

[1]Vereshchagin Institute for High Pressure Physics, RAS, Troitsk, Moscow, Russia
[2]Frank Laboratory of Neutron Physics, Joint Institute for Nuclear Research, Dubna, Russia
[3]Dzhelepov Laboratory of Nuclear Problems, Joint Institute for Nuclear Research, Dubna, Russia

In the $BiFeO_3$ multiferroic the antiferromagnetic and ferroelectic orders coexist at room temperature. Due to the non-centrosymmetric crystal and magnetic structures of the compound the linear magnetoelectric effect and weak ferromagnetism should exist. But these properties are suppressed by the long-range cycloid magnetic order of Fe magnetic spins. The substitution of Bi by rare-earth ions is one of the common approaches for improving the electrical, magnetic, and multiferroic properties of the most studied multiferroic material $BiFeO_3$.

In this work, $Bi_{1-x}Tb_xFeO_3$ compounds with $x = 0.05$, 0.1, and 0.3 were synthesized using a two-step process: standard solid-state synthesis and high-pressure annealing. The obtained samples were studied by means of X-ray diffraction at normal pressure and neutron powder diffraction at high pressure. It was shown that high-pressure annealing could increase the Tb solubility limit to 10 at.%. It is proposed that the maximum solubility limit is even higher and could be achieved with high-pressure annealing in bulk samples. The transition from the *R3c* phase to the *Pnma* phase for the compounds with $x = 0.05$, 0.1 occurs through a two-phase region and starts at $P = 4.4$ and 1.7 GPa, respectively. The *Pnma* phase is stable in the compound with $x = 0.3$ up to $P = 3.2$ GPa. The values of Fe magnetic moments decrease with an increase in the Tb concentration or with external pressure for the compounds with $x = 0.05$, 0.3 in one-phase regions. The results will help to optimize the synthesis of multiferroic materials with improved magnetoelectric coupling for use in technological applications [1].

This work was supported by Russian Science Foundation Grant No. 22-72-00014.

1. Salamatin D.A., Kichanov S.E., Kostyleva I.E. et al.: Appl. Phys. Lett. **122**, 211905 (2023)

Po13

Transient spin coherence behavior of metal-oxamidato complexes under multi-pulse sequences studied by solid-state ^{1}H NMR

Yu. Slesareva, Yu. Kandrashkin, R. Zaripov, E. Vavilova

Zavoisky Physical-Technical Institute, FRC Kazan Scientific Center of RAS, Kazan, Russia

When it comes to possible applications in quantum information and spintronics, the potential presented by metal-oxamidato complexes is intriguing to investigate. In this study, we have performed ^{1}H NMR experiments to compare the behavior of the Cu(II)-oxamidato complex with its diamagnetic Ni(II)-containing analog. The presence of magnetic ions induces inhomogeneous broadening and accelerates the relaxation processes. In this context, the pulse sequences deviate from those typical for the Carr-Purcell-Meiboom-Gill (CPMG) protocol, which is commonly used to extend the coherence time in the presence of spectral diffusion [1]. An improved CPMG pulse protocol proposed in [2] is used to mitigate unwanted echoes. The experiments reveal a transient phenomenon that needs to be considered carefully in the design of multi-pulse protocols.

1. Zaripov R. et al.: Phys. Rev. B. **88**, 094418 (2013)
2. Zaripov R. et al.: Beilstein J. Nanotechnol. **8**, 943–955 (2017)

Po14

Features of excited charge separation states and TADF effect in the naphthalene-phenothiazine dyads

A.A. Sukhanov[1], K. Ye[2], J. Zhao[2], V.K. Voronkova[1]

[1]Zavoisky Physical-Technical Institute, FRC Kazan Scientific Center of RAS, Kazan, Russia
[2]State Key Laboratory of Fine Chemicals, School of Chemical Engineering, Dalian University of Technology, Dalian, P. R. China

Thermally activated delayed fluorescence (TADF) molecular materials has attracted much attention for application in organic light emitting diodes (OLEDs) [1], upconversion [2], photocatalysis [3] and etc. Initially in the TADF molecule is designed so that the energy difference between the excited singlet charge separation (^{1}CS) state and the excited triplet charge separation (^{3}CS) state is much small to occur enables reverse intersystem crossing (RISC). Recently the three-state model is proposed to be responsible for the TADF process, considering ^{1}CS, ^{3}CS and triplet locally excited state [4]. In both models import role play to formation of triplet states. EPR techniques can study triplet states and can provide to understanding of TADF mechanism.

In the present work, we investigated the naphthalene (NI)-phenothiazine (PTZ) dyads by time resolved (TR) and pulse EPR. It was found inversion of polarization pattern of TR EPR signal (Fig. 1) for dyads appears as TADF emitters. Using pulse EPR technique we obtained life-times for inversion signal at different temperatures. The mechanism of spin polarization inversion is discussed.

The study was supported by the government assignment for FRC Kazan Scientific Centre of RAS.

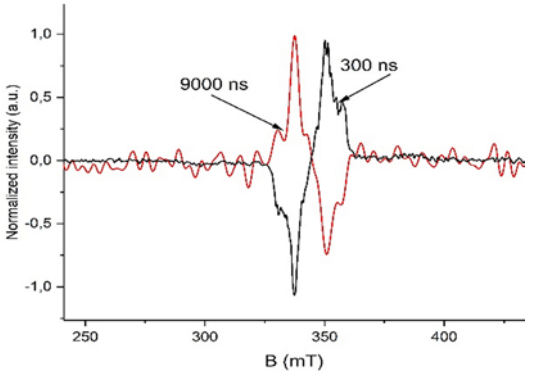

Fig. 1. TR EPR spectra of Ni-PTZ dyad for different value of delay after laser flash at 80 K.

1. Wu X., Su B.-K., Chen D.-G., Liu D., Wu C.-C., Huang Z.-X., Lin T.-C., Wu C.-H., Zhu M., Li E. Y., Hung W.-Y., Zhu W., Chou P.-T.: Nature Photonics **15**, 780 (2021)
2. Huang T., Jiang W., Duan L.: J. Mater. Chem. C **6**, 5577 (2018)
3. Lu J., Pattengale B., Liu Q., Yang S., Shi W., Li S., Huang J., Zhang J.: J. Am. Chem. Soc. **140**, 13719 (2018)
4. Samanta P.K., Kim D., Coropceanu V., Brédas J.-L.: J. Am. Chem. Soc. **139**, 4042 (2017)

Po15

Parametric excitation of magnetization waves in continuum model of diluted magnetic semiconductor

K.B. Tsiberkin

Perm State University, Perm, Russia

The study considers a parametric instability of the magnetization of DMS under harmonic perturbation of longitudinal magnetic field using the continuous medium model [1, 2]. The equations for ladder components of transversal magnetization are as follows:

$$\mathrm{i}\frac{\partial m}{\partial t} = \left(1 + 4Sa + h_0 \cos\omega t\right) m - Sp_{\mathrm{d}} Dm + 2\sigma a M + 4a\left|M\right|^2 m,$$

$$\mathrm{i}\frac{\partial M}{\partial t} = \left(\gamma + 4\sigma a + \gamma h_0 \cos\omega t\right) M + j\Delta M + 2Sam + 4a\left|m\right|^2 M,$$

$$a = Z\gamma p_{\mathrm{d}} n_S, \quad \gamma = \frac{\gamma_S}{\gamma_\sigma}, \quad p_{\mathrm{d}} = \frac{\hbar\gamma_\sigma^2}{\omega_0 a_0^3}, \quad j = S\left\langle J\right\rangle n_S^{-2/3},$$

where $m = m_x + \mathrm{i}m_y$ is the main lattice magnetization and $M = M_x + \mathrm{i}M_y$ is the admixture magnetization, where σ and S are the matrix and admixture spin operators, respectively; γ_σ and γ_S are their gyromagnetic ratios; n_S is the admixture concentration; p_{d} and j are dimensionless parameters of the dipole and exchange interaction, respectively; a_0 is a lattice constant, Z is the lattice coordination number, Δ is the Laplace operator, and the dipolar interaction in the bulk matrix is determined by the second-order differential operator D, which structure depends on the lattice geometry and direction of the external field. The time-scale is given in units of Larmor frequency of bulk matrix spins ω_0^{-1}. Parameter $\left\langle J\right\rangle$ is the volume-averaged magnitude of indirect exchange between the dopant ions. The perturbation amplitude h_0 is normalized to static field, and ω is measured in Larmor frequency units

The model equations are transformed into single second-order ODE considering the m and M as longitudinal waves ~exp(iqz). It is linearized assuming that $|m|^2$ and $|M|^2$ are constant. After the transformations and variable replacement [3], one obtains the double-forced Mathieu equation for the specific amplitude

$$\ddot{x} + \left[1 + \left(\beta\cos\nu t + \mathrm{i}\zeta\sin\nu t\right)h_0 + \delta h_0^2\cos 2\nu t\right]x = 0, \qquad \nu = \frac{\omega}{f_0},$$

where β, ζ, δ and f_0 combine the model parameters.

The instability analysis at wide range of the excitation frequency and magnitude is realized numerically by the standard numerical procedure [3]. It is based on direct solution of the obtained ODE by Runge-Kutta-Merson method with adaptive precision. It is realized as a self-written code in FORTRAN-90 language. A relative local precision is set at level 10^{-8}. The algorithm provides the automatic solution of the Mathieu equation and building the multipliers at a "frequency–forcing magnitude" plane with the grid $10^3 \times 10^3$.

Po15

The solution values after single period of forcing terms are applied to build the monodromy matrix and evaluate the solution multipliers. If the largest multiplier is > 1, the magnetization waves become unstable, and the system turns into non-linear regime.

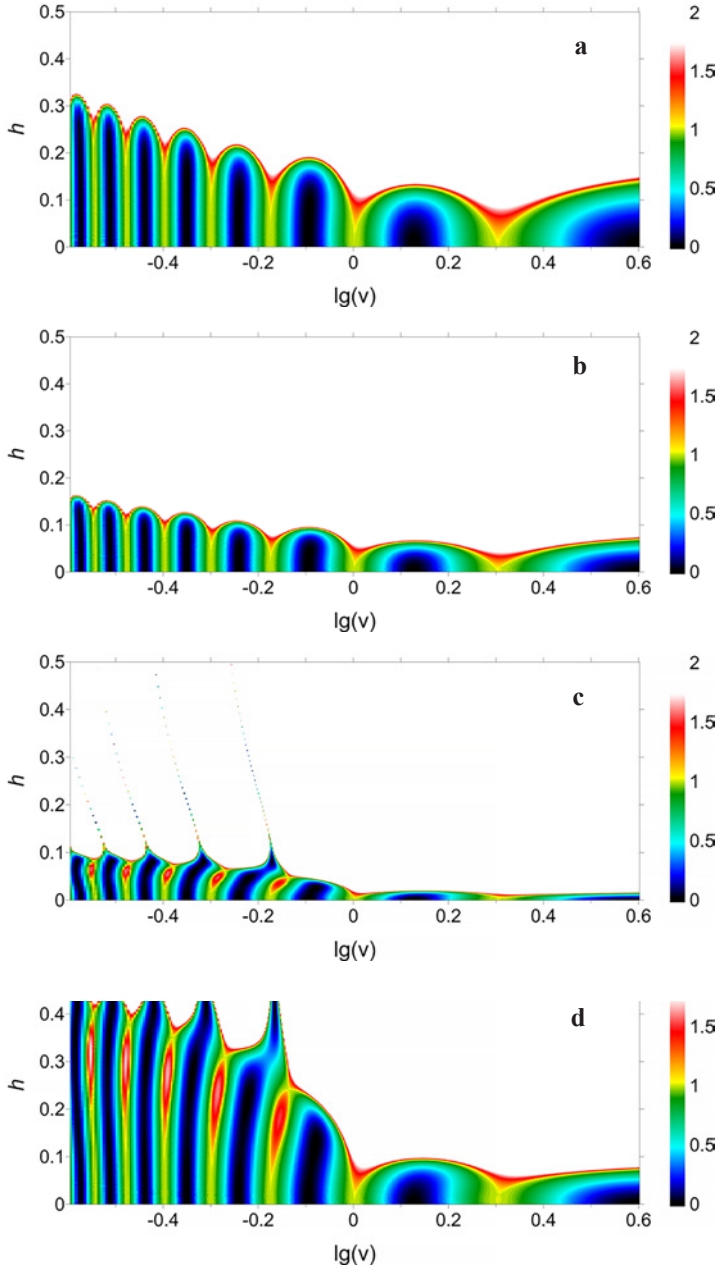

Fig. 1. Map of solution multiplier with different magnitude of exchange interaction: **a** $j = 0$; **b** $j = 0.015$; **c** $j = 0.021$; **d** $j = 0.025$; solution wavenumber $q = 10$; waves within the read and white areas are unstable.

Series of the numerical simulation is realized to consider the effect of main control parameters of the problem, namely the gyromagnetic parameter γ, wavenumber of spin wave q and interaction parameters j and p_d. The values $|m|^2$ and $|M|^2$ are set equal 0.2. The interaction parameters are close to the typical value for DMS, $p_d \approx j \approx 10^{-2}$. An admixture concentration n_S varies from 0.01 to 0.2.

In case of the relatively low gyromagnetic parameter ($\gamma < 2$), the system realizes the unstable regions qualitatively similar with the instability are of single-frequency forced Mathieu equation with resonances at $\nu = n/2$, n is a positive integer. If γ closes to 1, the system becomes less stable. If this parameter is small as well as large, the large stability areas realize even under relatively strong forcing.

The long-wave perturbations are insensitive to the variation of dipole and exchange interaction magnitude. At the same time, change of interaction parameters has a strong effect on the instability development of the finite-wave perturbations (Fig. 1). Increase of exchange magnitude stabilizes the system.

1. Tsiberkin K.B.: J. Magn. Magn. Mat. **523**, 167596 (2021)
2. Tsiberkin K.B.: Phys. Met. Metallogr. **122**, 358–361 (2021)
3. Kovacic I., Rand R., Mohamed Sah S.: ASME. Appl. Mech. Rev. **70**, 020802 (2018)

Po17

Mixed-valence iron complexes as multifunctional magnetic materials

A.R. Sharipova[1], E.E. Batueva[2], L.I. Savostina[1,2], E.N. Frolova[1], M.V. Ageeva[3], M.A. Cherosov[2], R.G. Batulin[2], O.A. Turanova[1], A.N. Turanov[1]

[1]Zavoisky Physical-Technical Institute, FRC Kazan Scientific Center of RAS, Kazan, Russia
[2]Institute of Physics, Kazan Federal University, Kazan, Russia
[3]Kazan Institute of Biochemistry and Biophysics, FRC Kazan Scientific Center of RAS, Kazan, Russia

Now, there is great interest in the search for materials that can be used to create fundamentally new devices for recording and storing information. This requires substances whose properties change reversibly under the influence of external factors. Molecular magnets are promising representatives of such compounds.

Multinuclear mixed-valence iron complexes have been synthesized, and their magnetic properties have been studied in this work. Three heptanuclear complexes with the general structural formula have been used as samples $[Fe(II)(CN)_6\{Fe(III)(L)\}_6]X_2$, where L = dianion of N,N′-bis[(2-hydroxyphenyl)methylene]-4-azaheptane-1,7-diamine (Salten), X = Cl (complex **1**), L = Salten, X = NCS (complex **2**), L = dianion of N,N′-

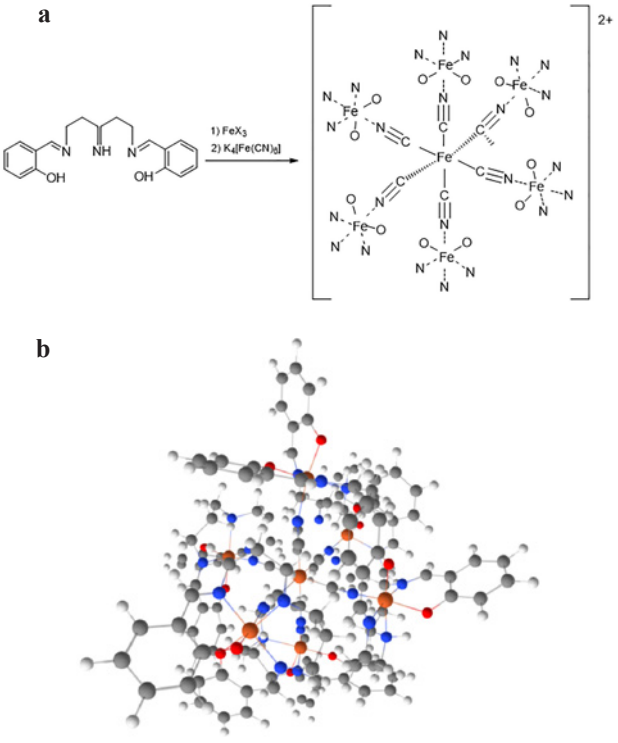

Fig. 1. a Synthetic route for preparation of the complex **2**; **b** 3D view of the complex **2**.

bis[(2-hydroxy-4-octadecyloxyphenyl)methylene]-4-azaheptane-1,7-diamine (18 Salten), X = Cl (complex **3**).

A liquid crystalline thermotropic phase for complex **3** has been identified by polarizing microscopy. The magnetic properties of these complexes have been studied by EPR and vibrational magnetometry in the temperature range from 5 to 300 K. The structure and properties of the synthesized compounds have been modeled by *ab initio* methods.

Po18

Hyperfine interactions in transition metal dichalcogenides Cr_xNbSe_2 (x = 0.33, 0.5) according to ^{93}Nb NMR data

N.A. Utkin[1], M.E. Kashnikova[1], A.G. Smolnikov[2], V.V. Ogloblichev[2], Y.V. Piskunov[2], A.F. Sadykov[2], D.F. Akramov[1,2]

[1]Institute of Physics and Technology, Ural Federal University, Ekaterinburg, Russian Federation
[2]M. N. Mikheev Institute of Metal Physics of the Ural Branch of the Russian Academy of Sciences, Ekaterinburg, Russian Federation

The paper presents the results of a ^{93}Nb NMR study of Cr_xNbSe_2 (x = 0.33, 0.5) – niobium dichalcogenide powders intercalated with chromium ions.

In recent works [1, 2] was revealed that the intercalation of 3d metal atoms (M) into 2H-NbS_2 and 2H-$NbSe_2$ not only suppresses superconductivity, but also generates various magnetic states in M_xNbX_2 depending on the type and concentration of intercalated M atoms as well as on the parent compound. It becomes possible to control the low-dimensional magnetic order in transition metal dichalcogenides.

Niobium spectra were obtained in a wide temperature range (from 35 to 293 K for x = 0.33 and from 28 to 293 K for x = 0.5) above and below the temperature point of the phase transition for a deeper understanding of the mechanisms responsible for changing the structural, magnetic and transport properties of the compound during intercalation of chromium ions. All spectra in the temperature range of the paramagnetic state of matter can be satisfactorily processed under the assumption of the presence of three lines in the entire NMR spectrum (Fig. 1). The position and shape of the line depends on the local charge and magnetic environments of the ^{93}Nb nuclei in the Cr_xNbSe_2 structure, and their intensity should correspond to the number of such nuclei.

Table 1 shows the values of the electric field gradient tensor (EFG-tensor) and magnetic shift for each of the three lines.

In the entire region of the paramagnetic state of matter, there is a change in the position and a homogeneous broadening in the spectrum of each of the three lines. At

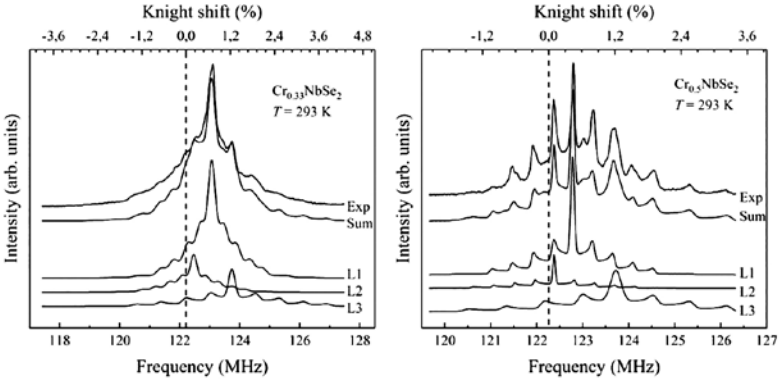

Fig. 1. Modeling of ^{93}Nb NMR spectra in Cr_xNbSe_2 (x = 0.33, 0.5) at temperature T = 293 K in an external magnetic field of 117.5 kOe with three lines.

Table 1. Parameters of the lines used to simulate the experimental ^{93}Nb NMR spectra presented in Fig. 1.

Sample	$Cr_{0.5}NbSe_2$			$Cr_{0.33}NbSe_2$		
Parameters of approximation	K_{iso} (%)	η	ν_Q (MHz)	K_{iso} (%)	η	ν_Q (MHz)
Line 1	0.444	0	0.89	0.683	0	0.89
Line 2	0.116	0	0.89	0.193	0	0.89
Line 3	1.224	0	1.63	1.241	0	1.63

the same time, the quadrupole frequency ν_Q and the asymmetry parameter η remain unchanged, which may indicate a change in the local magnetic environment of niobium nuclei while maintaining the local charge environment.

Figure 2 shows the dependence of the magnetic shift on temperature.

In the temperature region above the point of phase transition, line shifts repeat the behavior of magnetic susceptibility and are satisfactorily described by the Curie–Weiss law and can be associated with the spin magnetic susceptibility of chromium ions located near niobium nuclei. The proportionality of shifts and magnetic susceptibility is confirmed by the linear dependence of K–χ with a hidden parameter T. These data make it possible to determine the constants of the hyperfine Cr-Nb interaction in the studied compounds [3, 4].

Below the temperature point of the phase transition, there is a significant inhomogeneous broadening of the spectrum associated with the forming long-range magnetic order in the sublattice of chromium ions. NMR data below the Curie point allowed us to obtain information about the long-range magnetic order and the effect of an external magnetic field on the ferromagnetic phase transition.

This work was supported by the Russian Science Foundation (project no. 22-12-00220).

1. Cao Y., Huang Z., Yin Y. et al.: Mater. Today Adv. **7**, 100080 (2020)
2. Toporova N.M., Sherokalova E.M., Selezneva N.V. et al.: J. Alloys Compd. **848**, 156534 (2020)
3. Smol'nikov A.G., Ogloblichev V.V., Germov A.Yu. et al.: JETP Letters **107**, 134 (2018)
4. A.G. Smol'nikov, V.V. Ogloblichev, S.V. Verkhovskii et. al.: Physics of Metals and Metallography **118**, 134 (2017)

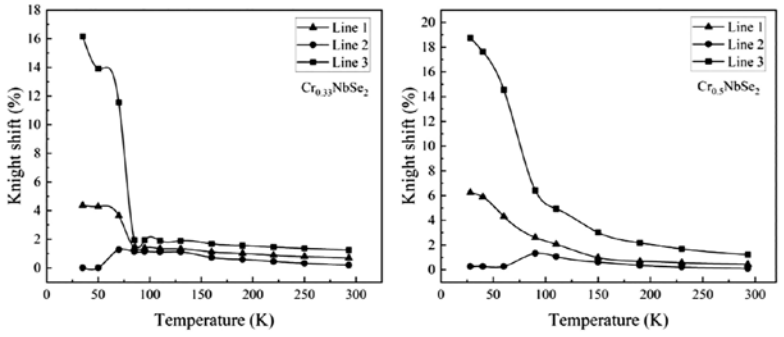

Fig. 2. Temperature dependence of the Knight shift of ^{93}Nb for the lines presented in Fig. 1.

Po19

Superconducting spin-valve structure Co1/Pb/Co2 with insulator layers in F/S interfaces

A.A. Validov, M.I. Nasyrova, R.R. Khabibullin, I.A. Garifullin

Zavoisky Physical-Technical Institute, FRC Kazan Scientific Center of RAS, Kazan, Russia,
e-mail: validov@kfti.knc.ru

Now the classical SSV structures have been studied in sufficient detail and well. Latest results show (see, e.g., [1, 2]), the limiting values of the SSV effect have already been practically achieved using various alloys and elemental materials in F1/F2/S structures. In this regard, it is necessary to study non-standard unusual SSV models. One of the such possible variants of models can be SSV structures with insulator layers. The possibility of observing a significant SSV effect ΔT_c ~0.3 K in SSV structures with insulator layers was demonstrated by Deutscher and Meunier in 1969 [3].

In present work are given our first experimental investigation of the superconducting properties of Co1/Pb/Co2 SSV structure with insulator layers. We created thin oxide layers into Co1/Pb and Pb/Co2 interfaces similarly [3]. Electrical resistivity measurements were carried out by standard DC four-point method. An external magnetic field was always applied in-plane of the sample in all measurements. The superconducting critical temperature T_c was defined as the midpoint of the transition curve.

Figure 1 depicts superconducting transition curves at P (H_0 = +1 kOe) and AP (H_0 = –1 kOe) orientations of the Co1 and Co2 layers's magnetization, respectively. The value of SSV effect ΔT_c = 0.2 K. The figure shows that the $\Delta T_c > \delta T_c$. Thus, the full SSV effect was observed.

Our results demonstrate the possibility of observing the SSV effects in SSV structures with insulator layers. It seems that the observation of SSV effects in such structures is not obvious, since S/F interface is bad. But from our experimental results and the results in [3] it follows that quite large SSV effects are observed.

We investigated superconducting properties of Co1/Pb/Co2 heterostructures with insulator layers. In these heterostructures thin oxide layers (insulator layers) were

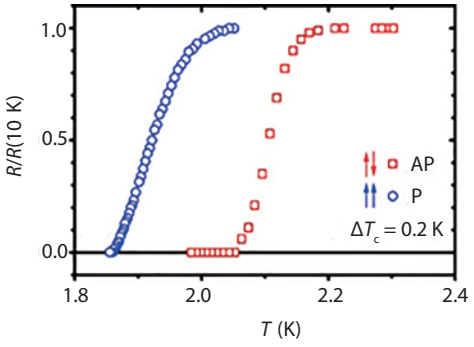

Fig. 1. Superconducting transition curves at P (H_0 = +1 kOe) (○) and AP (H_0 = –1 kOe) (□) orientations of the Co1- and Co2-layer's magnetizations, respectively.

formed into Co1/Pb and Pb/Co2 interfaces. We have observed full superconducting spin valve effect with value of ΔT_c reached 0.2 K. It can be assumed that investigation of SSV structure with insulator layers is a promising area of research. We have also studied superconducting properties of Co1/Pb/Co2 structures with similar parameters, but without insulator layers. T_c for these samples was not registered until 1.4 K. This is due to the free penetration of Cooper pairs from the S-layer into the F-layers.

The research was supported by the Russian Science Foundation grant No. 22-22-00916.

1. Gu Y., Hal'asz G.B., Robinson J.W.A., Blamire M.G.: Phys. Rev. Lett. **115**, 067201 (2015)
2. Singh A., Voltan S., Lahabi K., Aarts J.: Phys. Rev. X **5**, 021019 (2015)
3. Deutscher G., Meunier F.: Phys. Rev. Lett. **22**, 395 (1969)

Po20

Study of a series of the Fe(III) complexes with photoisomerizable axial ligands by NMR, EPR and UV-spectroscopy

M.Yu. Volkov, E.N. Frolova, O.A. Turanova, A.N. Turanov, L.V. Bazan, L.G. Gafiyatullin, I.V. Ovchinnikov

Zavoisky Physical-Technical Institute, FRC Kazan Scientific Center of RAS, Kazan, Russia

The study of spin crossover (SCO) materials based on transition metal ions is promising for the development of technical devices: displays and memory in electronic devices. In order to obtain such materials, bistable molecular systems are required, which can exist in two different electronic states. Spin-variable Fe(III) complexes are such systems. The spin transition in them can be induced by external exposures (temperature, light, etc.). The spin state of complexes also depends on many factors: the composition and structure of ligands, the presence or absence of a counterion and solvate, the intensity of intra- and intermolecular interactions. The problem of the relationship between the structure and magnetic properties of the complexes is relevant, so it is important to establish the correlation between them. The introduction of a photosensitive fragment (for example, a C=C or N=N group) into the ligand makes the complexes potentially photoisomerizable with the prospect of their application in devices where the magnetic properties of a substance can be controlled by light.

A series of complexes with the general chemical formula $[Fe(SB)(Sp)_2]BPh_4$ have recently been studied [1]. UV irradiation of such complexes leads not only to *cis-trans* isomerization of the 4-styrylpyridine axial ligands, but also to their cyclization with

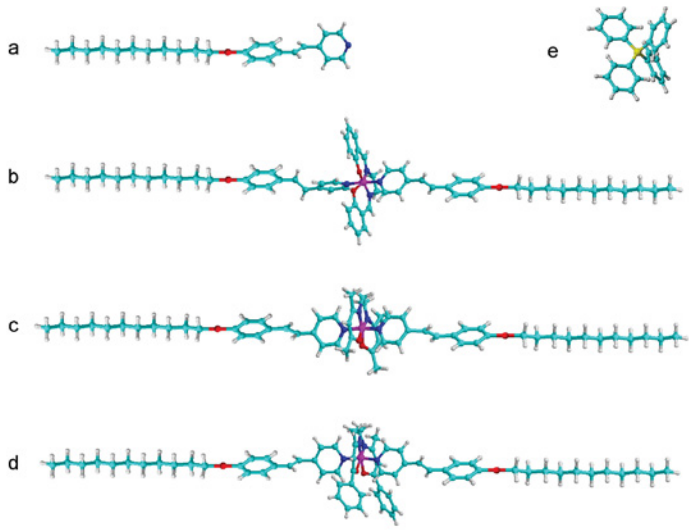

Fig. 1. Photoisomerizable ligand 4-undecyloxystyrylpyridine which mentioned below as Sp-11 (**a**). Structure of the synthesized Fe(III) complexes $[Fe(Salen)(Sp\text{-}11)_2]BPh_4$ (**b**), $[Fe(Acen)(Sp\text{-}11)_2]BPh_4$ (**c**), $[Fe(Bzacen)(Sp\text{-}11)_2]BPh_4$ (**d**), in which the axial ligands are Sp-11 and the counterion is BPh_4 (**e**).

Po20

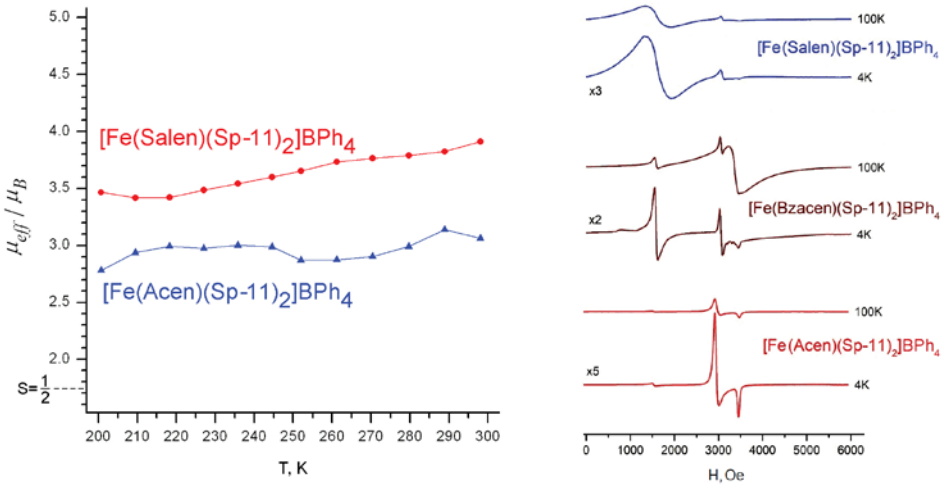

Fig. 2. EPR spectra of the complexes in powders (left). Temperature dependences of μ_{eff} for the solutions of the studied complexes in CH_2Cl_2 at C_M = 5 mmol/L obtained by NMR (right). The complex [Fe(Bzacen)(Sp-11)$_2$]BPh$_4$ was not studied by NMR due to its low solubility.

detachment from the central ion, i.e., to the destruction of the complexes. Therefore it is more reasonable to use 4-styrylpyridine with long alkyl chains, which is not subject to cyclization under UV irradiation, as axial ligands.

In this work, several Fe(III) complexes with photoisomerizable axial ligands have been first synthesized, characterized and studied. The general chemical formula of the complexes is [Fe(SB)(Sp-11)$_2$]BPh$_4$, where Sp-11 is 4-undecyloxystyrylpyridine (Fig. 1a), SB are dianions of Schiff bases: Salen, Bzacen and Acen [1]. The complexes were studied in solutions by UV-visible and NMR spectroscopy, in the solid state and in vitrified solutions by EPR spectroscopy.

The UV-vis spectra of the complexes show intense absorption bands in the region of 350 nm, which belong to the n–π* and π–π* transitions of the C=C and C=N groups of ligands. A weakly intense absorption band at 680–720 nm, which belongs to low-spin complexes, appears only in CH_2Cl_2 solutions. The effect of the chemical structure of the equatorial ligand on the spin state of the Fe(III) ion in complexes was studied in powders and in solutions of CH_2Cl_2 (Fig. 2). The EPR method revealed an incomplete spin crossover in the complexes in powders and vitrified solutions in the temperature range 4–340 K. The NMR measurements indicate that an incomplete smooth spin crossover between the LS and HS states is observed in the solution of the [Fe(Salen)(Sp-11)$_2$]BPh$_4$ complex. In a solution of the [Fe(Acen)(Sp-11)$_2$]BPh$_4$ complex, the number of LS ions noticeably exceeds the number of HS ions.

These conclusions differ from the results obtained for analogous complexes with unsubstituted 4-styrylpyridine [1]. Thus, in this work it is shown that long alkoxy chains in ligands lead to additional intermolecular interactions, which in turn cause a change in the spin properties of the complexes.

1. Turanova O.A., Volkov M.Y., Frolova E.N., Bazan L., Garifzianova G.G., Gafiyatullin L.G., Ovchinnikov I.V., Turanov A.N.: J. Chem. Phys. **152**, 014306 (2020)

Po16

A lipid system in the ionic liquid – water mixtures studied by magnetic resonance measurements and molecular dynamics

A.V. Khaliullina[1], A.R. Khakimzyanova[1], A.N. Sashina[1], A.M. Khakimov[2], A.N. Turanov[3], A.V. Filippov[4]

[1]Institute of Physics, Kazan Federal University, Kazan, Russia
[2]Institute of Civil Engineering, Kazan State University of Architecture and Engineering, Kazan, Russia
[3]Zavoisky Physical-Technical Institute, FRC Kazan Scientific Center of RAS, Kazan, Russia
[4]Division of Chemical Engineering, Luleå University of Technology, Luleå, Sweden

An ionic liquid (IL) is a salt in the liquid state. Ionic liquids have many potential applications. For instance, they can be used as electrolytes or powerful solvents. However, the toxic effects of ILs to biological objects are discussed if leaked into the environment. Investigations of the interaction of the ionic liquid with the biomembranes can be important to uncover the effects of ionic liquids on the biological bodies.

In this work, we discuss the features of the phase behavior and molecular mobility of a system consisting of lecithin at a concentration of 2% by weight in a mixture of solvents of ethylammonium nitrate (EAN) with deuterated water (D_2O).

Analysis of spectra by the ^{31}P NMR spectroscopy revealed two lipid phases in the systems: lamellar phase in the lecithin – D_2O system, and an isotropic phase in the lecithin – EAN system. In a D_2O – EAN mixture, the ratio of these two phases correlates with the proportions of D_2O and EAN solvents.

Diffusion NMR experiments were carried out using the pulsed-field gradient method. The self-diffusion coefficient (SDC) value related to lipids in EAN can be associated with the movement of diffusing micelles with a size ~20 nm recorded in the ^{31}P spectrum as an isotropic signal; the SDC related to lipids in D_2O may be associated with the movement of diffusing vesicles with a size of ~100 nm.

As the proportion of D_2O in the D_2O-EAN solvent mixture increases, the self-diffusion coefficients related to the ionic liquid and lipids increase, i.e. the system becomes more mobile, which may be due to a decrease in viscosity.

According to NMR relaxometry data, the transverse magnetization decays for the lipid system in a mixture of D_2O-EAN solvents (in the ratios from 80/20 to 20/80), are due to the sum of contributions from three components, which indicates the presence in the system of components with different molecular mobility: "liquid-phase" and components associated with the movement of diffusing micelles and vesicles observed in ^{31}P spectra.

Using molecular dynamics method, a uniform distribution of particles in the system (ratio of EAN/H_2O is 35/65) was observed with formation of a network of hydrogen bonds between ethylammonium and nitrate ions with H_2O molecules. For the EAN system with water, the SDC of the EAN components is increased significantly, as was observed in the diffusion NMR experiments. This can be explained by the fact that the hydration of EAN ions weakens the strong Coulomb and hydrogen interactions between cations and anions, which leads to a decrease in viscosity. An analysis of the radial distribution function showed that water hydrates the polar part of the $[NH_3]^+$ cation more preferentially than the $[NO_3]^-$ anion.

Po21

EPR study of the nitric oxide content in hippocampus and liver of rats in the simulation of cerebral ischemia followed by reperfusion

G.G. Yafarova[1,2], V.V. Andrianov[1,2], V.A. Kulchitchky[3], L.V. Bazan[1,2], T.K. Bogodvid[2,4], V.S. Iyudin[1], M.M. Bakirov[1], N.G. Shayakhmetov[5], E.V. Fedorova[3], T.A. Filipovich[3], A.V. Nagibovv[3], Kh.L. Gainutdinov[1,2]

[1]Zavoisky Physical-Technical Institute, FRC Kazan Scientific Center of RAS, Kazan, Russia
[2]Institute of Fundamental Medicine and Biology of Kazan Federal University, Kazan, Russia
[3]Institute of Physiology of Nat. Acad. of Sci. of Belarus, Minsk, Belarus
[4]Volga Region State University of Physical Culture, Sport and Tourism, Kazan, Russia
[5]Interregional Clinical Diagnostic Center, Kazan, Russia,
e-mail: kh_gainutdinov@mail.ru

With a decrease in the oxygen content in the inhaled air, violations of cerebral blood flow, leading to a lack of oxygen supply to the brain, cerebral ischemia occurs, which can result in an ischemic stroke, accompanied by damage to brain tissue and its functions [1]. During hypoxia and ischemia of the brain, the functioning of neurotransmitter systems, including the nitrogen monoxide system, is disrupted. Currently, there is no consensus on the role of endogenous NO in the processes occurring with damage to the nervous system [2]. In addition to vasodilating, neurotransmitter and stress-limiting properties, the involvement of NO in the reactions of oxidative stress, the glutamate-calcium cascade and inflammation has been demonstrated [3]. It has been shown that the development of cerebral ischemia and the subsequent occurrence of stroke are associated with a weakening of cerebral blood flow, as well as with violations of the regulation of blood supply to brain tissues by the NO system [4]. A violation of the oxygen supply to the brain also occurs when a vessel is thrombosed or an aneurysm ruptures, which often ends with an ischemic or hemorrhagic stroke [5]. Cerebral ischemia causes multiple and multidirectional changes in the NO content in the brain and in signal transmission. The available contradictory information suggests that there is currently no consensus on the role of endogenous NO in the processes occurring with damage to the nervous system [6]. According to the research results, the role of NO in these hypoxia-ischemia processes is contradictory: NO is able to perform both neurotoxic and neuroprotective functions [7]. The aim of our work was to study the intensity of NO production in the hippocampus of rats after ischemic brain damage by spectroscopy of electron paramagnetic resonance (EPR).

Ischemia was simulated at the Institute of Physiology of the National Academy of Sciences of Belarus, Minsk by means of a 10-minute violation of blood flow by ligation of both carotid arteries at the level of the vocal cords and taking 3 ml of blood from the common carotid artery. Measurement of NO content in brain tissue were performed by the method of electron paramagnetic resonance (EPR) [8, 9]. The method allows direct measurements, and is highly sensitive due to the use of spin traps. The components of the spin trap NO (DETC-Na, $FeSO_4$, sodium citrate) was injected 30 min before the extraction of studied tissue. The measurements of the spectra of the complex $(DETC)_2$-Fe^{2+}-NO were performed on the spectrometer EMX/plus with a temperature module ER 4112HV in the X band (9.50 GHz). The amplitude of the EPR-spectra was always normalized to the weight of the sample.

30 minutes after the introduction of the spin trap components, hippocampal and liver tissues were taken (one sample, about 100 mg). The selected areas were immediately frozen at liquid nitrogen temperature and transported from Minsk to Kazan in plastic containers with dry ice. A significant decrease in NO production in the hippocampus was shown 1 day after modeling an ischemic stroke caused by carotid artery ligation, and by 56% – during carotid artery ligation followed by taking 3 ml of blood from the common carotid artery.

Electron spin resonance measurements were performed with the financial support from the government assignment for FRC Kazan Scientific Center of RAS.

1. Donnan G.A. et al.: Lancet **371**, 1612–1623 (2008)
2. Calabrese C. et al.: Antioxidants and Redox Signaling **11**, 2717–2739 (2009)
3. Steinert J.R. et al.: Neuroscientist **16**(4), 435–452 (2010)
4. Terpolilli N.A. et al.: Cereb. Blood Flow Metab. **32** (7), 1332–1346 (2012)
5. Garry P.S. et al.: Experim. Neurol. **263**, 235–243 (2015)
6. Vanin A.F.: Biofizica **62**(4), 629–656 (2017)
7. Deryagin O.G. et al.: Neurosci. Behav. Physiol. **48**(1), 58–63 (2018)
8. Mikoyan V.D., Kubrina L.N. et al.: Biochim. Biophys. Acta **1336,** 225–234 (1997)
9. Vanin A.F., Huisman A. et al.: Methods in Enzymology **359**, 27–42 (2003)

Po22

Investigation of gallium iron oxide by the ESR method

I.V. Yatsyk[1], R.M. Eremina[1], E.M. Moshkina[2]

[1]Zavoisky Physical-Technical Institute, FRC Kazan Scientific Center of RAS, Kazan, Russia, e-mail: I.Yatsyk@gmail.com
[2]Kirensky Institute of Physics, Federal Research Center KSC SB RAS Krasnoyarsk, Russia

The multiferroic materials, which exhibit coexistence and coupling of magnetic and electric orders, have emerged as promising candidates for basic understanding of the coupling between magnetic and electronic properties and uses of the materials in magnetoelectric devices, such as memory, logic devices, sensors, and voltage-driven magnetic tunnel junctions [1–6]. The integration of naturally existing or artificially designed multiferroic materials into devices opens up a new field to achieve the energy-saving and miniaturization of the devices [7]. Some transition metal oxides ($BiFeO_3$, $TbMnO_3$, $BiMnO_3$, $HoMnO_3$, $DyFeO_3$, and $GaFeO_3$) have shown multiferroic properties [1–7] and majority of these oxides showed magnetic order at low temperatures.

The aim of this work is to study by ESR, magnetometry methods magnetic properties of $Fe_{1.21}Ga_{0.79}O_3$. Temperature and angular evolution of the ESR line in (*ab*) plane are shown in Fig. 1. At angle 70°, there is a sharp increase in the ESR linewidth and resonant field up to 700 mT. We believe that this is the ferromagnetic lines.

I.V.Y. and R.M.E. acknowledge the financial support from the government assignment for FRC Kazan Scientific Center of RAS.

1. Lone A.G., Bhowmik R.N.: J. Alloys and Comp. **905**, 164164 (2022)
2. Fiebig M., Lottermoser T., Meier D., Trassin M.: Nat. Rev. Mater. **1**, 16046 (2016)
3. Lu C., Wu M., Lin L., Liu J.M.: Natl. Sci. Rev. **6**, 4 (2019)
4. Spaldin N.A.: Proc. R. Soc. A **476**, 20190542 (2020)
5. Catalan G., Scott J.F.: Adv. Mater. **21**, 2463–2485 (2009)
6. Wang Y.J., Li J.F., Viehland D.: Mater. Today **17**, 269–275(2014)
7. Pyatakov A.P., Zvezdin A.K.: Phys. Usp. **55**, 557–581 (2012)

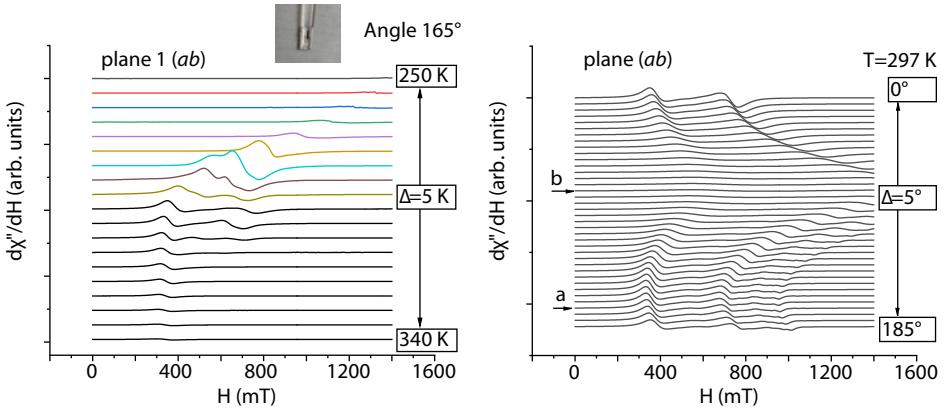

Fig. 1. Temperature (left) and angular (right) evolution of the ESR line in (*ab*) plane of $Fe_{1.21}Ga_{0.79}O_3$.

Po23

Influence of additional iron impurities on properties of Nb^{4+} paramagnetic centers embedded in BaF_2 crystals: results of EPR study

R.B. Zaripov[1], V.A. Ulanov[1,2]

[1]Zavoisky Physical-Technical Institute, FRC Kazan Scientific Center of RAS, Kazan, Russia
[2]Kazan State Power Engineering University, Kazan, Russia

In this work, we studied the effect of an additional iron impurity on the properties of an associate of niobium with two interstitial fluorine ions. The studies were carried out by the EPR spectroscopy in X and Q frequency bands. The figure 1 shows the EPR spectra of BaF_2:Nb and BaF_2:(Nb+Fe) single crystals.

It can be seen from the Fig. 1 that both spectra contain two types of Nb^{4+} centers characterized by almost the same parameters of hyperfine interaction with the magnetic moments of niobium nuclei. In the first type centers niobium ion does not have excess charge compensators (interstitial fluorine ions) in its immediate environment, but the second type centers are associates of the Nb^{4+} ion with two interstitial fluorine ions. The presence of an iron impurity in the BaF_2:(Nb+Fe) crystal significantly reduced the concentration of associates and, in addition, manifested itself in the appearance of new centers associated with impurity iron ions in the crystal.

Molecular structures and the nature of magnetic interactions in the niobium and iron centers formed during the synthesis of a BaF_2:(Nb+Fe) single crystal sample are discussed.

The research was supported financially by Russian Science Foundation (project #23-22-00402).

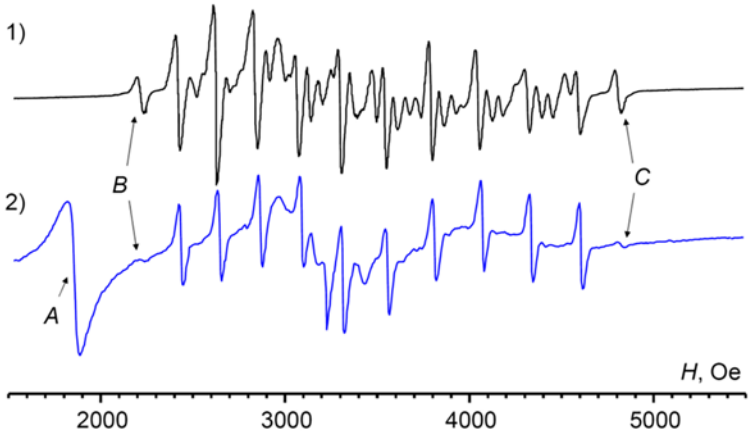

Fig. 1. EPR spectra of the BaF_2:Nb (1) and BaF_2:(Nb+Fe) (2) crystals registered in **H**||<001> orientation at 4.2 K (f = 9.3 GHz).

Po24

Nonthermal photoinduced reduction of the coercivity in thin epitaxial films of the $L1_0$-phase FePt and $FePt_{0.84}Rh_{0.16}$

A.V. Petrov[1], S.I. Nikitin[1], L.R. Tagirov[1,2], A.S. Kamzin[3], R.V. Yusupov[1]

[1]Kazan Federal University, Kazan, Russia, e-mail: flypetrov@yandex.ru
[2]Zavoisky Physical-Technical Institute, FRC Kazan Scientific Center of RAS, Kazan, Russia
[3]Ioffe Institute, St.-Petersburg, Russia

The time-resolved magneto-optical Kerr effect in epitaxial thin films of the FePt compound and the $FePt_{0.84}Rh_{0.16}$ solid solution with perpendicular magnetic anisotropy on the MgO (001) substrates was studied. Investigation of the hysteresis loop evolution on fast (100 fs – 1 ns) and slow (1 – 20 ms) time scales after the excitation with a femtosecond light pulse (Fig. 1) revealed an effect of long-lived non-thermal magnetic softening of the films. The value of the coercive field is restored on a time scale of milliseconds. A hypothesis relating the observed phenomenon to the excitation of high-Q acoustic resonances in the substrate/film system and strong magnetoelastic interaction in FePt and $FePt_{0.84}Rh_{0.16}$ films is proposed.

Comparison of the hysteresis loops under ultrashort pulse laser excitation with the data of static magnetometry indicates the nonthermal nature of the decrease in coercivity, since the temperature is restored after approximately 2 ns from the pump pulse.

The process of magnetization reversal of a continuous thin film with perpendicular magnetic anisotropy, includes two necessary stages, namely, the nucleation of domains with the opposite direction of magnetization and their growth due to the domain wall motion. Since both the nucleation and the motion of domain walls are of an activation origin, we suggest that a hypersonic wave induced by a femtosecond laser pulse increases the energy of the magnetic subsystem via inverse magnetostriction. The latter promotes domain nucleation and facilitates the overcoming by domain walls energy barriers arising from their pinning on defects.

Support by the Kazan Federal University Strategic Academic Leadership Program (PRIORITY-2030) is acknowledged.

1. Akulov N.S., Alizade Z.I., Belov K.P.: Doklady Akademii Nauk SSSR **65**, 815 **(**1949)

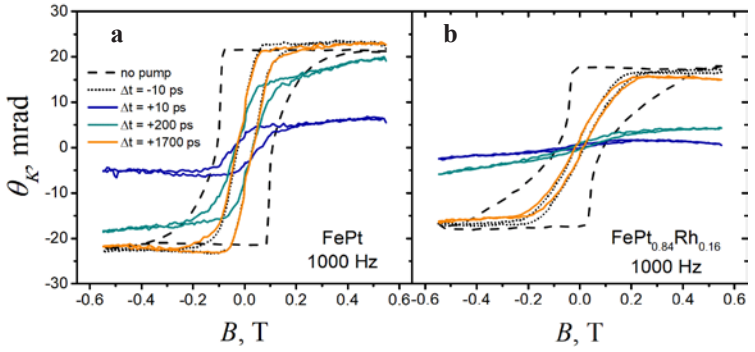

Fig. 1. Magnetization reversal curves of thin FePt (**a**) and $FePt_{0.84}Rh_{0.16}$ (**b**) epitaxial films in terms of the Kerr rotation angle at T = 300 K, pump pulse repetition rate 1 kHz, and pump density 6.4 mJ/cm^2. The colors and line types of the hysteresis curves correspond to different times (see the legend).

AUTHOR INDEX

SPONSORS

Element

Electron paramagnetic resonance spectrometers

X-band и W-band

Magnetic field 0.5-6 T

ZHONGTAI

a santai science company

SANTAI TECHNOLOGIES quality since 2004

Flash chromatographs

Purification and separation of organic synthesis products

Flash columns

WIGGENS THE MAGIC MOTION

General laboratory equipment

Rotary evaporators, centrifuges, mixers, homogenizers, heating blocks, shakers, etc.

Element

- supply of equipment
- installation
- training
- service maintenance

ZHONGTAI

NV magnetometer

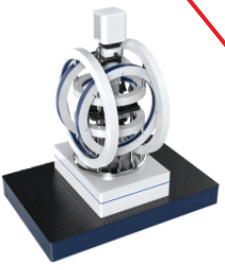

NV-Microscope

Important ELEMENT of your laboratory

УНИВЕРСАЛЬНАЯ СИСТЕМА НАГРЕВА И ОХЛАЖДЕНИЯ
THMS600

НАГРЕВ И ОХЛАЖДЕНИЕ	ОПТИЧЕСКИЕ МЕТОДЫ	ПЕРЕМЕННАЯ СКОРОСТЬ НАГРЕВА
Диапазон температур от <-195°C до 600°C	Поддержка конфокальной, рамановской, световой микроскопии, рентгенографии и др.	Точный контроль от 0,01°C до 150°C / мин

"НАУКА"
Центр Технического Сопровождения

Адрес: 129626, Россия, Москва, ул. Маломосковская, 22, стр. 1, «Технопарк»
Телефон: +7 (499) 322 06 62
E-mail: info@nauka-shop.ru
www.nauka-shop.ru

"НАУКА"

Центр Технического Сопровождения

Адрес: 129626, Россия, Москва,
ул. Маломосковская, 22, стр. 1, «Технопарк»
Телефон: +7 (499) 322 06 62
Моб.: +7 926 422 93 04
E-mail: info@nauka-shop.ru

КРИОГЕННЫЕ РЕФРИЖЕРАТОРЫ SHI CRYOGENICS СЕРИИ RDK

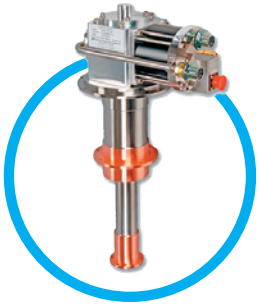

Компания «ЦТС Наука» предлагает приобрести криогенные рефрижераторы производства компании SHI Cryogenics:

- рефрижераторы Гиффорда-МакМагона,
- рефрижераторы с импульсной трубкой
- рефрижераторы Гиффорда-МакМагона/ Джоуля-Томпсона, с диапазонами температур от 4 K до 77+ K.
- Криогенные рефрижераторы SHI Cryogenics изготавливаются на производственных объектах мирового класса с использованием современных производственных и технологических возможностей в соответствии с концепцией «шести сигм». В результате получается продукция, отличающаяся высокой надежностью, удобством использования, поддерживаемая международными торговыми и обслуживающими сетями.
- Криогенные рефрижераторы Гиффорда-МакМагона на 4K от SHI Cryogenics Group — надежные и универсальные системы. Они гораздо выгоднее экономически, чем системы с незамкнутым циклом на основе жидкого гелия. Криогенные рефрижераторы RDK характеризуются высокой холодопроизводительностью, компактной конструкцией и универсальностью, признаны стандартными для МРТ. Рефрижераторы SHI применяют для охлаждения широкого спектра устройств в экспериментах и аналитических исследованиях.

SHI Cryogenics Group

ЛАБОРАТОРНОЕ ОБОРУДОВАНИЕ | РАСХОДНЫЕ МАТЕРИАЛЫ | СЕРВИС

КРИОСТАТЫ ЗАМКНУТОГО ЦИКЛА С ИЗМЕНЯЕМОЙ ТЕМПЕРАТУРОЙ С НИЗКИМ УРОВНЕМ ВИБРАЦИЙ И ПРИМЕНЕНИЕМ РЕЗИНОВОГО СИЛЬФОНА

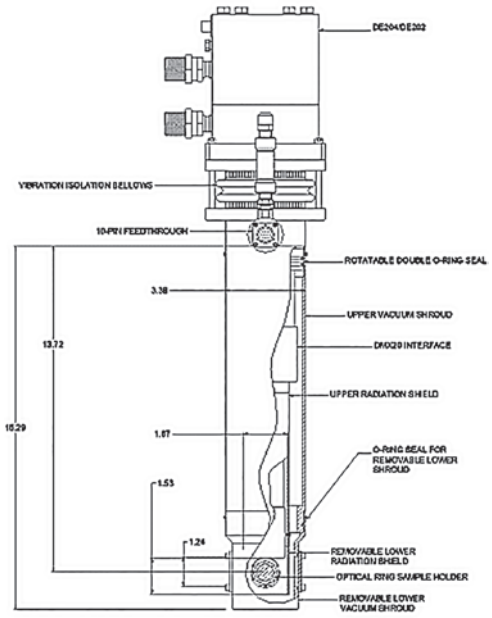

ПРИНЦИП РАБОТЫ

Этот инновационный криостат, изготовленный Cryo Industries, работающий по схеме «Образец в вакууме», имеет крайне низкий уровень вибраций благородя конструкции с гибким резиновым сильфоном и теплопередаче через газ. **Результатом является сверхнизкий уровень вибраций образца!**

Охлаждение для долгой роботы при низких температурах обеспечивается рефрижератором замкнутого цикла, работающим на пульсирующих трубках или по принципу Гиффорда-МакМагона. **Жидкий хладагент не требуется!**

Стандартная комплектация может быть с различными криостатами: трубчатым, оптическим со сверхвысоким вакуумом и с узким зазором. **Доступные диапазоны рабочих температур вплоть до 3 К.**

- Доступные диапазоны рабочих температур вплоть до 3 К.
- Доступны системы с охлаждающими головками на 10К, 6,5 К и 4 К с различной мощностью охлаждения
- Системы со сверхнизкой вибрацией доступны с четырьмя стационарными опорами и/или мобильной опорой с регулируемым креплением и подъёмным рычагом.

"НАУКА"

Центр Технического Сопровождения

Адрес: 129626, Россия, Москва, ул. Маломосковская, 22, стр. 1, «Технопарк»
Телефон: +7 (499) 322 06 62
E-mail: info@nauka-shop.ru
www.nauka-shop.ru

"НАУКА"

Центр Технического Сопровождения

Адрес: 129626, Россия, Москва,
ул. Маломосковская, 22, стр. 1, «Технопарк»
Телефон: +7 (499) 322 06 62
Моб.: +7 926 422 93 04
E-mail: info@nauka-shop.ru

CRYOGENIC

ПОЛНОСТЬЮ АВТОМАТИЗИРОВАННАЯ ИЗМЕРИТЕЛЬНАЯ СИСТЕМА

Диапазон температур
+ 1,6 K–400 K в стандартной версии
+ Минимальная температура 300 мк в версии с вставкой реконденсации He-3:
+ Минимальная температура 50 мК
+ Вставки для высоких температур: 700 / 1000 K
+ Стабильность температуры — мК во всем диапазоне магнитного поля
+ До 9 T версии mini-CEMIS
+ До 18 T в версии CFMS с сильным полем
+ Опция низких полей — для измерения полей в области практически нулевого поля

СУХИЕ КРИОГЕННЫЕ ИЗМЕРИТЕЛЬНЫЕ СИСТЕМЫ (CFMC)

ПРЕИМУЩЕСТВА БЕЗЖИДКОСТНОЙ ИЗМЕРИТЕЛЬНОЙ СИСТЕМЫ (CFMS)

Объекты общего пользования — для всех пользователей
+ Полное отсутствие криогенных жидкостей
+ Не требуется специальный опыт
+ Большие интервалы обслуживания

Высокий уровень безопасности и удобства
+ Отсутствие перекачивания криогенных жидкостей
+ Отсутствие опасности из-за испаряющихся газов
+ Полная зашита при отключении электроэнергии
+ Быстрая замена образца

Модульная архитектура
+ Совместимость с любыми измерительными модулями
+ быстрая взаимозаменяемость модулей

Автоматическое управление
+ Стабильные эксплуатационные характеристики поля и температуры.
+ Работа в автоматическом режиме (не требует присутствия)
+ Обеспечение возможности проведения сложных и длительных экспериментов

Поддержка в течение всего срока службы
+ Прямая поддержка со стороны производителя
+ Удаленная поддержка системы через Интернет
+ Международная команда обслуживания
+ Бесплатные обновления программного обеспечения

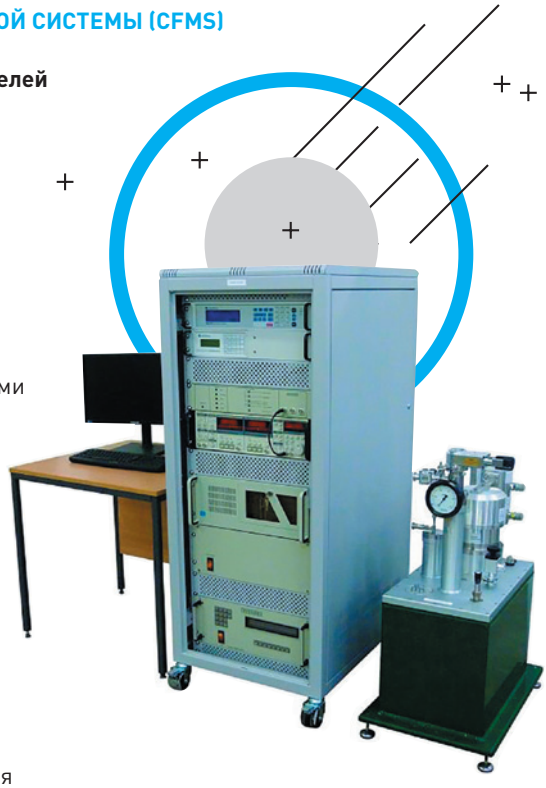

ООО «Криотрейд инжиниринг»
125367, г. Москва, Полесский проезд, дом 14А
Тел./факс: +7 (495) 374-69-52
Web: www.cryotrade.ru E-mail: sales@cryotrade.ru

ООО «Криотрейд инжиниринг» – это торгово-производственная компания, выполняющая поставки научного оборудования для лабораторий и промышленности на протяжении 15 лет. Основное направление деятельности – производство криостатов для научных исследований. Также выполняется гарантийное и постгарантийное сервисное обслуживание криостатов и криогенных систем, а также их модернизация под новые задачи. Наши высококвалифицированные технические специалисты всегда готовы помочь с подбором оборудования, максимально соответствующего требованиям заказчика.

Собственное оборудование:

- Компактные заливные азотные криостаты моделей LN-120 и LN-121-SPECTR (диапазон температур – от 77 до 500К);
- Азотные и гелиевые криостаты проточного и замкнутого типа – как стандартные, так под задачи пользователя;
- Гелиевые криостаты замкнутого типа со сниженными вибрациями для оптических экспериментов;
- Сверхпроводящие магниты любой конфигурации;
- Криостаты с базовой температурой 0.3 и 0.8К;

- Переливные устройства для LN_2 и LHe с ЭВТИ, а также системы выдачи азота (азотные питатели);
- Криовакуумные камеры и холодные экраны, а также температурные столы для вакуумных камер;

- Генераторы жидкого азота производительностью от 20 до 300 л/сутки.

ООО «Криотрейд инжиниринг»
125367, г. Москва, Полесский проезд, дом 14А
Тел./факс: +7 (495) 374-69-52
Web: www.cryotrade.ru E-mail: sales@cryotrade.ru

Поставляемое криогенное, холодильное и вакуумное оборудование:

- Гелиевые ожижители и реконденсаторы производительностью от 20 до 200 л/сутки;
- Термостатируемые столики с диапазоном температур -190…+ 1200 ºС, подходящие в том числе для микроскопии;
- Любое сопутствующее криогенное оборудование – криогенные провода, температурные датчики, мониторы и контроллеры температур, источники тока сверхпроводящих магнитов, сосуды Дьюара др.;

- Чиллеры и термостабилизаторы – от компактных настольных (в т.ч. для лазеров – с высокой стабилизацией температуры) до промышленных систем уличного исполнения с мощностью охлаждения до 100 кВт;

- Турбомолекулярные откачные посты, вакуумные датчики, насосы, а также сопутствующие товары и арматура;
- Криогенные рефрижераторы, в том числе компактные
- Оборудование для вакуумных систем – сверхвысоковакуумные переносные камеры, системы линейного перемещения (от 1 до 5 осей), высокотемпературные испарители, затворы и многое другое;
- LN_2 генераторы смесевого типа производительностью от 1 до 50 л/ч.

ООО «Криотрейд инжиниринг»
125367, г. Москва, Полесский проезд, дом 14А
Тел./факс: +7 (495) 374-69-52
Web: www.cryotrade.ru E-mail: sales@cryotrade.ru

Лабораторное и измерительное оборудование:

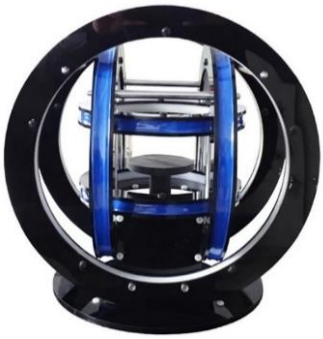

- Электромагниты, в том числе векторные, катушки Гельмгольца, а также установки на их основе (VSM, системы измерения эффекта Холла, Керра, установки размагничивания и другие);
- Гаусс-метры и флюксметры, а также зонды для них, в том числе криогенные;

- Электрическое измерительное оборудование (мультиметры, источники тока/ напряжения, LCR-метры, источники-измерители, импедансные анализаторы, тестеры проводов и батарей и т.п.);

- Синхронные усилители с частотным диапазоном до 60 МГц (с конца 2023 года доступны модели с частотой до 300 МГц);
- Лабораторные планетарные шаровые мельницы;

- Системы перемещения (линейное, вращение, качание) с пьезоприводами, в том числе криогенные пьезосканеры и пьезоступени;

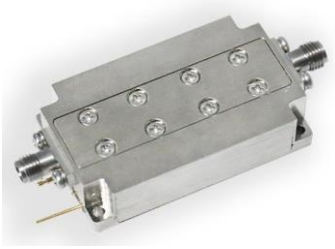

- Оборудование для СВЧ-измерений, в том числе для криогенных: детекторы, циркуляторы, изоляторы, коаксиальные провода, малошумящие усилители, фазовращатели, зонды, фильтры и другое;
- Оборудование для квантовых компьютеров;
- Возможна поставка любого оборудования под заказ и оснащение лабораторий «под ключ».

ООО «Криотрейд инжиниринг»
125367, г. Москва, Полесский проезд, дом 14А
Тел./факс: +7 (495) 374-69-52
Web: www.cryotrade.ru E-mail: sales@cryotrade.ru

Оптическое оборудование и фотоника:

- Узкополосные одночастотные лазеры с длиной волны от 185 до 2 371 нм и мощностью от 1 мВт до 18 Вт;
- Квантово-каскадные ИК-лазеры с длиной волны от 760 до 14 000 нм и мощностью от 1 мВт до 9 Вт;
- Импульсные твердотельные лазеры с длиной волны от 236 до 1 342 нм;
- Терагерцовые источники излучения от 1.3 до 4.7 ТГц мощностью от 0.1 до 5.0 мВт;

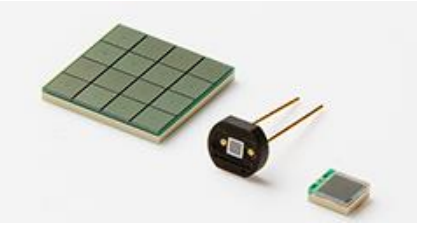

- Широкополосные источники излучения мощностью до 1 кВт;
- Волоконные оптические усилители;
- Лазерные диоды;
- Кремниевые фотоумножители;

- Электро- и акустооптические модуляторы;
- Микроскопы, в том числе стерео-микроскопы, конфокальные, сканирующие, биологические, металлургические и т.п.;
- Спектрометры комбинационного рассеяния;
- TCSPC системы, FLIM, конфокальные системы;
- Научные и промышленные камеры в таких спектральных диапазонах, как рентген, видимый, ближний и дальний ИК, с возможностью интеграции в систему заказчика;

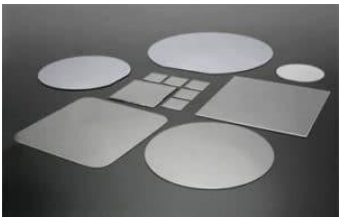

- виброизоляционные столы и аксессуары к ним;
- оптические компоненты, полупроводниковые подложки, сцинтилляторы, кристаллы для лазеров, окна прозрачности.

Кроме того, мы занимаемся ***выполнением обслуживания криогенных и вакуумных систем***. Наша производственная база имеет все необходимые инструменты, оборудование и ЗИП. Основные выполняемые работы: плановые ТО, диагностика неисправностей, вакуумирование объемов и проверка на течи, обслуживание криорефрижераторов и компрессоров, модернизация оборудования.

Ответственный редактор: Т. П. Гаврилова; редакторы В. К. Воронкова, Л. В. Мосина, Л. Р. Тагиров;
технические редакторы С. Г. Львов, О. Б. Яндуганова. Издательство ФИЦ КазНЦ РАН,
420029, Казань, Сибирский тракт, 10/7, лицензия № 0325 от 07.12.2000.